Genetic analysis of novel regulators of neuronal migration in *Caenorhabditis elegans*: the insulin/IGF-1 signaling pathway, a chromatin-binding factor ZFP-1 (AF10) and endogenous RNAi

Lisa Michelle Kennedy

Submitted in partial fulfillment of the requirements for the degree of
Doctor of Philosophy in the Graduate School of Arts and Sciences

COLUMBIA UNIVERSITY
2013

ABSTRACT

Genetic analysis of novel regulators of neuronal migration in *Caenorhabditis elegans*: the insulin/IGF-1 signaling pathway, a chromatin-binding factor ZFP-1 (AF10) and endogenous RNAi

Lisa M. Kennedy

The generation of functional neural circuitries requires neuronal migration, a central component of proper nervous system development. When defective, it can lead to devastating conditions including epilepsy and mental retardation. In the nematode *C. elegans*, neurons undergo both short- and long-range migrations that are regulated by conserved pathways. In my thesis study, I explore novel roles for both the insulin/IGF-1 signaling pathway and RNAi factors in neuronal migration by using the embryonic anterior migrations of the hermaphrodite-specific neurons (HSNs) of *C. elegans* as a model. I demonstrate that the insulin/IGF-1 signaling pathway modulates the activity of the conserved DAF-16/FOXO transcription factor non-autonomously in the hypodermis to regulate HSN migration. Furthermore, I identify PAK-1, a p21-activated kinase, as a downstream target of DAF-16 in the hypodermis. This study is the first to demonstrate a non-autonomous role for both FOXO and Pak1 in neuronal migration. I also implicate a conserved PHD zinc finger protein ZFP-1/AF10 and endogenous RNAi in the regulation of HSN migration. I determine that ZFP-1 affects HSN migration in part through its negative effect on the transcription of the conserved insulin/IGF-1 signaling kinase gene *pdk-1* and the modulation of downstream DAF-16 activity. This study expands the limited

understanding of the normal developmental roles of both ZFP-1/AF10 and RNAi. Combined, this thesis highlights a requirement for the coordinated activities of DAF-16/FOXO, ZFP-1/AF10 and endogenous RNAi in the establishment of proper neuronal positioning during development.

Table of Contents

List of Figures and Tables

Chapter One Figures and Tables

Chapter Two Figures

Chapter Three Figures and Tables

Chapter Four Figures and Tables

Appendix i Figures

Appendix ii Figures

Appendix iii Figures

Appendix iv Figures

Appendix v Figures

ACKNOWLEDGEMENTS

First and foremost, I would like to express my sincerest gratitude to my advisor Dr. Alla Grishok. Her enthusiasm for her research has motivated me throughout my years as a Ph.D. student. I am especially thankful for her generosity of time, scientific guidance, and most of all for always encouraging me to think "outside the box."

I would like to thank my training and thesis committee members: Dr. Iva Greenwald, Dr. Richard Mann and Dr. Lori Sussel for their many insights and guidance over the years. I am especially grateful to Iva for her mentorship and encouragement throughout my Ph.D. experience. I would also like to acknowledge Richard as the first reader of my thesis; I am grateful for his time and valuable comments. I would like to thank Lori for joining my committee as an Endocrinology Training Grant advisor and the long-term NIH Endocrinology Training Grant (T32 DK0007328) for multiple years of funding. Thanks also to my qualifying committee members: Dr. Oliver Hobert and Dr. Andrew Tomlinson; especially Oliver for continuing to keep an open door and providing me with invaluable scientific advice.

I would like to thank all members of the Grishok lab, past and present, for contributing to my scientific growth over the past 5 years. I would especially like to thank Germano Cecere for being generous with both his knowledge and friendship. I owe Steven Pham my heartfelt appreciation for his tremendous help over the past year and a half; his specific contributions to the work in this thesis are acknowledged at the start of various chapters.

One: General Introduction

Neuronal migration

Neuronal migration is central to proper nervous system development. Newly born neurons migrate from their place of birth to assume specific positions within the nervous system and permit the generation of functional neural circuitries. In vertebrates, neural progenitor cells originate from two major proliferative zones: the ventricular zone (VZ) of the neural tube, which eventually forms the embryonic ventricles of the brain (the forebrain, midbrain and hindbrain) and the ventral telencephalon, which is derived from the embryonic forebrain and is composed of the medial, lateral and caudal ganglionic eminences and later develops into the basal ganglia (reviewed in Stiles and Jernigan, 2010). Billions of neural progenitors travel, some at distances up to centimeters in length, throughout the central nervous system (CNS) to reach their final positions.

The cerebral cortex, which covers the surface of the two cerebral hemispheres and is a component of the forebrain, is required for higher cognitive functioning. During cortex formation, extensive cell migrations are coordinated to create six highly ordered horizontal neuronal layers (reviewed in Marín et al., 2010) (Figure 1-1). Specifically, the first wave of post-mitotic neurons to migrate out of the VZ forms the preplate of the cerebral cortex. Next, subsequent waves of neurons split the preplate into two layers: the marginal zone (MZ or layer I), which is made up of Cajal-Retzius cells and a deeper layer called the subplate (SP), which is populated by pyramidal neurons. Together these two layers make up what is termed the cortical plate (CP). Progressive cohorts of neurons continue to migrate and take up occupancy in increasingly more superficial layers within the CP. Consequently, layers II-VI are generated in an “inside-out” sequence; neurons generated earlier reside in deeper layers than those of neurons

born at a later time, which migrate past existing layers to form the superficial layers of the cerebral cortex.

Cortical malformations resulting from incomplete or excessive neuronal migrations during development can have profound and devastating consequences, including epilepsy and mental retardation (reviewed in Spalice et al., 2009). The methods utilized by migrating neurons and molecular pathways required during normal neuronal migration will be discussed in greater detail below and the specific disruptions that lead to human migration disorders will also be highlighted.

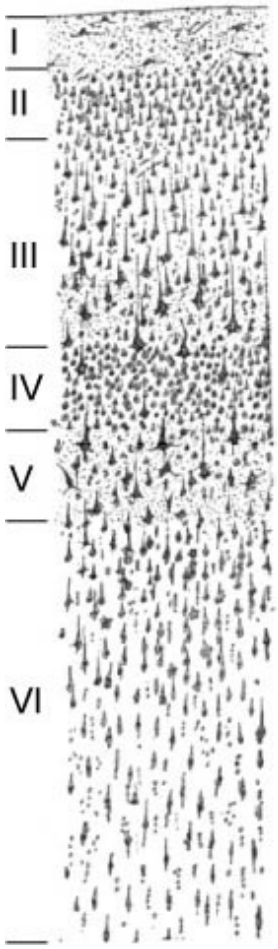

Figure 1-1. Hand drawing of the motor cortex of a human adult by Santiago Ramon y Cajal. The six developed layers of the cerebral cortex are indicated. The embryonic subplate (SP), marginal zone (MZ) and cortical plate (CP) are transient embryonic structures that are not illustrated. Image drawn from a Nissl-stained motor cortex. Image adapted from Ramon y Cajal, Santiago. *Comparative Study of the Sensory Areas of the Human Cortex.* Worcester: Clark University, 1899. Print.

Mechanics and methods of neuronal migration

Neuronal migration occurs in two distinct phases: extension of the leading process, which is followed by the movement of the cell body and nucleus (nucleokinesis) (reviewed in Tsai and Gleeson, 2005). Time-lapse observations of neuronal migration have revealed that a leading process is first extended in the direction of migration, followed by the advancement of the centrosome, which remains in front of the cell and emanates microtubules that extend both anteriorly into the leading process and posteriorly to encompass the nucleus. Next, the nucleus translocates forward in a saltatory fashion—short bursts of forward movements interrupted by inactive phases—followed by remodeling of the trailing process. This sequence of events is repeated until migration is complete (Solecki et al., 2004).

Migrating neurons travel by one of two main methods: radial or tangential migration (reviewed in Marín and Rubenstein, 2003). Radial migration is the process by which neurons travel a trajectory that is perpendicular to the ventricular surface, moving parallel to radial glial cells. Tangential migration occurs when neurons move in a trajectory that is parallel to the ventricular surface and orthogonal to the radial glial. The intricate formation of the cerebral cortex highlights how both radial and tangential migration are integrated during brain development.

In all species, the cerebral cortex is defined by its striking organization, which consists of neurons arranged in horizontal layers intersected by radial columns. In the cortex, radial glial cells span the radial axis to create a scaffold for directing newly born postmitotic neurons from the VZ towards the pial surface (outer brain surface), past previously generated neuronal layers. The glutamatergic cortical projection neurons (also called pyramidal cells) of the adult cerebral cortex use the process of radial migration to reach the top of the developing cerebral cortex

(cortical plate) and assemble into distinct layers (reviewed in Rakic, 2007). Furthermore, radial migration can occur in two distinct modes: somal translocation or locomotion (Nadarajah et al., 2001). Early-generated neurons have been shown to use somal translocation to travel from the VZ to their positions beneath the pial surface. During somal translocation, a process largely independent of glial cells, neurons extend a long basal process from the VZ to the pial surface, which is then followed by rapid nucleokinesis and shortening of the basal process. On the other hand, neurons that undergo locomotion extend a free leading process in the direction of migration and proceed in a slow saltatory fashion, while using glial cells to guide them.

Migrating simultaneously to the cortical projection neurons are the GABAergic interneurons (cortical interneurons), which undergo long tangential migrations to reach the cerebral cortex. In contrast to radial migration, tangential migration does not require specific interactions with radial glial cells. Instead, neurons use a variety of different types of substrates to promote their migration, including other neurons, growing axons or in some cases, no substrate at all (reviewed in Marín and Rubenstein, 2003).

Major molecular pathways

An extensive signaling network that ultimately converges upon the involvement of the cytoskeleton in the migrating cell controls neuronal migration. Cytoskeletal components that allow for the movement of a cell, signaling pathways that regulate the dynamics of the cytoskeleton and extracellular guidance cues are all required for neuronal migration.

The actin network

Disruption of actin dynamics can have profound effects on neuronal migration. For example, a mutation in Filamin 1, an actin crosslinking protein, prevents neurons from migrating

out of the VZ and into the cerebral cortex and causes the X-linked dominant human disorder periventricular heterotopia (PH) (Fox et al., 1998). Females with PH suffer from epilepsy and other conditions, while hemizygous males die embryonically. Filamin 1 can interact with many transmembrane proteins and provides a scaffold for signaling proteins of the Rho family of GTPases, which also regulate actin dynamics (reviewed in Ayala et al., 2007).

The evolutionarily conserved mammalian Ena (Mena), vasodilator-stimulated phosphoprotein (VASP), and Ena-VASP-like protein (EVL) are another family of actin regulators. Ena/VASP proteins promote actin polymerization and are found at the leading edge of lamellipodia and the tips of filopodia. Inhibition of Ena/VASP results in the ectopic localization of early-born neurons to more superficial layers (reviewed in Krause et al., 2003).

Furthermore, the actin-based motor, non-muscle myosin II (NMII), is another important regulator of neuronal migration. The myosin II motor has been demonstrated to accumulate behind the nucleus during migration and create a forward "pushing" force that aids in nuclear movement during nucleokinesis (reviewed in Ayala et al., 2007). Mice that are mutated for myosin IIB show abnormal migration of cerebellar granular neurons and abnormal tangential migration of neurons born in the medial ganglionic eminence (MGE) (Ma et al., 2004).

The microtubule network

The microtubules play a crucial role in associating the centrosome with the nucleus during nucleokinesis, as well as in providing stability to the leading process. The microtubule – associated proteins (MAPs) are required to stabilize microtubules during migration. Classical MAPs, such as MAP1A, MAP1B, MAP2, and Tau, as well "nonclassical" MAPs, including Lis1 and DCX family members, have been shown to stabilize microtubules during migration (reviewed in Ayala et al., 2007). Strikingly, humans that contain a deletion of *lis1* present with

type I lissencephaly, a brain developmental disorder that results in a smooth brain surface, disordered cortical layering, enlarged ventricles and neuronal heterotopias (displaced neurons) (Ozmen et al., 2000). The *DCX* (*doublecortin)* gene when mutated is responsible for X-linked lissencephaly in males and subcortical heterotopia (or doublecortex) in females.

Kinases

A large number of kinases mediate neuronal migration by activating multiple pathways (reviewed in Ayala et al., 2007). The Cdk5-mediated pathway has been studied in great detail. In mice deleted for *Cdk5* or both of its two regulators *P35* and *P39*, failed regulation of key cytoskeleton proteins results in abnormal neuronal positioning in the brain (reviewed in Dhavan and Tsai, 2001). Among the many targets of Cdk5 that are misregulated in the mutant are the actin regulatory proteins, such as the p21-activated kinase (Pak1) and microtubule-associated proteins, including DCX.

Another crucial kinase involved in neuronal migration is the phosphoinositide 3-kinase (PI3K), which generates phospholipid second messengers that stimulate downstream signaling pathways to regulate the actin cytoskeleton. One of the major downstream effectors of PI3K is Akt, which can, for example, negatively regulate glycogen synthase kinase 3 (GSK-3β) or modulate mammalian target of rapamycin (mTOR) activity to control microtubule dynamics and protein translation, respectively (reviewed in van Diepen and Eickholt, 2008).

Extracellular molecules

Guidance cues that were originally identified for controlling axonal navigation have shown significant overlap with those required for neuronal migration, and include the Netrins, Semaphorins, and Slits (reviewed in Tessier-Lavigne and Goodman, 1996). Netrin and its receptor Deleted in Colorectal Cancer (DCC) mediate neuronal positioning of pontine neurons in

the cerebellum (Yee et al., 1999). Migrating pontine cells express DCC and are attracted to Netrin-1 present at the ventral midline of the developing rat hindbrain. In addition to chemoattractive roles, Netrin-1 has also been shown to exhibit chemorepulsive roles during murine development (reviewed in Bradford et al., 2009). The major downstream effectors of netrin receptor signaling are the small GTPases, which in turn regulate cytoskeletal dynamics, including lamellipodium and filopodium extension or, in the case of the chemorepulsive response to Netrin-1, the regulation of cytoskeletal collapse (reviewed in Wen and Zheng, 2006).

Although, the secreted Slit glycoproteins and their receptors Roundabout (Robo) have been implicated in neuronal migration due to their expression in migrating cortical interneurons, the knockout mouse mutants have failed to display a neuronal migration phenotype (reviewed in Andrews et al., 2008). Recently, however, Slit2 and Robo3 have been shown to modulate the migration of the Gonadotropin-releasing hormone (GnRH) neurons (Cariboni et al., 2012) and the novel Robo family member, Robo4, has been demonstrated to regulate the radial migration of newborn cortical neurons (Zheng et al., 2012).

The semaphorins and their co-receptors neuropilin and plexin are involved in regulating cortical and striatal interneuron sorting from the MGE (reviewed in Marin and Rubenstein, 2001). Additionally, the plexin receptors serve as scaffolds for numerous Rho family GTPases, thus also linking the semaphorins and their co-receptors to the regulation of actin dynamics. Plexins, moreover, regulate the tyrosine kinases Fes and Fyn, which are linked to microtubule dynamics (reviewed in Ayala et al., 2007).

Glycosyltransferases

Loss-of-function mutations in the glycosyltransferases POMGnT1, POMT1 or the putative glycosyltransferase fukutin cause different subtypes of muscular dystrophy: muscle-eye-

brain disease (MEB), Walker-Warburg syndrome (WWS) and Fukuyama-type congenital muscular dystrophy (FCMD), respectively (reviewed in Yamamoto et al., 2004). All of these subtypes are associated with cobblestone lissencephaly (also called type II lissencephaly), which is characterized by the overmigration of cortical neurons in the cerebral cortex, such that neurons penetrate the pia mater above the cortex instead of stopping short of this surface (Gelot et al., 1995). The enzymes POMGnT1, POMT1 and fukutin have all been implicated in the glycosylation of α-dystroglycan, a heavily glycosylated protein, which links dystrophin and extracellular matrix proteins at the basement membrane, and may play an important role in the formation of basement membrane at the glia limitans in order to prevent the overmigration of neurons (reviewed in Yamamoto et al., 2004).

Reelin signaling

The reelin signaling pathway is one of the most well studied signaling mechanisms required during cerebral cortex formation and has been extensively reviewed (Rice and Curran, 2001; Stranahan et al., 2013). Reelin is a large extracellular glycoprotein that binds to members of the lipoprotein family of receptors VLDLR and ApoER2 and induces tyrosine phosphorylation of the adaptor protein Dab1. Mice with mutations in Reelin, Dab1 or a compound receptor mutant exhibit the same reeler phenotype: perturbation of the normal inside-out layering of the cerebral cortex, such that cortical neurons are layered in an outside-in order. Furthermore, during human cerebral cortex development, reduced reelin expression gives rise to neuronal migration defects that are associated with the development of lissencephaly (Hong et al., 2000).

The molecular mechanisms for how reelin is functioning as a positional signal during development is still an active area of research, however, there is evidence to suggest that the

actin regulatory network is a major downstream target (reviewed in Stranahan et al., 2013). Dab1, for instance, is required for somal translocation and stabilization of the leading processes (Franco et al., 2011) and reelin stabilizes the cytoskeleton by activating LIMK1, which inactivates cofilin and inhibits actin depolymerization (Chai et al., 2009).

C. elegans as a model for studying neuronal migration

The nematode *Caenorhabditis elegans* is an excellent model organism for studying the conserved process of neuronal migration; its invariant cell lineage and the abundance of genetic tools available to visualize individual neurons make it an advantageous system. The *C. elegans* nervous system is composed of 302 neurons that are largely clustered in several ganglia in the head and tail regions, as well as along the body itself (White et al., 1986). Neurons and their axons develop between the cell membrane and the basal lamina of the epidermis (also called the hypodermis) (Sulston et al., 1983) (Figure 1-2).

During *C. elegans* embyrogenesis, many cells move short distances, including the intestinal, germline, pharynx and body muscle precursors, however, a few cells undergo long, longitudinal migrations and include the anterior lateral microtubule neurons (ALMs), canal-associated neurons (CANs) and hermaphrodite-specific neurons (HSNs), as well as the mesoblasts M, Z1 and Z4, the right intestinal muscle and the coelomocyte mother cells (Sulston et al., 1983). Interestingly, of these cells, the HSNs are the only ones to undergo anteriorly directed migrations; the others undergo posteriorly directed migrations. During larval development, additional cells undergo migration along the body wall, these include the neuroblasts derived from the QV5 and T epidermal cells; descendants of the M, Z1 and Z4

mesoblasts and cells of the hermaphrodite and male body wall also undergo significant rearrangements (reviewed in Hedgecock et al., 1987).

Our understanding of neuronal migration and nervous system physiology has been greatly improved by studies in *C. elegans.* The following sections will discuss the major mechanisms that mediate neuronal migration in *C. elegans* as well as introduce the hermaphrodite-specific neurons (HSNs) as a model for studying neuronal migration during development.

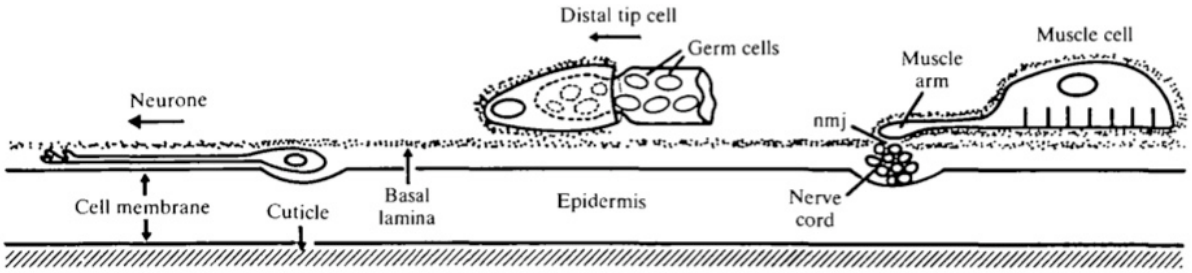

Figure 1-2. Embryonic body wall of *C. elegans*. Neurons and their axons develop sandwiched between the cell membrane and basal lamina of the epidermis. Figure from (Hedgecock et al., 1987).

Neuronal guidance cues along the dorsal-ventral body axis

UNC-6/Netrin

The conserved *unc-6/Netrin1* pathway, composed of the products of three genes, *unc-5, unc-6,* and *unc-40,* was first discovered in *C. elegans* (Hedgecock et al., 1990; Ishii et al., 1992; Leung-Hagesteijn et al., 1992; Chan et al., 1996; Wadsworth et al., 1996) and is the most well studied pathway required for migrations along dorsal-ventral (DV) axis of the *C. elegans*

epidermis. Specifically, *unc-5* mutations affect the dorsal migrations on the epidermis, including the major classes of motor axons, excretory canal cells, head mesodermal cells, linker cell, and the hermaphrodite distal tip cells. Mutations in *unc-40*, on the other hand, affect the ventral migrations, including several classes of sensory and motor axons, linker cell and anchor cell. Unlike *unc-5* and *unc-40* mutants, *unc-6* mutants affect migrations in both directions. The migration of the HSN pioneer axon along the epidermis during the L4 larval stage provides an example how mutations in *unc-6* and *unc-40* disrupt growth cone guidance. Normally, HSN axons extend ventrally and enter the ventral nerve cord in the midbody, they then extend anteriorly in the nerve cord. However, in *unc-6* and *unc-40* mutants 90% of HSN axons fail to reach the ventral nerve cord and instead run longitudinally along the lateral epidermal ridges (Desai et al., 1988).

In addition to the major role *unc-6/Netrin1* signaling plays in axon guidance along the DV body axis, mild defects in the posterior embryonic migrations of the ALM cell body have also been reported in *unc-40* and *unc-6* loss-of-function mutants (Levy-Strumpf and Culotti, 2007; Watari-Goshima et al., 2007).

After the initial discovery of this genetic pathway, the *unc-6* gene was shown to encode a laminin-related, secreted protein that is expressed in 12 types of neuroglia and neurons along the ventral midline and is used by cells to orient their movements either towards or away from the UNC-6 source (Ishii et al., 1992; Wadsworth et al., 1996). Furthermore, *unc-5* was cloned and identified as a cell surface receptor required cell-autonomously in migrating cells and growth cones to guide dorsal movements away from UNC-6 sources (Leung-Hagesteijn et al., 1992). Similarly, *unc-40* encodes a homolog of the vertebrate cell adhesion molecules DCC and

neogenin and is expressed cell-autonomously in motile cells and axons to guide ventral movements towards UNC-6 sources (Chan et al., 1996).

SLT-1/slit

Slit was first identified as a *Drosophila* mutant exhibiting severe cell and axon defects at the midline (Rothberg et al., 1990) and was later shown in both *Drosophila* and vertebrates to bind directly to Robo receptors (Brose et al., 1999; Li et al., 1999). In *C. elegans,* one *sax-3/robo* gene and one *slt-1/slit* gene are present in the genome, although a SAX-3 co-receptor EVA-1 has also been identified (Fujisawa et al., 2007). SLT-1 has roles in both DV guidance of pioneer axons in larvae and anterior-posterior (AP) guidance of neuron migrations during embryogenesis (Hao et al., 2001). The *slt-1* gene acts in parallel to *unc-6* to guide growing axons along the DV axis during larval development (Hao et al., 2001). In larval muscles, SLT-1 is expressed in a high to low dorsal-ventral gradient and acts as a repellent through the SAX-3/Robo receptor, which functions cell-autonomously, to direct axons away from the dorsal body walls (Zallen et al., 1999; Hao et al., 2001). Using the AVM and/or HSN neurons as a model for ventral directed axon migration, cooperation between UNC-6/Netrin and SLT-1/Slit signaling was subsequently shown to induce neuronal asymmetry and define the site of axon outgrowth through MIG-10/RIAM/Lamellopodin and its binding partner UNC-34/Enabled/VASP, presumably via the reorganization of the actin cytoskeleton (Chang et al., 2006; Quinn et al., 2006).

In embryos, SLT-1 expression is first observed at the comma stage in the most anterior epidermal cells, including hyp4 and hyp1, and is later observed at lower levels in the tail and excluded from the center of the embryo (Hao et al., 2001). Consistent with this expression pattern and SLT-1 acting as a repellent, posterior migrations of both the CAN and ALM neurons, which travel from the head to the midbody during embryogenesis, are terminated prematurely in

sax-3 and *slt-1* mutant animals (Hao et al., 2001; Fleming et al., 2005). To a lesser extent, the embryonic anterior migrations of the HSNs from the tail to the midbody of the animal are also disrupted in *sax-3* mutants (Zallen et al., 1999).

Neuronal guidance cues along the anterior-posterior body axis

Wnt proteins

The Wnt proteins (Wingless in *Drosophila)* are a family of highly conserved secreted glycoproteins that were originally discovered in *Drosophila*. Wingless (Wg) was first identified as a recessive mutation affecting wing development and embryonic segmentation (reviewed in Buechling and Boutros, 2011) and later shown to function as a gradient morphogen across developing tissues (Zecca et al., 1996). Wnt proteins can signal through different members of the Frizzled (Fz) receptor family, which are atypical G-protein-coupled receptors (GPCRs), as well as via the receptor tyrosine kinase RYK to regulate downstream transcriptional and posttranscriptional processes through either canonical (β-catenin-dependent) or noncanonical (β-catenin-independent) pathways.

In *C. elegans,* the Wnts control many processes including cell fate, cell polarity, axon outgrowth and cell migration (reviewed in Killeen and Sybingco, 2008). However, I will only focus on the role of Wnts in AP neuronal migration below. The *C. elegans* genome encodes five Wnts: EGL-20, LIN-44, CWN-1, CWN-2, MOM-2 and four Frizzled receptors of Wnt: MOM-5, CFZ-2, MIG-1, LIN-17, in addition to the Ryk homolog LIN-18. The Wnt proteins are expressed in partially overlapping domains along the AP body axis that are already defined by the comma stage embryo and persist throughout L1 larval development (Harterink et al., 2011). LIN-44, EGL-20 and CWN-1 are expressed in the embryonic tail region and continue to be expressed in

the tail throughout larval development, which has lead to the suggestion that they may form a posterior-to-anterior concentration gradient enabling them to function as directional cues during cell migration (Herman et al., 1995; Whangbo and Kenyon, 1999; Gleason et al., 2006; Pan et al., 2006). In fact, an EGL-20 gradient that extends from the tail to the midbody of the animal has been observed (Coudreuse et al., 2006). The other Wnts, MOM-2 and CWN-2, have been reported to be more widely expressed along the AP body axis during embryonic and larval development (Gleason et al., 2006). Recently, MOM-2 was shown to be more restricted than previously thought, with transcripts detected by single-molecule fluorescent in situ hybridization (smFISH) present primarily in the germ cell precursors Z2 and Z3, their descendants and a few unidentified tail cells (Harterink et al., 2011).

Wnt signaling in *C. elegans* has been extensively studied for its role in regulating the migration of the Q neuroblasts and their descendants (reviewed in Silhankova and Korswagen, 2007). The two Q neuroblasts are born at similar positions on the left (QL) and right (QR) sides of the animal towards the end of embryogenesis, but along with their descendants migrate in opposite directions during the first larval stage (Sulston and Horvitz, 1977). At the beginning of the L1 larval stage, the QL neuroblast migrates a short distance posteriorly and the QR neuroblast migrates a short distance anteriorly. Their descendants continue migrating to asymmetric posterior or anterior positions, respectively. Each Q lineage produces a mechanosensory neuron (AVM/PVM), a sensory neuron (AQR/PQR), an interneuron (SDQR/L) and two programmed cell deaths (Salser and Kenyon, 1992).

The guidance cue that specifies the migration direction of the Q neuroblasts and its descendants is the Wnt EGL-20 (Harris et al., 1996; Maloof et al., 1999), which activates a canonical Wnt/β-catenin pathway in the QL neuroblast, likely through the Frizzled receptors

MIG-1 and LIN-17 to turn on the expression of the homeotic gene *mab-5*. The migration of QL and its descendants is subsequently directed posteriorly by MAB-5 (Salser and Kenyon, 1992; Harris et al., 1996). The anterior migration of the QR neuroblast and its descendants, on the other hand, is dependent on multiple Wnts including EGL-20, CWN-1 and CWN-2 to activate a β-catenin-independent Wnt signaling pathway (Zinovyeva and Forrester, 2005) through any of the four Frizzled receptors (Zinovyeva et al., 2008). Interestingly, EGL-20/Wnt appears to have a permissive role in regulating the Q neuroblast migrations; asymmetric EGL-20/Wnt levels do not mediate the differential migratory responses of QR and QL, rather it is the difference in neuroblast sensitivity to EGL-20 that dictates the migratory direction taken by individual Q neuroblasts (Whangbo and Kenyon, 1999).

In addition to having a permissive role in regulating neuronal migration, Wnt signaling has also been demonstrated to play an instructive role in guiding the embryonic migrations of the hermaphrodite-specific neurons (HSNs), which migrate from the posterior to the midbody region (Sulston et al., 1983; Pan et al., 2006). The EGL-20/Wnt protein functions as a repellent to direct the anterior migrations of the HSNs away from the tail region and towards the midbody during embryogenesis (Pan et al., 2006). Although *egl*-20 mutants exhibit the strongest HSN undermigration phenotype, the other Wnts contribute a subtler role: double mutant combinations among *cwn-1, cwn-2*, *lin-44*, *mom-2* and *egl-20* enhance the HSN undermigration phenotype of single mutants alone. Furthermore, three of the four Frizzled and the one Derailed/Ryk tyrosine kinase receptor in *C. elegans* are also required for HSN migration: *mig-1/fz* mutations affect HSN migration to the greatest extent, while mutations in the other receptors MOM-5/Fz, CFZ-2/Fz and LIN-18/Ryk show no phenotype as single mutants but enhance a *mig-1* mutant (Pan et

al., 2006). Additionally, MIG-1/Fz function was shown to be required cell-autonomously in the HSN neurons, suggesting that Wnt may act through this receptor (Pan et al., 2006).

In addition to affecting the anterior migrations of the HSN neurons, Wnts have also been shown to affect the posteriorly oriented migrations of the ALM and CAN neurons during embryogenesis, which migrate from the anterior to the midbody region (Sulston et al., 1983; Zinovyeva and Forrester, 2005). ALM posterior migration is stopped short in *cwn-1; cwn-2* double mutants, as well as in *cfz-2*/Fz single mutants (Zinovyeva and Forrester, 2005; Zinovyeva et al., 2008). For the CAN neurons, only single mutations in *cwn-2* prevent the posterior-directed migrations, however it can be enhanced by a mutation in *cfz-2*/Fz. Interestingly, the Wnts CWN-1, EGL-20 and MOM-2 have also been implicated regulating CAN migration, however, they appear to function redundantly and antagonistically to CFZ-2/Fz and CWN-2 to produce a "stop signal" as mutant combinations of these proteins often lead to a CAN overmigration phenotype (Zinovyeva et al., 2008).

Negative regulators of Wnt

The sole *C. elegans* Receptor tyrosine kinase-like orphan receptor (Ror), CAM-1, can function as a negative regulator of Wnt signaling. CAM-1 is expressed beginning at the 200-cell stage in most cells of the embryo (Forrester et al., 1999). Mutations in *cam-1* affect the AP migrations of several neurons, including the long-range migrations of the HSN, CAN, ALM and Q neuroblasts (Forrester and Garriga, 1997). The relationship between CAM-1 and EGL-20/Wnt during HSN migration has been well studied (Forrester et al., 1999; Kim and Forrester, 2003; Forrester et al., 2004). The observation that *cam-1* loss-of-function mutants and *egl-20* loss-of-function mutants cause reciprocal HSN migration phenotypes (overmigration in *cam-1* mutants and undermigration in *egl-20* mutants) lead to further studies demonstrating that CAM-1

overexpression phenocopies the *egl-20* loss-of-function HSN undermigration phenotype and that EGL-20 overexpression phenocopies the *cam-1* loss-of-function HSN overmigration phenotype (Forrester et al., 2004). Thus, CAM-1 and EGL-20 appear to have an antagonistic relationship in regards to HSN migration, which is further supported by the observation that *egl-20* mutants can suppress the HSN overmigration phenotype in *cam-1* mutants (Forrester et al., 2004).

Interestingly, the intracellular kinase domain of CAM-1 is not required for AP neuronal migrations, suggesting that kinase activity may not be required for some CAM-1 functions (Forrester et al., 1999; Kim and Forrester, 2003). In fact, experiments using engineered *cam-1* deletions demonstrated that the membrane anchored CAM-1 extracellular Cys-rich-domain (CRD) alone was sufficient to rescue *cam-1* mutant HSN migration defects. Consistently, CAM-1 transgenes deleted for the CRD failed to rescue the embryonic CAN and ALM migrations (Kim and Forrester, 2003). Furthermore, overexpression of the CAM-1 CRD was shown to reduce *mab-5* expression in the QL and descendants, causing anterior migrations instead of posteriorly directed migrations during the larval L1 stage—just as occurs in *egl-20* mutants (Forrester et al., 2004). Combined, these results led to the model that CAM-1 directs HSN and QL descendant cell migrations by negatively regulating EGL-20 and specifically by functioning as a "sink" for Wnt through its CRD domain. It has been shown that vertebrate Ror proteins bind Wnt through their CRD domains (reviewed in Green et al., 2008). This was later also confirmed in *C. elegans* in a study demonstrating that the CAM-1 CRD can bind to Wnts CWN-1, EGL-20 and MOM-2 in vitro (Green et al., 2007). It should also be noted that in addition to acting as a "sink," CAM-1 appears to also facilitate Wnt signaling as in the case for CAN migration. Mutations in *cam-1* give a CAN undermigration phenotype, as do mutations in CWN-2. In double *cam-1; cwn-2* mutants there is no enhancement of this migration defect, suggesting that

Wnts and CAM-1 can also function together to coordinate cell migration (Zinovyeva et al., 2008).

The activity of Wnt proteins can also be modulated by secreted Frizzled-related proteins (SFRPs), which, like CAM-1, are characterized by an N-terminal CRD and have been shown to act as both inhibitors and facilitators of Wnt signaling (reviewed in Esteve and Bovolenta, 2010). Recently, a *C. elegans* ortholog of SFRP, *sfrp-1,* has been identified (Harterink et al., 2011). In *C. elegans*, SFRP-1 functions exclusively as an inhibitor of Wnt signaling (Harterink et al., 2011). Mutations in SFRP-1 affect the migrations of the QR neuroblast and descendants, ALM and CAN; the HSN migrations are unaffected. In all cases the final positions of these cells are shifted anteriorly, which can be suppressed by a mutation in the Wnt CWN-2 for the QR cells and mutations in either CWN-1 or CWN-2 for the ALM and CAN neurons. Combined with the predominately anterior expression of SFRP-1 in the head body wall muscles, these findings have suggested that SFRP-1 controls AP migration by inhibiting the most anteriorly expressed Wnts: CWN-1 and CWN-2 (Harterink et al., 2011).

The hermaphrodite-specific neuron (HSN) as a model for neuronal migration

The HSNs of *C. elegans* are among the farthest migrating cells in the developing embryo and of those cells, the only ones to undergo anterior-directed migrations (Sulston et al., 1983). The HSNs are a pair of bilaterally symmetric motor neurons that are born in the tail of the embryo 400 minutes after fertilization when each of two HSN/PHB precursors divides to give rise to an HSN and a PHB phasmid chemosensory neuron. Ten minutes after being born, the HSNs migrate to the mid-body of the animal (reviewed in Hedgecock et al., 1987) (Figure 1-3). During the fourth larval stage, the HSNs begin morphological maturation and differentiation,

resulting in axonal outgrowth and serotonin biosynthesis (Desai et al., 1988). In the adult hermaphrodite, the HSNs innervate the vulval muscles and stimulate egg-laying by releasing the neurotransmitter serotonin (Desai et al., 1988). Forward genetic screens have identified many genetic components required for HSN migration (Desai et al., 1988; Manser and Wood, 1990; Forrester and Garriga, 1997), and I have compiled a table summarizing all of the currently known genes required for HSN migration (Table 1-1). A subset of the genes identified exhibit HSN migration defects due to the fact that they act cell-autonomously to promote HSN cell-fate and includes the homeodomain transcription factor *egl-5* (Trent et al., 1983; Desai et al., 1988). Of those genes identified to have a role specifically in the migration process, the Wnt family of signaling molecules is the most well studied pathway in controlling anterior-posterior directed neuronal migration of the HSN, to date (Silhankova and Korswagen, 2007). Also of note is that many of the genes identified to be required for HSN migration have not been well-characterized; they lack a cellular focus or a clearly identified genetic pathway (Table 1-1).

The HSN is an excellent model for identifying novel and conserved components of neuronal migration, not only because of its long range embryonic migrations but also because many of the same genes that have been implicated in HSN migration (Table 1-1) have also been identified as functioning in migrating vertebrate neural crest cells (Kee et al., 2007), suggesting conservation between species. Specifically, using comparative genomic analysis, vertebrate orthologs of genes required for HSN migration in *C. elegans* were identified and then examined for both their expression and functional conservation in the vertebrate neural crest. Of the 15 genes examined, only two did not show expression in the neural crest cells of chicken embryos and 6 of those genes, using gain- and loss-of-function studies, were shown to affect the migrations of neural crest cells in *Xenopus* embryos (Kee et al., 2007). The HSN has been used

as a model to investigate novel pathways required for neuronal migration in the work presented throughout this thesis.

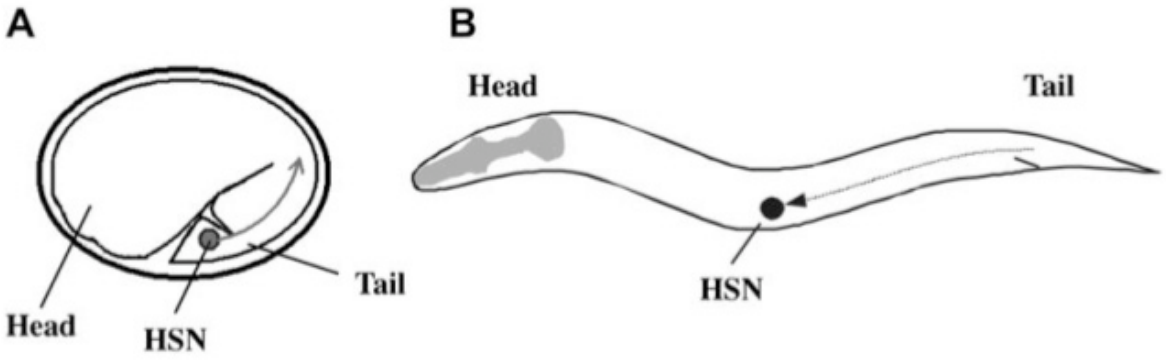

Figure 1-3. Schematic diagram of HSN migratory route. A. Diagram of an embryo showing the birthplace of the HSN in the tail and its migration route (arrow). **B.** Diagram of a first-stage larva and the final position of the HSN after its migration (arrow). Figure from (Pan et al., 2006).

Table 1-1. Summary of genes required for HSN migration

Gene	Description	Cellular Focus	References
egl-5	Homeodomain transcription factor	Autonomous; required for HSN fate	Desai et al., Nature, 1988; Baumeister & Ruvkun, G&D, 1996; Baum et al., G&D, 1999, Singhvi, Genetics, 2008
ham-2	C2H2 Zinc-finger containing protein	Autonomous; required for HSN fate	Desai et al., Nature, 1988; Baum et al., G&D, 1999
egl-43	Zinc-finger protein	Likely Autonomous; expressed in the HSN during migration	Garriga & Horvitz, G&D, 1993; Baum et al., G&D, 1999
ham-1	Novel protein	Autonomous; acts in the HSN/PHB precursor cells to specify cell fate	Desai et al., Nature, 1988; Guenther & Garriga, Development, 1996
ham-3	BAF60 homolog, a subunit the BAF chromatin remodeling complex	Likely autonomous; expressed in the HSN	Desai et al., Nature, 1988; Weinberg et al., Genetics 2013
egl-44	Transcription factor	Autonomous	Desai et al., Nature, 1988; Wu et al., G&D, 2001
egl-46	Transcription factor	Autonomous	Desai et al., Nature, 1988; Wu et al., G&D, 2001
Wnt family (*cwn-1, cwn-2, lin-44, egl-20, mom-2)*	Wnt proteins	Non-autonomous (tail cells)	Desai et al., Nature, 1988; Herman et al., Cell, 1995; Harris et al., Development, 1996; Pan et al., Dev. Cell, 2006
Wnt receptors (*mig-1*/FZ, *mom-5*/FZ, *cfz-2*/FZ, *lin-18*/Ryk)	Frizzled and Derailed/Ryk tyrosine kinase Wnt receptors	Autonomous (only *mig-1* tested)	Desai et al., Nature, 1988; Harris et al., Development, 1996; Pan et al., Dev. Cell, 2006
sdn-1	Heparan sulfate proteoglycan	Neuronal & possibly hypodermal	Rhiner et al., Development, 2005
mig-10	Actin-regulatory pleckstrin homology (PH) domain protein (lamellipodin)	Possibly autonomous; ventrally localized in the HSN during L2	Desai et al., Nature, 1988; Manser & Wood, Dev. Genetics, 1990; Adler et al., Nature, 2006
ina-1	α integrin subunit	Likely autonomous; INA-1::GFP expressed in migrating HSNs	Baum & Garriga, Neuron, 1997
mig-2	RhoG homolog	Likely autonomous; MIG-2::GFP expressed in migrating HSN	Desai et al., Nature, 1988; Zipkin et al., 1997
epi-1	Structural gene of laminin alpha chain	Unknown	Forrester & Garriga, Development, 1997
vab-8	Novel protein containing an atypical kinesin-like motor domain	Unknown	Manser & Wood, Dev. Genetics, 1990; Wightman et al., Development, 1996; Forrester & Garriga, Development, 1997
fam-2	Unknown	Unknown	Forrester & Garriga, Development, 1997
unc-34	Ena/VASP homolog	Unknown	Desai et al., Nature, 1988, Forrester & Garriga, Development, 1997
unc-71	Disintegrin and metalloprotease (ADAM) protein	Unknown	Desai et al., Nature, 1988
egl-18	GATA transcription factor	Unknown	Desai et al., Nature, 1988
egl-27	Metastasis-associated gene (MTA)	Unknown	Desai et al., Nature, 1988
tbx-2	T-box protein	Unknown	Singhvi et al., Genetics, 2008
unc-73	Guanine nucleotide exchange factor (GEF)	Unknown	Desai et al., Nature, 1988
hda-1	Histone deacetylase	Unknown	Zinovyeva et al., Dev. Bio, 2006
mig-12	Unknown	Unknown	Desai et al., Nature, 1988
cam-1	Receptor tyrosine kinase	Unknown	Forrester & Garriga, Development, 1997; Forrester et al., Nature, 1999; Forrester et al., Genetics, 2004

Insulin signaling in neuronal development

Insulin signaling

Insulin/insulin-like growth factor-1 (IGF-1) signaling (IIS) is highly conserved from invertebrates to mammals and has been best studied in *C. elegans* for its role in regulating longevity (reviewed in Lapierre and Hansen, 2012). The single IIS pathway of nematodes corresponds in structure and function to two distinct pathways of mammals that signal through either the insulin receptor (IR) to mediate metabolic responses to insulin or the insulin-like growth factor 1 receptor (IGF1R) to effect a growth response (reviewed in Kenyon, 2005). In *C. elegans,* the insulin/IGF-1 receptor is encoded by a single gene *daf-2* (Kimura et al., 1997). Interestingly, despite having one insulin-like receptor, the *C. elegans* genome encodes 39 insulin-like peptides, which can function as either agonists or antagonists of DAF-2/IR (Pierce et al., 2001; Li et al., 2003).

Agonist binding to DAF-2/IR activates its tyrosine kinase activity leading to the recruitment and phosphorylation of AGE-1, a phosphatidylinositol 3-kinase (PI3K) (Morris et al., 1996). Activated AGE-1 then adds a phosphate to phosphatidylinositol 4, 5-diphosphate (PIP2) at the inositol-ring 3-position, converting it to phosphatidylinositol 3,4,5-triphospate (PIP3), which activates the AKT family of kinases (Hertweck et al., 2004) in a 3-phosphoinositide-dependent kinase (PDK-1) dependent manner (Paradis et al., 1999). Next, these active AKT kinases (AKT-1/2 and SGK-1) phosphorylate the forkhead transcription factor DAF-16/FOXO (Henderson and Johnson, 2001; Lee et al., 2001; Lin et al., 2001), which prevents DAF-16 from entering the nucleus and regulating the transcription of its target genes (Lin et al., 1997; Ogg et al., 1997) (Figure 1-4).

Not surprisingly, reduced insulin/IGF-1 signaling relieves the repression of DAF-16, allowing it to translocate into the nucleus and turn on its target genes including metabolic, stress protective and antimicrobial genes (reviewed in Murphy, 2006) (Figure 1-4). Interestingly, gene expression profiling (McElwee et al., 2003; Murphy et al., 2003; McElwee et al., 2004; Halaschek-Wiener et al., 2005) and chromatin immunoprecipitation (ChIP) (Oh et al., 2006) studies using *daf-2/*IR mutants as well as genome-wide analysis of DAF-16::GFP binding regions in wild type worms (modENCODE; Snyder project) identified hundreds of DAF-16/FOXO-regulated genes, suggesting that DAF-16 may function in biological processes other than longevity and the stress response. These expression analyses in combination with direct binding techniques have revealed that DAF-16 can function to both activate (class I genes) and repress (class II genes) its transcriptional targets (Kenyon and Murphy, 2006; Murphy, 2006).

In addition to reduced insulin/IGF-1 signaling there are several other methods by which DAF-16 can be signaled to move into the nucleus. DAF-18, the phosphatase and tensin (PTEN) homolog in *C. elegans* dephosphorylates AGE-1 (PI3K) generated PIP3, thereby inhibiting PI3K signaling and preventing DAF-16 phosphorylation by downstream kinases (Ogg and Ruvkun, 1998; Solari et al., 2005). Furthermore, DAF-16 can be directly activated by the c-Jun N-terminal kinase (JNK) upon heat stress (Oh et al., 2005). Nuclear translocation of DAF-16 is also regulated by PRMT-1, an arginine methyltransferase, which blocks DAF-16 phosphorylation by AKT (Takahashi et al., 2011). Moreover, DAF-16 nuclear translocation can also be terminated. For example, RLE-1, an E3 ubiquitin ligase catalyzes ubiquitination of DAF-16 and targets it for degradation by the proteasome (Li et al., 2007). Additional modulators of DAF-16 activity include the Ras/LET-60 MAPK pathway, the histone deacetylase SIR-2.1, the LET-7/LIN-4 target LIN-14 and germline ablation (reviewed in Wolff and Dillin, 2006).

Nuclear entry of DAF-16 is not sufficient for some functions (Lin et al., 2001); therefore it is not surprising that DAF-16 has several nuclear co-regulators that function together to modulate its activity in response to reduced insulin/IGF-1 signaling. SMK-1, a homolog of SMEK (suppressor of MEK null), for example, is required to mediate the longevity, innate immune, UV and oxidative stress functions of DAF-16 (reviewed in Wolff and Dillin, 2006). The *C. elegans* homolog of host cell factor 1 (HCF-1) physically associates with DAF-16 in the nucleus and prevents it from accessing a selection of its target genes involved in longevity and environmental stress (Li et al., 2008). Other co-regulators include the heat-shock factor 1 (HSF-1), which is required to mediate DAF-16 transcriptional activity of the genes encoding the small heat-shock proteins (Hsu et al., 2003) and the transcription factor Skinhead (SKN)-1/Nrf, which cooperates with DAF-16 to mediate the detoxification response (Tullet et al., 2008).

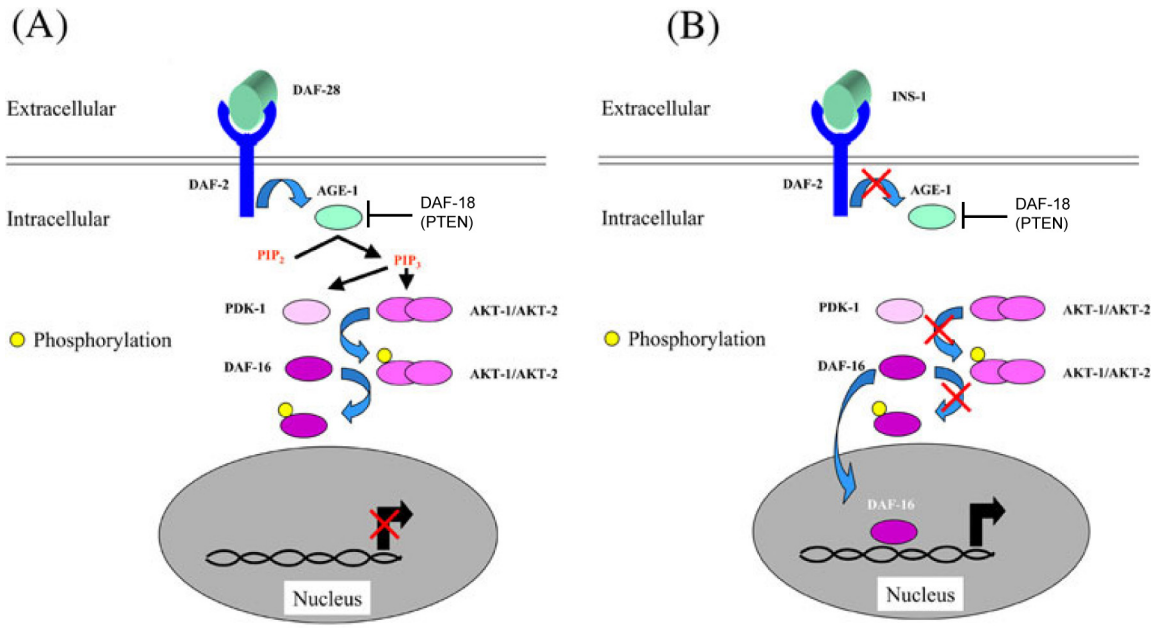

Figure 1-4. The insulin/IGF-1 signaling (IIS) pathway. A. Agonist binding to the DAF-2/IR activates downstream kinases, which phosphorylate DAF-16 to retain it in the cytoplasm. **B.** Antagonist binding to the DAF-2/IR inactivates the downstream kinases, consequently, DAF-16 is not phosphorylated and can translocate to the nucleus to regulate its target genes. See text for details. Figure adapted from Ewbank, J. J. Signaling in the immune response (January 23, 2006), *WormBook*, ed. The *C. elegans* Research Community, WormBook, doi/10.1895/wormbook.1.83.1, http://www.wormbook.org.

Insulin signaling and nervous system physiology of *C. elegans*

The sole *C. elegans* DAF-2/IR has been shown to be expressed at its highest levels in the nervous system, with weaker expression observed in other tissues, including the hypodermis during larval and adult stages (embryos were not examined) (Kimura et al., 2011). Downstream of DAF-2, there are three functionally characterized *daf-16* isoforms: *daf-16a, daf-16b* and *daf-*

16d/f (Ogg et al., 1997; Lee et al., 2001; Lin et al., 2001; Kwon et al., 2010). DAF-16a and DAF-16b proteins are expressed during embryogenesis (Ogg et al., 1997; Henderson and Johnson, 2001; Lee et al., 2001) and all three isoforms exhibit neuronal expression in developing larvae (Ogg et al., 1997; Henderson and Johnson, 2001; Lee et al., 2001; Kwon et al., 2010). Therefore, it is not surprising that novel roles for insulin signaling and DAF-16/FOXO in nervous system physiology of the worm have begun to emerge in the last few years.

Recently, a role for PI3K-regulated signaling through DAF-16 has been shown to cell-autonomously promote neurite outgrowth in the *C. elegans* AIY interneurons during embryonic development (Christensen et al., 2011). Interestingly, PI3K signaling in this case appears to function independently of the DAF-2 receptor, as a *daf-2* loss-of-function allele did not suppress the truncated AIY neurites present in *daf-18/*PTEN mutants, whereas both *age-1*/PI3K and *pdk-1* loss-of-function alleles were capable of suppression, presumably by enabling DAF-16 nuclear translocation and subsequent activity. Furthermore, the DAF-16b isoform was sufficient to rescue the AIY truncations present in the *daf-16* null mutant animals and neither DAF-16a nor DAF-16d/f were capable of rescuing activity. This study also demonstrated that the axon outgrowth-promoting role of DAF-16/FOXO is conserved in mammalian neurons, as FOXO was shown to be required for both axon outgrowth and inhibition of dendritic length in primary cerebellar granular neurons (Christensen et al., 2011).

In addition to a role in neurodevelopment, DAF-16 activity mediated by decreased insulin/IGF-1 signaling has been implicated in the progression of neuronal aging (Pan et al., 2011; Tank et al., 2011). The ALM and PLM touch receptor neurons (two classes of bilaterally symmetric mechanosensory neurons), as well as the cholinergic axons in the ventral nerve cord (VNC), have been shown to undergo age-dependent morphological defects including

cytoskeletal disorganization in the cell body, defasiculation and axon beading (Pan et al., 2011). Insulin signaling was identified as one regulator of neuronal aging; *daf-2* mutants exhibited delayed aging and *daf-16* mutants displayed premature aging. Interestingly, restoring DAF-16 activity in the neurons or in the body-wall muscles did not rescue the age-dependent defects seen in the touch neurons of *daf-16* null mutants, suggesting that DAF-16 acts non-autonomously to regulate neuronal aging (Pan et al., 2011). Similarly, in another study, insulin/IGF-1 signaling and DAF-16 have been shown to regulate neurite branching in aging worms (Tank et al., 2011). In contrast to the first study, insulin/IGF-1 signaling was shown to function autonomously within neurons to inhibit DAF-16 activity and promote branching (Tank et al., 2011).

Another recent study has implicated the downregulation of the IIS pathway in the prevention of neuronal degeneration, another age-associated process (Calixto et al., 2012). It utilized worms that express *mec-4d*, a constitutively active degenerin, which causes degeneration of neuronal somas and axons in the touch neurons, as a model. Entry into dauer, a diapause state triggered by a lack of nutrients, and the subsequent downregulation of the IIS pathway prevented *mec-4d* triggered neuronal degeneration (Calixto et al., 2012). The study further shows that cell-autonomous down-regulation of the IIS pathway within the touch cells acts in a DAF-16-dependent manner to activate antioxidant enzymes, such as superoxide dismutases (SODs) and catalases to prevent neuronal degeneration.

Recently, we have identified a novel and non-autonomous role for DAF-16/FOXO in neuronal migration and implicated PAK-1, a P21-activated kinase, as a downstream mediator of insulin/IGF-1-DAF-16 signaling in the non-autonomous control of HSN migration (see chapter 2).

Insulin signaling in vertebrate neurodevelopment

Similar to *C. elegans* DAF-16/FOXO expression in the nervous system, the FOXO transcription factors are widely expressed in the developing mammalian brain (Brunet et al., 1999; Hoekman et al., 2006; de la Torre-Ubieta et al., 2010) and only recently have begun to be implicated in neurodevelopment. For example, recently, the FOXOs were shown to be required cell-autonomously for neuronal polarity in the mammalian brain; knockdown of FOXOs in the cerebellum of rat pups resulted in cortical neurons having multiple long processes and the absence of defined ascending axons (de la Torre-Ubieta et al., 2010). In addition, this study identified PAK1, a P21-activated kinase, as a direct transcriptional target of FOXO required to mediate FOXO-dependent neuronal polarity. Additionally, a role for FOXO3a, a member of the FOXO subfamily, in the maintenance of neuronal survival during *zebrafish* brain development has been described (Peng et al., 2010).

In contrast to the newly described roles for FOXO in neurodevelopment, IGF-1-induced signaling has been implicated in mammalian brain development for some time now. Early observations in homozygous *Igf1*$^{-/-}$ mice reported reduced brain size resulting from a loss in neural progenitors (Beck et al., 1995) and the reciprocal phenotype of increased brain size in mice overexpressing IGF-1 has also been noted (Carson et al., 1993). Consistently, IGF1R is highly expressed in the embryonic brain and *Igf1r*$^{-/-}$ mice also show a reduced brain size and altered brain structures (Liu et al., 1993). Although a direct link between IGF-1 and FOXO has not been established, phenotypic analysis suggests that FOXO is inhibited downstream of IGF-1 to mediate brain development. FOXO3 overexpression, for example, leads to a reduced brain size and a decrease in neural progenitors, similar to the phenotype of *Igf1*$^{-/-}$ mice (Schmidt-Strassburger et al., 2012) and consistently, decreased FOXO activity results in larger brain size

and increased neural progenitor proliferation (Paik et al., 2009; Renault et al., 2009), congruent with the results of IGF-1 overexpression on the brain (Carson et al., 1993).

As expected from these initial observations, IGF-1 has been identified as an important factor that supports neuronal survival, differentiation and maturation by activating the PI3K/Akt signaling pathway (reviewed in Varela-Nieto et al., 2003; Bateman and McNeill, 2006; Otaegi et al., 2006). Moreover, IGF-1 has also been shown to influence the organization of olfactory bulb layering in the mammalian brain by promoting neuronal migration in a PI3K-dependent manner (Hurtado-Chong et al., 2009).

The insulin receptor (IR) is also expressed in the nervous system, however, IR expression is mostly restricted to the adult brain (reviewed in Bateman and McNeill, 2006) and neuron-specific disruption of the *Ir* gene in mice does not appear to affect brain development or neuronal survival (Bruning et al., 2000), suggesting that the IGF1R receptor may play a larger role in vertebrate neurodevelopment. Despite this, insulin has been shown to stimulate neurite outgrowth, proliferation, differentiation and antiapoptotic effects in neurons (reviewed in Candeias et al., 2012).

RNA interference (RNAi)

We have uncovered a role for ZFP-1, an RNAi promoting chromatin-binding protein, and the RNAi factors RDE-4, CSR-1 and DRH-3 in the process of HSN migration (see chapter 3). Historically, the initial observation that classical RNAi factors, ZFP-1 and DAF-16 are likely to regulate common biological processes based on expression analysis (Murphy et al., 2003; Grishok et al., 2008), led us to create complex mutants among these genes to look for phenotypic changes. This subsequently led to the identification of egg-laying defects in double mutant

combinations between mutants of DAF-16 and RNAi components and prompted us to examine the HSN neurons, which are responsible for egg-laying in the adult animal. The result of this was the identification of HSN migration defects in mutants of the insulin signaling pathway (see chapter 2) and the endo-RNAi pathway (see chapter 3).

RNAi was discovered in *C. elegans* as a gene silencing phenomenon induced by double-stranded RNA (dsRNA) introduced by either injection or bacterial feeding (Fire et al., 1998; Timmons and Fire, 1998). This phenomenon is now regarded as a highly conserved process of gene silencing found in organisms ranging from fission yeast to humans (Figure 1-5). The first step in the RNAi process is the generation of short interfering RNAs (siRNAs) of about 21-30 nucleotides. The second step is the targeting of specific mRNA molecules complementary to these short RNAs for gene silencing, which can occur through a variety of different mechanisms. Silencing can occur at the posttranscriptional level, termed posttranscriptional gene silencing (PTGS), where the mature mRNA is targeted in the cytoplasm (Fire et al., 1998; Montgomery et al., 1998), or alternatively, it can occur at the transcriptional level, where the pre-mRNA is targeted in the nucleus (Grishok et al., 2005; Guang et al., 2010; Burton et al., 2011; Gu et al., 2012) and is termed RNAi-induced transcriptional gene silencing (RNAi-TGS).

Exogenous RNAi pathway

The complex that acts to initiate gene silencing in response to exogenous RNAi (exo-RNAi), a silencing response mediated by foreign dsRNA, is composed of RDE-4, a dsRNA binding protein; Dicer, an RNase III family ribonuclease; DRH-1, a dicer-related helicase and the Argonaute protein RDE-1 (Tabara et al., 2002). It has been suggested that the main role of RDE-4-bound dsRNA is in the recruitment of the Dicer/RDE-1/DRH-1 complex for processing

dsRNA into siRNAs (Parker et al., 2006). RDE-4 acts cell non-autonomously to promote RNAi, as *rde-4* null progeny of animals carrying a functional *rde-4* gene respond to an exo-RNAi trigger introduced in the parent (Blanchard et al., 2011) and exo-RNAi induced in *rde-4 (+)* tissue can induce silencing in *rde-4 (-/-)* cells (Jose et al., 2011). Dicer is required for the processing of dsRNA into siRNAs (reviewed in Meister and Tuschl, 2004) and DRH-1 may function to alter the conformation or placement of dsRNA for efficient complex activity (Tabara et al., 2002). RDE-1, one of 26 Argonaute proteins in *C. elegans*, is required for exo-RNAi and binds the primary siRNA duplex generated by Dicer (reviewed in Hutvagner and Simard, 2008). RDE-1, which exhibits RNase H activity, cleaves the "passenger" strand in the siRNA duplex so that the "guide" strand can bind to its target mRNA and likely recruit an RNA-dependent RNA polymerase (RdRP) complex for subsequent secondary siRNA production and mRNA cleavage (Steiner et al., 2009).

Secondary siRNAs arise from *de novo* synthesis by RdRPs, independent of Dicer activity (Aoki et al., 2007), and contain 5' triphosphates (Pak and Fire, 2007; Sijen et al., 2007) (Figure 1-5). The RdRPs RRF-1 and EGO-1 are required for exo-RNAi in the soma and germline (Sijen et al., 2001; Gu et al., 2009) and just in the germline, respectively (Smardon et al., 2000). RRF-1 and EGO-1 exist in a complex with the Dicer-related helicase DRH-3 (Aoki et al., 2007; Gu et al., 2009) and tudor domain protein EKL-1 (Gu et al., 2009; Thivierge et al., 2012). These secondary siRNAs are directly loaded onto Worm specific Argonautes (WAGOs) (Yigit et al., 2006; Gu et al., 2009). Since WAGOs lack key catalytic residues in their RNase H-related PIWI domain, they are unlikely to retain endocatalytic activity and presumably require additional co-factors to mediate target mRNA degradation (Yigit et al., 2006).

Endogenous RNAi pathway

Endogenous RNAi (endo-RNAi) is an RNAi response initiated by endogenous double-stranded RNA triggers that can be derived from a variety of sources, including RdRP generated dsRNA, inverted and repeated sequences and convergent transcription (snapshot in Flamand and Duchaine, 2012) (Figure 1-5). Endogenous small interfering RNAs (endo-siRNAs) have been identified in many organisms, including plants, fungi, nematodes, flies and mammals (reviewed in Li and Liu, 2011). In *C. elegans*, a large number of endo-siRNAs have been cloned. They map to regions throughout the genome, including protein coding genes and transposons (Ambros et al., 2003; Lee et al., 2006; Ruby et al., 2006; Pak and Fire, 2007; Claycomb et al., 2009; Gu et al., 2009). The endo-RNAi pathways in *C. elegans* involve some shared components with exogenous RNAi, these include DCR-1, RDE-4 and DRH-3 (Lee et al., 2006; Gu et al., 2009) as well as some factors that are specific to endogenous RNAi, including the RdRP RRF-3 and the exonuclease ERI-1 (Lee et al., 2006).

One large class of endo-siRNAs has been termed 22G-RNAs due to the fact that they preferentially begin with guanosine and are 22 nucleotides in length (Gu et al., 2009). There are two main classes of 22G-RNAs, which are designated according to their interacting Argonaute protein. The first are the 22G-RNAs antisense to protein-coding genes, which are in complex with the Argonaute CSR-1 (Chromosome Segregation and RNAi-deficient) (Claycomb et al., 2009; Gu et al., 2009). The second are the 22G-RNAs antisense to transposons, pseudogenes, cryptic loci and some coding genes, which are in complex with the WAGO family of Argonautes (Gu et al., 2009).

Another class of endo-siRNAs, called 26G-RNAs, are produced by the ERI (Enhanced RNAi) pathway (Gent et al., 2009; Han et al., 2009; Vasale et al., 2010). The ERI pathway is a

two-step process in which 26G-RNAs produced during embryogenesis drive the biogenesis of 22G-RNAs, which subsequently maintain silencing of target genes in later developmental stages (Vasale et al., 2010). Specifically, the ERI complex containing Dicer, RDE-4 and the RdRP RRF-3 is required for the production of 26G-RNAs which are loaded onto the ERGO-1 Argonaute. The subsequent rounds of 22G-RNA biogenesis require the RdRP RRF-1 and the WAGO family of Argonautes (Vasale et al., 2010).

Biological roles of endoRNAi

A major role of endo-RNAi in *C. elegans* is in genome surveillance. Germline enriched 22G-RNAs bound by the WAGO family of Argonautes silence transposable elements and aberrant transcripts (Gu et al., 2009), and the 22G-RNAs generated by the ERI pathway silence gene duplications (Vasale et al., 2010; Fischer et al., 2011). The ERI pathway has also been implicated in regulating genes required for spermatogenesis and fertility (Han et al., 2009; Conine et al., 2010).

Mutations in the dsRNA binding protein RDE-4 result in decreased lifespan (Welker et al., 2007; Mansisidor et al., 2011), increased sensitivity to oxidative stress (Mansisidor et al., 2011) and a decreased tolerance for high temperatures (Blanchard et al., 2011). In *rde-4* mutant worms the expression of the insulin signaling component *pdk-1* is upregulated, which is responsible for the decrease in lifespan and increased sensitivity to oxidative stress in the *rde-4* mutant, as shown by genetic epistasis experiments (Mansisidor et al., 2011). Furthermore, WAGO-bound 22G-RNAs map to the *pdk-1* promoter and dsRNA is produced from this region, suggesting that these siRNAs may be used to modulate the expression of *pdk-1* (Mansisidor et al., 2011).

Mutations in *csr-1, ego-1, ekl-1* and *drh-3* all show similar phenotypes: germline abnormalities (Smardon et al., 2000; She et al., 2009) and chromosome segregation defects in the embryo (Duchaine et al., 2006; Yigit et al., 2006; Nakamura et al., 2007; Claycomb et al., 2009). The finding that the 22G-RNAs associated with CSR-1 are mostly antisense to protein-coding genes led to the model that these siRNAs act to influence the global architecture of the holocentric chromosomes in *C. elegans*, thereby affecting chromosome segregation (Claycomb et al., 2009). Recently, however, it was shown that knockdown by RNAi of *csr-1, ego-1* or *drh-3* causes depletion of core histone proteins and defective histone mRNA processing (Avgousti et al., 2012). The overexpression of a transgene containing one copy of each core histone rescued the embryonic lethality of the RNAi mutants, suggesting that histone depletion is responsible for the sterility and chromosome segregation defects seen in the CSR-1 pathway mutants (Avgousti et al., 2012). Importantly, this study demonstrates that in addition to negatively regulating genes, some endo-siRNAs in *C. elegans* have a positive role in gene regulation.

CSR-1, EGO-1, EKL-1 and DRH-3 have also been implicated in the specification of the excretory duct, a component of the worms renal system, during embryogenesis (Rocheleau et al., 2008). A genome wide RNAi screen demonstrated that these RNAi pathway genes act redundantly with the KSR-1 (kinase suppressor of Ras) scaffolding protein and are required maternally for Ras-mediated Excretory duct cell specification. However, it is not clear if the CSR-1 endoRNAi pathway is acting positively to regulate Ras signaling and/or negatively to regulate negative regulators of Ras signaling (Rocheleau et al., 2008).

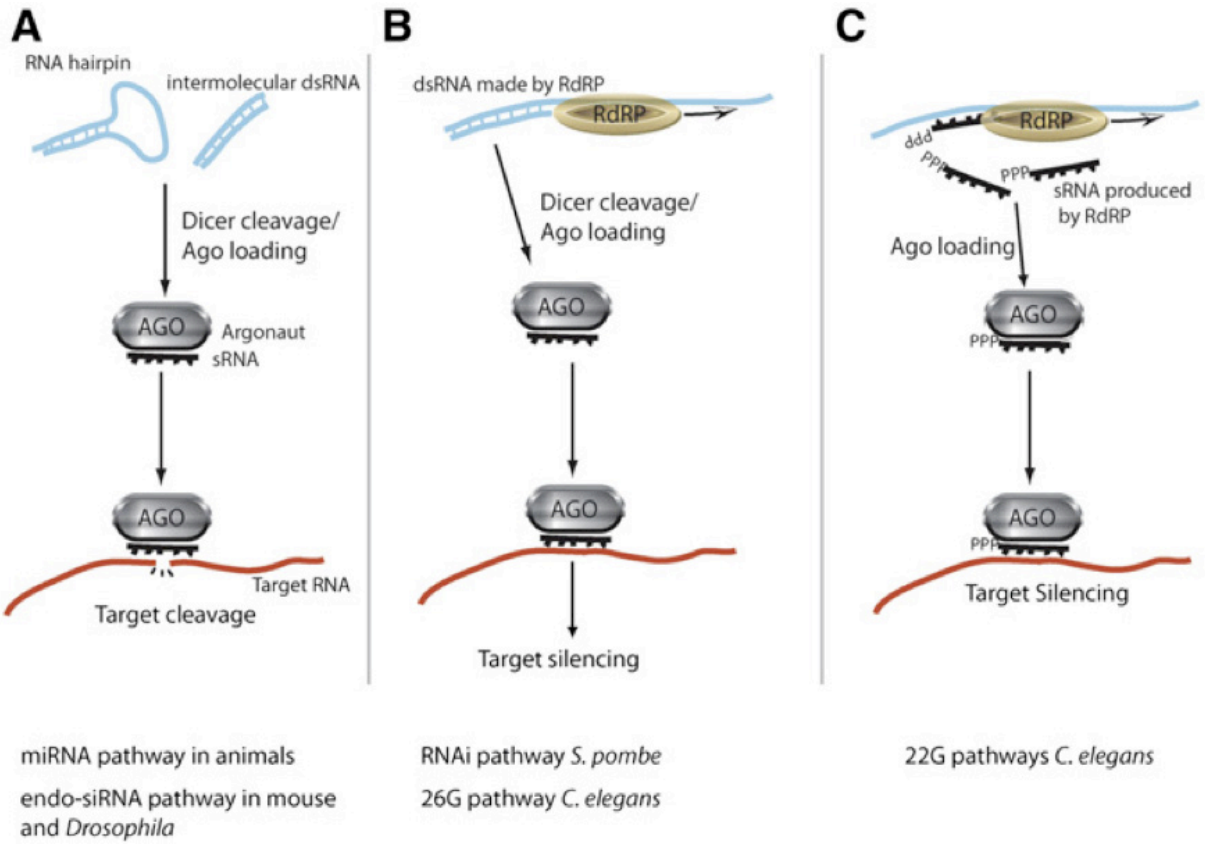

Figure 1-5. RNAi pathways. A. Classical RNAi pathway initiated by foreign or endogenous dsRNA. **B.** dsRNA can be synthesized by RNA-dependent RNA Polymerase (RdRP) and further processed by Dicer in *C. elegans*. **C.** RdRPs can synthesize siRNAs *de novo* from target mRNA. See text for details. Figure from (Ketting, 2011)

Zinc Finger Protein 1 (ZFP-1)

Genome-wide RNAi screens in *C. elegans* have identified novel factors required for RNAi, including the protein ZFP-1 (Dudley et al., 2002; Kim et al., 2005), a chromatin-binding protein, that has since been shown to be enriched at promoters of highly expressed genes (Mansisidor et al., 2011; Avgousti et al., 2013). ZFP-1 has also been shown to be required for

RNAi-TGS of a repetitive transgene (Grishok et al., 2005). Interestingly, a genome-wide expression study revealed that both ZFP-1 and RDE-4 regulate close to 250 overlapping genes and that endo-siRNA target genes show a significant enrichment among genes upregulated in *zfp-1* (P-value $1.4x10^{-22}$) and *rde-4* (P-value $9.6x10^{-18}$) mutants, suggesting that RNAi may negatively regulate numerous target genes in *C. elegans* (Grishok et al., 2008). Interestingly, genes with decreased expression, and therefore not predicted to be direct targets of both RDE-4 and ZFP-1, were enriched in metabolic and stress-related factors; a profile strikingly similar to that of DAF-16 "class I" target genes (genes that are upregulated in *daf-2* mutants) (Murphy et al., 2003). Consistent with this observation, both RDE-4 and ZFP-1 were subsequently shown to negatively regulate the conserved insulin signaling kinase *pdk-1* and to promote *C. elegans* fitness in a DAF-16-dependent manner (Mansisidor et al., 2011).

ZFP-1 is a homolog of mammalian AF10 (Acute Lymphoblastic Leukemia 1-Fused gene from chromosome 10), which is best known for its role in leukemia caused by its fusion to the mixed lineage leukemia (MLL) gene to create the MLL-AF10 oncogene (Chaplin et al., 1995). The inappropriate recruitment of the histone methyltransferase Dot1 by the C-terminus of AF10 to MLL target genes contributes to oncogenesis (Okada et al., 2005). The normal developmental role of AF10 is largely unknown; therefore, studying the role of its homolog ZFP-1 in *C. elegans* development may help to shed light on this matter. In fact, recently, the highly conserved N-terminal plant homeodomain (PHD) fingers of ZFP-1 were shown to be essential for viability (Avgousti et al., 2013). Furthermore, the *drosophila* homolog of AF10, named *Alhambra* (also called *Dalf* or dAF10), is also required for viability as well as for maintaining neuronal EVE expression during embryogenesis (Bahri et al., 2001).

Chapter Two: Nonautonomous Regulation of Neuronal Migration by Insulin Signaling, DAF-16/FOXO, and PAK-1

(An adapted chapter has been accepted at *Cell Reports*)

Lisa M. Kennedy,[1] Steven C.D.L. Pham[2] and Alla Grishok[2]

[1]Department of Genetics and Development, [2]Department of Biochemistry and Molecular Biophysics, Columbia University, New York, NY 10032, USA

Author Contributions

The experiments presented in this chapter were conceived and designed by L.M.K. and A.G. The Analysis of the *daf-2/*IR receptor phenotype was performed by S.C.D.L.P and L.M.K.; all other experiments were performed and analyzed by L.M.K.

Summary

Neuronal migration is essential for nervous system development in all organisms and is regulated in the nematode, *C. elegans,* by signaling pathways that are conserved in humans. Here, we demonstrate that the insulin/IGF-1-PI3K signaling pathway modulates the activity of the DAF-16/FOXO transcription factor to regulate the anterior migrations of the hermaphrodite-specific neurons (HSNs) during embryogenesis of *C. elegans*. When signaling is reduced, DAF-16 is activated and promotes migration, conversely, when signaling is enhanced, DAF-16 is inactivated and migration is inhibited. We show that DAF-16 acts non-autonomously in the hypodermis to promote HSN migration. Furthermore, we identify PAK-1, a p21-activated kinase, as a downstream mediator of insulin/IGF-1-DAF-16 signaling in the non-autonomous control of HSN migration. As a FOXO-Pak1 pathway was recently shown to regulate mammalian neuronal polarity, our findings indicate that the roles of FOXO and Pak1 in neuronal migration are likely conserved from *C. elegans* to higher organisms.

Introduction

The process of neuronal migration, when the cell bodies of newly born neurons migrate from their birthplace to their final positions within the nervous system, is a conserved and critical part of proper nervous system development (reviewed in Marín et al., 2010). When defective, it can lead to several human disorders of cortex development, including lissencephaly or the related disorder double cortex, epilepsy and severe mental retardation (reviewed in Ross and Walsh, 2001). Furthermore, Schizophrenia has also been associated with defective neuronal migration (Nopoulos et al., 1995; Falkai et al., 2000).

Specific neurons that migrate during *C. elegans* development are well characterized (reviewed in Hedgecock et al., 1987) and have been used to identify a variety of conserved genes and pathways implicated in neuronal migration not only in *C. elegans* but *Drosophila* and vertebrates as well (reviewed in Montell, 1999; Hatten, 2002; Silhankova and Korswagen, 2007). One of the best examples comes from pioneering genetic analyses, which identified a group of genes encoding a secreted protein UNC-6/Netrin and its receptors as required for the guidance of cells and axons along the dorsoventral axis of *C. elegans* (Hedgecock et al., 1990; Ishii et al., 1992; Leung-Hagesteijn et al., 1992; Chan et al., 1996; Wadsworth et al., 1996). Subsequently, UNC-6/Netrin signaling was shown to be critical for cell migrations in vertebrates as well (Ackerman et al., 1997; Leonardo et al., 1997).

The hermaphrodite-specific neurons (HSNs) of *C. elegans* are among the farthest migrating cells in the developing embryo and the only cells that undergo posterior to anterior long-range migrations at this stage (Sulston et al., 1983). They are a pair of bilaterally symmetric motor neurons that are born in the tail and migrate to the mid-body of the animal during embryogenesis (Figure 2-1A). In the adult hermaphrodite, the HSNs stimulate egg-laying by

releasing the neurotransmitter serotonin (Desai et al., 1988). Forward genetic screens have identified many genetic components required for HSN migration (Desai et al., 1988; Manser and Wood, 1990; Forrester and Garriga, 1997); moreover, many of these same components have been identified as being expressed in migrating vertebrate neural crest cells (Kee et al., 2007), suggesting conservation between species. A subset of the genes identified, which includes the homeodomain transcription factor *egl-5* (Trent et al., 1983; Desai et al., 1988), exhibit HSN migration defects when mutated due to the fact that they normally act cell-autonomously to promote HSN cell-fate. Of those genes identified to have a role specifically in the migration process, the Wnt signaling components represent the most well studied pathway implicated in controlling the anteriorly directed HSN migrations, to date (reviewed in Silhankova and Korswagen, 2007).

The conserved transcription factor DAF-16/FOXO is the best-known target negatively regulated by insulin/insulin-like growth factor-1 (IGF-1) signaling through a conserved phosphatidylinositol 3-kinase (PI3K)/Akt pathway in *C. elegans* (Lin et al., 1997; Ogg et al., 1997; Henderson and Johnson, 2001; Lee et al., 2001; Lin et al., 2001). This negative regulation of FOXO through IGF-1-mediated signal transduction and PI3K/Akt signaling is conserved in mammalian cells, including neurons, and promotes cell survival by inhibiting the pro-apoptotic function of FOXO (Brunet et al., 1999; Leinninger et al., 2004; reviewed in Wen et al., 2012). In *C. elegans,* the biological function of DAF-16 has been well studied in the context of aging: enhanced DAF-16 activity through the inactivation of the insulin/IGF-1 signaling pathway promotes extended lifespan and increased stress resistance (Lin et al., 1997; Ogg et al., 1997; Henderson and Johnson, 2001; Lee et al., 2001). More recently, PI3K-regulated signaling through DAF-16 has been demonstrated to promote neurite outgrowth in the *C. elegans* AIY

interneurons during development (Christensen et al., 2011), and a role for insulin/IGF-1 signaling in the progression of neuronal aging, in part, by inhibition of DAF-16 (Pan et al., 2011; Tank et al., 2011) has been reported.

Here, we describe a role for insulin/IGF-1 signaling through DAF-16/FOXO in modulating the migration of HSNs during development. We demonstrate that null mutations in the *daf-16* gene as well as inhibition of DAF-16 activity due to a *daf-18*/PTEN mutation and activation of PI3K signaling cause an HSN undermigration phenotype, while an increase in DAF-16 activity resulting from decreased insulin/IGF-1 signaling leads to HSN overmigration. Surprisingly, our data indicate that DAF-16 promotes HSN migration cell non-autonomously from the hypodermal tissue. We also implicate *pak-1*, which encodes a p21-activated kinase, as a downstream effector of DAF-16 activity in the hypodermis during HSN migration. To our knowledge, FOXO and Pak1 acting non-autonomously in nervous system development has not been described previously.

Results

C. elegans DAF-16/FOXO regulates the migration of the HSNs

While studying the biological roles of the endogenous RNA interference (RNAi) factors we discovered a synergy between the RNAi pathway and *daf-16* in the regulation of egg-laying (L.M. Kennedy and A. Grishok, unpublished data). This prompted us to look for possible HSN defects in *daf-16* mutant animals. We found that *daf-16(mu86)* and *daf-16(mgDf50)* null mutants displayed HSN undermigration defects (Figure 2-1B-D). We used a tryptophan hydroxylase GFP reporter (*tph-1::gfp*) for identifying HSN neurons and their migration defects. TPH-1 is required for serotonin biosynthesis and is expressed in all serotonergic neurons (Rand and Nonet, 1997).

Most of them are located in the head of the hermaphrodite animal making it easy to recognize a pair of HSNs flanking the vulva. However, because *tph-1* is expressed late in development and allows HSN identification only in late L4 and adult animals, we used an additional reporter, *kal-1::gfp*, which is expressed in the HSN during both larval and adult stages (Bulow et al., 2002) to confirm that the *daf-16 (null)* HSN undermigration phenotype was also present in newly hatched L1 larvae (Figure 2-2A-C). These results indicate that DAF-16 is required for proper HSN migration during development rather than having a role in adult neuronal maintenance.

Furthermore, we stained wild type worms and *daf-16* mutant worms with an anti-serotonin antibody (Garriga et al., 1993) to exclude the possibility that the transgenes used to visualize the HSNs were possibly enhancing or causing the *daf-16* mutant undermigration phenotype, as transgene artifacts have been reported for other migration and axon guidance phenotypes (Forrester et al., 1998; Toms et al., 2001). The extent of HSN undermigration was similar in stained and transgenic worms indicating that all defects seen with the reporters were due to the relevant mutant backgrounds and not to the reporters themselves (Figure 2-2D-F). In addition, these results suggest that DAF-16 specifically affects the process of HSN migration rather than HSN identity, since undermigrated HSNs still express the neurotransmitter serotonin, a late step in HSN maturation (Desai et al., 1988).

There are three functionally characterized *daf-16* isoforms: *daf-16a*, *daf-16b* and *daf-16d/f* (Ogg et al., 1997; Lee et al., 2001; Lin et al., 2001; Kwon et al., 2010). DAF-16a and DAF-16b proteins are expressed during embryogenesis (Ogg et al., 1997; Henderson and Johnson, 2001; Lee et al., 2001) and all three isoforms show neuronal expression in developing larvae (Ogg et al., 1997; Henderson and Johnson, 2001; Lee et al., 2001; Kwon et al., 2010). Therefore, DAF-16 may function in multiple aspects of neuronal development. We determined which DAF-

16 isoforms are involved in the regulation of HSN migration by performing anti-serotonin staining using *daf-2(e1370ts); daf-16(mgDf50)* mutant worms or isogenic strains expressing isoform-specific DAF-16 proteins under the control of the corresponding *daf-16* promoters (Kwon et al., 2010) grown at 20°C. We found that isoforms DAF-16a and DAF-16b, but not the DAF-16d/f isoform, rescued the undermigration defect of the *daf-16* mutant (Figure 2-1E); in contrast, DAF-16d/f has been shown to contribute most significantly to the regulation of lifespan (Kwon et al., 2010). Mutation of *daf-2* leads to enhanced DAF-16 activity and therefore may facilitate the rescue of *daf-16(mgDf50)* by the transgenic arrays. Therefore, we have confirmed that *daf-2(e1370ts)* mutants lack HSN migration defects when grown at the permissive temperatures of 15°C or 20°C (data not shown). Moreover, to confirm that the *daf-2(e1370ts)* allele was not contributing to the rescue observed in Figure 2-1E, we also show that the DAF-16a and DAF-16b isoforms can rescue the HSN undermigration defects of the *daf-16* mutant to a similar extent in the wild type and *daf-2(e1370ts)* backgrounds (compare Figure 2-1E and 2-2G). This is consistent with *daf-2(e1370)* being a temperature-sensitive allele (Vowels and Thomas, 1992; Kimura et al., 1997). Combined, these results suggest that two isoforms of DAF-16 (a and b) may regulate the transcription of genes required to promote HSN migration during development. Consistently, the DAF-16b isoform was recently shown to control neurite outgrowth in *C. elegans* (Christensen et al., 2011) and a role for DAF-16a in regulating neuronal aging has been reported (Pan et al., 2011; Tank et al., 2011)

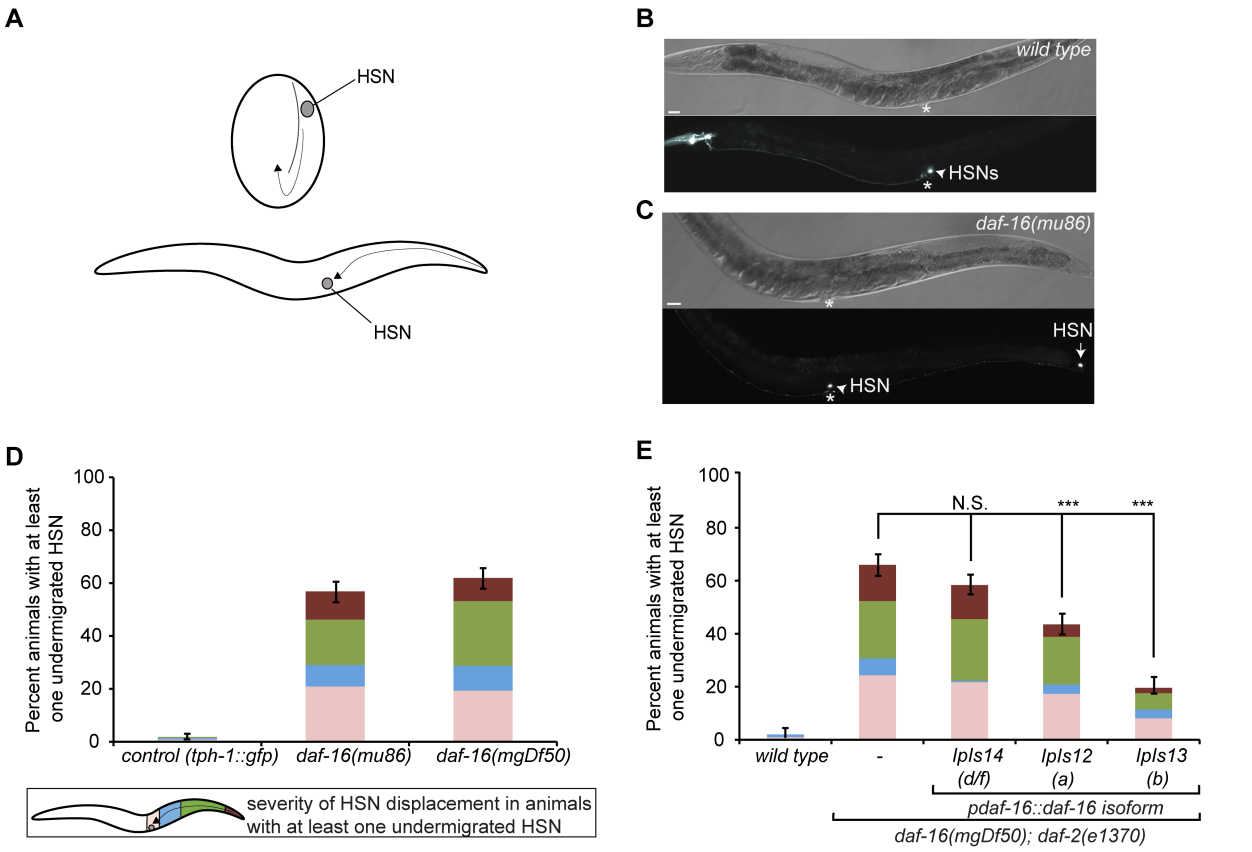

Figure 2-1. HSN undermigration defects in *daf-16* mutants. (A) Schematic representation of the HSN migratory route from the tail to the gonad primordium during embryogenesis (top) and the corresponding location of the HSN in newly hatched L1 larvae (bottom). Note that only one of two bilaterally symmetric HSNs is illustrated. **(B-C)** Differential Interference Contrast (DIC) image of adult hermaphrodite (top) and corresponding epifluorescent image of the HSN (bottom) in wild type (B) and *daf-16(mu86)* mutant animals (C), HSN is visualized with a tryptophan hydroxylase GFP reporter (*tph-1::gfp)*. Images are oriented with the posterior of the animal to the right. Asterisks indicate the vulva and arrowheads denote the position of properly migrated HSN(s). The arrow in (C) illustrates a HSN that has failed to migrate from its birthplace in the tail of the *daf-16(mu86)* mutant animal **(D)** Quantification of the percentage of animals with an

undermigrated HSN from a minimum of two pooled independent experiments per strain in control *tph-1::gfp* (n=165), *daf-16(mu86)* (n=160) and *daf-16(mgDf50)* (n=155) mutants. **(E)** Quantification of the percentage of animals with an undermigrated HSN in wild type (n=50), *daf-16(mgDf50); daf-2(e1370)* mutant animals (n=150) and mutant animals containing the *pdaf-16d/f::daf-16d/f* (n=168), *pdaf-16a::daf-16a* (n=170), or *pdaf-16b::daf-16b* (n=179) array. Note that rescue was observed in animals carrying the *pdaf-16::daf-16a* or *pdaf-16::daf-16b* arrays. HSNs were visualized by anti-serotonin staining. The stacked bars show information about the position of all HSNs in the affected worms, see the description below. Worm schematic legend: Stacked bars represent the proportion of HSNs at different positions along the A-P body axis within only those animals containing at least one undermigrated HSN. Thus, since there are two HSNs within each animal and not every HSN is affected, one colored region (light pink) represents the wild type HSN that remains unaffected in animals containing a second undermigrated HSN, which is represented by either the red, green or blue region. ***$p<0.001$ (*z*-test). For all figures, error bars represent standard error of the proportion (SEP) for the entire stacked column. Scale bars: 20 μm.

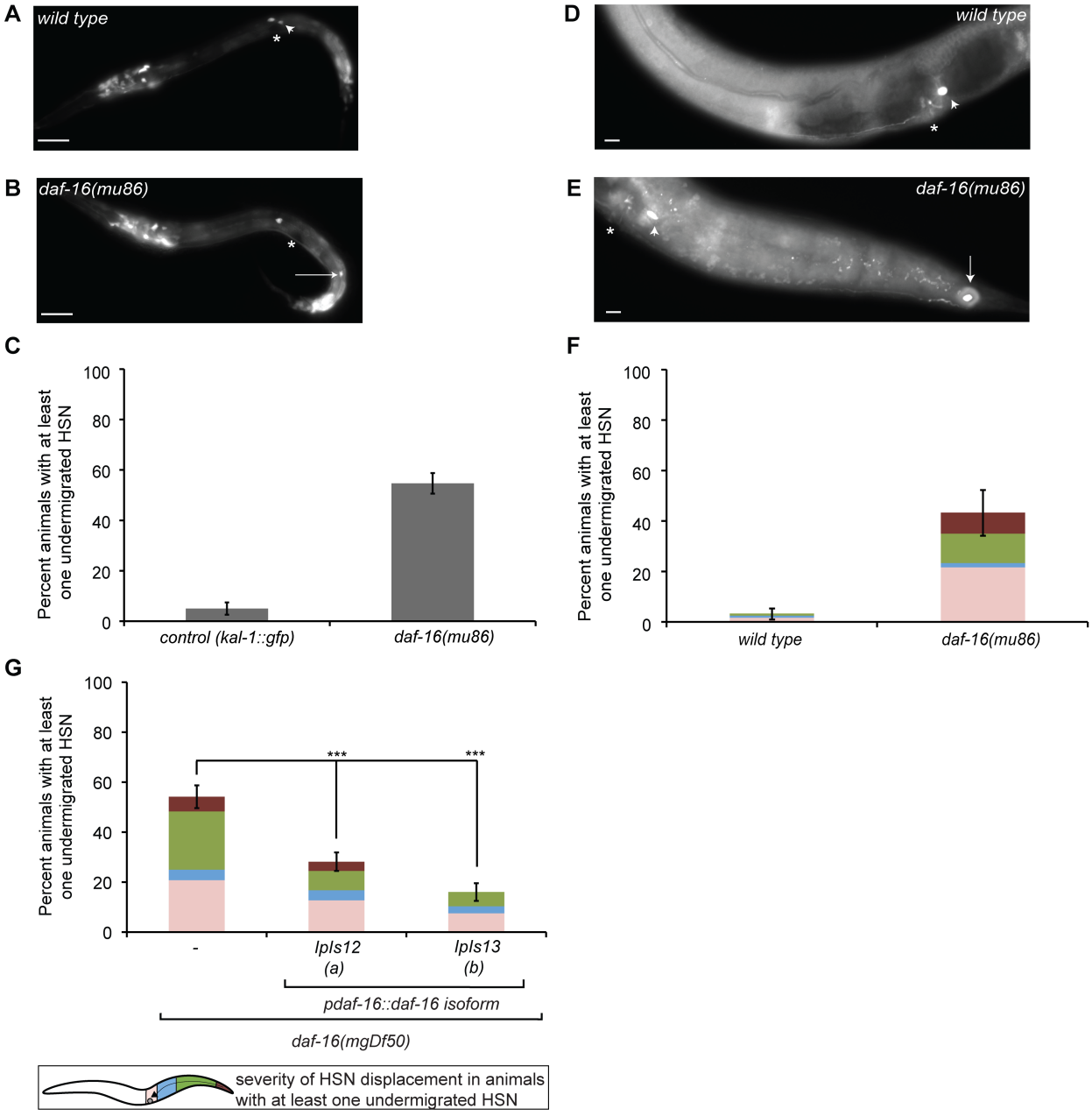

Figure 2-2. DAF-16 is required during development to specifically regulate the process of HSN migration. (A-B) Epifluorescent images of the HSN in newly hatched L1 larvae of wild type (A) and *daf-16(mu86)* mutant animals (B), visualized with the *kal-1::gfp* reporter. Asterisks indicate the developing gonad and the arrowhead in (D) denotes the position of a properly

migrated HSN. The arrow in (B) indicates a HSN that has prematurely terminated in its migratory route to the gonad primordium in the *daf-16(mu86)* mutant animal. **(C)** Quantification of the percentage of animals with an undermigrated HSN from at least two pooled independent experiments per strain in control *kal-1::gfp* (n=80) and *daf-16(mu86)* (n=150) animals. **(D-E)** Epifluorescent images of the HSN stained with anti-serotonin in wild type (D) and *daf-16(mu86)* animals (E). Asterisks indicate the vulva and the arrowheads denote the position of properly migrated HSNs. The arrow in (E) indicates a HSN that has failed to migrate from its birthplace in the tail of the *daf-16(mu86)* mutant animal. Note that undermigrated HSNs still differentiate, as they express the neurotransmitter serotonin, a late step in HSN development. Images are oriented with the posterior of the animal to the right. **(F)** Quantification of the percentage of animals with an undermigrated HSN in wild type (n=60) and *daf-16(mu86)* (n=30) animals. **(G)** Quantification of the percentage of animals with an undermigrated HSN from two pooled independent experiments per strain in *daf-16(mgDf50)* mutant animals (n=120) and mutant animals containing the *pdaf-16a::daf-16a* (n=149), or *pdaf-16b::daf-16b* (n=106) integrated array. HSNs were visualized with the *tph-1::gfp* reporter. Note that because *tph-1::gfp* and *pdaf-16a::daf-16a* are integrated on the same chromosome *pdaf-16a::daf-16a* / *tph-1::gfp* animals were scored. Figure 2-1 for detailed worm schematic legend. Error bars represent standard error of the proportion. Scale bars: 20 μm.

DAF-16 interacts with other known pathways regulating HSN migration

Many genes have been implicated in the process of HSN migration (Desai et al., 1988). Of those genes shown to affect the process of HSN migration, rather than HSN identity, the Wnt and Frizzled families of genes are best studied (reviewed in Silhankova and Korswagen, 2007).

Specifically, the EGL-20 Wnt ligand and other posteriorly expressed Wnts function as repellents to direct the HSNs anteriorly and are believed to act directly on the HSN since the Wnt receptor MIG-1/Fz was shown to act cell-autonomously in the HSNs (Pan et al., 2006). We show that the HSN undermigration defect in a *daf-16* null mutant is enhanced by an *egl-20* null mutation (Coudreuse et al., 2006) (Figure 2-3A), which suggests that *daf-16* and *egl-20* act in parallel pathways. However, because of the redundancy between Wnt ligands, this result allows us only to rule out the possibility that DAF-16 is exclusively acting through EGL-20 to influence HSN migration. It is still possible that DAF-16 functions in the same genetic pathway with the Wnts to control HSN migration, for example, by regulating Wnt expression and/or function.

C. elegans contains one syndecan gene, *sdn-1*, which encodes a transmembrane heparan sulfate proteoglycan (HSPG) and has been shown to act in the nervous system to promote HSN migration (Rhiner et al., 2005). Interestingly, the absence of mammalian syndecan-4 leads to decreased Akt activation and reduced FOXO phosphorylation (Partovian et al., 2008). Also, mammalian syndecan-1 can suppress the insulin-signaling components phosphoinositide-dependent protein kinase 1 (PDK-1) and Akt to induce apoptosis in human prostate cancer cells (Hu et al., 2010). In light of the mammalian syndecan family interaction with insulin/IGF-1 signaling components, we investigated the *C. elegans sdn-1* interaction with *daf-16*. We observed an enhancement in HSN undermigration in a strain with null mutations of these two genes compared to either single mutant alone (Figure 2-3B), placing *daf-16* and *sdn-1* in parallel genetic pathways.

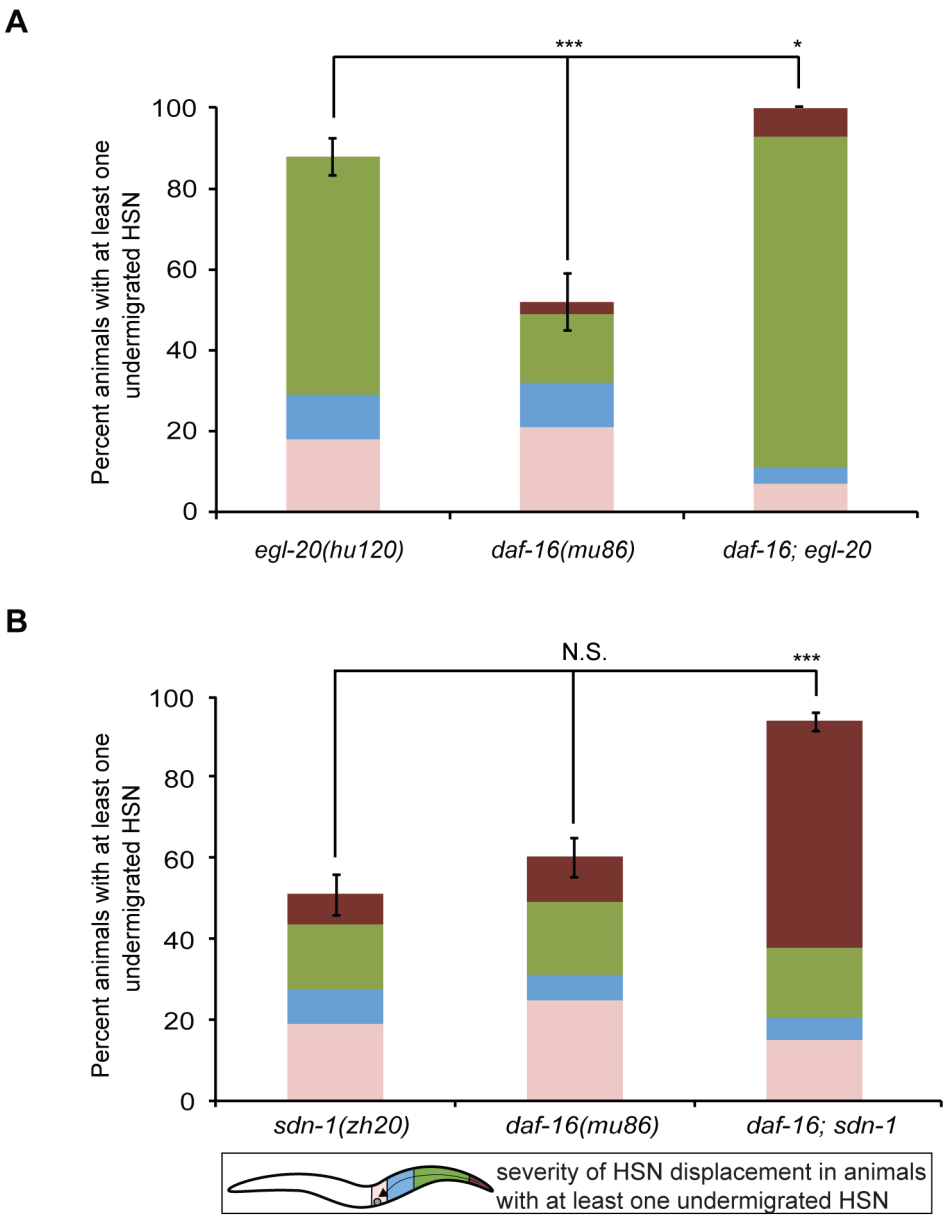

Figure 2-3. DAF-16 acts in parallel to other known genes controlling HSN migration (A) *daf-16(mu86)* and *egl-20(hu120)* null mutations enhance each other. *egl-20* encodes a posteriorly expressed Wnt. Quantification of the percentage of animals with an undermigrated HSN in *egl-20(hu120)* (n=50), *daf-16(mu86)* (n=50) and *daf-16(mu86); egl-20(hu120)* (n=50). **(B)** *daf-16(mu86)* and *sdn-1(zh20)* null mutations enhance each other. *sdn-1* encodes a transmembrane

heparan sulfate proteoglycan (HSPG). Quantification of the percentage of animals with an undermigrated HSN from two pooled independent experiments per strain in *sdn-1(zh20)* (n=100), *daf-16(mu86)* (n=103), *daf-16(mu86); sdn-1(zh20)* (n=110). See Figure 2-1 for detailed worm schematic legend. Error bars represent SEP.

The PI3K signaling pathway regulates DAF-16 activity to control HSN migration

DAF-18, the phosphatase and tensin homolog (PTEN) in *C. elegans* acts in the insulin/IGF-1 signaling pathway to promote DAF-16 activity by dephosphorylating AGE-1 PI3 kinase-generated PIP3 and inhibiting PI3K signaling (Ogg and Ruvkun, 1998; Solari et al., 2005) (Figure 2-4A). Therefore, a loss-of-function of PTEN leads to inhibition of DAF-16 by activated PI3K signaling. We observed undermigration of the HSN in the *daf-18* (PTEN) null mutant background, consistent with reduced DAF-16 activity (Figure 2-4B-D). The penetrance of HSN undermigration in *daf-18(ok480)* was similar to that in *daf-16(mu86)*; moreover, a combination of *daf-16(mu86); daf-18(ok480)* null alleles did not enhance the HSN undermigration phenotype of either single mutant (Figure 2-4D), indicating that *daf-16* and *daf-18* act in the same pathway to control neuronal migration. Furthermore, we found that a transgenic array expressing DAF-18 under the control of its endogenous promoter (Masse et al., 2005) rescued the HSN undermigration phenotype of the *daf-18(mg198)* null mutant (Figure 2-4E). Together, these observations suggest that the PI3K signaling pathway works upstream of DAF-16 to control its activity required for promoting HSN migration.

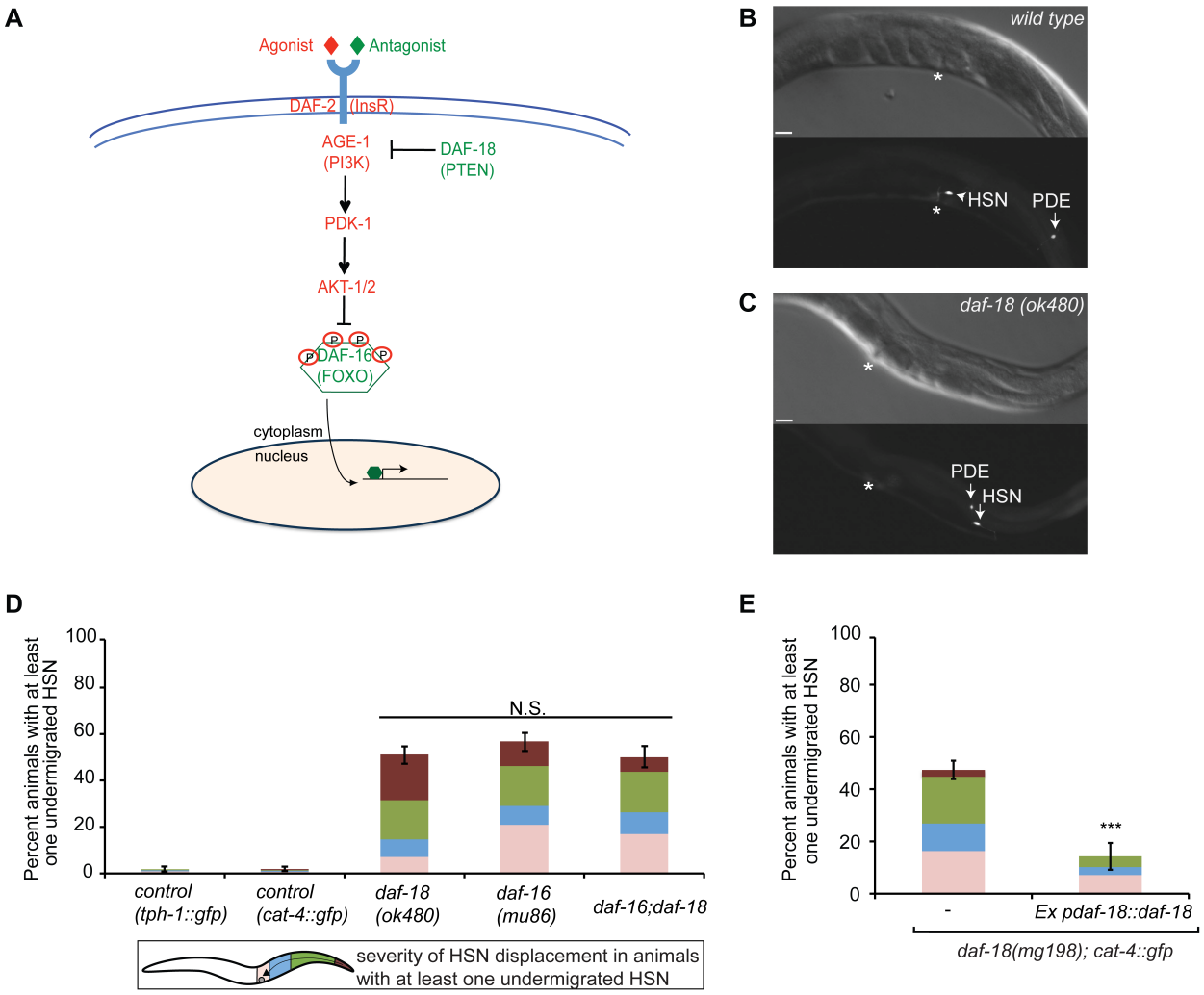

Figure 2-4. PI3K signaling regulates DAF-16 activity to control HSN migration. A) DAF-18 acts in the insulin/IGF-1 signaling pathway to promote DAF-16 activity by inhibiting PI3K signaling. When pathway components in red are active, DAF-16 is phosphorylated and inactive due to its retention in the cytoplasm. When pathway components in green are active, DAF-16 is no longer phosphorylated and can translocate into the nucleus to regulate its target genes. **(B-C)** DIC images of adult hermaphrodites (top) and corresponding epifluorescent images of the HSNs (bottom) in wild type (B) and *daf-18(ok480)* mutant animals (C), HSN is visualized with a GTP cyclohydrolase GFP reporter (*cat-4::gfp*), which is expressed in all dopaminergic and

serotonergic neurons (Flames and Hobert, 2009). Images are oriented with the posterior of the animals to the right. Asterisks indicate the vulva and arrowheads denote the position of properly migrated HSN(s). The arrow in (C) illustrates a HSN that has failed to migrate the full distance and terminates near the PDE neuron, which is also marked by an arrow in (B) and (C). **(D)** Quantification of the percentage of animals with an undermigrated HSN from three pooled independent experiments per strain in *tph-1::gfp* (n=165) and *cat-4::gfp* (n=213) controls, *daf-16(mu86)* (n=160), *daf-18(ok480)* (n=211) and *daf-16(mu86); daf-18(ok480)* (n=112) mutant animals. Note that the *cat-4::gfp* reporter was used to visualize the HSNs in the *daf-18* single and double mutant backgrounds. There is no significant difference among the *daf-16, daf-18* single and double mutants (*z*-test). **(E)** Quantification of the percentage of animals with an undermigrated HSN from two pooled independent experiments in *daf-18(mg198)* mutant animals (n=95) and mutant animals containing the *Ex pdaf-18::daf-18* (n=98) rescuing transgenic array. The *daf-18(mg198)* mutants that had the rescuing transgenic array (+) or their siblings that had lost the array (-) were scored. See Figure 2-1 for detailed description of worm schematic legend. ***$p<0.001$ (*z*-test). Error bars represent SEP. Scale bars: 20 μm.

PI3K signaling and DAF-16 act non-autonomously in HSN migration

To determine which tissue DAF-16/FOXO activity is required in for promoting the anterior HSN migrations, we first utilized published transgenic strains where a *daf-18* cDNA is expressed under various tissue-specific promoters in a *daf-2; daf-18* mutant background (Masse et al., 2005). We began with *daf-18* rescue for two reasons: first, there is only one DAF-18 isoform compared to the two DAF-16 isoforms that rescue HSN migration (Figure 2-1E, 2-4E) and second, since the *daf-18* undermigration phenotype arises due to a decrease in DAF-16 activity

(Figure 2-4D), rescuing the *daf-18* mutant is the equivalent of restoring DAF-16 function. We performed anti-serotonin staining using *daf-2(e1370); daf-18(mg198)* mutant worms or isogenic strains expressing *daf-18* cDNA under the control of various tissue-specific promoters (Figure 2-5A) and determined that *daf-18* cDNA driven by the pan-neuronal *unc-119* promoter rescued the *daf-18* mutant. However, given that this promoter is also active in the embryonic hypodermal tissue (Hardin et al., 2008), and since HSN migration occurs during embryogenesis, the rescue observed from this promoter could have resulted from DAF-18 expression in neuronal tissue, hypodermal tissue or both.

To narrow down these possibilities, we generated transgenic animals that used the *unc-119* promoter (Maduro et al., 2000) or the hypodermal *dpy-7* promoter (Gilleard et al., 1997) to drive expression of a *daf-18* cDNA. Expression of DAF-18 under the control of both these promoters rescued the HSN migration defects in *daf-18* mutants (Figure 2-6A), suggesting that hypodermal expression of DAF-18 is sufficient for rescue. Next, we crossed the two transgenic lines to each other to create animals that simultaneously expressed DAF-18 under both the *unc-119* promoter and the *dpy-7* promoter, as we reasoned that if DAF-18 is required in the neuronal tissue as well as the hypodermal tissue then a more complete rescue would be observed in animals expressing DAF-18 from both promoters as compared to either single promoter alone. We determined that rescue of the HSN migration defects in *daf-18* mutants was not enhanced in animals expressing DAF-18 from the two promoters (Figure 2-6B), suggesting that DAF-18 acts predominately in the hypodermal tissue to control HSN migration.

Consistently, we found that a second pan-neuronal promoter, *rab-3*, which is active during embryogenesis and is not expressed in the hypodermis (N. Stefanakis, I. Carrera and O. Hobert, personal communication), does not rescue the *daf-18* null phenotype when used to

express a full-length *daf-18* cDNA (Figure 2-5B). Moreover, we find that *daf-18* cDNA driven from the *unc-86* promoter, which is expressed in a subset of neurons including the HSN (Baumeister et al., 1996), does not rescue the *daf-18* null mutant (Figure 2-6A). Notably, this same promoter has been used previously to rescue the HSN undermigration defects present in *mig-1/Fz* mutants (Pan et al., 2006). Furthermore, in agreement with our observations that DAF-18 does not work cell autonomously to regulate HSN migration, we find that the cDNA of *daf-16b* fused to TagRFP driven by the *unc-86* promoter fails to rescue the HSN undermigration defects seen in the *daf-16* null mutant (Figure 2-6B-C).

Next, we tested whether or not hypodermal expression of DAF-16 could rescue the HSN migration defects in *daf-16* mutants. To do this, we generated transgenic animals that used the hypodermal *dpy-7* promoter to drive expression of the *daf-16b* cDNA fused to TagRFP, since this isoform rescued the *daf-16* mutant most significantly (Figure 2-1E). Expression of DAF-16b::TagRFP in the hypodermis rescued the HSN migration defects of *daf-16* mutants (Figure 2-7C). We observed that plasmid constructs with the *dpy-7* or *unc-119* promoters expressing either DAF-18 or DAF-16b did not rescue the *daf-18* or *daf-16* mutant phenotypes to the same extent as the constructs with their endogenous promoters. This likely reflects the fact that expression of DAF-16 in the hypodermis is toxic to the worm, as has been previously reported (Libina et al., 2003). Also, we found worms expressing the *pdpy-7::daf-18* transgenic array to be slow growing and sick, with many dead larvae produced. Thus, it is likely that we selected for transgenic lines expressing low levels of both DAF-18 and DAF-16 in the hypodermal tissue.

Importantly, and consistent with the rescue by DAF-18 and DAF-16 expressed in the hypodermis, we found that DAF-16b::TagRFP was localized in the nuclei of hypodermal cells during the 1.5-fold stage of embryogenesis (Figure 2-7D, top panels) when HSN migration takes

place (Sulston et al., 1983; Pan et al., 2006), but not during the L1 stage when HSN migration is complete (Figure 2-7D, bottom panels). This result demonstrates that DAF-16b nuclear translocation is actively regulated in the hypodermal tissue during embryonic development. To our knowledge, dynamic DAF-16 nuclear localization in wild type worms during development has not been previously observed. Taken together, our results indicate that DAF-16 activity is required in the embryonic hypodermal tissue to non-autonomously promote the migration of the HSNs.

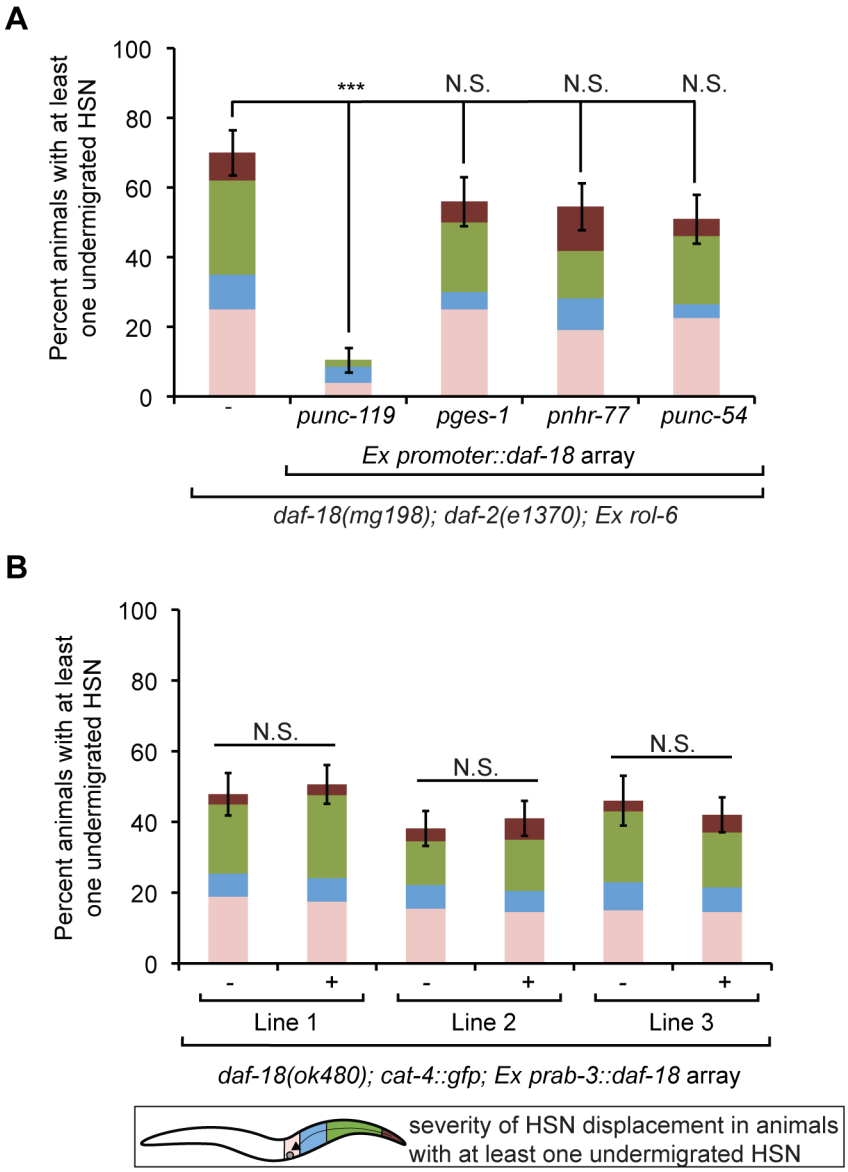

Figure 2-5. HSN migration in *daf-18* mutants with tissue-specific DAF-18 expression. (A) Quantification of the percentage of animals with an undermigrated HSN in *daf-18(mg198); daf-2(e1370); Ex rol-6* mutant animals (n=50) and mutant animals containing the *Ex punc-119::daf-18* (n=76), *Ex pges-1::daf-18* (n=50), *Ex pnhr-77::daf-18* (n=55) or *Ex punc-54::daf-18* (n=51) array. *punc-119* drives expression in neurons as well as the embryonic hypodermis. *pges-1* drives expression in the intestinal cells. *pnhr-77* drives expression in the seam cells and *punc-54* drives

expression in the body wall muscles. Note that only the *punc-119* driven expression of *daf-18* rescued the HSN undermigration phenotype. HSNs were visualized by anti-serotonin staining. **(B)** Expression of DAF-18 driven by the *rab-3* pan-neuronal promoter does not rescue the HSN undermigration defect in *daf-18(ok480)* mutants. The *daf-18(ok480)* mutants that had the rescuing array (+) or their siblings that had lost the array (-) were scored. Number of animals scored from two pooled independent experiments per line are: Line 1: (-) n=69 and (+) n=83; Line 2: (-) n=97 and (+) n=100; Line 3: (-) n=50 and (+) n=100. See Figure 2-1 for detailed description of worm schematic legend. ***$p<0.001$ (*z*-test). Error bars represent SEP.

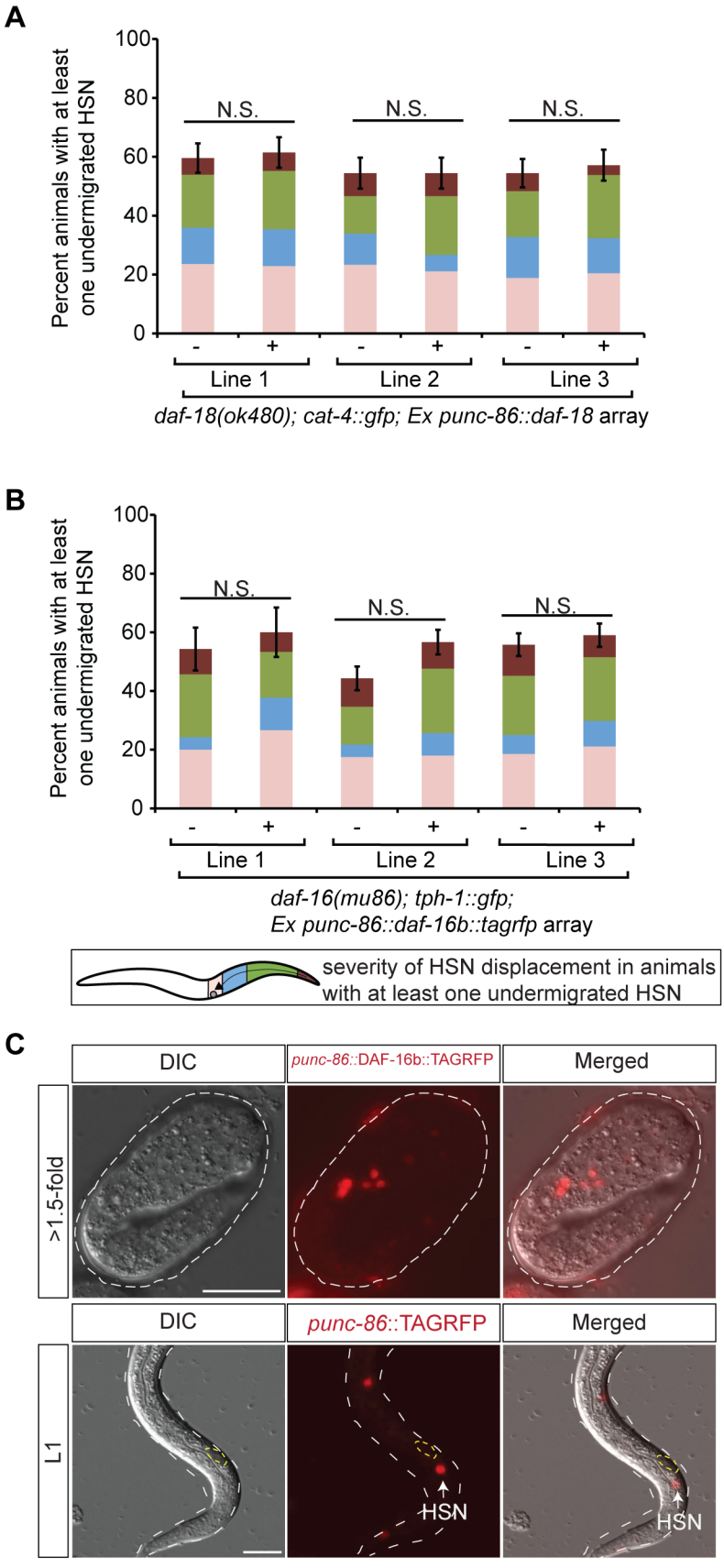
A
Percent animals with at least one undermigrated HSN
100
80
60
40
20
0
N.S.
N.S.
N.S.
-
+
-
+
-
+
Line 1
Line 2
Line 3
daf-18(ok480); cat-4::gfp; Ex punc-86::daf-18 array
B
Percent animals with at least one undermigrated HSN
100
80
60
40
20
0
N.S.
N.S.
N.S.
-
+
-
+
-
+
Line 1
Line 2
Line 3
daf-16(mu86); tph-1::gfp;
Ex punc-86::daf-16b::tagrfp array
severity of HSN displacement in animals with at least one undermigrated HSN
C
DIC
punc-86::DAF-16b::TAGRFP
Merged
>1.5-fold
DIC
punc-86::TAGRFP
Merged
L1
HSN
HSN

Figure 2-6. DAF-18 and DAF-16b do not act cell-autonomously to promote HSN migration. **(A)** Expression of DAF-18 driven by the *unc-86* promoter does not rescue the HSN undermigration defect in *daf-18(ok480)* mutants. The *daf-18(ok480)* mutants that had the rescuing transgenic array (+) or their siblings that had lost the array (-) were scored. Number of animals scored from three pooled independent experiments per line are Line 1: (-) n=89 and (+) n=96; Line 2 (-) n=90 and (+) n=90; Line 3 (-) n=90 and (+) n=105. **(B)** Expression of DAF-16b::TagRFP in HSN does not rescue the HSN undermigration defect of *daf-16(mu86)* mutants. The *daf-16(mu86)* mutants that had the rescuing array (+) or their siblings that had lost the array (-) were scored. Number of animals scored from four pooled independent experiments for line 2 and 3 and one experiment for line 1 are: Line 1: (-) n=35 and (+) n=45; Line 2: (-) n=140 and (+) n=150; Line 3: (-) n=156 and (+) n=161. See Figure 2-1 for detailed description of worm schematic legend. Significance determined by the *z*-test. Error bars represent SEP. **(C)** The *unc-86* promoter-driven TagRFP constructs are expressed in a subset of neurons in *daf-16* null mutants including the HSN. Images of a 1.5-fold embryo (top) and L1 larva (bottom) are shown. The yellow dotted outlines denote the developing gonad. Scale bars: 20 μm.

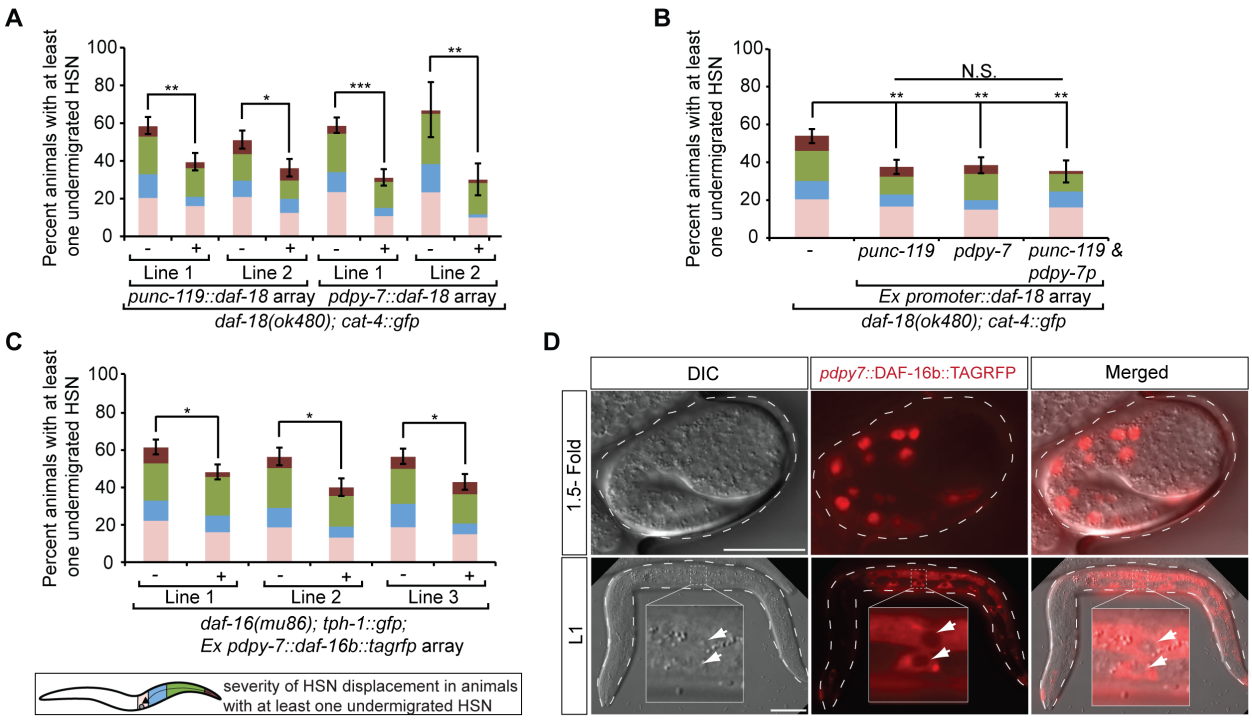

Figure 2-7. DAF-16 functions cell non-autonomously in the hypodermal tissue to promote HSN migration. (A) Expression of DAF-18 driven by either the *unc-119* or *dpy-7* promoter rescues the HSN undermigration defect in *daf-18(ok480)* mutants. The *daf-18(ok480)* mutants that had the rescuing transgenic array (+) or their siblings that had lost the array (-) were scored. Number of animals scored for the *punc-119* rescue from three pooled independent experiments per line are: Line 1: (-) n=120 and (+) n=112; Line 2: (-) n=123 and (+) n=113. Number of animals scored for the *pdpy-7* rescue from three pooled independent experiments for line 1 and one experiment from line 2 are: Line 1: (-) n=147 and (+) n=116; Line 2: (-) n=30 and (+) n=30. **(B)** Expression of DAF-18 driven simultaneously by both the *unc-119* and *dpy-7* promoters in the same animal does not enhance the rescue of either array alone. The *daf-18(ok480)* mutants that had both rescuing arrays or their siblings that contained only the *punc-119* array, only the *pdpy-7* array or had lost both arrays (-) were scored. Number of animals scored are: (-), n=176;

punc-119 only, n=165; *pdpy-7* only, n=130; both arrays, n=65. **(C)** Expression of DAF-16b::TagRFP in the hypodermis rescues the HSN undermigration defect of *daf-16(mu86)* mutants. The *daf-16(mu86)* mutants that had the rescuing array (+) or their siblings that had lost the array (-) were scored. Number of animals scored from at least two pooled independent experiments per line are: Line 1: (-) n=153 and (+) n=162; Line 2: (-) n=110 and (+) n=110; Line 3: (-) n=147 and (+) n=140. See Figure 2-1 for detailed description of worm schematic legend. **(D)** The rescuing construct *pdpy-7::*DAF-16b::TagRFP is localized to the hypodermal nuclei during the embryonic stages when HSN migration is occurring (see also Figure 2-11C for images of nuclear hypodermal GFP for comparison) and is mostly cytoplasmic or perinuclear during the L1 stage when HSN migration has finished. Arrows in L1 magnification panel point to hypodermal nuclei to illustrate that DAF-16b::TagRFP is not nuclear localized at this stage. *p<0.05, **p<0.01, ***p<0.001 (*z*-test). Error bars represent SEP. Scale bars: 20 μm.

Enhanced DAF-16 activity leads to HSN overmigration

DAF-16 in *C. elegans* is negatively regulated by insulin/IGF-1 signaling (Lin et al., 1997; Ogg et al., 1997) in part through excluding its nuclear localization (Henderson and Johnson, 2001; Lee et al., 2001; Lin et al., 2001); therefore, DAF-16-dependent transcription is activated in insulin/IGF-1 signaling mutants. Since *daf-16* null mutants exhibit an HSN undermigration defect, we investigated whether activation of DAF-16 could cause HSN overmigration, meaning that the HSNs migrate beyond their normal destination flanking the vulva. We tested the *age-1(hx546)* (PI3K) mutant (Friedman and Johnson, 1988; Tissenbaum and Ruvkun, 1998) for HSN migration defects and found an HSN overmigration phenotype in a small number of adult animals grown at 20°C. Notably, the dramatic extent of HSN overmigration in these few affected

animals (Figure 2-8A) was never observed in the wild type population. Since DAF-16 can be directly activated by the c-Jun N-terminal kinase (JNK) upon heat stress (Oh et al., 2005), we tested whether or not a combination of heat stress and *age-1* loss-of-function could enhance the overmigration phenotype seen at 20°C by increasing DAF-16 nuclear activity. In order to enhance DAF-16 nuclear activity during embryogenesis specifically, we let *age-1(hx546)* embryos develop at a higher temperature of 27°C and then shifted the L1 larvae back to 20°C and allowed them to grow to adulthood. We then scored HSN migration defects in these adult animals and found a significant increase in frequency of HSN overmigration compared to wild type (Figure 2-8B). This enhanced overmigration at higher temperature was DAF-16-dependent since it did not take place in *daf-16; age-1* double mutant animals (Figure 2-8B).

HSN overmigration has also been observed in animals with missing or anteriorly displaced canal-associated neurons (CANs) (Forrester and Garriga, 1997), a pair of bilaterally symmetric neurons that are born in the head and migrate posteriorly to the center of the embryo just anterior to the HSNs (Figure 2-8C) (Sulston et al., 1983). In order to rule out the possibility that the DAF-16-dependent overmigration we describe could be contributed to by anteriorly displaced CANs in the *age-1* mutant background we examined the position of the CANs in larvae using the *kal-1::gfp* reporter, which marks the CANs in addition to the HSNs (Rugarli et al., 2002). We did not observe a defect in CAN migration in the *age-1* mutant at 27°C, and in fact the HSN even migrated past the CAN in some cases (Figure 2-8D). Together, these observations indicate that HSN overmigration in the *age-1* mutant is due strictly to an increase in DAF-16 activity mediated by the loss of PI3K activity and JNK activation during embryogenesis.

Our data predicts that DAF-16-dependent overmigration is occurring independently of pathways controlling the posterior migration of the CANs, since the CAN neurons migrate normally in *age-1* mutants. Therefore, we reasoned that if we disrupted CAN migration in the *age-1* mutant background that HSN overmigration might be enhanced due to the combined effect of *age-1* loss-of-function and CAN displacement. To do this, we combined the *age-1* mutant with a null allele of *vab-8. vab-8* encodes a kinesin-related protein, which is required for most posterior migrations, including the CANs (Manser and Wood, 1990; Wightman et al., 1996; Wolf et al., 1998). In the *vab-8* mutant background the CANs fail to migrate out of the head and the HSNs can migrate past their normal stopping point in 34% of animals (Figure 2-8E). In addition, we also noted that in the *vab-8* mutant background the HSN undermigrated in 32% of animals (Figure 2-8E), suggesting that *vab-8* is also partially required for the anterior migrations of the HSNs. Consistent with our observation, this undermigration phenotype has been previously reported (Manser and Wood, 1990). At 20°C in the *age-1; vab-8* double mutant, we observed that the positions of the HSNs along the anterior-posterior body-axis were shifted anteriorly in a DAF-16-dependent manner, such that the *age-1* mutant suppressed the *vab-8* HSN undermigration phenotype (Figure 2-8E). This result indicates that a loss of PI3K signaling in a *vab-8* sensitized mutant background can shift the HSNs anteriorly even in the absence of JNK signaling. Consistently, we also observed enhanced HSN overmigration in a DAF-16-dependent manner when the *age-1; vab-8* double mutant was grown under heat stress at 27°C (Figure 2-9). Combined, our results demonstrate that DAF-16-dependent HSN overmigration occurs in parallel to pathways controlling the posterior migration of the CANs and that increased DAF-16 activity can shift the HSNs anteriorly along the A-P body axis.

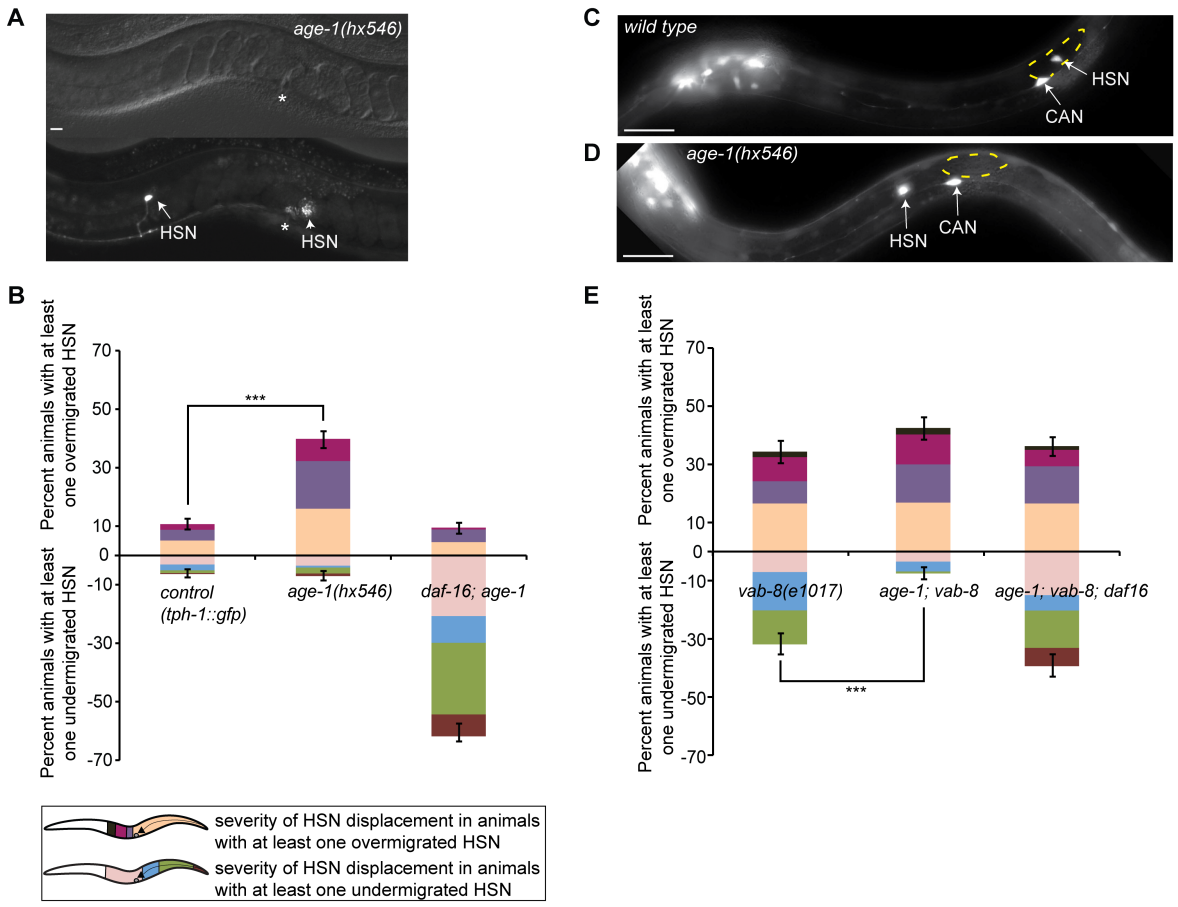

Figure 2-8. Enhanced DAF-16 activity during embryogenesis causes the HSNs to overmigrate. (A) A DIC (top) and an epifluorescent images (bottom) of an *age-1(hx546)* mutant adult animal observed at 20°C. The asterisk marks the vulva and the arrowhead indicates an out-of-focus HSN that has migrated to the proper location. The arrow points to an HSN that has migrated anterior to the vulva. The HSNs were visualized using *tph-1::gfp*. **(B)** The HSN overmigration phenotype in *age-1* mutant animals is DAF-16-dependent. Quantification of the percentage of animals with an overmigrated HSN (top) and animals with an undermigrated HSN (bottom) from five pooled independent experiments per strain in control *tph-1::gfp* (n=273), *age-1(hx546)* (n=241) and *daf-16(mu86); age-1(hx546)* (n=241) animals. Embryogenesis occurred at 27°C under heat stress, after which animals were shifted to 20°C at the L1 stage and allowed to

grow to adulthood before the HSNs were scored using *tph-1::gfp*. **(C-D)** Epifluorescent images of the HSN and CAN in wild type (C) and *age-1(hx546)* mutant larvae (D) that underwent embryogenesis at 27°C. After hatching, neurons were visualized with a *kal-1::gfp* transcriptional reporter. The yellow dotted outlines denote the developing gonad and arrows indicate the positions of the HSN and CAN relative to the gonad. The CAN migrates normally in *age-1(hx546)* mutants and an example of a HSN overmigrating to a distance beyond the CAN is depicted (D). **(E)** Increased DAF-16 activity shifts the HSNs anteriorly along the A-P body axis. Quantification of the percentage of animals with an overmigrated HSN (top) and animals with an undermigrated HSN (bottom) from three pooled independent experiments per strain in *vab-8(e1017)* (n=163), *age-1(hx546); vab-8(e1017)* (n=160) and *age-1(hx546); vab-8(e1017); daf-16(mu86)* (n=160) animals. Animals were grown at 20°C and scored as adults using the *tph-l::gfp* reporter. Worm schematic legend: Stacked bars represent the proportion of HSNs at different positions along the A-P body axis within only those animals containing at least one under- or overmigrated HSN. Top worm: the light peach region represents HSNs that have not overmigrated (i.e. are wild type or in few cases have undermigrated). The black region represents the most severely overmigrated HSNs. Bottom worm: The light pink region represents HSNs that have not undermigrated (i.e. are wild type or in few cases have overmigrated) and the red region represents the most severely undermigrated HSNs. ***$p<0.001$ (*z*-test). Error bars represent SEP. Images are oriented with the posterior of the animal to the right. Scale bars: 20 μm.

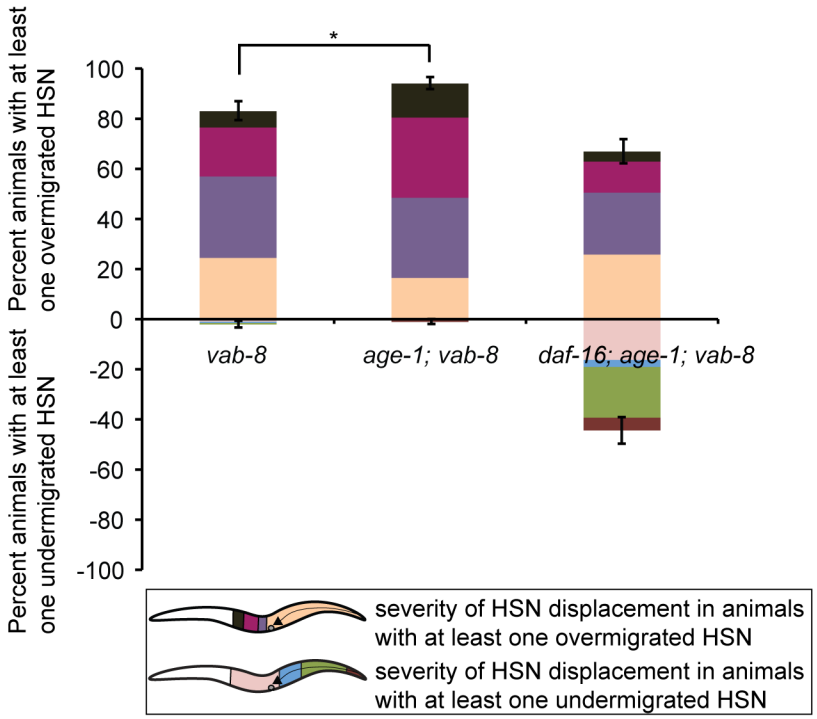

Figure 2-9. DAF-16-dependent HSN overmigration is enhanced in the absence of CAN migration. The HSNs can migrate past their normal stopping point in *vab-8* mutants due to the failure of CAN migration. Increased DAF-16 activity induced by the loss of PI3K signaling and simultaneous heat shock enhances HSN overmigration in *vab-8(e1017)*. Quantification of the percentage of animals with an overmigrated HSN (top) and animals with an undermigrated HSN (bottom) from two pooled independent experiments per strain in *vab-8(e1017)* (n=100), *age-1(hx546)*; *vab-8(e1017)* (n=100) and *daf-16(mu86); age-1(hx546); vab-8(e1017)* (n=89). Embryogenesis for all strains occurred at 27°C (heat stress) before L1 animals were shifted to 20°C, where they completed their development. The HSNs were scored using the *tph-1::gfp* reporter. Worm schematic legend: stacked bars represent the proportion of HSNs at different positions along the A-P axis. See Figure 2-8 for detailed description of worm schematic legend. *$p<0.05$ (*z*-test). Error bars represent SEP.

The DAF-2 insulin/IGF-1 receptor acts upstream of DAF-16 to control HSN migration

In *C. elegans* the insulin/IGF-1 receptor is encoded by a single gene *daf-2* (Kimura et al., 1997) and acts upstream of PI3K signaling to inhibit DAF-16 activity (Morris et al., 1996; Lin et al., 1997; Ogg et al., 1997; Ogg and Ruvkun, 1998; Paradis and Ruvkun, 1998). In order to determine if HSN migration is controlled through DAF-2 receptor signaling, we examined the temperature-sensitive *daf-2(e1370)* mutant containing a missense mutation in a highly conserved residue of the kinase domain (Kimura et al., 1997). Embryos were allowed to develop at the restrictive temperature of 27°C before being shifted as L1 larvae to the permissive temperature of 20°C, where they completed their development. Consistent with a release of DAF-16 inhibition and increased DAF-16 activity, *daf-2* mutants displayed a DAF-16-dependent HSN overmigration phenotype (Figure 2-10AC). Interestingly, in addition to an overmigration phenotype, *daf-2* mutants also exhibited an HSN undermigration phenotype that did not enhance the null *daf-16* mutant (Figure 2-10B-C). This suggests that the undermigration phenotype in *daf-2(e1370)* is due to decreased DAF-16 activity. To further confirm this, we performed epistasis analysis using the *age-1(hx546)* allele, which we have shown to cause a DAF-16-dependent HSN overmigration phenotype. We observed that removing AGE-1 activity suppressed the *daf-2* mutant undermigration phenotype *(*Figure 2-10D), which is consistent with its dependence on DAF-16. In *C. elegans*, the insulin-like peptides have been shown to function as either DAF-2 agonists or antagonists (Kawano et al., 2000; Pierce et al., 2001; Li et al., 2003; Murphy et al., 2003; Murphy et al., 2007; Matsunaga et al., 2012). Therefore, misregulation of HSN migration in both directions is likely due to an inconsistent control of signaling and downstream DAF-16 activity in the *daf-2(e1370)* mutant, which is not null. We also observed animals with HSN under and overmigration defects using another loss-of-function allele *daf-*

2(m65) (Patel et al., 2008) (data not shown). Although a model of regulation of HSN migration through a combination of DAF-2 agonists and antagonists acting on hypodermal cells along the HSN migration route is very attractive, we cannot exclude the possibility that HSN undermigration seen in *daf-2* loss-of-function mutants is due to inappropriate *age-1*-dependent signaling initiated through other receptors.

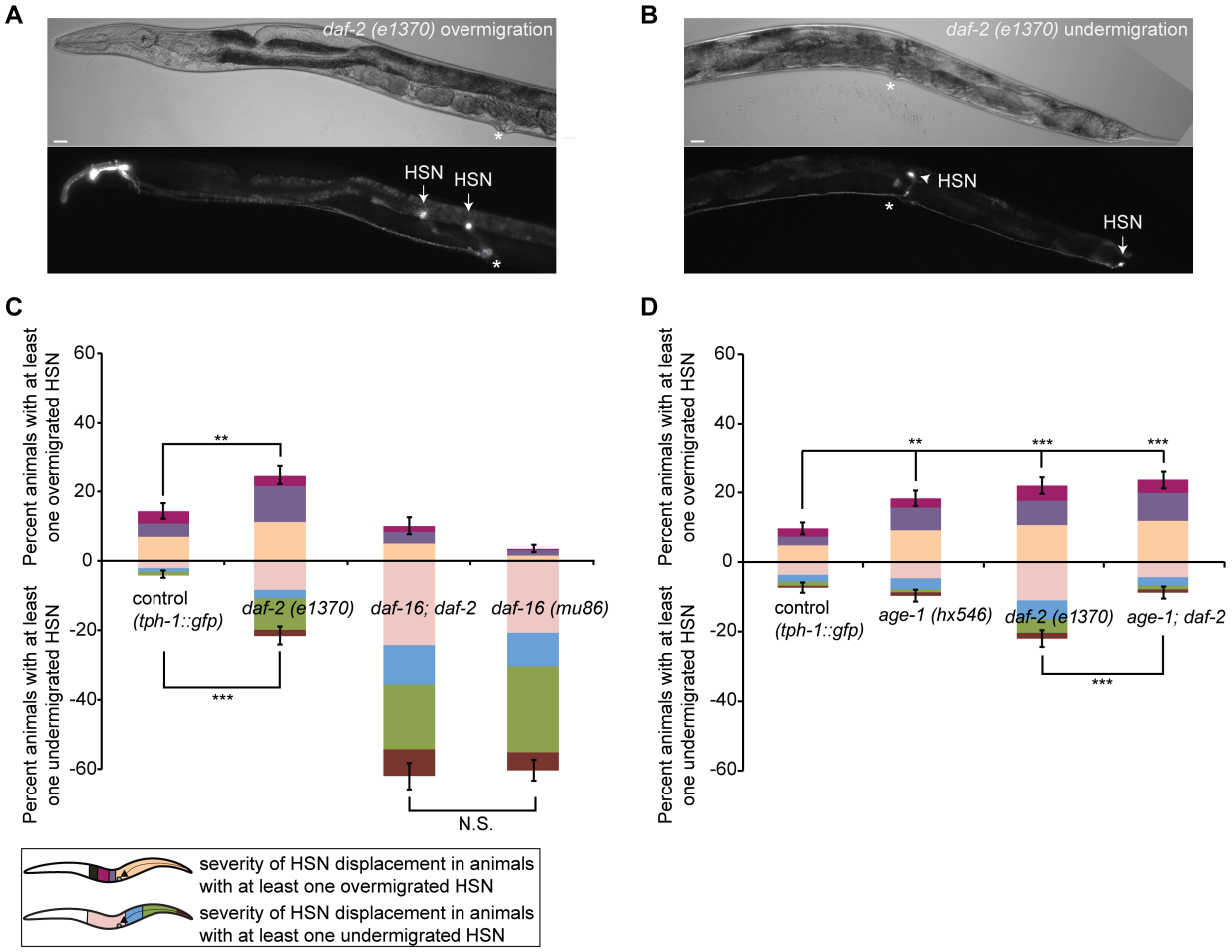

Figure 2-10. The DAF-2 receptor regulates HSN migration by modulating DAF-16 activity. **(A-B)** DIC images of adult hermaphrodites (top) and corresponding epifluorescent images of the HSNs (bottom) in *daf-2(e1370)* mutants. The asterisk marks the vulva and the arrowhead denotes

the position of a properly migrated HSN (B). Images are oriented with the posterior of the animal to the right. The HSNs were visualized using *tph-1::gfp*. The arrows indicate HSNs that have overmigrated to positions anterior to the vulva (A) and to an undermigrated HSN that remains in the tail (B). **(C)** The HSNs over- and undermigrate in the temperature-sensitive *daf-2(e1370)* mutant. Quantification of the percentage of animals with an overmigrated HSN (top) and animals with an undermigrated HSN (bottom) from a minimum of three pooled independent experiments per strain in control *tph-1::gfp* (n=238), *daf-2(e1370)* (n=250), *daf-16(mu86); daf-2(e1370)* (n=150) and *daf-16(mu86)* (n=260) animals. Note that the undermigration phenotype of *daf-2* mutants does not enhance the *daf-16* undermigration phenotype. **(D)** Reducing AGE-1 activity suppresses the *daf-2* mutant undermigration phenotype. Quantification of the percentage of animals with an overmigrated HSN (top) and animals with an undermigrated HSN (bottom) from two pooled independent experiments per strain in control *tph-1::gfp* (n=300), *age-1(hx546)* (n=300) *daf-2(e1370)* (n=300) and *age-1(hx546); daf-2(e1370)* (n=274) animals. Embryogenesis for all strains occurred at the *daf-2(e1370)* restrictive temperature of 27°C before L1 animals were shifted to the permissive temperature 20°C, where they completed their development. The HSNs were scored using the *tph-1::gfp* reporter (C-D). See Figure 2-8 for detailed description of worm schematic legend. **p<0.01, ***p<0.001 (*z*-test). Error bars represent SEP. Scale bars: 20 μm.

PAK1 acts non-autonomously and downstream of insulin/IGF-1-DAF-16 signaling in HSN migration

Recently, FOXO transcription factors have been identified as regulators of neuronal polarity in the mammalian brain through their direct activation of the gene *pak1*, which encodes

a p21-activated kinase (de la Torre-Ubieta et al., 2010). To determine whether FOXO-dependent Pak1 regulation is conserved and whether it is relevant to the regulation of HSN migration, we analyzed the orthologous *pak-1* in *C. elegans*. First, we determined that a putative null allele, *pak-1(ok448)*, which removes most of the kinase region (Lucanic et al., 2006), causes HSN undermigration defects similar to that of the *daf-16* null mutant (Figure 2-11A, 2-12A) and that *pak-1(ok448)* does not enhance the HSN undermigration phenotype of *daf-16* (Figure 2-11A). However, because the *daf-16 (null)* phenotype displays a stronger expressivity than the *pak-1 (null)* allele, that is the degree of HSN undermigration is more severe in *daf-16 (null)* (Figure 2-11A), DAF-16 is likely to have additional downstream effectors. Epistasis analysis using the *age-1* loss-of-function mutant further places *pak-1* downstream of insulin/IGF-1 signaling. The *pak-1* mutant suppressed the HSN overmigration phenotype observed in the *age-1* mutant, which we have shown to be DAF-16-dependent (Figure 2-11B). Altogether, these results are consistent with *pak-1* acting as a downstream effector of DAF-16 in HSN migration.

We examined the expression pattern of *pak-1* during embryogenesis using a *pak-1p::NLS-TagRFP* transcriptional reporter. The HSNs are born in the tail of the comma stage embryo and begin migrating ten minutes later (Sulston et al., 1983). We determined that *pak-1* is expressed in the hypodermal tissue before and during the HSN migrations (Figure 2-11C), consistent with earlier PAK-1 expression pattern reports (Chen et al., 1996; Iino and Yamamoto, 1998). Next, we tested whether or not hypodermal expression of PAK-1 could rescue the HSN migration defects in *pak-1* mutants. To do this, we expressed *pak-1* cDNA fused to TagRFP using the *dpy-7* hypodermal promoter. Expression of PAK-1::TagRFP in the hypodermis rescued the HSN migration defects of *pak-1* mutants (Figure 2-11D), placing the focus of PAK-1 activity in the same tissue as that of DAF-16. Hypodermal expression of PAK-1, however, was

insufficient to rescue the *daf-16 (null)* phenotype (data not shown), consistent with the suggestion of our genetic data that DAF-16 likely regulates multiple genes to affect HSN migration, just as it does for lifespan (Murphy, 2006).

Next, we determined that *pak-1* contains consensus DAF-16 binding site sequences in its promoter (Furuyama et al., 2000; Murphy et al., 2003), which are conserved among the nematodes (Figure 2-12B). Furthermore, we analyzed a ChIP-seq data set available from the modENCODE project to show that a DAF-16::GFP fusion protein occupies the endogenous *pak-1* promoter (Figure 2-12C). In order to test whether DAF-16 regulates *pak-1* expression in the hypodermis during HSN migration we performed single-molecule fluorescent in situ hybridization (smFISH) (Raj et al., 2008) to examine the endogenous *pak-1* mRNA expression levels during embryogenesis in wild type and *daf-16(mu86)* null embryos. First, consistent with a role in HSN migration, *pak-1* transcripts were abundantly expressed prior to and after HSN migration has begun before decreasing in the 3-fold embryo (Figure 2-13A). Second, we observed a small but significant decrease in *pak-1* transcripts in the hypodermal cells of comma stage embryos in the *daf-16* null mutant compared to wild type (Figure 2-13B), but not in the CAN during late embryogenesis (Figure 2-13C), suggesting that DAF-16 specifically regulates *pak-1* activity in the embryonic hypodermal tissue. We identify the CANs based on their positions in the developing embryo and the high expression of a *pak-1* transcriptional reporter in the CANs of newly hatched L1 larvae (Figure 2-14).

DAF-16 is known to act as a master regulator of transcription in stress response and longevity pathways (reviewed in Murphy, 2006), and none of its downstream target genes were shown to rescue *daf-16* mutant phenotypes when overexpressed. Therefore, it is possible that DAF-16 modulates the expression of a variety of factors, including *pak-1*, at the transcriptional

level in the embryonic hypodermis to promote HSN migration. Embryos stained with an antibody against PAK-1 have revealed its localization to the plasma membrane of hypodermal cells during morphogenesis (Chen et al., 1996). Thus, DAF-16 may also regulate factors required for PAK-1 activation and/or for its localization to the hypodermal cell boundaries during HSN migration. Overall, our results are consistent with a model wherein nuclear localization of DAF-16 in the embryonic hypodermal cells, specifically at the time of HSN migration, promotes expression of multiple target genes, including *pak-1*, that are required to control the robustness of the migration process in a cell non-autonomous manner.

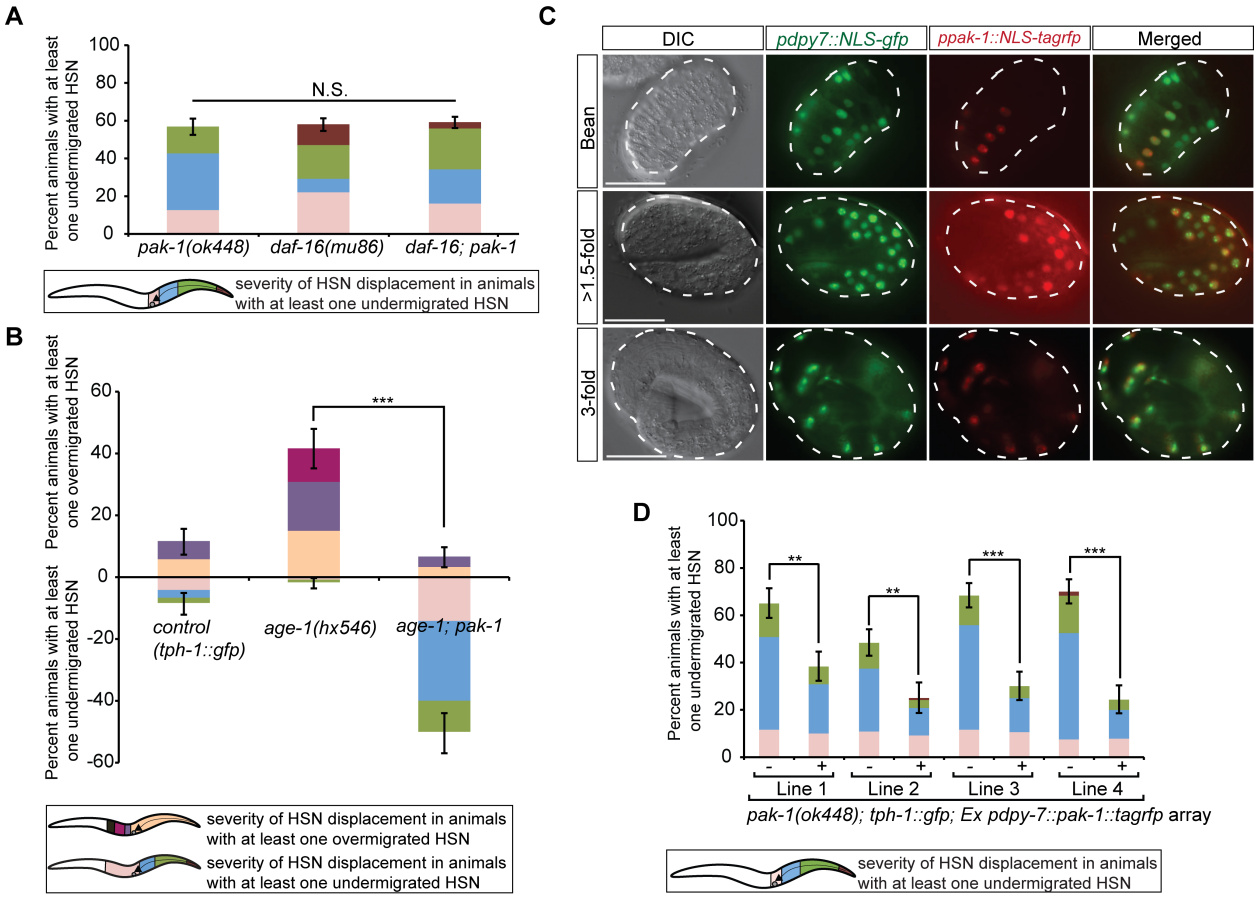

Figure 2-11. PAK-1 acts cell non-autonomously and downstream of insulin/IGF-1 signaling in HSN migration. (A) *pak-1* mutants phenocopy *daf-16* mutants and a *pak-1* null allele does not enhance a *daf-16* null allele. Quantification of the percentage of animals with an undermigrated HSN from a minimum of three pooled experiments per strain in *pak-1(ok448)* (n=130), *daf-16(mu86)* (n=210) and *daf-16(mu86); pak-1(ok448)* (n=90) mutant animals. **(B)** *age-1(hx546)* HSN overmigration is *pak-1*-dependent. Quantification of the percentage of animals with an overmigrated HSN (top) and animals with an undermigrated HSN (bottom) from two pooled independent experiments per strain in control *tph-1::gfp* (n=60), *age-1(hx546)* (n=60) and *age-1(hx546); pak-1(ok448)* (n=60). **(C)** Representative TagRFP expression in embryos carrying the *ppak-1::NLS-tagrfp* reporter. Expression is restricted to the hypodermal tissue throughout embryogenesis beginning prior to HSN migration (bean stage, top) and during HSN migration (1.5-fold, middle) and continues to be expressed in the hypodermis during late embryogenesis (3-fold, bottom). A GFP fusion gene driven by the hypodermal promoter *pdpy-7* (mnIs61) was present in the same animals to confirm that *pak-1* is expressed in the hypodermal tissue. **(D)** Expression of PAK-1::TagRFP in the hypodermis rescues the HSN undermigration defect of *pak-1(ok448)* mutants. The *pak-1(ok448)* mutants that had the rescuing array (+) or their siblings that had lost the array (-) were scored. Number of animals scored, from two pooled independent experiments per line are: Line 1: (-) n=60 and (+) n=60; Line 2: (-) n=60 and (+) n=60; Line 3: (-) n=60 and (+) n=80; Line 4: (-) n=60 and (+) n=70. See Figure 2-1 and 2-8 for detailed description of worm schematic legends. **p<0.01, ***p<0.001 (*z*-test). Error bars represent SEP. Scale bars: 20 μm.

A

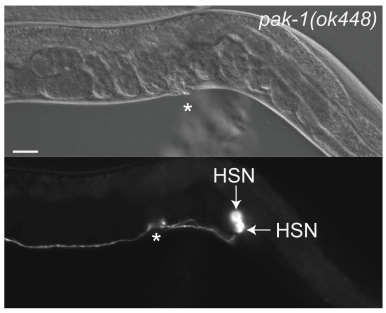

B

Caenorhabditis species	DAF-16 binding site sequence in *pak-1* promoter	position relative to ATG	Strand
C. elegans	TATTTAC	-1350, -2918	-
C. briggsae	-------		
C. remanei	-------		
C. brenneri	-------		
C. japonica	TATTTAC	-16	+
C. elegans	CTTATCA	-1867	-
C. briggsae	CTTATCA	-2582	-
C. remanei	CTTATCA	-1707, 2784	-
C. brenneri	CTTATCA	-2006	-
C. japonica	-------		
C. elegans	TGTTTAC	-3238	+
C. briggsae	TGTTTAC	-1572	+
C. remanei	TGTTTAC	-2994	+
C. brenneri	TGTTTAC	-1439, -3663	-, +
C. japonica	TGTTTAC	-1391	-

C

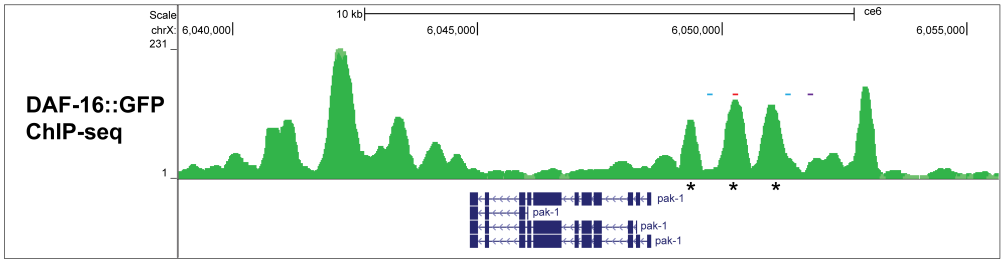

Figure 2-12. *pak-1* mutants phenocopy *daf-16* mutants and the *pak-1* promoter contains conserved DAF-16 binding sites capable of binding DAF-16::GFP. (A) A DIC image of an adult worm (top) and an epifluorescent image of the HSNs (bottom) in a *pak-1(ok448)* animal. HSNs were visualized with a tryptophan hydroxylase GFP reporter (*tph-1::gfp)*. Image is oriented with the posterior of the animal to the right. Asterisk indicates the vulva and arrows denote both HSNs, which have failed to migrate the full distance from the tail to the vulva. Scale bar: 20 μm. **(B)** DAF-16 binding site sequences in the *pak-1* promoter and the homologous sequences found in *C. briggsae, C. remanei, C. brenneri* and *C. japonica*. **(C)** ChIP/seq data

from modENCODE (Michael Snyder group) performed in L4 young adult animals shows that a DAF-16::GFP fusion protein occupies the endogenous *pak-1* promoter. Asterisks indicate peaks in the promoter that were ruled significant by modENCODE. Colored lines above peaks represent positions of DAF-16 binding site sequences (B). Note that the conserved binding site CTTATCA (red) is bound by DAF-16::GFP (C).

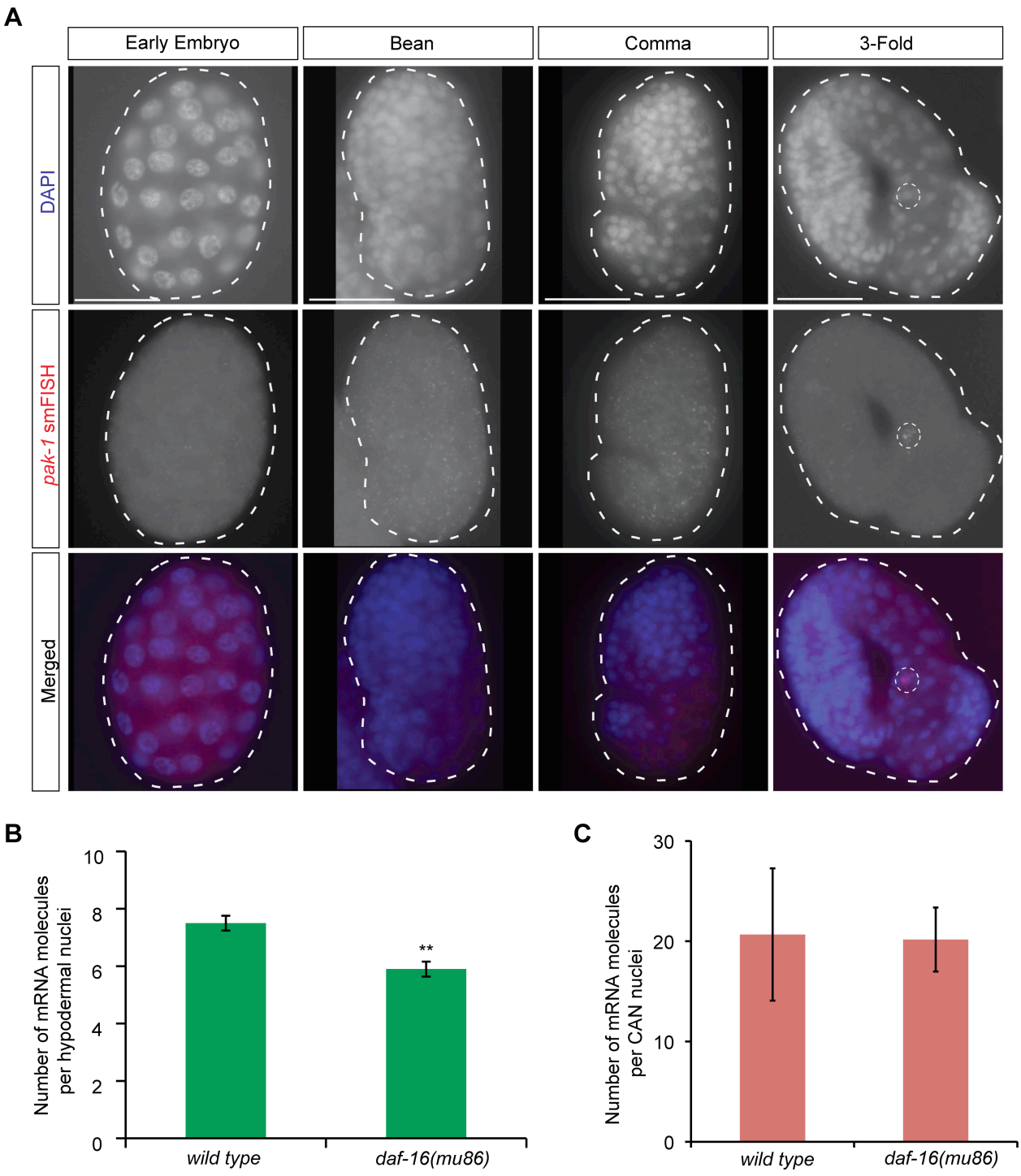

Figure 2-13. *pak-1* expression is high in hypodermal cells during the time of HSN migration and is enhanced by DAF-16. (A) Single-molecule FISH against *pak-1* mRNA in

embryos. *pak-1* expression is seen in the early embryo and continues throughout all stages of embryogenesis. Expression is highly localized to the hypodermal cells beginning in the bean stage and occurring through the 1.5-fold stage, which is consistent with the timing of HSN migration. We assume these are hypodermal cells based on the *pak-1* transcriptional reporter overlap with marked hypodermal cells (Figure 2-11C). *pak-1* expression is dramatically reduced in the 3-fold embryo and becomes restricted mainly to the CAN. Outlined is what we assume to be the CAN neuron based on the high expression of a *pak-1* transcriptional reporter in the CAN of a newly hatched L1 (Figure 2-14) and the position of this cell in the embryo. **(B)** *pak-1* expression is partially dependent on DAF-16 in the hypodermal cells during HSN migration. Quantification of single mRNA molecules in wild type (n=3) and *daf-16(mu86)* (n=3) comma-stage embryos. **(C)** *pak-1* expression is not dependent on DAF-16 in the CAN. Quantification of single mRNA molecules in wild type (n=6) and *daf-16(mu86)* (n=6) CANs of 3-fold embryos. See Experimental Procedures for details on quantification method. Error bars represent the standard deviation. **p<0.01 (*t*-test). Scale bars: 20 μm.

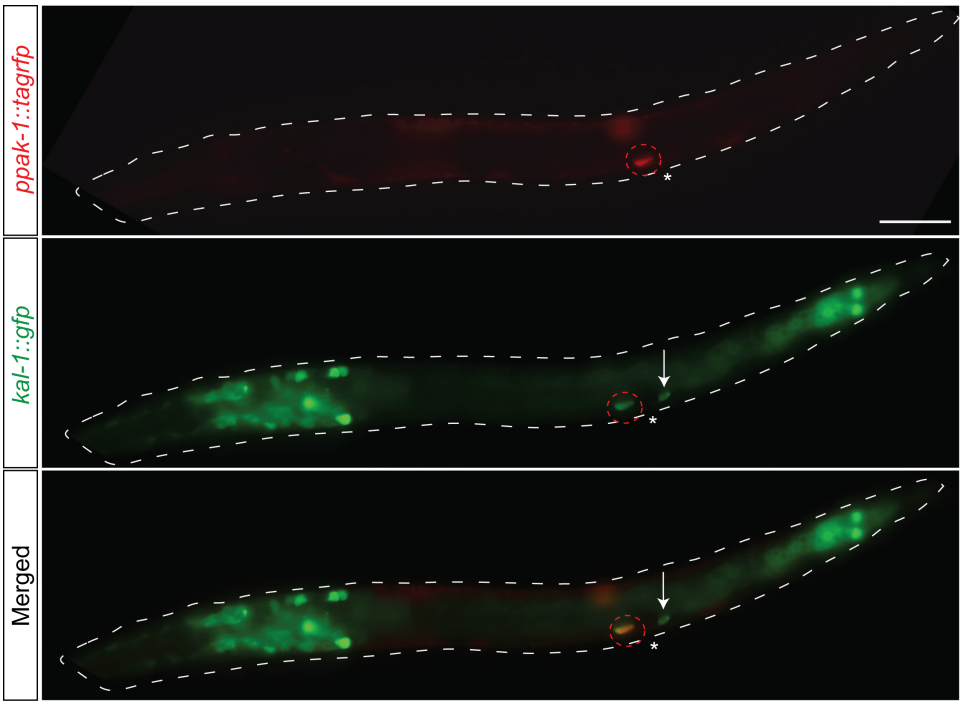

Figure 2-14. A *ppak-1::tagrfp* transcriptional reporter is expressed highly in the CAN of newly hatched L1 larvae. Representative TagRFP expression in L1 larvae carrying the *ppak-1::tagrfp* reporter. GFP expression from the *kal-1::gfp* reporter marks the CAN (outlined in red) and HSN (arrow). TagRFP expression overlaps with GFP expression in the CAN. Images are oriented with the posterior of the animal to the right. Scale bar: 20 μm.

Discussion

In this study, we have uncovered a function of insulin/IGF-1 signaling through DAF-16/FOXO as a regulator of neuronal migration during *C. elegans* development. We demonstrate that DAF-16 activity is required in the hypodermal tissue to non-autonomously promote the HSN migrations and that this activity relies on the release of insulin/IGF-1-mediated inhibition of DAF-16. We show that a loss of DAF-16 activity leads to an HSN undermigration phenotype and that an increase in DAF-16 activity can cause the HSN to migrate past its normal stopping point. We also identify a non-autonomous role for PAK-1 as a downstream effector of DAF-16 activity in HSN migration. Taken together, our findings describe a genetic mechanism by which the extent of HSN migration can be regulated. Suppression of the insulin/IGF-1 pathway can potentiate HSN migration since DAF-16 inhibition is released and DAF-16-dependent transcription takes place, and conversely, activation of the insulin/IGF-1 pathway can terminate HSN migration through inhibition of DAF-16-dependent transcription (Figure 2-15).

The FOXO transcription factors are widely expressed in the developing mammalian brain (Hoekman et al., 2006; de la Torre-Ubieta et al., 2010) and are likely to play important roles during neurodevelopment. However, their specific roles are only just beginning to be elucidated. Recently, the FOXOs were shown to be required cell-autonomously for neuronal polarity in the mammalian brain (de la Torre-Ubieta et al., 2010) and a study in *C. elegans* and mammalian neurons demonstrated a conserved and cell-autonomous role for DAF-16 and FOXO in the control of axon outgrowth (Christensen et al., 2011). Furthermore, a role for FOXO3a in the maintenance of neuronal survival during *zebrafish* brain development has also been recently described (Peng et al., 2010). Here, we identify a non-autonomous role for DAF-16 in neuronal

migration and build on growing evidence that FOXO transcription factors play important roles during neurodevelopment.

Previous studies have implicated IGF-1 signaling in mammalian brain development; a loss of IGF-1 causes reduced brain size due to a loss of neural progenitors (Beck et al., 1995) and overexpression of IGF-1 leads to increased brain size (Carson et al., 1993). It has been suggested that a major output of IGF-1 signaling in this process is inhibition of FOXO, since FOXO3 overexpression also leads to reduced brain size and a decrease in neural progenitors (Schmidt-Strassburger et al., 2012) and, consistently, decreased FOXO activity has been reported to result in larger brain size and increased neural progenitor proliferation (Paik et al., 2009; Renault et al., 2009). Furthermore, IGF-1 has also been shown to influence the organization of olfactory bulb layering by promoting neuronal migration in a PI3K-dependent manner (Hurtado-Chong et al., 2009).

It is well known that the PI3K signaling pathway controls many aspects of nervous system development, including neuronal migration, through multiple downstream effectors (reviewed in van Diepen and Eickholt, 2008; Waite and Eickholt, 2010). Interestingly, there still remains a discrepancy on whether or not PI3K signaling affects neuronal migration in a cell-autonomous or non-autonomous fashion (Backman et al., 2001; Kwon et al., 2001; Marino et al., 2002; Yue et al., 2005). Although multiple outputs of PI3K signaling have been implicated in neurodevelopment, the connection between insulin/IGF-1-PI3K signaling and DAF-16/FOXO in the non-autonomous regulation of neuronal migration has not been described previously.

Pak1, a member of the PAK protein kinase family, was previously identified as a direct target of FOXO in controlling neuronal polarity in the mammalian brain (de la Torre-Ubieta et al., 2010). Here, we demonstrate that the orthologous PAK-1 in *C. elegans* also acts downstream

of DAF-16/FOXO in HSN migration, suggesting conservation for this regulatory connection in neurodevelopment. Although a role for Pak1 in cell migrations has been previously described in both *C. elegans* (Lucanic et al., 2006; Peters et al., 2013) and mammals (reviewed in Kreis and Barnier, 2009), to our knowledge, a non-autonomous role for Pak1 in regulating the process of migration has not been reported. It will be interesting for future studies to determine whether or not FOXO-Pak1 is also non-autonomously required for mammalian neuron migration.

Pak1 has many substrates that control cytoskeletal dynamics (reviewed in Ye and Field, 2012). It is thought to primarily mediate the migration of cells in a cell-autonomous manner through the activation of LIM-kinase, which phosphorylates and inhibits cofilin, an actin-regulatory protein, in order to stimulate actin polymerization and cell movement (Edwards et al., 1999; reviewed in Ye and Field, 2012). From the genetic model we describe in this study, we can propose three possible scenarios for how PAK-1 might regulate HSN migration non-autonomously in *C. elegans*: First, PAK-1 could remodel the actin cytoskeleton and/or regulate cell adhesion at hypodermal cell boundaries to help guide the HSN along its migratory route, second, PAK-1 could regulate the expression of an extracellular molecule that is secreted from the hypodermis to act on the HSN and promote its migration and third, PAK-1 could be required for repressing inappropriate signaling from the hypodermis to the HSN during migration.

The negative regulation of DAF-16/FOXO by insulin/IGF-1 signaling was initially established in the regulation of longevity and stress response in *C. elegans* (Lin et al., 1997; Ogg et al., 1997) and was later shown to be conserved in mammals (reveiwed in Kops and Burgering, 2000). Given the conservation of the genetic networks regulating long-range cell migrations (Kee et al., 2007), it is likely that the control of neuronal migration in vertebrates includes a similar insulin/IGF-1-FOXO branch.

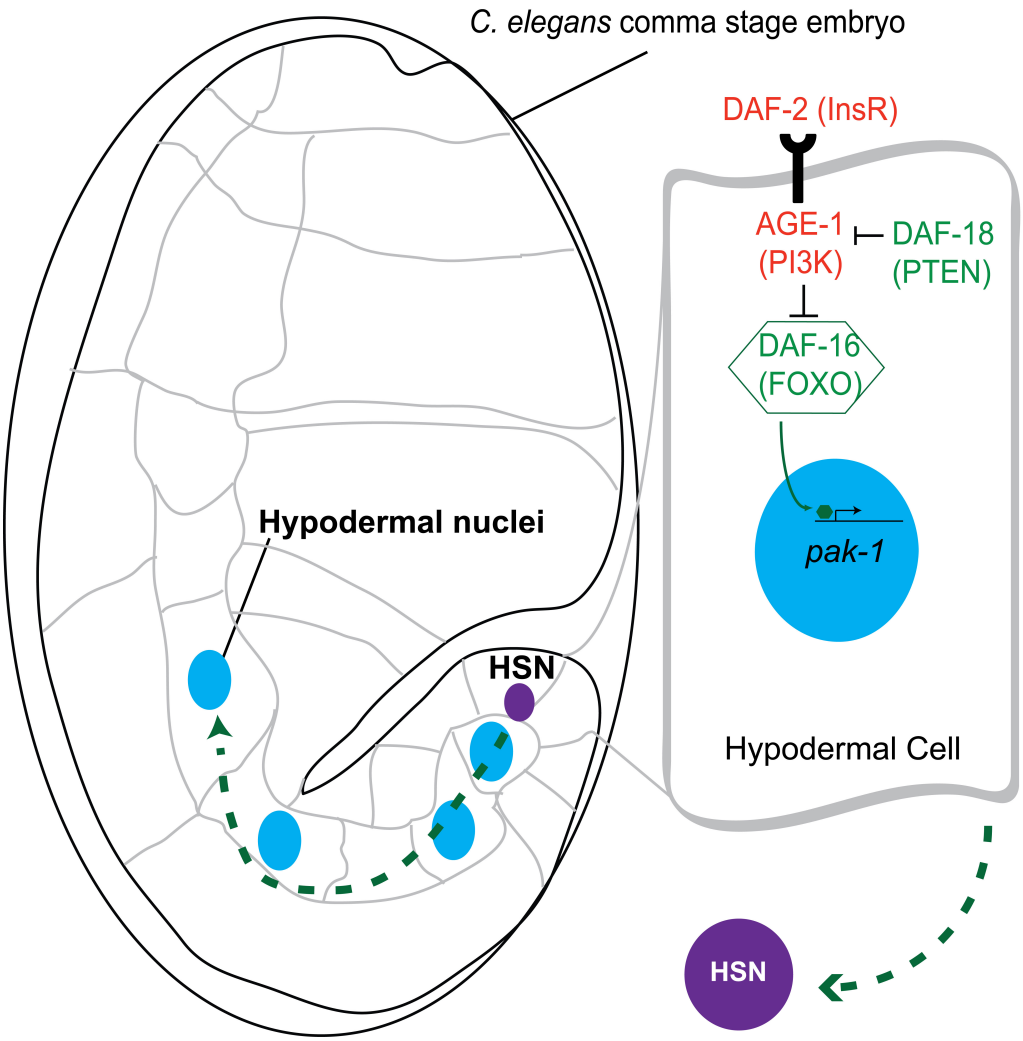

Figure 2-15. Insulin signaling, DAF-16/FOXO and PAK-1 act in the hypodermis to regulate HSN migration. Schematic model of *C. elegans* embryo, hypodermal cells and HSN.

Material and Methods

C. elegans Strains

Strains were maintained at 20°C using standard methods (Brenner, 1974). Bristol N2 was the wild-type strain used. *daf-16(mgDf50) I; daf-2(e1370) III* was provided by the Tissenbaum lab. The following strains were provided by the Hobert lab: SK4013 *zdIs13*(*tph-1::gfp)* (Clark and Chiu, 2003) and OH8482 *otIs225(cat-4::gfp) II; him-8 IV*. The following strains originally generated by the Tissenbaum lab were provided by the Colón-Ramos lab: HT1881 *daf-16(mgDf50) I; daf-2(e1370) unc-119(ed3) III; IpIs12*, HT1882 *daf-16(mgDf50) I; daf-2(e1370) unc-119(ed3) III; IpIs13*, HT1883 *daf-16(mgDf50) I; daf-2(e1370) unc-119(ed3) III; IpIs14* (Kwon et al., 2010). The following strains were provided by the Solari lab: SO18 *daf-18(mg198); daf-2(e1370)*, FS54 *daf-2(e1370); daf-18(mg198); fsEx54[pRF4]*, FS84 *daf-2(e1370); daf-18(mg198); fsEx84[pdaf-18::daf-18* cDNA], FS87 *daf-2(e1370); daf-18(mg198); fsEx87[punc-119::daf-18* cDNA], FS77 *daf-2(e1370); daf-18(mg198); fsEx77[pnhr-77::daf-18* cDNA], FS100 *daf-2(e1370); daf-18(mg198); fsEx100[pges-1::daf-18* cDNA], FS120 *daf-2(e1370); daf-18(mg198); fsEx120[punc54::daf-18* cDNA]. The following mutant and transgenic strains were obtained through the *Caenorhabditis* Genetics Center: *LGI:* CF1038 *daf-16(mu86),* GR1307 *daf-16(mgDf50); LGII*: TG1052 *age-1(hx546); LGIII:* CB1370 *daf-2(e1370),* DR410 *daf-2(m65)/unc-32(e189); LGIV:* RB712 *daf-18(ok480)*, OH904 *otIs33[kal-1::GFP]*, KN387 *egl-20(hu120); LGV:* CB1017 *vab-8(e1017); LGX:* AH205 *sdn-1(zh20),* RB689 *pak-1(ok448)*. Linkage group unknown: mnIs61 [*dpy-7p::unc-52(exons 15-19)::GFP + unc-36(+)*]. Compound mutant and transgenic strains are as follows: AGK580: *daf-16(mu86)*I; *tph-1::gfp*IV, AGK122: *daf-16(mgDf50)*I; *tph-1::gfp*IV, AGK214: *daf-18(ok480)*IV*; cat-4::gfp*II, AGK275: *daf-16(mu86)*I*; daf-18(ok480)IV; cat-4::gfp*II, AGK573: {*daf-18(ok480)*IV;

*cat-4::gfp*II; armEx218 [*punc-119::daf-18* pRF4 (*rol-6)*]} (Line 1 in this chapter), AGK575: {*daf-18(ok480)*IV; *cat-4::gfp*II; armEx220 [*punc-119::daf-18* pRF4 (*rol-6)*]} (Line 2 in this chapter), AGK567: {*daf-18(ok480)*IV; *cat-4::gfp*II; armEx217 [*pdpy-7::daf-18 pdpy-7::tagrfp* pPD118.33 *(pmyo-2::gfp)*]} (Line 1 in this chapter), AGK645: {*daf-18(ok480)*IV; *cat-4::gfp*II; armEx255 [*pdpy-7::daf-18 pdpy-7::tagrfp* pPD118.33 *(pmyo-2::gfp)*]} (Line 2 in this chapter), AGK650: {*daf-16(mu86)*I; *tph-1::gfp*IV; armEx257 [*pdpy-7::daf-16b::tagrfp* pPD118.33 *(pmyo-2::gfp)*]} (Line 1 in this chapter), AGK643: {*daf-16(mu86)*I; *tph-1::gfp*IV; armEx254 [*pdpy-7::daf-16b::tagrfp* pPD118.33 *(pmyo-2::gfp)*]} (Line 2 in this chapter), AGK646: {*daf-16(mu86)*I; *tph-1::gfp*IV; armEx256 [*pdpy-7::daf-16b::tagrfp* pPD118.33 *(pmyo-2::gfp)*]} (Line 3 in this chapter), AGK470: *age-1(hx546)*II; *tph-1::gfp*IV, AGK213: *daf-16(mu86)*I; *age-1(hx546)*II; *tph-1::gfp*IV, AGK651: *vab-8(e1017)*V; *tph-1::gfp*IV, AGK577: *age-1(hx546)*II; *vab-8(e1017)*V; *tph-1::gfp*IV, AGK652: *daf-16(mu86)*I; *age-1(hx546)*II; *vab-8(e1017)*V; *tph-1::gfp*IV, AGK572: *age-1(hx546)*II; *kal-1::gfp*IV, AGK186: *daf-2(e1370)*III; *tph-1::gfp*IV, AGK393: *daf-16(mu86)*I; *daf-2(e1370)*III; *tph-1::gfp*IV, AGK653: *age-1(hx546)*II; *daf-2(e1370)*III; *tph-1::gfp*IV, AGK545: *pak-1(ok480)*X; *tph-1::gfp*IV, AGK386: *daf-16(mu86)*I*; pak-1(ok480)*X; *tph-1::gfp*IV; AGK565: *age-1(hx546)*II; *pak-1(ok480)*X; *tph-1::gfp*IV, AGK369: *armEx*227 [*ppak-1-NLS::tagrfp* pRF4]*; mnIs61* [*dpy-7p::unc-52(exons 15-19)::GFP + unc-36(+)*], AGK635: {*pak-1(ok480)*X; *tph-1::gfp*IV; *armEx251* [*pdpy-7::pak-1::tagrfp* pPD118.33 *(myo-2::gfp)*]} (Line 1 in this chapter), AGK634: {*pak-1(ok480)*X; *tph-1::gfp*IV; *armEx250* [*pdpy-7::pak-1::tagrfp* pPD118.33 *(myo-2::gfp)*]} (Line 2 in this chapter), AGK632: {*pak-1(ok480)*X; *tph-1::gfp*IV; *armEx249* [*pdpy-7::pak-1::tagrfp* pPD118.33 *(myo-2::gfp)*]} (Line 3 in this chapter), AGK640: {*pak-1(ok480)*X; *tph-1::gfp*IV; *armEx252* [*pdpy-7::pak-1::tagrfp* pPD118.33 *(myo-2::gfp)*]} (Line 4 in this chapter), AGK388: *daf-16(mu86)*I; *kal-*

*1::gfp*IV, AGK489: *egl-20(hu120)*IV; *cat-4::gfp*II, AGK492: *daf-16(mu86)*I*; egl-20(hu120)*IV; *cat-4::gfp*IV, AGK191: *sdn-1(zh20)*X; *tph-1::gfp*IV, AGK190: *daf-16(mu86)*I; *sdn-1(zh20)*X; *tph-1::gfp*IV, AGK559: *armEx215* [*ppak-1::tagrfp* pRF4 (*rol-6)*]; *kal-1::gfp*IV. AGK442: {*daf-18(ok480)*IV; *cat-4::gfp*II; *armEx137* [*punc-86::daf-18 punc-86::tagrfp* pPD118.33 (*myo-2::gfp)]}* (Line 1 in this chapter), AGK 443: {*daf-18(ok480)*IV; *cat-4::gfp*II; *armEx138* [*punc-86::daf-18 punc86::tagrfp* pPD118.33 (*myo-2::gfp)]}* (Line 2 in this chapter), AGK441: {*daf-18(ok480)*IV; *cat-4::gfp*II; *armEx136* [*punc-86::daf-18 punc-86::tagrfp* pPD118.33 (*myo-2::gfp)]}* (Line 3 in this chapter), AGK405: {*daf-16(mu86)*I; *tph-1::gfp*IV; *armEx105* [*pun86::daf-16b::tagrfp* pPD118.33 *(myo-2::gfp)]}* (Line 1 in this chapter), AGK407: {*daf-16(mu86)*I; *tph-1::gfp*IV; *armEx107* [*pun86::daf-16b::tagrfp* pPD118.33 *(myo-2::gfp)]}* (Line 2 in this chapter), AGK406: {*daf-16(mu86)*I; *tph-1::gfp*IV; *armEx106* [*pun86::daf-16b::tagrfp* pPD118.33 *(myo-2::gfp)]}* (Line 3 in this chapter), AGK671: {*daf-18(ok480)*IV; *cat-4::gfp*II; *armEx261* [*prab-3::daf-18 prab-3::NLS-tagrfp* pPD118.33 (*myo-2::gfp)]}* (Line 1 in this chapter), AGK678: {*daf-18(ok480)*IV; *cat-4::gfp*II; *armEx264* [*prab-3::daf-18 prab-3::NLS-tagrfp* pPD118.33 (*myo-2::gfp)]}* (Line 2 in this chapter), AGK680: {*daf-18(ok480)*IV; *cat-4::gfp*II; *armEx266* [*prab-3::daf-18 prab-3::NLS-tagrfp* pPD118.33 (*myo-2::gfp)]}* (Line 3 in this chapter).

Molecular Biology and Transgenic Lines

Standard molecular biology techniques were used to construct transgenes. Germline transformation was performed by direct injection of various plasmid DNAs into the gonads of adult wild type animals as described (Mello et al., 1991). A *daf-18* cDNA was obtained by PCR with N2 cDNA as a template, with the forward primer containing a KpnI site 5'-

ATTGAAGGTACCATGGTTACTCCTCCTCCAGATGTG-3' and the reverse primer containing an AdeI site 5'-GCCGGCGCACCTCGTCTTACAAATAAATAGCTTGATCAAAA-3.' The *unc-119* (Maduro et al., 2000), dpy-7 (Gilleard et al., 1997) and *unc-86* (Baumeister et al., 1996) promoters were obtained by PCR with N2 genomic DNA as a template. The *unc-119* promoter was amplified with the forward primer containing a SphI site 5'-ATGAAGAATGCATGCCTATTCCTAGACGATTATTGGTTCC-3' and the reverse primer containing a SalI site 5'-CCAATGCATTGGTTGTCGACATATGCTGTTGTAGCTGAAAATTTTGG-3.' The *dpy-7* promoter was amplified with the forward primer containing a SphI site 5'-GTTATTGCATGCTCCACGATTTCTCGCAACACATCCC-3' and the reverse primer containing a SalI site 5'-GCGTCGGTCGACAAAGAACAGGGTGTGATAAATGAAT-3.' A 5.1 kb fragment upstream of the *unc-86* transcriptional start site was isolated with the forward primer containing an SphI site 5'-CGTGACACTGCATGCTTCAAAAACTGTCAACTAACAAGAT -3' and the reverse primer containing a SalI site 5'-CGGATGCGGTTGTCGACTCATTCAATTTCACTTTTTCATTCG -3.' The *rab-3* promoter subcloned into a modified Fire Kit vector pPD95.75 was provided as a generous gift from the Hobert lab. DNA was inserted into a modified Fire Kit vector pPD95.75, in which we replaced the GFP with a TAGRFP sequence using the KpnI/EcoRI sites. *Promoter::tagrfp* and *Promoter::daf-18* cDNA constructs were created. A *daf-16b* cDNA was obtained by PCR with N2 cDNA as a template with the forward primer containing a XmaI site 5'-TAGGAACCCGGGATGAACGACTCAATA-3' and the reverse primer containing an AgeI site 5'-GTCGCTACCGGTCCCAAATCAAAATGAAT-3.' *Pdpy-7::daf-16b::tagrfp* was

generated by inserting a SphI/SalI *dpy-7* fragment and XmaI/AgeI *daf-16b* cDNA fragment into our modified pPD95.75 vector. *Punc-86::daf-16b:;tagrfp* was generated by inserting a SphI/SalI *unc-86* fragment and XmaI/AgeI *daf-16b* cDNA fragment into our modified pPD96.75 vector. A *pak-1* cDNA was obtained by PCR with N2 cDNA as a template with the forward primer containing a XmaI site 5'-GGACTACCCGGGATGAAAGCTTTCTCATCGTA-3' and a reverse primer containing a KpnI site 5'-AATATAGGTACCCCTGAGTTGCTAGCTTCGGCGATGCT-3.' *Pdpy-7::pak-1::tagrfp* was generated by inserting a SphI/SalI *dpy-7* fragment and XmaI/KpnI *pak-1* cDNA fragment into our modified pPD95.75 vector. A 4kb fragment upstream of the *pak-1* ATG was isolated from genomic DNA by PCR and cloned into our modified fire vector with the forward primer containing a HindIII site 5'-CCGGCCAAGCTTCAATTCGATGCAATCCATTTAAAAG-3' and the reverse primer containing a BamHI site 5'-ATACGAGGATCCTTTGGCAAGCCTGGAAAATTGAAAC-3.' The same primers were used to insert the 4kb *pak-1* promoter into a modified Fire Kit Vector pPD95.75 containing 2x NLS sequences and a gene encoding TagRFP (generously provided by the Greenwald Lab). For each tissue-specific promoter, the corresponding transgenes encoding *daf-18* cDNA and *tagrfp* were co-injected at 20 ng/µl together with either pRF4 (*rol-6)* at 100 ng/µl for the *punc-119* construct or pPD118.33 (*myo-2::gfp)* at 2.5 ng/µl for the *pdpy-7* construct. The corresponding transgenes encoding *daf-18* cDNA and *tagrfp* were co-injected at 5 ng/µl together with pPD118.33 (*myo-2::gfp)* at 2.5 ng/µl for the *prab-3* construct. The corresponding transgeens encoding *daf-18* cDNA and *tagrfp* were co-injected at 1 ng/µl together with pPD118.33 (*myo-2::gfp)* at 2.5 ng/µl for the *punc-86* construct. Tissue-specific TagRFP expression was confirmed using Nomarski and fluorescence microscopy. We observed the expected TagRFP pattern for both promoters in

embryos and adults at 20°C and 16°C. For hypodermal expression of DAF-16b and PAK-1, the corresponding transgenes encoding *daf-16b cDNA*::tagrfp or *pak-1 cDNA::tagrfp* were injected at 20 ng/µl together with pPD118.33 (*myo-2::gfp)* at 2.5 ng/µ1. The corresponding transgene encoding *daf-16b cDNA::tagrfp* was injected at 1 ng/µl together with pPD118.33 (*myo-2::gfp)* at 2.5 ng/µl for the *punc-86* construct. To create the *pak-1* transcriptional reporter lines, the corresponding transgenes were injected at 10 ng/µl together with pRF4 *(rol-6)* at 100 ng/µ1. At least there independent transgenic lines have been analyzed for each *pak-1* transcriptional reporter to confirm the expression pattern.

Visualization of the HSN and CAN neurons

The HSN neurons were detected by staining adult hermaphrodites with rabbit anti-serotonin antibody (Sigma) as previously described (Garriga et al., 1993) or by using the *zdIS13[tph-1::gfp]* or *otIs225[cat-4::gfp]* transcriptional reporters. The HSN and CAN in L1 larvae were detected using the *otIs33[kal-1::gfp]* transcriptional reporter.

Microscopy and quantification

Live animals or embryos were mounted on 2% agarose pads and immobilized with 25 mM sodium azide (Sigma). Worms were examined using a Zeiss AxioImager Z1. All phenotypes were scored as percent animals with at least one undermigrated or overmigrated HSN and results are presented as stacked bar graphs to represent the proportion of HSNs in positions along the A-P body axis in these animals. When one or both HSN cell bodies were located posterior or anterior to the vulva in adult animals, the animal was scored as mutant. In the L1 larvae when

one or both HSN cell bodies were located posterior to the developing gonad the animal was scored as mutant. Statistical significance was calculated using the *z*-test.

Single-molecule (sm) FISH

smFISH was done as previously described (Raj et al., 2008). Probes were designed by using the Stellaris RNA FISH probe designer and were received, already conjugated and purified, from Biosearch Technologies. The *pak-1* probe was conjugated to CAL Fluor Red 590. Quantification of smFISH was performed using ImageJ software (Schneider et al., 2012) and the cell counter plug-in to manually count mRNA molecules. Stacks of images were taken automatically with 0.3 microns between z-slices. The quantification of the number of mRNA molecules per hypodermal cell was estimated by counting the number of molecules in each of three z-slices per comma stage embryo and then dividing by 78, the number of embryonic hypodermal cells (Sulston et al., 1983). Statistical significance was calculated using the unpaired *t*-test.

Acknowledgements

We thank I. Greenwald, O. Hobert. J. Canman, and members of the Grishok lab for helpful discussions; Heidi Tissenbaum, Daniel Colón-Ramos, Florence Solari and Oliver Hobert for strains; X. Zhou for help in generating plasmid-based transgenic lines and I. Greenwald for a generous offer of technical assistance by her staff. The *daf-18(ok480)* and *pak-1(ok448)* strains were provided by the *C. elegans* Gene Knockout Project at Oklahoma Medical Research Foundation, which is part of the International *C. elegans* Gene Knockout Consortium. Some strains were provided by the CGC, which is funded by NIH Office of Research Infrastructure Programs (P40 OD010440). This work was supported by "Hormones: Biochemistry and

Molecular Biology" Training Grant T32 DK0007328 and Genetics and Development Training Grant T32 GM007088 to L.M.K. and the Irma T. Hirschl Career Scientist Award to A.G.

Chapter Three: Endogenous RNAi and Chromatin Factor ZFP-1/AF10 Regulate Neuronal Migration in *Caenorhabditis elegans*

(This chapter has not yet been published, but we plan to submit it for publication within the next few months)

Author Contributions

The experiments presented in this chapter were conceived and designed by L.M.K. and A.G. All experiments were carried out and analyzed by L.M.K.

Summary

Endogenous RNAi and the conserved PHD zinc finger protein ZFP-1/AF10 regulate overlapping sets of genes in *C. elegans*, which suggests that they control common biological pathways. We have shown recently that the RNAi factors RDE-4 and ZFP-1 negatively modulate transcription of the insulin/PI3 signaling-dependent kinase PDK-1 to promote *C. elegans* fitness. Moreover, we have demonstrated that the insulin/IGF-1-PI3K signaling pathway regulates the activity of the DAF-16/FOXO transcription factor in the hypodermis to non-autonomously promote the anterior migrations of the hermaphrodite-specific neurons (HSNs) during embryogenesis of *C. elegans*. In this study, we implicate the PHD containing isoform of ZFP-1 and endogenous RNAi in the regulation of HSN migration. ZFP-1 affects HSN migration in part through its negative effect on *pdk-1* transcription and modulation of downstream DAF-16 activity. We also identify a novel role for ZFP-1 and RNAi pathway genes, including RDE-4, in the regulation of HSN migration in parallel to DAF-16. Therefore, the coordinated activities of DAF-16, ZFP-1 and endogenous RNAi contribute to gene regulation during development to ensure proper neuronal migration.

Introduction

With the identification of endogenous small interfering RNAs (endo-siRNAs) in many organisms including plants, fungi, flies, nematodes and mammals (reviewed in Li and Liu, 2011), has come the challenge of identifying their biological and physiological roles. One large class of endo-siRNAs has been termed 22G-RNAs due to the fact that they preferentially begin with guanosine and are 22 nucleotides in length (Gu et al., 2009). There are two main classes of 22G-RNAs, which are designated according to their interacting Argonaute protein. The first are the 22G-RNAs antisense to protein-coding genes, which are in complex with the Argonaute CSR-1 (Chromosome Segregation and RNAi-deficient) (Claycomb et al., 2009; Gu et al., 2009). The second are the 22G-RNAs antisense to transposons, pseudogenes, cryptic loci and some coding genes, which are in complex with the WAGO family of Argonautes (Gu et al., 2009).

RDE-4 is a double stranded RNA (dsRNA)-binding protein and member of the Dicer complex required to initiate silencing in response to exogenous RNAi (Tabara et al., 2002) and for the expression of some endo-siRNAs (Lee et al., 2006; Vasale et al., 2010) in *Caenorhabditis elegans*. It was also shown to cooperate with the RNAi-promoting factor Zinc Finger Protein 1 (ZFP-1) (Dudley et al., 2002; Grishok et al., 2005; Kim et al., 2005) in modulating insulin/IGF-1 signaling (IIS) through its negative effect on transcription of the conserved 3-phosphoinositide-depedent kinase-1 *(pdk-1)* (Mansisidor et al., 2011). The upregulation of *pdk-1* in *rde-4(ne299)* and *zfp-1(ok554)* mutants was shown to be responsible for the increased sensitivity to stress and shortened lifespan observed in these animals (Mansisidor et al., 2011). Since we have recently discovered a novel non-autonomous function of the IIS pathway in the hypodermis, which serves to regulate hermaphrodite-specific neuron (HSN) migration in a DAF-16-dependent manner (Kennedy et al., *in press*), we were intrigued by the possibility that RNAi factors also contribute

to the regulation of IIS during embryogenesis to influence neuronal migration. Indeed, here we describe a role for both RNAi factors and the chromatin factor ZFP-1 in the regulation of HSN migration, in part through the modulation of DAF-16 activity.

ZFP-1 is a homolog of mammalian AF10 (Acute Lymphoblastic Leukemia 1-Fused gene from chromosome 10) and is best known for its role in leukemia caused by its fusion to the mixed lineage leukemia (MLL) gene to create the MLL-AF10 oncogene (Chaplin et al., 1995). However, the normal developmental roles of AF10 remain elusive; therefore, studying the role of its homolog ZFP-1 in *C. elegans* development may help advance our understanding of this protein. In fact, recently, the highly conserved N-terminal plant homeodomain (PHD) fingers of ZFP-1 were shown to be essential for *C. elegans* viability and for its localization to the promoters of target genes (including *pdk-1*) enriched in methylated H3K4 during embryogenesis (Avgousti et al., 2013).

Here we demonstrate that the long isoform of ZFP-1, which contains the N-terminal PHD fingers, is required for HSN migration. Using epistasis analysis we show that the upregulation of *pdk-1* in *zfp-1(ok554)* loss-of-function mutants contributes to the observed HSN undermigration phenotype by limiting DAF-16 activity. Furthermore, we implicate a number of RNAi factors, which include the dsRNA binding protein RDE-4, the dicer-related helicase DRH-3 and the Argonaute CSR-1, in HSN migration. However, these genes are likely to function in parallel to DAF-16. Our study expands the limited understanding of the normal developmental roles of both ZFP-1/AF10 and endogenous RNAi by highlighting their requirement in establishing proper neuronal positioning during development.

Results

C. elegans ZFP-1/AF10 regulates the migration of the HSNs

In our recent study (Kennedy et al., *in press*) we showed that the insulin/IGF-1-PI3K signaling modulates the activity of the DAF-16/FOXO transcription factor in the hypodermis to non-autonomously regulate the anterior migrations of the two bilaterally symmetric HSNs during embryogenesis of *C. elegans*. With the discovery that ZFP-1 negatively regulates *pdk-1*, a component of the IIS pathway, via direct repression of *pdk-1* transcription (Mansisidor et al., 2011), we were prompted to investigate the connection between ZFP-1 and IIS during HSN migration. We found that the *zfp-1(ok554)* loss-of-function mutant (Cui et al., 2006b; Avgousti et al., 2013) and a *zfp-1(op481)* mutant (a generous gift from the Hengartner lab), both of which lead to the generation of mRNAs that contain premature stop codons after the PHD fingers displayed HSN undermigration defects (Figure 3-1A-C). We used a tryptophan hydroxylase GFP reporter (*tph-1::gfp)* to mark the HSNs in adult animals. Furthermore, we stained wild type worms and *zfp-1* mutant worms with an anti-serotonin antibody (Garriga et al., 1993) to exclude the possibility that the *tph-1::gfp* transgene was enhancing or causing the *zfp-1* mutant undermigration phenotype. The extent of HSN undermigration was similar in stained and transgenic worms, thereby ruling out the above possibility (Figure 3-2A-C). These results also suggest that ZFP-1 specifically affects the process of HSN migration, rather than cell fate, since all undermigrated HSNs showed expression of the neurotransmitter serotonin, a late step in HSN maturation (Desai et al., 1988). This is consistent with previous observations in *daf-16* null mutants (Kennedy et al., *in press*).

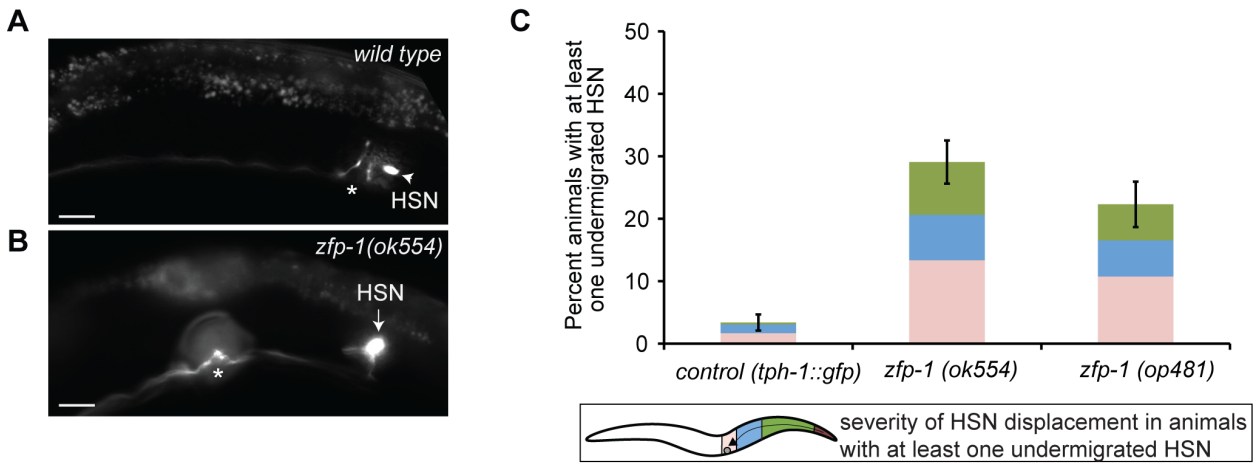

Figure 3-1. HSN undermigration defects in *zfp-1* mutants. (A) Epifluorescent images of the HSN in adults of wild type (A) and *zfp-1(ok554)* mutant animals (B), visualized with a tryptophan hydroxylase GFP reporter (*tph-1::gfp)*. Images are oriented with the posterior of the animal to the right. Asterisks indicate the vulva and arrowheads denote the position of properly migrated HSN(s). The arrow in (B) illustrates a HSN that has failed to migrate the full distance in the *zfp-1(ok554)* mutant animal **(C)** Quantification of the percentage of animals with an undermigrated HSN from a minimum of two pooled independent experiments per strain in control *tph-1::gfp* (n=177) versus *zfp-1(ok554)* (n=172) and *zfp-1(op481)* (n=130) mutants. The stacked bars show information about the position of all HSNs in the affected worms, see the description below. Worm schematic legend: Stacked bars represent the proportion of HSNs at different positions along the A-P body axis within only those animals containing at least one undermigrated HSN. Thus, since there are two HSNs within each animal and not every HSN is affected, one colored region (light pink) represents the wild type HSN that remains unaffected in animals containing a second undermigrated HSN, which is represented by either the red, green or

blue region. For all figures, error bars represent standard error of the proportion (SEP) for the entire stacked column. Scale bars: 20 μm.

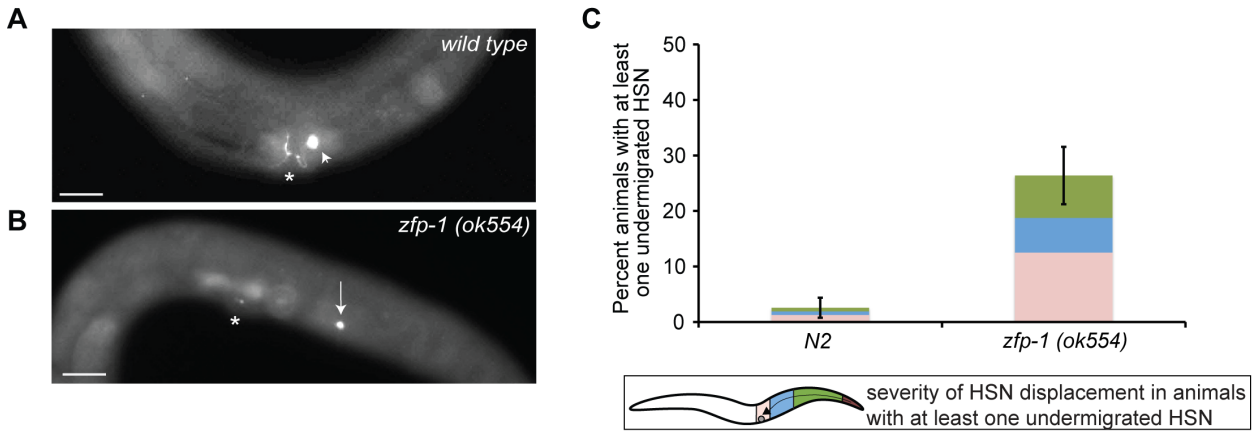

Figure 3-2. HSN migration defects in *zfp-1(ok554)* determined by anti-serotonin staining. **(A)** Epifluorescent images of the HSN stained with anti-serotonin in wild type (A) and *zfp-1(ok554)* adult animals (B). Asterisks indicate the vulva and the arrowhead denotes the position of a properly migrated HSN. The arrow in (B) indicates a HSN that has failed to migrate the full distance from its birthplace in the tail of the *zfp-1(ok554)* mutant animal. Note that undermigrated HSNs still differentiate, as they express the neurotransmitter serotonin, a late step in HSN development. Images are oriented with the posterior of the animal to the right. **(C)** Quantification of the percentage of animals with an undermigrated HSN from two pooled independent experiments in wild type (n=78) versus *zfp-1(ok554)* (n=72) animals. See Figure 3-1 for detailed explanation of worm schematic legend. Error bars represent standard error of the proportion (SEP). Scale bars: 20 μm.

The long isoform of ZFP-1 is required for HSN migration

There are two predicted isoforms of ZFP-1 (Figure 3-3A): a long isoform that encodes a protein containing two PHD fingers, an octapeptide motif (OM) and a leucine zipper motif (LZ), and a shorter isoform that encodes a protein that lacks the PHD fingers but retains the OM and LZ. The OM-LZ motifs present in both the long and short isoforms have been shown to be required for MLL-AF10 mediated oncogenesis (DiMartino et al., 2002), whereas the PHD fingers present in the long isoform of ZFP-1 have recently been shown to be required for early development of *C. elegans* independent of the OM-LZ motifs (Avgousti et al., 2013). Moreover, it was shown that the long isoform of ZFP-1 is enriched at the *pdk-1* promoter during embryogenesis, when HSN migration is occurring (Avgousti et al., 2013). Therefore, we sought to determine if the long isoform of ZFP-1 was required for HSN migration.

First, we made use of two different *zfp-1* fosmid constructs that express recombinant ZFP-1 protein tagged with either GFP or FLAG at the C-terminal portion of the protein (Mansisidor et al., 2011) (Figure 3-3A) to rescue the *zfp-1(ok554)* HSN undermigration phenotype. These constructs express both the long and short isoforms of ZFP-1 along with all the regulatory sequences present at the *zfp-1* locus. We found that both fosmid constructs significantly rescued the HSN undermigration defects present in the *zfp-1(ok554)* mutant (Figure 3-3B). Next, to clarify which isoform(s) were required for rescue we made use of another *zfp-1* fosmid that introduces a FLAG tag downstream of the PHD fingers followed by a stop codon, thereby leaving only the short isoform intact (Avgousti et al., 2013) (Figure 3-3A). In contrast to the fosmids that express both isoforms, this construct was unable to rescue the HSN undermigration defects present in the *zfp-1* mutant (Figure 3-3B). Interestingly, the lethality of *zfp-1* mutant animals when placed in trans to a deficiency chromosome (nDf17) was rescued

using this fosmid expressing the PHD finger region (Avgousti et al., 2013). Combined these results indicate that the short isoform is not sufficient to rescue the migration defects present in the *zfp-1(ok554)* mutant and that the presence of the long isoform containing both the PHD fingers and the C-terminus portion of the protein is required for proper HSN migration.

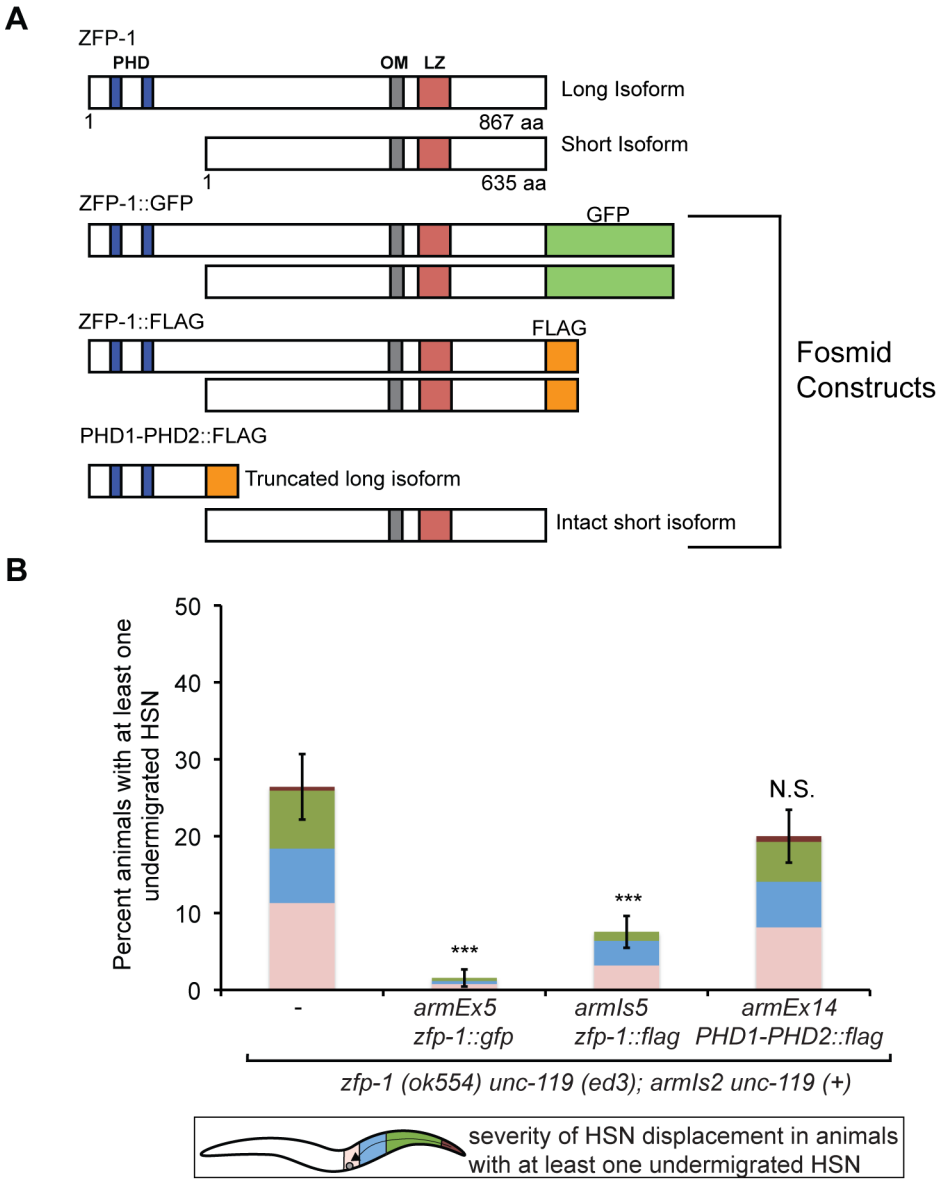

Figure 3-3. The long isoform of ZFP-1 is required for HSN migration. (A) The long isoform of ZFP-1 (867 aa) has two predicted plant homeodomains (PHDs) in the N terminus and an octapeptide motif and leucine zipper in the C-terminus. The short isoform of ZFP-1 (635 aa) lacks the PHD fingers but retains the OM-LZ motifs. *zfp-1* fosmid constructs used to rescue the HSN undermigration defects present in *zfp-1(ok554)* mutant are illustrated below the ZFP-1 proteins. **(B)** Two different ZFP-1 fosmid constructs rescue the HSN undermigration defects in the *zfp-1(ok554)* mutants. The ZFP-1 fosmid construct expressing only an intact short isoform did not rescue the HSN undermigration defects present in the *zfp-1* mutant. Quantification of the percentage of animals with an undermigrated HSN from a minimum of two pooled independent experiments per strain in the (-) control *armIs2 Unc-119 (+); zfp-1(ok554) unc-119 (ed3)* (n=106) versus the addition of the *armEx5 zfp-1::gfp* (n=128), *armIs5 zfp-1::flag* (n=172) or *armEx14 PHD1-PHD2::flag* (n=135) fosmids into the (-) control background. HSNs were visualized with a *tph-1::gfp* reporter. See Figure 3-1 for detailed description of worm schematic legend. ***p<0.001 (*z*-test). Error bars represent SEP.

ZFP-1 works in parallel and through DAF-16 to control HSN migration

ZFP-1 has been shown to negatively regulate *pdk-1* expression at multiple developmental stages (Mansisidor et al., 2011), including the embryo (Figure 3-4). To determine whether the HSN undermigration phenotype present in *zfp-1* loss-of-function mutants was due to a de-repression of *pdk-1* expression and increased insulin/IGF-1 signaling leading to decreased nuclear DAF-16 activity (Figure 3-5A) we performed epistasis analysis between *zfp-1* and IIS pathway components. We created a double mutant strain between *zfp-1(ok554)* and the null allele *daf-16(mu86)* (Lin et al., 1997) to establish whether DAF-16 is the sole output of ZFP-1

involved in HSN migration. We observed a significant enhancement of the *daf-16(mu86)* HSN undermigration phenotype, indicating that the undermigration phenotype present in *zfp-1(ok554)* mutants cannot be attributed exclusively to decreased DAF-16 activity (Figure 3-5B).

Next, we asked whether or not the HSN undermigration defects in *zfp-1(ok554)* could be contributed, in part, to reduced DAF-16 activity due to increased *pdk-1* expression. We performed epistasis analysis between the *pdk-1(sa709)* loss-of-function mutant (Paradis et al., 1999; Mansisidor et al., 2011) and the *zfp-1(ok554)* mutant to determine whether decreasing *pdk-1* expression in the *zfp-1* mutant background could suppress the HSN undermigration defects. We observed a significant suppression of HSN undermigration defects in the double mutant (Figure 3-5C), suggesting that repression of *pdk-1* by ZFP-1 plays a role in regulating HSN migration.

In order to further demonstrate that enhanced insulin/IGF-1 signaling in the *zfp-1(ok554)* mutant is responsible for inhibiting HSN migration we also performed epistasis analysis between *zfp-1(ok554)* and *age-1(hx546)/*PI3K reduction-of-function mutants (Friedman and Johnson, 1988; Tissenbaum and Ruvkun, 1998). Similar to our analysis of *pdk-1* and *zfp-1* mutants we also observed a significant suppression of HSN undermigration defects in *age-1; zfp-1* double mutants (Figure 3-5D). To determine whether the suppression of the *zfp-1* mutant phenotype in IIS pathway mutants was due to a release of DAF-16 inhibition, we created a triple mutant: *daf-16(mu86); age-1(hx546); zfp-1(ok554)* to remove *daf-16* activity from the *age-1; zfp-1* double mutant. We determined that a loss of *daf-16* activity in the *age-1; zfp-1* double mutant background now prevented the suppression of the *zfp-1(ok554)* mutant phenotype by *age-1(hx546)* (Figure 3-5D). Together, our results suggest that the negative regulation of the IIS pathway by ZFP-1 contributes to the control of HSN migration in a DAF-16-dependent manner.

Furthermore, consistent with our observations that ZFP-1 regulates the IIS pathway, which functions non-autonomously in HSN migration (Kennedy et al., *in press*), we find that the cDNA of the long isoform fused to GFP driven by the *unc-86* promoter, which is expressed in a subset of neurons including the HSN (Baumeister et al., 1996), does not rescue the HSN undermigration defects seen in *zfp-1(ok554)* mutants (Figure 3-6). This suggests that ZFP-1 is likely to also function non-autonomously to promote HSN migration.

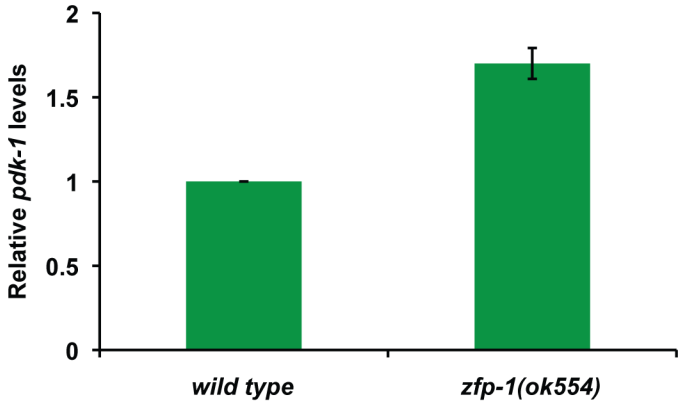

Figure 3-4. Relative *pdk-1* mRNA expression in mixed embryos. mRNA expression of *pdk-1* in *zfp-1(ok554)* and wild type worms was measured by RT-qPCR and normalized to wild type. Actin (*act-3)* was used as an internal control. Results of two biological replicas are shown; error bars represent Standard deviation.

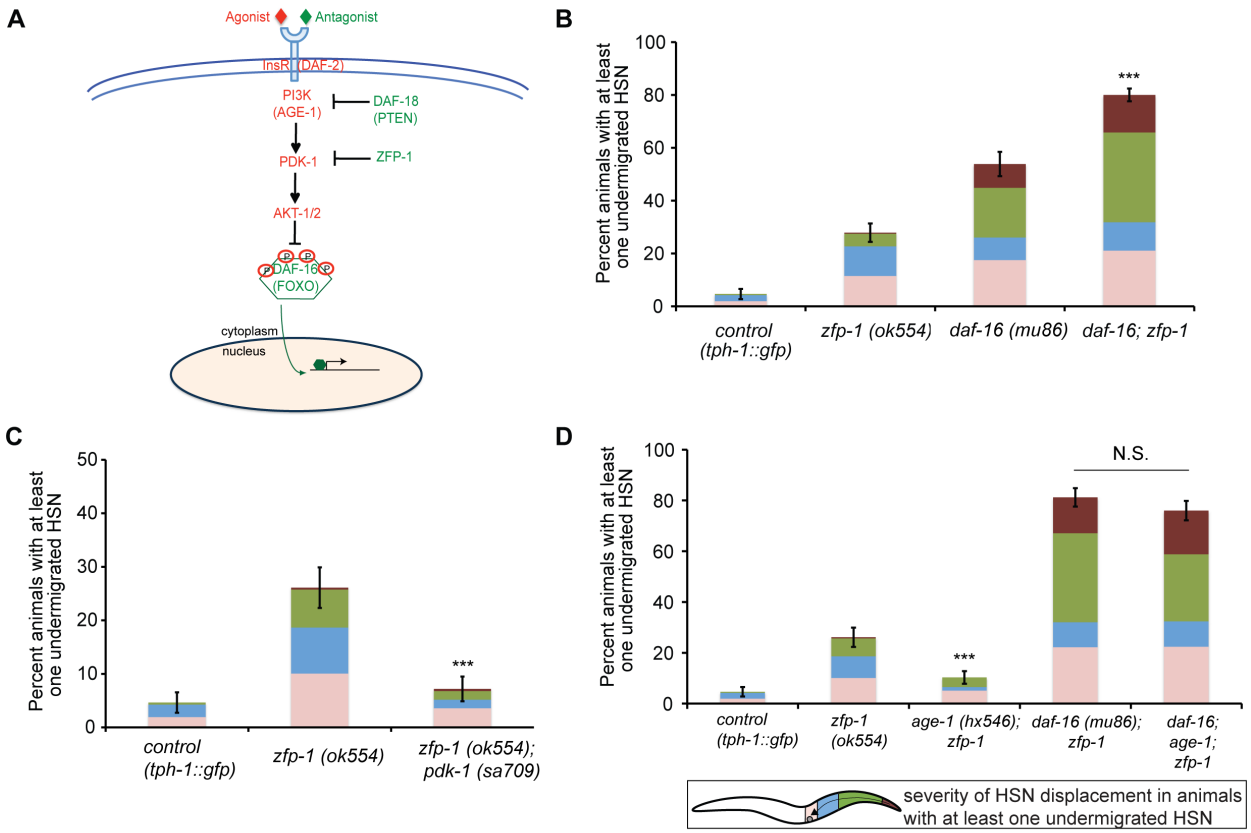

Figure 3-5. ZFP-1 functions through DAF-16 and in parallel to DAF-16 to regulate HSN migration. (A) The IIS pathway. When pathway components in red are active, DAF-16 is phosphorylated and inactive due to its retention in the cytoplasm. When pathway components in green are active, DAF-16 is no longer phosphorylated and can translocate into the nucleus to regulate its target genes. **(B)** The *zfp-1(ok554)* mutant enhances the *daf-16(mu86)* null mutant. Quantification of the percentage of animals with an undermigrated HSN from at least two pooled independent experiments per strain in control *tph-1::gfp* (n=129) versus *zfp-1(ok554)* (n=165), *daf-16(mu86)* (n=117) and *daf-16(mu86); zfp-1(ok554)* (n=275) mutant animals. **(C)** A *pdk-1* loss-of-function mutant suppresses the HSN undermigration defects in *zfp-1* mutant animals. Quantification of the percentage of animals with an undermigrated HSN from two pooled

independent experiments per strain in control *tph-1::gfp* (n=129), *zfp-1(ok554)* (n=134) and *zfp-1(ok554); pdk-1(sa709)* (n=125) mutant animals. Note that *pdk-1(sa709)* animals do not exhibit HSN migration defects at 20 °C (not shown). **(D)** An *age-1(hx546)* loss-of-function mutant suppresses the HSN undermigration defects in *zfp-1* mutant animals in a DAF-16-dependent manner. Quantification of the percentage of animals with an undermigrated HSN from two pooled independent experiments per strain in control *tph-1::gfp* (n=129) versus *zfp-1(ok554)* (n=134), *age-1(hx546); zfp-1(ok554)* (n=146) and *daf-16(mu86); age-1(hx546); zfp-1(ok554)* (n=125). Note that *age-1(hx546)* animals do not exhibit HSN migration defects at 20 °C (not shown). HSNs were visualized with a *tph-1::gfp* reporter. See Figure 3-1 for detailed description of worm schematic legend. ***p<0.001 (*z*-test). Error bars represent SEP.

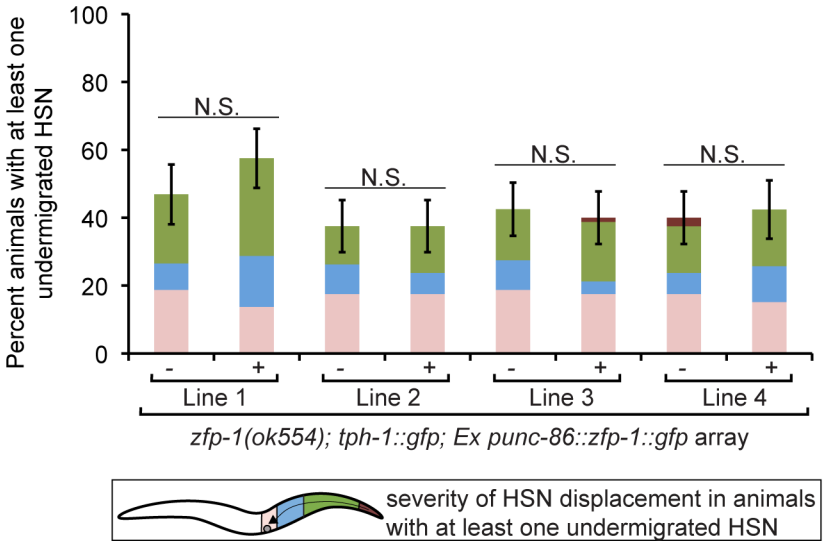

Figure 3-6. ZFP-1 may function non-autonomously to promote HSN migration. Expression of ZFP-1::GFP in the HSN does not rescue the HSN undermigration defect of *zfp-1(ok554)* mutants. The *zfp-1(ok554)* mutants that had the transgenic array (+) or their siblings that had lost

the array (-) were scored. Number of animals scored per line are: Line 1: (-) n=32 and (+) n=40; Line 2: (-) n=40 and (+) n=40; Line 3: (-) n=40 and (+) n=40; Line 4: (-) n=40 and (+) n=33. HSNs were visualized with a *tph-1::gfp* reporter. See Figure S3-1 for detailed description of worm schematic legend. The *z*-test was used to determine significance. Error bars represent SEP.

RNAi factors RDE-4, DRH-3 and CSR-1 regulate HSN migration

A genome-wide expression study has revealed that ZFP-1 and RDE-4, a dsRNA binding protein required for the initiation of exogenous RNAi (Tabara et al., 2002), regulate close to 250 overlapping genes (Grishok et al., 2008). Consistent with this finding, both RDE-4 and ZFP-1 have been shown to affect longevity and the stress response by negatively regulating the conserved IIS kinase *pdk-1* (Mansisidor et al., 2011). Therefore, we examined a null allele of *rde-4* (Tabara et al., 2002), as well as 11 other RNAi components for their involvement in HSN migration (Table 3-1). We crossed RNAi mutants to a *tph-1::gfp* reporter strain and identified three mutants that display HSN migration defects: *rde-4(ne299)* null mutant (Tabara et al., 2002), *drh-3(ne4253)* loss-of-function mutant (Gu et al., 2009), and a *csr-1(tm892)* partially rescued strain (Claycomb et al., 2009) (Table 3-1 and Figure 3-7A). Strikingly, the highest percentage of migration defects was observed in *rde-4* null mutants, with almost all affected animals exhibiting migration defects in both HSNs, as shown by the relatively small proportion of HSNs in the wild type position (pink stack on column). *drh-3* encodes a dicer-related helicase, which participates in multiple branches of endogenous RNAi in *C. elegans* (Gu et al., 2009), and *csr-1* encodes an Argonaute, which binds 22G-RNAs antisense to protein-coding genes (Claycomb et al., 2009; Gu et al., 2009). Consistent with only a reduction-of-function in the *drh-3* and *csr-1* mutants, fewer animals exhibited HSN migration defects compared to the *rde-4* null

mutant (Figure 3-7A). We used a *drh-3* loss-of-function allele since null mutants are infertile (Gu et al., 2009). Since *csr-1(tm892)* mutants are also sterile we used a partially rescued transgenic strain, where CSR-1 is expressed in the germline to produce 38% viable progeny (Claycomb et al., 2009) that we could analyze for migration defects.

To further confirm that the HSN undermigration defect we observed in *rde-4* null mutants is due to mutations in *rde-4* and not to the background of the strain we placed the *rde-4(ne299)* allele over a deficiency allele, nDf17, which is balanced by chromosome qC1 [*dpy-19(e1259) glp-1(q339)*] (Edgley et al., 2006). We crossed *rde-4(ne299)* males to nDf17/qC1 animals and scored F1 animals for HSN migration defects. We determined the genotypes of the F1 animals by the presence or absence of the qC1 phenotypes, which are dumpy and sterile, segregating in the F2 generation. Only F1 animals carrying the deficiency allele, nDf17, displayed penetrant HSN undermigration defects (Figure 3-7B). Moreover, we also stained *rde-4(ne299)* worms with an anti-serotonin antibody (Garriga et al., 1993) to further exclude the possibility that the HSN undermigration defects observed in *rde-4* null animals were the result of transgene background effects. We observed HSN undermigration defects in stained worms without the *tph-1::gfp* transgene (Figure 3-8). Similar to *zfp-1* mutants, *rde-4* mutants are not affected in the production of serotonin since undermigrated HSNs still express the neurotransmitter. In addition, we have also determined that RDE-4 is likely to be required zygotically for HSN migration since all *rde-4* null animals obtained from *rde-4/+* mothers exhibited HSN migration defects to the same extent as animals derived from *rde-4/rde-4* mothers (data not shown).

Table 3-1. RNAi mutants surveyed for HSN migration defects

RNAi pathway gene	Class	Nature of mutation	HSN migration defect?
alg-1 (gk214)	Argonaute	Lof	No
C04f12.1(tm1637)	Argonaute	Lof	No
csr-1 (tm892)	Nuclear Argonaute	Partially rescued mutant	Yes
drh-3 (ne4253)	Helicase	Lof	Yes
ergo-1 (tm1860)	Argonaute	Lof	No
nrde-3 (gg066)	Argonaute	Null	No
rde-1 (ne300)	Argonaute	Putative null	No
rde-3 (ne298)	Nucleotidyl-transferase	Strong lof	No
rde-4 (ne299)	dsRNA binding	Null	Yes
rrf-1 (pk1417)	RdRP	Null	No
rrf-2 (ok210)	RdRP	Null	No
rrf-3 (pk1426)	RdRP	Null	No

A

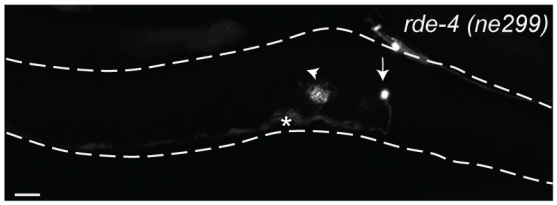
rde-4 (ne299)

B

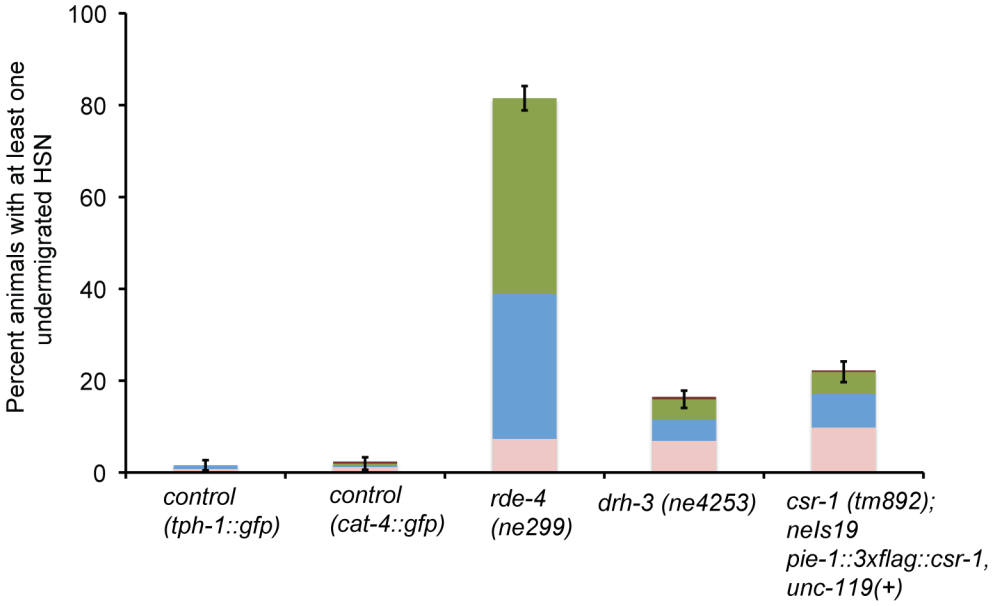
Percent animals with at least one undermigrated HSN
100
80
60
40
20
0
control (tph-1::gfp)
control (cat-4::gfp)
rde-4 (ne299)
drh-3 (ne4253)
csr-1 (tm892); neIs19 pie-1::3xflag::csr-1, unc-119(+)

C

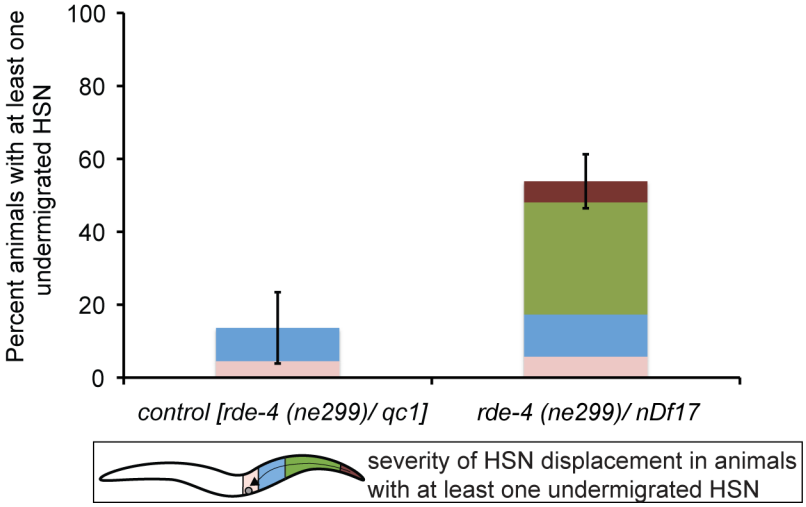
Percent animals with at least one undermigrated HSN
100
80
60
40
20
0
control [rde-4 (ne299)/ qc1]
rde-4 (ne299)/ nDf17
severity of HSN displacement in animals with at least one undermigrated HSN

Figure 3-7. RNAi pathway genes *rde-4, drh-3* and *csr-1* affect HSN migration.

(A) Epifluorescent image of the HSNs in an adult *rde-4(ne299)* mutant animal visualized with a tryptophan hydroxylase GFP reporter (*tph-1::gfp)*. Image is oriented with the posterior of the animal to the right. Asterisk indicates the vulva and the arrowhead denotes the position of a properly migrated HSN. The arrow illustrates a HSN that has failed to migrate the full distance from its birthplace in the tail. **(B)** Quantification of the percentage of animals with an undermigrated HSN from a minimum of three pooled independent experiments per strain in *tph-1::gfp* (n=127) and *cat-4::gfp* (n=127) controls versus *rde-4(ne299)* (n=211), *drh-3(ne4253)* (n=376) and the partially rescued *csr-1(tm982)* (n=342) mutant animals. Note that the *cat-4::gfp* reporter was used to visualize the HSNs in the partially rescued *csr-1(tm892)* strain. **(C)** Placing *rde-4(ne299)* over a deficiency allele, nDf17, also resulted in HSN undermigration defects. Quantification of the percentage of animals with an undermigrated HSN in control animals (*rde-4(ne299)/*qC1) (n=22) versus *rde-4(ne299)*/nDf17 animals (n=26). HSNs were visualized with a *tph-1::gfp* reporter. See Figure 3-1 for detailed description of worm schematic legend. Error bars represent SEP.

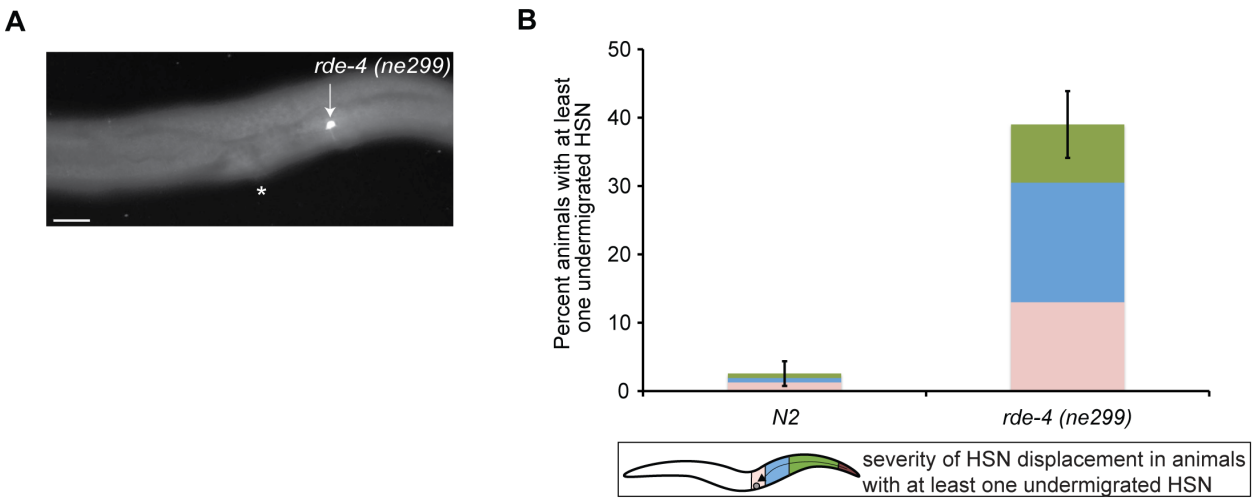

Figure 3-8. HSN migration defects in *rde-4(ne299)* determined by anti-serotonin staining. **(A)** Epifluorescent image of the HSN stained with anti-serotonin in *rde-4(ne299)* animals (B). Asterisks indicate the vulva and the arrow indicates a HSN that has failed to migrate the full distance from its birthplace in the tail to flank the vulva. Note that undermigrated HSNs still differentiate, as they express the neurotransmitter serotonin, a late step in HSN development. Image is oriented with the posterior of the animal to the right. **(B)** Quantification of the percentage of animals with an undermigrated HSN from two pooled independent experiments in wild type (n=78) versus *rde-4(ne299)* (n=100) animals. See Figure 3-1 for detailed description of worm schematic legend. Error bars represent SEP. Scale bars: 20 μm.

RDE-4 works in parallel to DAF-16

Since RDE-4 was shown to inhibit *pdk-1* transcription (Mansisidor et al., 2011), we performed genetic epistasis between the *rde-4* mutant and IIS pathway components to determine if RDE-4, like ZFP-1, also regulates HSN migration in part by inhibiting IIS to promote DAF-16 nuclear localization. First, we combined the *rde-4(ne299)* null allele with the *daf-16(mu86)* null

allele and observed a significant enhancement of the *daf-16* null phenotype (Figure 3-9A). Furthermore, although the *rde-4* null phenotype is not enhanced for the percentage of animals affected, the severity of the undermigrated HSNs along the anterior-posterior body axis resemble the *daf-16* phenotype, suggesting an additive effect between the two mutants (Figure 3-9A). Combined, these results suggest that *rde-4* and *daf-16* are working in parallel genetic pathways to affect HSN migration.

Since we found that the *zfp-1* mutant phenotype can be suppressed by a reduction in *pdk-1* and *age-1* expression we also performed epistasis analysis between *rde-4(ne299)* and either the *pdk-1(sa709)* mutant or the *age-1(hx546)* mutant to determine if *rde-4(ne299)* could also be suppressed by reduced IIS. In contrast to epistasis experiments with *zfp-1,* we observed no suppression of the HSN undermigration defects in either double mutant combination (Figure 3-9B-C). These results indicate that RDE-4 is unlikely to contribute to the regulation of HSN migration through repression of *pdk-1*.

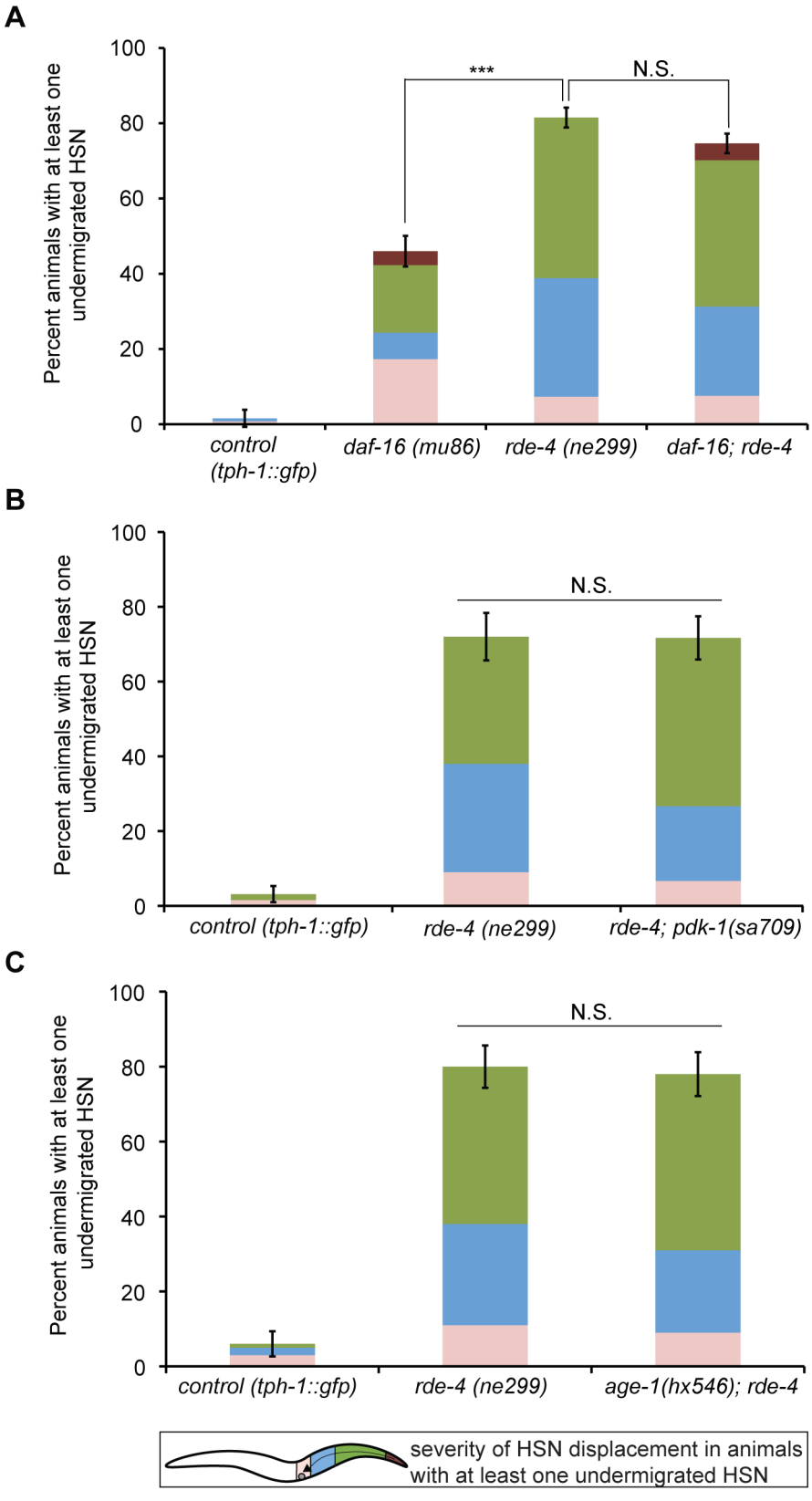
A
Percent animals with at least one undermigrated HSN
100
80
60
40
20
0
***
N.S.
control (tph-1::gfp)
daf-16 (mu86)
rde-4 (ne299)
daf-16; rde-4
B
Percent animals with at least one undermigrated HSN
N.S.
control (tph-1::gfp)
rde-4 (ne299)
rde-4; pdk-1(sa709)
C
Percent animals with at least one undermigrated HSN
N.S.
control (tph-1::gfp)
rde-4 (ne299)
age-1(hx546); rde-4
severity of HSN displacement in animals with at least one undermigrated HSN

Figure 3-9. RDE-4 works in parallel to DAF-16 to regulate HSN migration. (A) Quantification of the percentage of animals with an undermigrated HSN from a minimum of two pooled independent experiments per strain in control *tph-1::gfp* (n=127) versus *daf-16(mu86)* (n=150), *rde-4(ne299)* (n=211) and *daf-16(mu86); rde-4(ne299)* (n=270) mutant animals. **(B)** A *pdk-1* loss-of-function mutant does not suppress *rde-4* null HSN undermigration defects. Quantification of the percentage of animals with an undermigrated HSN in control *tph-1::gfp* (n=64) versus *rde-4(ne299)* (n=50), *rde-4(ne299); pdk-1(sa709)* (n=60). **(C)** An *age-1* loss-of-function mutant does not suppress *rde-4* null HSN undermigration defects. Quantification of the percentage of animals with an undermigrated HSN in control *tph-1::gfp* (n=50) versus *rde-4(ne299)* (n=50) and *age-1(hx546); rde-4(ne299)* mutant animals. HSNs were visualized with a *tph-1::gfp* reporter. See Figure 3-1 for detailed description of worm schematic legend. ***p<0.001 (*z*-test). Error bars represent SEP.

Discussion

Our genetic analysis has identified the conserved chromatin factor ZFP-1/AF10, the dsRNA binding protein RDE-4, the dicer-related helicase DRH-3 and the Argonaute CSR-1 as regulators of neuronal migration during *C. elegans* embryogenesis. We demonstrate that ZFP-1 affects HSN migration in part through its negative regulation of the conserved IIS kinase *pdk-1* (Mansisidor et al., 2011) and the modulation of downstream DAF-16/FOXO activity, which we have previously shown to act in the hypodermis to promote HSN migration (Kennedy et al., *in press*). We also show that both ZFP-1 and RDE-4 work in parallel to DAF-16 to regulate HSN migration during embryogenesis.

Recently, mammalian AF10 has been shown to exist in a complex with the H3K79 histone methyltransferase DOT1L (Mohan et al., 2010). The Oncogenic MLL fusion protein MLL-AF10 has previously been implicated in the recruitment of DOT1L to chromatin by the OM-LZ motifs of AF10 (Okada et al., 2005). The DOT1L complex, called DotCom, is involved in mediating global H3K79 methylation by DOT1L (Mohan et al., 2010). Interestingly, β-catenin, an important downstream mediator of Wnt signaling was shown to co-immunoprecipitate with DOT1L complex components in HEK293T cells (Mohan et al., 2010). Moreover, reduced expression of Wingless/Wnt targets in *drosophila* larvae was observed after knockdown of the AF10 ortholog *Alhambra* (or *Dalf,)*, as well as after the knockdown of other DotCom orthologs (Mohan et al., 2010). Additionally, AF10 was independently found in a complex with the downstream effectors of Wnt signaling TCF4 and β-catenin in colorectal cancer cells and implicated in the regulation of Wnt target genes in these cells as well as in *zebrafish* (Mahmoudi et al., 2010).

It is well known that Wnt signaling controls HSN migration in a β-catenin-independent manner (Harris et al., 1996; Forrester et al., 2004) by acting as a repellent to guide the HSN out of the embryonic tail and into the mid-body of the animal (Pan et al., 2006). However, the connection between AF10 and canonical Wnt signaling (β-catenin-dependent) in vertebrates highlights the intriguing possibility that the interaction between ZFP-1/AF10 and Wnt pathway components may be conserved in *C. elegans.* Based on our observations that ZFP-1 regulates the IIS pathway, which functions non-autonomously in HSN migration (Kennedy et al., *in press*), and the failure of an HSN-specific promoter driving the expression of a ZFP-1::GFP transgene to rescue the HSN undermigration defects in *zfp-1* mutant animals (this study, Figure S3-3), it is likely that ZFP-1 functions non-autonomously to promote HSN migration. One possibility is that

ZFP-1, independently or in combination with DAF-16, regulates the transcription of the Wnts, which affect HSN migration non-autonomously (Pan et al., 2006). Another possibility is that ZFP-1 regulates the transcription of negative regulators of Wnt signaling, such as CAM-1, that can function as a sink to limit extracellular Wnt and impede HSN migration (Kim and Forrester, 2003; Forrester et al., 2004; Green et al., 2007). Future studies will elucidate these potential roles of ZFP-1 in the regulation of Wnt signaling during HSN migration.

There are multiple endo-siRNA pathways in *C. elegans* including the CSR-1 RNAi pathway (Claycomb et al., 2009; Gu et al., 2009), the WAGO RNAi pathway (Gu et al., 2009) and the ERI RNAi pathway (Lee et al., 2006; Gent et al., 2009; Han et al., 2009; Vasale et al., 2010). The determinants that differentiate these pathways from one another include whether they are Dicer-dependent or independent, the length of the endo-siRNAs produced (26 nucleotides (26G) versus 22 nucleotides (22G)) and the interacting Argonaute(s). Dicer-independent endo-siRNAs produced de novo by RNA-dependent polymerases (RdRPs) (Ruby et al., 2006; Aoki et al., 2007; Pak and Fire, 2007) are termed 22G-RNAs.

The biological roles of the endo-RNAi pathways in *C. elegans* remain largely uncharacterized. A major known role of the WAGO endo-RNAi pathway is in genome surveillance: the silencing of transposable elements, aberrant transcripts (Gu et al., 2009) and gene duplications (Vasale et al., 2010; Fischer et al., 2011). The ERI (Enhanced RNAi) pathway has been implicated in regulating genes required for spermatogenesis and fertility (Han et al., 2009; Conine et al., 2010). Moreover, the CSR-1 RNAi pathway has been recently shown to positively regulate histone mRNA expression (Avgousti et al., 2012). Mutations in *rde-4*, on the other hand, have been associated with decreased lifespan (Welker et al., 2007; Mansisidor et al., 2011) and increased sensitivity to oxidative stress (Mansisidor et al., 2011) and temperature

(Blanchard et al., 2011). An increase in stress sensitivity and reduced lifespan of *rde-4* mutants has been attributed to the upregulation of *pdk-1*(Mansisidor et al., 2011). Here, we describe a novel zygotic role for RDE-4 in embryonic neuronal migration, which is consistent with the previous observations that some somatic 22G-RNAs are dependent on RDE-4 (Lee et al., 2006; Gu et al., 2009).

The majority of 22G-RNAs that are in the complex with the Argonaute CSR-1 are antisense to protein-coding genes (Claycomb et al., 2009), suggesting that multiple genes and genetic pathways may be regulated by endo-siRNAs. Similar to the regulation of embryonic HSN migration, both CSR-1 and DRH-3 have been implicated in another embryonic process: the specification of the excretory duct cell, a component of the worms renal system (Rocheleau et al., 2008). A genome-wide RNAi screen identified these RNAi pathway genes to act redundantly with the KSR-1 (kinase suppressor of Ras) scaffolding protein for Ras-mediated excretory duct cell specification (Rocheleau et al., 2008). Since DRH-3 is a component of the RdRP complex (Gu et al., 2009; Thivierge et al., 2012) required for the biogenesis of all 22G-RNAs, including those present in the complex with CSR-1 (Gu et al., 2009), it is most likely that DRH-3-dependent CSR-1-bound endo-siRNAs regulate a number of genes affecting HSN migration.

Furthermore, a regulatory pathway involving a two-step process for endo-siRNA production implicated RDE-4 and Dicer in the production of 26G-RNAs, which subsequently drive the biogenesis of some WAGO-bound 22G-RNAs (Vasale et al., 2010). Therefore, it is possible that RDE-4 works upstream of the CSR-1 22G-RNA pathway to cooperate in regulating genes affecting HSN migration. Surprisingly, none of the RdRPs implicated in 26G-RNA production (Vasale et al., 2010) displayed an HSN migration phenotype when examined in a null

mutant background (Table 3-1). One possible explanation for this is redundancy among the RdRPs required for HSN migration.

Our work has highlighted a novel biological role for the conserved chromatin factor ZFP-1/AF10 and the endo-siRNA pathway in neuronal migration of *C. elegans*. Future studies will determine if ZFP-1 and RNAi cooperate to regulate specific 22G-RNA target genes required for HSN migration and whether these small RNAs act positively, which has been shown recently for the core histones (Avgousti et al., 2012), or negatively to influence gene expression.

Material and Methods

C. elegans Strains

Strains were maintained at 20°C using standard methods (Brenner, 1974). Bristol N2 was the wild-type strain used. The following strains were provided by the Hobert lab: SK4013 *zdIs13*(*tph-1::gfp)*IV (Clark and Chiu, 2003) and OH8482 *otIs225(cat-4::gfp)II; him-8IV*. The following strain was provided by the Hengartner lab: *zfp-1(op481)*III. The following mutant and transgenic strains were obtained through the *Caenorhabditis* Genetics Center: LGI: CF1038 *daf-16(mu86),* WM153 *C04F12.1(tm1637),* WM206 *drh-3(ne4253),* WM30 *rde-3(ne298),* NL2098 *rrf-1(pk1417),* EL476 *rrf-2(ok210),* LGII: TJ1052 *age-1(hx546),* NL2099 *rrf-3(pk1426),* LGIII: RB774 *zfp-1(ok554),* WM49 *rde-4(ne299),* CB4681 nDf17/qC1 dpy-19(e1259) glp-1(q339), LGIV: WM193 {*csr-1(tm892)*IV; *neIs20* [pie-1::3xFLAG::csr-1 + unc-119(+)]}, LGV: WM158 *ergo-1(tm1860), rde-1(ne300),* LGX: JT709 *pdk-1(sa709),* VC446 *alg-1(gk214).* Compound mutant strains and transgenes used are as follows: AGK82: *zfp-1(ok554)*III; *tph-1::gfp*IV, AGK153: *zfp-1(op481)*III*; tph-1::gfp*IV, AGK154: {*zfp-1(ok554) unc-119(ed3)*III; *tph-1::gfp*IV; *armIs5* [ZFP-1::FLAG *unc-119*(+)]}, AGK133: {*zfp-1(ok554) unc-119(ed3)*III; *tph-1::gfp*IV;

armEx5 [ZFP-1::GFP *unc-119*(+)]}, AGK156: {*zfp-1(ok554) unc-119(ed3)*III; *tph-1::gfp*IV; *armEx14* [PHD1-PHD2::FLAG ZFP-1 short *unc-119*(+)]}, AGK211: {*zfp-1(ok554) unc-119(ed3)*III; *tph-1::gfp*IV; *armIs2* [*unc-119*(+)]}, AGK343: {*zfp-1(ok554)*III; *tph-1::gfp*IV; *armEx91* [*punc-86::zfp-1(long isoform)::gfp* pPD118.33 (*myo-2::gfp)*]} (line 1 in this paper), AGK335: {*zfp-1(ok554)*III; *tph-1::gfp*IV; *armEx85 armEx91* [*punc-86::zfp-1(long isoform)::gfp* pPD118.33 (*myo-2::gfp)*]} (line 2 in this paper), AGK336: {*zfp-1(ok554)*III; *tph-1::gfp*IV; *armEx86 armEx91* [*punc-86::zfp-1(long isoform)::gfp* pPD118.33 (*myo-2::gfp)*]} (line 3 in this paper), AGK339 {*zfp-1(ok554)*III; *tph-1::gfp*IV; *armEx89 armEx91* [*punc-86::zfp-1(long isoform)::gfp* pPD118.33 (*myo-2::gfp)*]} (line 3 in this paper), AGK580: *daf-16(mu86)*I; *tph-1::gfp*IV, AGK236: *pdk-1(sa709)*X; *tph-1::gfp*IV, AGK155: *zfp-1(ok554)*III; *pdk-1(sa709)*X; *tph-1::gfp*IV, AGK470: *age-1(hx546)*II; *tph-1::gfp*IV, AGK285: *age-1(hx546)*II; *zfp-1(ok554)*III; *tph-1::gfp*IV, AGK277: *daf-16(mu86)*I; *age-1(hx546)*II; *zfp-1(ok554)*III; *tph-1::gfp* IV, AGK98: *rde-4(ne299)*III; *tph-1::gfp*IV, AGK246: *rde-4(ne299)*III; *pdk-1(sa709)*X; *tph-1::gfp*IV, AGK268: *age-1(hx546)*II; *rde-4(ne299)*III; *tph-1::gfp*IV, AGK124: *alg-1(gk214)*X; *tph-1::gfp*IV, AGK81: *C04F12.1(tm1637)*I; *tph-1::gfp*IV, AGK208: {*csr-1(tm892)*IV; *tph-1::*gfpIV; *neIs20* [pie-1::3xFLAG::csr-1 + unc-119(+)]}, AGK654: *drh-3(ne4253)*I; *tph-1::gfp*IV, AGK146: *tph-1::gfp*IV; *ergo-1(tm1860)*V, AGK144: *nrde-3(gg066)*; *tph-1::gfp*IV, AGK218: *tph-1::gfp*IV; *rde-1(ne300)*V, AGK194: *rde-3(ne298)*I; *tph-1::gfp*IV, AGK123: *rrf-1(pk1417)*I; *tph-1::gfp*IV, AGK121: *rrf-2(ok210)*I; *tph-1::gfp*IV, AGK145: *rrf-3(pk1426)*II; *tph-1::gfp*IV, AGK276: *daf-16(mu86)*I; *rde-4(ne299)*III; *tph-1::gfp* IV, AGK85: *daf-16(mu86)*I; *zfp-1(ok554)*III; *tph-1::gfp*IV.

Molecular Biology and Transgenic Lines

Standard molecular biology techniques were used to construct transgenes. Germline transformation was performed by direct injection of various plasmid DNAs into the gonads of adult wild type animals as described (Mello et al., 1991). A *zfp-1(long isoform)* cDNA was obtained by PCR with N2 cDNA as a template with the forward primer containing a BalI site 5'-ATGAAGAAGTGGCCAATGAAGGAGATGGTAGGTGGATGC-3' and the reverse primer containing an AgeI site 5'-CAAGTTATTGGTTACCGGTCCTTTTCCATTCGGAGTTGCAGATG-3.' A 5.1 kb fragment upstream of the *unc-86* transcriptional start site was isolated by PCR from genomic DNA with the forward primer containing an SphI site 5'-CGTGACACTGCATGCTTCAAAAACTGTCAACTAACAAGAT -3' and the reverse primer containing a SalI site 5'-CGGATGCGGTTGTCGACTCATTCAATTTCACTTTTTCATTCG -3.' The *zfp-1* cDNA and the *unc-86* promoter were subcloned into the Fire Kit GFP vector pPD95.75. The resulting *punc86::zfp-1::gfp* transgene was injected at 0.5 ng/µl with the co-injection marker pPD118.33 (*myo-2::gfp)* at 4 ng/µl. Tissue-specific GFP expression was confirmed using Nomarski and fluorescence microscopy.

Visualization of the HSN neurons

The HSN neurons were detected by staining adult hermaphrodites with rabbit anti-serotonin (Sigma) as previously described (Garriga et al., 1993) or by using the *zdIS13[tph-1::gfp]* or *otIs225[cat-4::gfp]* transcriptional reporters.

Microscopy and quantification

Live animals or embryos were mounted on 2% agarose pads and immobilized with 25 mM sodium azide (Sigma). Worms were examined using a Zeiss AxioImager Z1. All phenotypes were scored as percent animals with at least one undermigrated HSN and results are presented as stacked bar graphs to represent the proportion of HSNs in positions along the A-P body axis in these animals. When one or both HSN cell bodies were located posterior to the vulva in adult animals, the animal was scored as mutant. Statistical significance was calculated using the *z*-test.

RNA extraction and RT-PCR. RNA extraction and reverse transcriptase PCR (RT-PCR) was carried out as described previously (Mansisidor et al., 2011). The following primers were used to detect the *pdk-1* transcript: 5'-CCTACAGCCAGGTATTCCG-3' (Forward) and 5'-GATCACGAAATAAATTCTAGCCTGG-3.'

Acknowledgements

We thank I. Greenwald, O. Hobert and members of the Grishok lab for helpful discussions; G. Cecere and A. Mansisidor for generating the fosmid-based transgenic strains; M. Hengartner and Stephan Gysi for providing the *zfp-1(op481)* allele and for sharing data before publication; X. Zhou for help in generating plasmid-based transgenic lines and I. Greenwald for a generous offer of technical assistance by her staff. The *zfp-1(ok554)* and *rrf-2(ok210)* strains were provided by the *C. elegans* Gene Knockout Project at Oklahoma Medical Research Foundation, which is part of the International *C. elegans* Gene Knockout Consortium. Some strains were provided by the CGC, which is funded by NIH Office of Research Infrastructure Programs (P40 OD010440). The *ergo-1(tm1860)*, *C04F12.1(tm1637),* and *csr-1(tm892)* alleles were generated by the

National Bioresource Project (Japan). This work was supported by “Hormones: Biochemistry and Molecular Biology” Training Grant T32 DK0007328 and Genetics and Development Training Grant T32 GM007088 to L.M.K. and the Irma T. Hirschl Career Scientist Award to A.G.

Chapter Four: General Discussion

Author Contributions

The experiments presented in this chapter were conceived and designed by L.M.K. and A.G. Steven C.D.L. Pham and L.M.K. performed the insulin RNAi experiments, all other experiments were performed and analyzed by L.M.K.

I. DAF-16/FOXO functions non-autonomously to regulate HSN migration

We have found that transcription factor DAF-16/FOXO functions in the hypodermis to influence the migration of the HSNs (Chapter 2). This finding was unexpected since DAF-16 has recently been shown to influence embryonic neurite outgrowth (Christensen et al., 2011) and neuronal aging (Tank et al., 2011) in a cell-autonomous fashion. Moreover, we have identified PAK-1, a p21-activated kinase, as one of what is likely to be multiple downstream effectors of DAF-16 required in the hypodermis to control HSN migration (Chapter 2). PAK-1 will be discussed in greater detail in section IV below.

Our finding that insulin/IGF-1-PI3K signaling modulates DAF-16/FOXO activity in the hypodermis is the first to demonstrate that a signaling pathway can function non-autonomously to influence HSN migration. The secreted Wnt molecules are the only other characterized factors that have been shown to affect HSN migration non-autonomously (Pan et al., 2006). EGL-20/Wnt has the strongest effect on HSN migration: loss-of-function mutants exhibit HSN undermigration defects and overexpression of EGL-20 leads to an HSN overmigration phenotype (Forrester et al., 2004; Pan et al., 2006). This phenotypic profile is strikingly similar to what we observe in cases of enhanced insulin/IGF-1-PI3K signaling (HSN undermigration) and reduced signaling (HSN overmigration), which both exert their effects in a DAF-16-dependent manner (Chapter 2).

One intriguing possibility is that the insulin/IGF-1 signaling (IIS) pathway modulates expression of the Wnts via DAF-16-mediated transcriptional activation in the hypodermis. This idea is supported by the fact that of the five Wnts, all of which have been implicated in HSN migration (Pan et al., 2006), LIN-44/Wnt (Herman et al., 1995; Harterink et al., 2011) and EGL-20/Wnt (Whangbo and Kenyon, 1999; Harterink et al., 2011) are expressed in multiple cells,

including the hypodermal cells hyp8-hyp11 and P11/P12, respectively, during the embryonic stages when HSN migration is occurring. We have shown that HSN undermigration in a *daf-16* null is enhanced by an *egl-20* null mutation (Figure 2-3), which suggests they act in parallel pathways. However, because of the redundancy between the Wnt ligands this result allows us only to rule out the possibility that DAF-16 is exclusively activating *egl-20* to influence HSN migration. It is still possible that DAF-16 contributes to the expression of a subset of Wnts (i.e. both the *egl-20* and *lin-44* hypodermal expressed Wnts).

It is well documented that Wnt ligands are produced by multiple tissues, including the hypodermis (Herman et al., 1995; Whangbo and Kenyon, 1999; Gleason et al., 2006), muscles (Whangbo and Kenyon, 1999; Gleason et al., 2006), neurons (Gleason et al., 2006; Song et al., 2010) and intestine (Kennerdell et al., 2009; Song et al., 2010). Therefore, if DAF-16 were contributing to the expression of Wnt ligands from multiple sources, we would have expected to observe at least partial rescue of the *daf-16* null mutant with multiple tissue-specific promoters driving a functional DAF-16 protein. It should be noted that for these experiments we utilized transgenic arrays expressing DAF-18 under various tissue-specific promoters instead of DAF-16 for two reasons: first, there is only one DAF-18 isoform compared to the two DAF-16 isoforms that rescue HSN migration (Figure 2-1E, 2-4E) and second, since the *daf-18* undermigration phenotype arises due to a decrease in DAF-16 activity (Figure 2-4D), rescuing the *daf-18* mutant should be the equivalent of restoring DAF-16 function. Our tissue-specific rescue experiments demonstrate that DAF-16 is unlikely to function in the nervous system (Figure 2-6B), muscles or intestine to influence HSN migration (Figure 2-5), therefore, it is unlikely that DAF-16 is a master regulator of Wnt expression.

Another possible scenario for the interaction between DAF-16 and Wnt is that DAF-16 may modulate the expression of genes required for the secretion of Wnts from the Wnt-producing hypodermal cells. Further experiments will be required to clarify these possibilities. For example, (1) transcriptional reporters or single-molecule fluorescent in situ hybridization (smFISH) can be used to monitor the effect of a *daf-16* null mutation on the expression of the hypodermal-expressed Wnt genes and (2) translational reporters and/or immunostaining to monitor the secretion of EGL-20 and LIN-44 from the hypodermal cells of *daf-16* null mutants.

II. DAF-16/FOXO as a potential repressor of transcription during HSN migration

DAF-16 can function to both activate (class I genes) and repress (class II genes) its transcriptional targets (Kenyon and Murphy, 2006; Murphy, 2006). Therefore, it is possible that DAF-16 is functioning in the hypodermis to repress a target(s) that would otherwise inhibit HSN migration. In this scenario, *daf-16* null mutations would relieve this repression leading to ectopic activation of target gene(s) that subsequently inhibit HSN migration. The SynMuv (Synthetic Multivulva) genes offer a conceptually similar illustration of this potential scenario. During normal development, three of the six vulval precursor cells (VPCs) are induced to adopt vulval fates in the third larval stage by LIN-3/EGF signaling from the gonadal anchor cell (AC), while the distal-most VPC cells, which receive no LIN-3 signal, eventually fuse with the hyp7 syncytium to become part of the hypodermis (reviewed in Sternberg, 2005). The functionally redundant SynMuv genes negatively regulate vulval induction and are divided into the SynMuv A, B (Ferguson and Horvitz, 1989) and C (Ceol and Horvitz, 2004) classes. Mutations in either SynMuv A, B or C genes alone do not cause a vulval phenotype, however, double mutant combinations between SynMuv gene classes cause a Multivulva (Muv) phenotype in

hermaphrodites due to all six VPCs adopting vulval fates. Specifically, the SynMuv genes act non-autonomoulsy in the hyp7 syncytium (Herman and Hedgecock, 1990; Myers and Greenwald, 2005) to regulate VPC fate by repressing the *lin-3* gene in the neighboring hypodermis (Cui et al., 2006a). In SynMuv double mutant combinations, *lin-3/EGF* is depressed in the hyp7 syncytium, which consequently leads to vulval induction in all six VPCs and the Muv phenotype (Cui et al., 2006a). Thus, the SynMuv genes provide an example of how the non-autonomous expression of repressors can function to prevent inappropriate interactions between tissues/cells during development.

One possibility for the role of DAF-16 in the *C. elegans* hypodermis may be to negatively regulate Wnt antagonists to prevent inappropriate dampening of the Wnt signal during HSN migration. Interestingly, mammalian FOXOs have been identified as direct regulators (although positive and not negative) of the soluble frizzled receptors (*sfrp1/2)* and sclerostin (*Sost)*, which act as antagonists of Wnt ligands to affect neural stem/progenitor cell (NSC) homeostasis in the brain (Paik et al., 2009). Consistent with this possibility, the overexpression of the *C. elegans* SFRP ortholog inhibits the EGL-20-dependent anterior migrations of the HSNs (Harterink et al., 2011).

Furthermore, the *C. elegans* Ror, CAM-1, another negative regulator of Wnt signaling, has been shown to antagonize EGL-20/Wnt during HSN migration (Forrester et al., 2004). The discovery that CAM-1 can bind Wnts through its Cys-rich-domain (CRD) (Green et al., 2007) and the observation that the CRD domain is sufficient to rescue *cam-1* mutant HSN overmigration defects (Kim and Forrester, 2003) has led to the model that CAM-1 functions as a "sink" for Wnt ligands. CAM-1 overexpression causes the HSNs to undermigrate (Forrester et al., 1999; Kim and Forrester, 2003; Forrester et al., 2004). Therefore, it is possible that increased

hypodermal *cam-1* expression in *daf-16* null animals may contribute to the HSN undermigration phenotype observed in this mutant. Interestingly, a *cam-1* putative null allele was identified in a screen for dauer-constitutive (daf-c) mutants at higher temperatures (Ailion and Thomas, 2003), a phenotype opposite to that of *daf-16* loss-of-function dauer-defective (daf-d) mutants (Vowels and Thomas, 1992). However, due to a synthetic lethal phenotype in *cam-1; daf-16* double mutants it was not possible to determine whether CAM-1 and DAF-16 act antagonistically in the same genetic pathway to affect dauer formation. Nevertheless, there is one line of evidence suggesting that CAM-1 acts in the TGF-β pathway, in parallel to IIS-DAF-16: a mutation in the transcription factor *daf-5*/SNO/SKI, which functions in the TGF-β pathway to regulate dauer formation (reviewed in Fielenbach and Antebi, 2008), was shown to partially suppress the *cam-1* (daf-c) mutant (Ailion and Thomas, 2003). However, since the *daf-5* allele used for suppression analysis is most likely not a null (da Graca et al., 2004), further studies will be required to determine if CAM-1 functions solely in the TGF-β pathway, or if crosstalk with the IIS pathway exists as well. Furthermore, the possibility that CAM-1 and DAF-16 work in the same genetic pathway to regulate HSN migration but in parallel pathways to regulate dauer formation cannot be ruled out and is supported by the observation that CAM-1 protein domains have differential functions. For example, the kinase domain of CAM-1 is required for dauer regulation (Ailion and Thomas, 2003) but is dispensable for regulating HSN migration (Forrester et al., 1999; Kim and Forrester, 2003).

Future studies will be required to determine whether DAF-16 is functioning in the hypodermis to repress transcriptional target(s) that have to be inhibited during the time of HSN migration to ensure its precision. Examples of future experiments include: (1) epistasis analysis to test whether the HSN undermigration phenotype of *daf-16* null mutants is suppressed by the

mutations in the candidate target genes, (2) knockdown of the candidate target genes in the hypodermis by RNAi to observe HSN overmigration, as would be predicted by this model, and (3) analysis of mRNA levels of the candidate target genes in the hypodermis using smFISH to determine whether their expression is elevated in *daf-16* null mutants.

III. The DAF-16b isoform regulates HSN migration

The discovery that the DAF-16b isoform is the major regulator of HSN migration (Figure 2-1E) is consistent with a recent study demonstrating that DAF-16b is responsible for another embryonic process: neurite outgrowth (Christensen et al., 2011). This presents the intriguingly possibility that DAF-16b may have specific functions during embryonic development. In mammals, there are four FOXO proteins: FOXO1, FOXO3, FOXO4 and FOXO6 that exhibit both distinct and overlapping functions (reviewed in Arden, 2008). Similar to the family of mammalian FOXOs, the multiple DAF-16 isoforms in *C. elegans* have been shown to function both individually and cooperatively, depending on the biological context.

Of the multiple DAF-16 isoforms that have been identified (www.wormbase.org), only three have been functionally characterized: DAF-16a (al or a2), DAF-16b and DAF-16d/f. The "a" isoform has been implicated in lifespan regulation (Lee et al., 2001; Lin et al., 2001; Kwon et al., 2010), dauer formation (Henderson and Johnson, 2001; Lee et al., 2001; Lin et al., 2001; Kwon et al., 2010), heat stress (Kwon et al., 2010), neuronal aging (Pan et al., 2011; Tank et al., 2011; Calixto et al., 2012) and germline proliferation (Qi et al., 2012). The role of "d/f" isoform has been described in lifespan regulation, heat stress and fat metabolism (Kwon et al., 2010), and the "b" isoform, in addition to its roles in neuronal development (Chapter 2), (Christensen et al., 2011), has been shown to contribute to dauer formation (Lee et al., 2001; Kwon et al., 2010).

Many recent studies have not focused on identifying the details of specific DAF-16 isoform involvement, but instead have utilized DAF-16 transgenic constructs that often express only the "a" (a1 or a2) isoform (Gaglia and Kenyon, 2009; Pan et al., 2011; Tank et al., 2011; Qi et al., 2012; Driver et al., 2013). Therefore, it is likely that there are additional distinct and overlapping functions of the DAF-16 isoforms that have not yet been revealed. Furthermore, promoter-swapping experiments have shown that the promoter regions of the DAF-16 isoforms are important for their function (Lee et al., 2001; Kwon et al., 2010), as are the N-terminus-coding regions of each DAF-16 isoform (Kwon et al., 2010). Both promoters and N-termini are likely important, at least in part, for regulating the subcellular localization of DAF-16 proteins (Kwon et al., 2010). Combined, these observations reinforce the importance of differentiating between DAF-16 isoforms, since both biological context and surrounding gene regulatory regions can influence their activity in varying ways.

Additionally, many biochemical studies to identify direct DAF-16-binding regions have been performed in one developmental stage and with a specific DAF-16 isoform. For example, chromatin profiling by DNA adenine methyltransferase identification (DamID) was performed only in adults using the DAF-16a1 isoform (Schuster et al., 2010). Also, genome-wide ChIP-seq analysis was performed in L4-young adult worms using the DAF-16a2 isoform fused to GFP (modENCODE; Snyder project 2009). Therefore, a significant number of DAF-16 targets are likely to be missing from these data sets. Another study (Oh et al., 2006) performed chromatin immunoprecipitation (ChIP) (Oh et al., 2006) in mixed embryos with a DAF-16 antibody raised against the conserved C-terminus region present in all DAF-16 isoforms and identified 103 potential DAF-16 direct targets. However, this study was performed prior to recently developed

high-throughput next generation sequencing technologies and therefore likely only represents a fraction of DAF-16 targets in the embryo.

Moreover, all expression profiling studies using *daf-2/*IR mutants to identify DAF-16-regulated genes (McElwee et al., 2003; Murphy et al., 2003; McElwee et al., 2004; Halaschek-Wiener et al., 2005) have been performed in adults. Future expression and genome-localization studies performed in the *C. elegans* embryo, in combination with the use of specific DAF-16 isoforms, have the potential to uncover developmentally regulated targets of DAF-16, including those mediating the control of HSN migration.

IV. PAK-1 acts downstream of DAF-16 to non-autonomously promote neuronal migration

The p21-activated kinases (Paks) function in signal transduction and regulation of cytoskeletal organization. They are characterized by a shared kinase domain and the ability to be bound and regulated by the Cdc42 and Rac small GTPases (reviewed in Bokoch, 2003). In mammals there are six Pak proteins, which are divided into two groups: Group A and Group B. The Group A proteins are activated by Cdc42 or Rac, whereas Group B activation is independent of the small GTPases, despite the presence of a p21-binding domain (PBD), which is capable of binding Cdc42 or Rac (Arias-Romero and Chernoff, 2008).

Pak1, a member of the PAK protein kinase family, was previously identified as a direct target of FOXO in regulating neuronal polarity in the mammalian brain (de la Torre-Ubieta et al., 2010). We have demonstrated that the orthologous PAK-1 in *C. elegans* also acts downstream of DAF-16/FOXO, in the novel context of HSN migration, suggesting conservation for this pathway in neurodevelopment (Chapter 2). Although a role for Pak1 in cell migrations has been previously described in both *C. elegans* (Lucanic et al., 2006; Peters et al., 2013) and mammals

(reviewed in Kreis and Barnier, 2009), to our knowledge this is the first study describing a non-autonomous role for Pak1 in regulating the process of migration.

The *C. elegans* genome encodes three Pak proteins: PAK-1, PAK-2 and MAX-2 (Chen et al., 1996; reviewed in Hofmann et al., 2004). PAK-1 is the most similar to Group A mammalian Paks. It can bind both CDC-42 and CED-10/Rac and colocalizes with these GTPases at the plasma membrane of hypodermal cells during embryogenesis (Chen et al., 1996). The presence of PAK-1 at all hypodermal cell boundaries during the time of HSN migration is consistent with the non-autonomous role we have identified for PAK-1 in regulating HSN migration (Chapter 2). Moreover, we have found that CDC-42 is also required for HSN migration (Figure 4-1) and is therefore likely to be required for upstream activation of PAK-1 in the hypodermis.

Pak1 is thought to primarily mediate the migration of cells in a cell-autonomous manner through the activation of LIM-kinase, which phosphorylates and inhibits cofilin, an actin-regulatory protein, in order to stimulate actin polymerization and cell movement (Edwards et al., 1999; reviewed in Ye and Field, 2012). From the genetic model we describe (Chapter 2), we can imagine several possible scenarios for how PAK-1 might regulate HSN migration non-autonomously in *C. elegans*, including: (1) PAK-1 could remodel the actin cytoskeleton and/or regulate cell adhesion at hypodermal cell boundaries to help guide the HSN along its migratory route, (2) PAK-1 could regulate the expression of an extracellular molecule that is secreted from the hypodermis to act on the HSN and promote its migration and (3) PAK-1 could be required for repressing inappropriate signaling from the hypodermis to the HSN during migration, much in the same way as discussed in section II for DAF-16. Possibilities for (1) and (2) will be discussed below.

The timing of HSN migration (Sulston et al., 1983) corresponds with that of embryo elongation, which takes place largely between 395-520 minutes after first cleavage and reflects the elongation of epidermal cells along the anterior-posterior axis (reviewed in Priess and Hirsh, 1986). Therefore, an intriguing possibility is that the localization of PAK-1 protein to the hypodermal cell boundaries during embryo elongation (Chen et al., 1996) concomitantly affects the migration of the HSN, which migrates along the hypodermal cells in a position sandwiched between the cell membrane and the basal lamina (reviewed in Hedgecock et al., 1987).

To begin addressing this possibility, we started by examining the epidermal (or hypodermal) *C. elegans* apical junctions (ceAJ). We hypothesized that PAK-1 may contribute to the formation of these junctions to provide a pathway for migrating HSNs. We used a *ajm-1::gfp* reporter, which marks the apical junction molecule (AJM), a novel coiled-coil membrane-associated protein that is expressed in the apical junctions of all epithelia cells (Bossinger et al., 2001; Koppen et al., 2001), to examine the epidermal junctions in both *pak-1* null and *daf-16* null mutants. The result was that we observed no obvious change in the integrity of the junctions (Figure 4-2). This finding is consistent with mammalian studies demonstrating that PAKs are not required for junction formation (Lozano et al., 2008; Liu et al., 2010), thereby suggesting that PAKs are not necessary for the establishment of cell-cell contacts but rather may affect the signaling events that occur after junction assembly.

Alternatively, PAK-1 may be required for junction stability. One possibility is that PAK-1 contributes to the formation of circumferential actin filament bundles (CFBs), which are linked to the apical junctions and required to maintain the shape of the embryo during elongation (Priess and Hirsh, 1986; Costa et al., 1997). In view of the fact that CFBs form at the 1.5-fold stage when HSN migration is occurring (Sulston et al., 1983), abnormalities in this structure may

impede HSN migration along its migratory path. Interestingly, in mammalian epithelial cells Pak1 has been observed at regions of E-cadherin-mediated cell-cell contacts (Zegers et al., 2003) and shown to be required for F-actin recruitment to cadherin complexes (Nola et al., 2011). This raises the possibility that in *C. elegans* a role for PAK-1 in recruiting F-actin to the cadherin-catenin complex composed of E-cadherin, α-catetin and β-catenin, which is required for embryo elongation (Costa et al., 1998), may be conserved. Phalloidin staining of F-actin in *pak-1* null mutants would address these possibilities. It should be noted that *pak-1* null mutants do not exhibit gross morphological defects during embryogenesis, but instead show a redundant role with another *C. elegans* PAK family member, MAX-2, in ventral enclosure (Lucanic et al., 2006). Therefore, if PAK-1 influences HSN migration through its role in embryo elongation, it is likely through more subtle defects than through a complete abolishment of components present at the hypodermal cell boundaries.

Furthermore, mammalian Pak1 has been shown to be necessary for Rac1-dependent downregulation of E-cadherin at human keratinocyte cell junctions by a mechanism that has not yet been elucidated (Lozano et al., 2008). The function of E-cadherin in cell-cell adhesion is highly conserved and is required for epithelial tissue cohesion in *C. elegans*, flies and vertebrates (reviewed in Gumbiner, 2005). The downregulation of E-cadherin at cell-cell junctions allows epithelial cells to detach from one another and migrate; a process that is required during gastrulation and epithelial wound healing (reviewed in Thiery, 2003). Therefore, another distinct possibility for the involvement of PAK-1 at the hypodermal cell boundaries in *C. elegans* may be in the downregulation of E-cadherin, an event that could stimulate HSN detachment from the basal lamina of the hypodermis during its migration. Immunostaining *pak-1* null mutants with anti-HMR-1/E-cadherin antibodies (Costa et al., 1998) would be useful for testing the hypothesis

that in *pak-1* null mutants E-cadherin levels remain higher than in wild type animals at the hypodermal cell boundaries.

Pak1 has been demonstrated to localize and affect focal adhesion assembly, maturation and turnover in mammalian epithelial cells through a PAK-PIX-GIT signaling module. Formation of this module is mediated by the binding of Pak1 to PIX proteins (Rac/Cdc42 guanine-nucleotide exchange factors), which subsequently associate with G protein-coupled receptor kinase interactor (GIT) proteins that bind directly to paxillin, a central cytoskeletal protein of focal adhesions (reviewed in Parrini, 2012). Focal adhesions provide a mechanical link to the extracellular matrix (EM), as well as support the formation of signaling hubs on the inner side of the plasma membrane. Integrins, which are a group of cell surface transmembrane receptors, are the key mediators of these attachments. In light of the fact that the HSN migrates between the basal lamina and the cell membrane of the hypodermis—an ideal location for bidirectional signaling between the HSN and hypodermal EM—it is tempting to suggest a role for PAK-1-dependent focal adhesion organization in regulating HSN migration. Analyzing the organization of focal adhesion sites present at the hypodermal membranes during HSN migration in *pak-1* null mutants could be of benefit. The ortholog of paxillin in *C. elegans* is PXL-1, and it can be visualized with either an antibody against PXL-1 or a PXL-1::GFP translational fusion, which localizes to adhesion sites (Warner et al., 2011).

Another possibility for the role of PAK-1 at the hypodermal cell membranes, as either a component of focal adhesions or not, is in mediating the interaction between an extracellular signaling molecule and the HSN. An interesting idea may be that PAK-1 stimulates the interaction between the migrating HSNs and the extracellular Wnts by either inducing their production and/or aiding in their secretion from the hypodermis. Recently, Pak1 has been shown

to positively regulate canonical Wnt signaling in colon cancer cells by directly phosphorylating β-catenin and stabilizing its accumulation in the nucleus (Zhu et al., 2012). However, in this context Pak1 is acting downstream of the Wnt ligands to affect Wnt signaling. Further studies will be required to elucidate a potential connection between PAK-1 and the Wnt proteins.

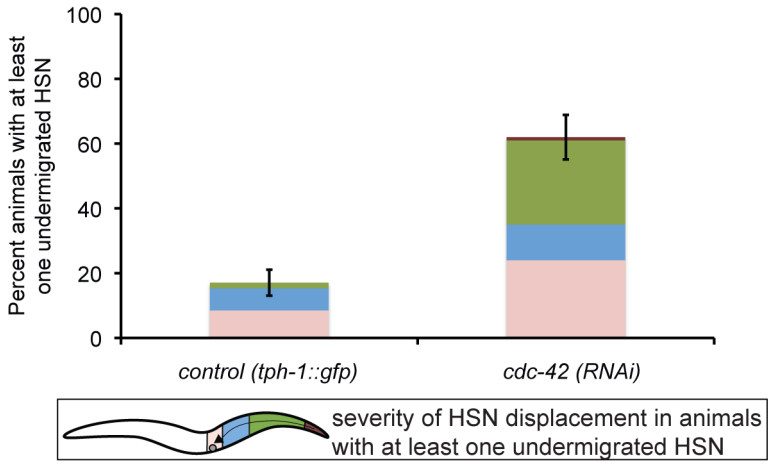

Figure 4-1. HSN undermigration defects in *cdc-42* (*RNAi*) animals. Quantification of the percentage of animals with an undermigrated HSN from two pooled independent experiments in control *tph-1::gfp* (n=88) versus *cdc-42 (RNAi)* (n=50) animals. Worm schematic legend: Stacked bars represent the proportion of HSNs at different positions along the A-P body axis within only those animals containing at least one undermigrated HSN. Thus, since there are two HSNs within each animal and not every HSN is affected, one colored region (light pink) represents the wild type HSN that remains unaffected in animals containing a second undermigrated HSN, which is represented by either the red, green or blue region. Error bars represent standard error of the proportion (SEP) for the entire stacked column.

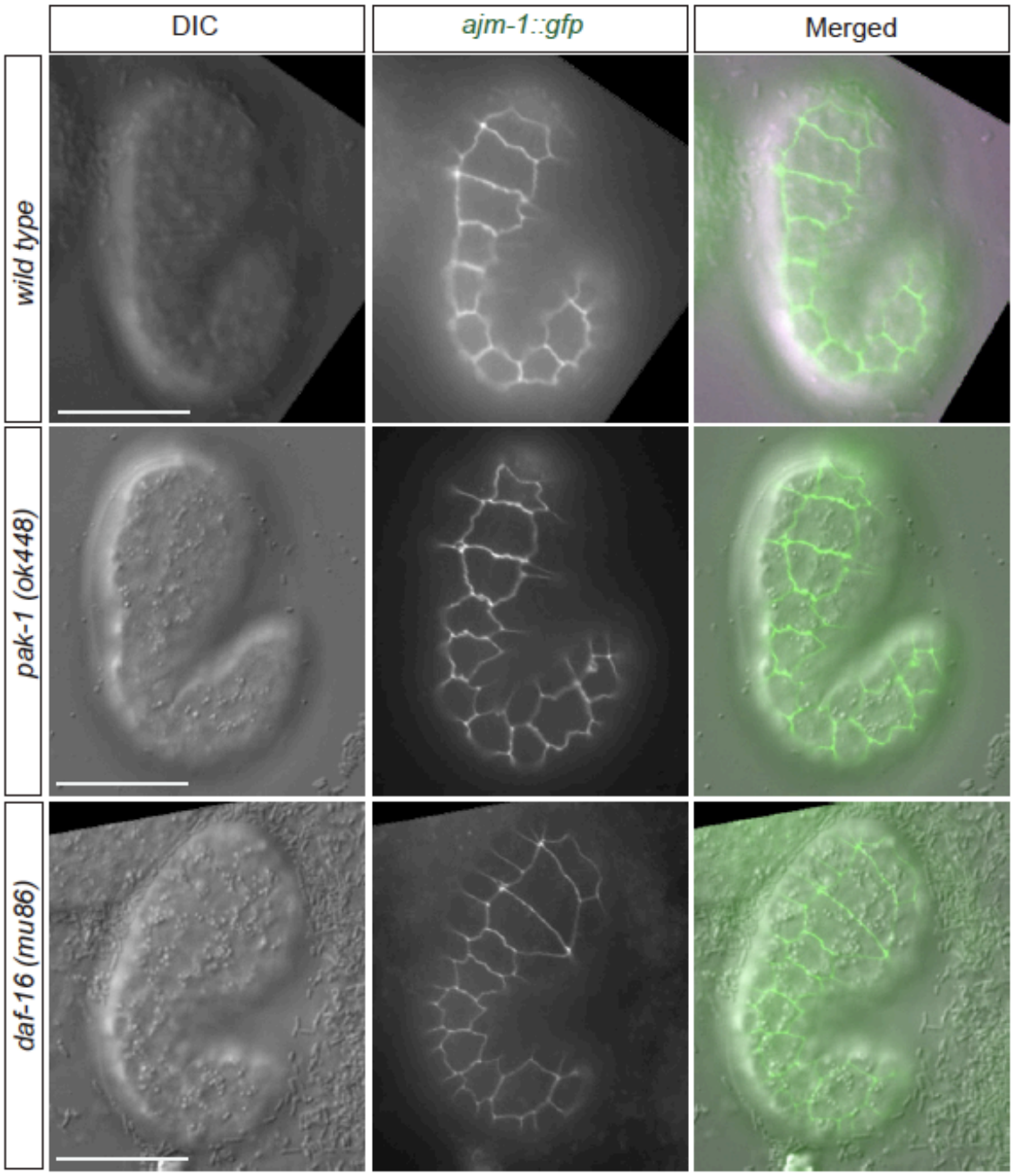

Figure 4-2. The hypodermal apical junctions are not disrupted in *daf-16* and *pak-1* null mutants. Epifluorescent and DIC images of comma/1.5-fold stage embryos expressing *ajm-1::gfp*, a transcriptional reporter that is expressed at all hypodermal cell boundaries.

V. The neuron-glial-like interaction between the *C. elegans* hypodermis and HSN

Much like the pyramidal cells of the developing cerebral cortex use radial glia as a scaffold for directing their radial migrations (reviewed in Rakic, 2007), the *C. elegans* hypodermis may have an analogous function in directing the anterior migrations of the HSNs. The movement of cortical neurons along glial fibers occurs in part through the formation of an adhesion junction along the length of the cell body and the leading process, which projects short filopodia extensions along the glia fiber (Edmondson and Hatten, 1987). Neuron-glial adhesion molecules, including the integrins, are required for migrations along radial glia (reviewed in Solecki, 2012). Furthermore, Glial cells of the developing mammalian midbrain have been shown to secrete Wnt-5a (Castelo-Branco et al., 2006) and the mammalian floor plate, a structure at the ventral midline of the neural tube, which is rich in glia-like cells, secretes a variety of molecules including sonic hedgehog, netrin 1, the Wnts and bone morphogenetic proteins (reviewed in Placzek and Briscoe, 2005), all of which can affect neuronal development. Similar to the interactions between neurons and glia, the *C. elegans* hypodermis and HSN may also dynamically communicate during HSN migration. It will be interesting to determine if the mechanisms by which the HSN and hypodermis interact are conserved in mammalian neuron-glial communications.

VI. The insulin-like peptides of *C. elegans*

Although the *C. elegans* genome contains one insulin-like receptor, it encodes 39 insulin-like peptides (Pierce et al., 2001; Li et al., 2003), and very little is known about the function of each. In order to identify the insulin(s) that activate or inactivate DAF-2/IR to regulate HSN migration we turned our attention first to *ins-7* and *ins-18,* since both are expressed during

embryogenesis (Kawano et al., 2000; Pierce et al., 2001) and are most well characterized in relation to their genetic interaction with the *daf-2* receptor (Kawano et al., 2000; Pierce et al., 2001; Murphy et al., 2007). We observed that neither down regulation of *ins-7* by RNAi nor a null mutant resulted in an HSN migration phenotype (Table 4-1). Furthermore, we observed no phenotype after *ins-18 (RNAi)* (Table 4-1). We recently acquired the *ins-18(tm0339)* deletion mutant generated by the National Bioresource Project (Japan) and will analyze the HSN migration phenotype in this mutant in the future. Moreover, we have utilized the 19 available RNAi clones targeting insulin genes from the *C. elegans* bacterial RNAi feeding library (Kamath et al., 2003), but have not observed obvious HSN phenotypes in RNAi experiments (Table 4-1). Future analysis using deletion mutants will be required to definitively rule out the involvement of individual insulins in HSN migration. It is possible that one or more insulins function redundantly to regulate HSN migration.

Table 4-1. Insulin gene down-regulation by RNAi and deletion mutants examined for the HSN migration phenotype

Insulin gene	RNAi phenotype (performed in wild type background)	Deletion mutant phenotype	Previous literature
ins-1	No RNAi clone available	N/A	* Most closely related to human insulin by primary sequence, structural homology models * Characterized as a possible antagonist because it enhanced dauer arrest when it was overexpressed (Pierce et al., 2001 Genes & Dev)
ins-2	No phenotype	N/A	* Expressed in bean-stage embryo (Pierce et al., 2001 Genes & Dev)
ins-3	No RNAi clone available	N/A	N/A
ins-4	No phenotype	N/A	N/A
ins-5	No phenotype	N/A	N/A
ins-6	No phenotype	N/A	N/A
ins-7	No phenotype	No phenotype at 20°C *ins-7(ok1573)*	* Described as possible agonist because of extended lifespan in ins-7 null mutants & ins-7 RNAi showed enhanced daf-16::gfp nuclear localization (Murphy et al., 2007 PNAS)
ins-8	No phenotype	N/A	* Described as "not likely an antagonist" because *ins-8(tm4144)* mutants were not dauer defective (Ritter et al., 2013 Genome Res)
ins-9	No RNAi clone available	N/A	N/A
ins-10	No RNAi clone available	N/A	N/A
ins-11	No phenotype	No phenotype at 20°C *ins-11(tm1053)*	* Described as possible antagonist because mutant suppressed the *ins-7* RNAi lifespan extension (Kawano et al., 2006 Biosci Biotechnol Biochem)
ins-12 through *ins-17*	No RNAi clone available	N/A	N/A
ins-18	No phenotype	N/A	* *ins-18* described as an antagonist based on its effect on lifespan and dauer diapause when mutated (Matsunaga et al., 2012 Biochem Biophys Res Commun)
ins-19	No phenotype	N/A	N/A
ins-20	No RNAi clone available	N/A	N/A
ins-21 through *ins-24*	No phenotype	N/A	N/A
ins-25 through *ins-29*	No RNAi clone available	N/A	N/A
ins-30	No phenotype	N/A	N/A
ins-31	No RNAi clone available	N/A	N/A
ins-32	No phenotype	N/A	N/A
ins-33	No RNAi clone available	N/A	N/A
ins-34	No RNAi clone available	N/A	N/A
ins-35	No phenotype	N/A	N/A
ins-36	No phenotype	N/A	N/A
ins-37	No phenotype	N/A	N/A
ins-38	No RNAi clone available	N/A	N/A
ins-39	No phenotype	N/A	N/A

VII. The involvement of endogenous RNAi and ZFP-1/AF10 in HSN migration

The discovery that both RNAi factors and the chromatin factor ZFP-1/AF10 regulate HSN migration (Chapter 3) is consistent with a genome-wide expression study, which established that both ZFP-1 and the dsRNA-binding protein RDE-4 regulate close to 250 overlapping genes (Grishok et al., 2008). Moreover, the finding that ZFP-1 regulates HSN migration in part through the modulation of DAF-16/FOXO activity is in agreement with the discovery that ZFP-1 affects longevity and stress response by negatively regulating the conserved IIS kinase *pdk-1* (Mansisidor et al., 2011). Therefore, we have identified a system in which the activities of DAF-16, ZFP-1 and endogenous RNAi cooperate to influence gene regulation during the process of HSN migration (Chapter 2 and 3).

Although we have determined that ZFP-1 contributes to the regulation of HSN migration in part through the repression of *pdk-1* and release of DAF-16 inhibition and in part in parallel to DAF-16, RDE-4 appears to function only in parallel to DAF-16. Further studies will be required to determine whether ZFP-1 and RNAi cooperate to regulate common target genes necessary for HSN migration, to identify the identity of those genes and the mechanism of their regulation.

Based on our observations that ZFP-1 regulates the IIS pathway, which functions non-autonomously in HSN migration (Kenney et al., *in press*), and the failure of a ZFP-1::GFP transgene expressed specifically in the HSN to rescue the HSN undermigration defects of *zfp-1* mutant animals (Figure 3-6), it is likely that ZFP-1 functions non-autonomously to promote HSN migration. Future studies will address whether ZFP-1 functions exclusively in the hypodermis to regulate HSN migration. Tissue-specific promoters driving expression of a full-length *zfp-1* cDNA in the background of the *zfp-1* mutant will be used to assess for rescue of the HSN undermigration phenotype.

Direct ZFP-1 targets are enriched among genes upregulated in *zfp-1* mutants and not among the down-regulated genes (Mansisidor et al., 2011; Cecere et al., 2013). Furthermore, ZFP-1 is enriched specifically at target gene promoter regions and has been shown to negatively regulate the expression of these genes by opposing H2B ubiquitylation and slowing down transcriptional elongation (Cecere et al., 2013). Therefore, it is likely that ZFP-1 is functioning to inhibit additional target(s) affecting HSN migration, much in the same way ZFP-1 was shown to repress *pdk-1* (Mansisidor et al., 2011) (Chapter 3). To begin addressing the question of what these additional targets are, we compared the list of known genes required for HSN migration (Table 1-1) to that of genes directly bound by ZFP-1 (ChIP/chip data generated by modENCODE). We examined the overlap for any known negative regulators of HSN migration, since we hypothesized that in *zfp-1* mutants HSN undermigration is likely caused by a derepression of target gene(s), which subsequently impedes HSN migration.

We determined that the only known negative regulator of HSN migration, *cam-1*, discussed in section II above and in Chapter I, is directly bound by ZFP-1 at the promoters of all three isoforms (Figure 4-3). The *cam-1* gene encodes a Receptor tyrosine kinase-like orphan receptor (Ror) that negatively regulates EGL-20/Wnt signaling, likely by binding and depleting soluble Wnts, and inhibits HSN migration when overexpressed (Forrester et al., 1999; Kim and Forrester, 2003; Forrester et al., 2004). Thus, we propose that a derepression of *cam-1* in *zfp-1* loss-of-function mutants could contribute to the HSN undermigration phenotype. Future experiments will focus on (1) determining the site-of-action of both ZFP-1 and CAM-1, (2) epistasis analysis to test whether HSN undermigration in the *zfp-1* loss-of-function mutant is suppressed by the *cam-1* null mutant, (3) identifying whether *cam-1* mRNA is upregulated in the *zfp-1* mutant embryos and specifically in the tissue we implicate in (1).

Interestingly, *cam-1* is also an endo-siRNA target gene of the CSR-1 RNAi pathway (Claycomb et al., 2009) (Figure 4-3). Future studies will determine whether endogenous RNAi cooperates with ZFP-1 to negatively regulate *cam-1* and promote HSN migration. Additionally, identifying the site-of-action for the RNAi factors that we have implicated in HSN migration (Chapter 3) will be necessary in order to understand mechanistically how they are affecting this developmental process.

There are multiple endo-siRNA pathways in *C. elegans,* including the CSR-1 RNAi pathway (Claycomb et al., 2009; Gu et al., 2009), the WAGO RNAi pathway (Gu et al., 2009) and the ERI RNAi pathway (Lee et al., 2006; Gent et al., 2009; Han et al., 2009; Vasale et al., 2010). The determinants that differentiate these pathways from one another include whether they are Dicer-dependent or independent, the length of the endo-siRNAs produced (26 nucleotides (26G) versus 22 nucleotides (22G)) and the interacting Argonaute(s). Dicer-independent endo-siRNAs produced de novo by RdRPs (Ruby et al., 2006; Aoki et al., 2007; Pak and Fire, 2007) are termed 22G-RNAs. The group of 22G-RNAs that are mostly anti-sense to protein coding genes bind the Argonaute CSR-1 and are produced by the RdRP EGO-1 (Claycomb et al., 2009) present in complex with the Dicer-related helicase DRH-3 (Gu et al., 2009; Thivierge et al., 2012). Moreover, a requirement for the dsRNA-binding protein RDE-4 in the accumulation of some EGO-1-depedent endo-siRNAs has been identified (Maniar and Fire, 2011). We have implicated CSR-1, RDE-4 and DRH-3 in the process of HSN migration (Chapter 3), thus, it is likely that the CSR-1 RNAi pathway regulates genes required for HSN migration. It will be interesting to determine how RDE-4 fits into this pathway, since it is well known that RDE-4 is a member of the Dicer complex required to process dsRNA (Tabara et al., 2002). Recently, a regulatory pathway involving a two-step process for endo-siRNA production implicated RDE-4

and Dicer in the production of 26G-RNAs, which subsequently drive the biogenesis of some WAGO-bound 22G-RNAs (Vasale et al., 2010). Therefore, it is possible that RDE-4 works upstream of the CSR-1 22G-RNA pathway to cooperate in regulating genes affecting HSN migration.

Since the CSR-1 RNAi pathway has been recently shown to positively regulate the expression of the core histones (Avgousti et al., 2012), the possibility remains that the CSR-1 RNAi pathway, which we have also implicated in HSN migration (Chapter 3), positively regulates the expression of genes required during development to ensure proper neuronal migration. The positive effect on histone gene expression by endogenous RNAi, however, presents a unique example, since the maturation of histone mRNAs is different from that of other mRNAs; it requires processing of their 3'UTRs through an endonucleolytic cleavage downstream of a conserved stem loop, guided by U7 snRNA (reviewed in Marzluff et al., 2008). In *C. elegans,* the U7 snRNA is not encoded by the genome and thus a direct role for endo-siRNAs in the endonucleolytic cleavage of histone 3'UTRs has been proposed (Avgousti et al., 2012). However, other mechanisms exist by which the CSR-1 RNAi pathway positively affects gene expression at the transcriptional level (Germano Cecere, unpublished). CSR-1 has known endonucleolytic capabilities (Aoki et al., 2007); therefore, one possibility is that CSR-1 is involved in the processing of pre-mRNA. The fact that CSR-1-bound siRNAs are often complementary to regions found along the entire length of its target transcripts (Claycomb et al., 2009) suggests that there are likely multiple mechanisms by which CSR-1 affects gene regulation. Therefore, future studies aimed at identifying direct targets of endogenous RNAi should not exclude the possibility that genes required for HSN migration may be downregulated in the RNAi mutants.

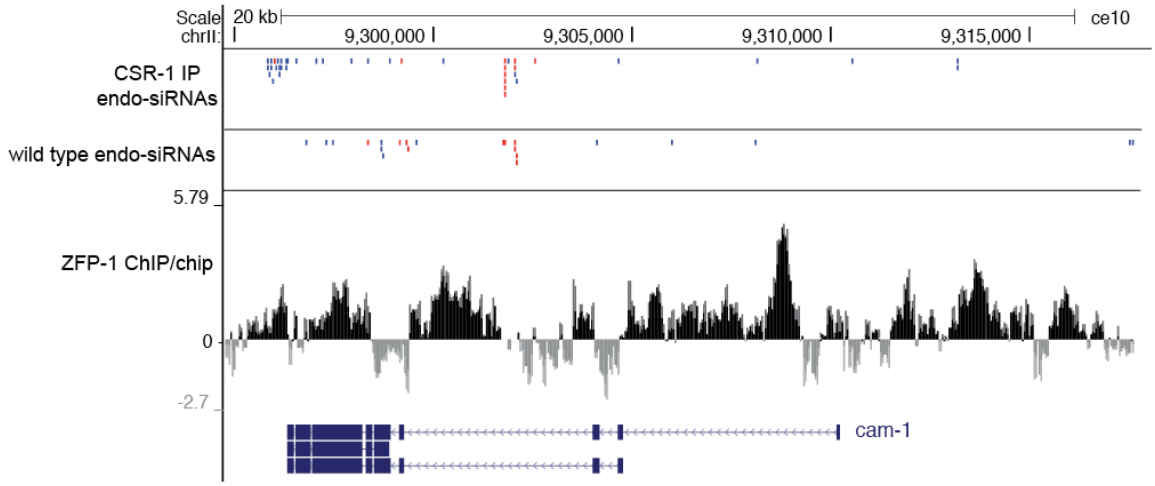

Figure 4-3. ZFP-1 and siRNAs localize to the promoter of *cam-1*. A screen shot of the *cam-1* locus generated using the UCSC genome browser indicating ZFP-1 localization peaks (ChIP/chip modENCODE data), cloned endo-siRNAs from wild type worms (Gu et al., 2009) and cloned endo-siRNAs enriched in read count in CSR-1 IP complexes (Claycomb et al., 2009). Antisense siRNAs are indicated in blue, sense siRNAs in red.

VIII. Environmental influence on neuronal development

The environment can influence the activity of both the endogenous RNAi pathway and the insulin/IGF-1 signaling pathway. The involvement of these pathways in regulating neuronal migration during development serves to highlight the "nurture versus nature" debate. It is intriguing to reflect on the possibility that the stress we subject ourselves to or the amount of calories we consume could significantly impact neuronal migration in the fetal brain during pregnancy. Moreover, in light of the growing obesity epidemic, a focus on understanding the connection between diabetes during pregnancy and fetal brain development is a point of interest. In fact, gestational diabetes has already been linked to an increased risk of schizophrenia in

offspring (Van Lieshout and Voruganti, 2008). Interestingly, schizophrenia has also been associated with neuronal migration defects (Nopoulos et al., 1995; Falkai et al., 2000), providing evidence for a direct connection between environmental signals and neuronal migration during fetal development.

Thus, the discovery that the insulin/IGF-1 signaling pathway modulates the expression of genes, such as *pak-1*, by regulating the activity of the transcription factor DAF-16/FOXO to affect neuronal migration (Chapter 2), emphasizes the importance of understanding the full set of genes and developmental processes that require insulin signaling. Similarly, dissecting the regulatory networks of other pathways subject to environmental inputs, such as endogenous RNAi, which also influence neuronal development (Chapter 3), will serve to build a greater comprehension of the link between nurture and gene expression (i.e. nature) during nervous system development.

C. elegans can arrest at an alternative larval stage called the dauer diapause under unfavorable conditions, which includes lack of nutrients, high temperatures and overcrowding. The entry into dauer diapause is regulated by multiple conserved pathways including insulin/IGF-1, TGF-β and steroid hormone signaling (reviewed in Fielenbach and Antebi, 2008). In view of the fact that we have described a role for the insulin/IGF-1 pathway in regulating neuronal migration during development, determining whether other pathways coupled to environmental signals also regulate HSN migration could offer further insight into conserved connections between the environment and neuronal migration.

Material and Methods

C. elegans Strains

Strains were maintained at 20°C using standard methods (Brenner, 1974). Bristol N2 was the wild type strain used. The following strains were provided by the Hobert lab: SK4013 *zdIs13*(*tph-1::gfp)*IV (Clark and Chiu, 2003) and *jcIs1(ajm-1::gfp)*IV. The following mutant and transgenic strains were obtained through the *Caenorhabditis* Genetics Center: LGI: CF1038 *daf-16(mu86),* LGX*:* RB689 *pak-1(ok448)*.

RNAi

RNA interference (RNAi) experiments were carried out by feeding at 20°C in the wild type background. L4 worms were fed dsRNA-producing bacteria, and their progeny scored for HSN migration defects. The following clones from the *C. elegans* feeding library (Kamath et al., 2003) were used: *cdc-42* (JA: R07G3.1), *ins-2* (JA: ZK75.2), *ins-4* (JA: ZK75.1), *ins-5* (JA: ZK84.3), *ins-6* (JA: ZK84.6), *ins-7* (ZK1251.2), *ins-8* (ZK1251.11), *ins-11* (C17C3.4), *ins-18* (T28B8.2), *ins-19* (T10D4.13), *ins-21* (M04D8.1), *ins-22* (M04D8.2), *ins-23* (M04D8.3), *ins-24* (ZC334.3), *ins-30* (ZC334.2), *ins-32* (Y8A9A.6), *ins-35* (K02E2.4), *ins-36* (Y53H1A.4), *ins-37* (F08G2.6), *ins-39* (F21E9.4). Bacteria containing each RNAi clone were grown via standard methods.

Microscopy and quantification

Live animals or embryos were mounted on 2% agarose pads and immobilized with 25 mM sodium azide (Sigma). Worms were examined using a Zeiss AxioImager Z1. All phenotypes were scored as percent animals with at least one undermigrated HSN and results are presented as

stacked bar graphs to represent the proportion of HSNs in positions along the A-P body axis in these animals. When one or both HSN cell bodies were located posterior to the vulva in adult animals, the animal was scored as mutant. Statistical significance was calculated using the *z*-test.

Acknowledgements

We thank I. Greenwald, O. Hobert and members of the Grishok lab for helpful discussions. The *pak-1(ok448)* strain was provided by the *C. elegans* Gene Knockout Project at Oklahoma Medical Research Foundation, which is part of the International *C. elegans* Gene Knockout Consortium. Some strains were provided by the CGC, which is funded by NIH Office of Research Infrastructure Programs (P40 OD010440). This work was supported by "Hormones: Biochemistry and Molecular Biology" Training Grant T32 DK0007328 and Genetics and Development Training Grant T32 GM007088 to L.M.K. and the Irma T. Hirschl Career Scientist Award to A.G.

References

Ackerman, Kozak, Przyborski, Rund, Boyer and Knowles (1997) 'The mouse rostral cerebellar malformation gene encodes an UNC-5-like protein', *Nature* 386(6627): 838-42.

Ailion, M. and Thomas, J. H. (2003) 'Isolation and characterization of high-temperature-induced Dauer formation mutants in Caenorhabditis elegans', *Genetics* 165(1): 127-44.

Ambros, V., Lee, R. C., Lavanway, A., Williams, P. T. and Jewell, D. (2003) 'MicroRNAs and other tiny endogenous RNAs in C. elegans', *Curr Biol* 13(10): 807-18.

Andrews, W., Barber, M., Hernadez-Miranda, L. R., Xian, J., Rakic, S., Sundaresan, V., Rabbitts, T. H., Pannell, R., Rabbitts, P., Thompson, H. et al. (2008) 'The role of Slit-Robo signaling in the generation, migration and morphological differentiation of cortical interneurons', *Dev Biol* 313(2): 648-58.

Aoki, K., Moriguchi, H., Yoshioka, T., Okawa, K. and Tabara, H. (2007) 'In vitro analyses of the production and activity of secondary small interfering RNAs in C. elegans', *EMBO J* 26(24): 5007-19.

Arden, K. C. (2008) 'FOXO animal models reveal a variety of diverse roles for FOXO transcription factors', *Oncogene* 27(16): 2345-50.

Arias-Romero, L. E. and Chernoff, J. (2008) 'A tale of two Paks', *Biol Cell* 100(2): 97-108.

Avgousti, Cecere and Grishok (2013) 'The conserved PHD1-PHD2 domain of ZFP-1/AF10 is a discrete functional module essential for viability in Caenorhabditis elegans', *Mol Cell Biol* 33(5): 999-1015.

Avgousti, D. C., Palani, S., Sherman, Y. and Grishok, A. (2012) 'CSR-1 RNAi pathway positively regulates histone expression in C. elegans', *EMBO J* 31(19): 3821-32.

Ayala, R., Shu, T. and Tsai (2007) 'Trekking across the brain: the journey of neuronal migration', *Cell* 128(1): 29-43.

Backman, Stambolic, Suzuki, Haight, Elia, Pretorius, Tsao, Shannon, Bolon, Ivy et al. (2001) 'Deletion of Pten in mouse brain causes seizures, ataxia and defects in soma size resembling Lhermitte-Duclos disease', *Nat Genet* 29(4): 396-403.

Bahri, S. M., Chia, W. and Yang, X. (2001) 'The Drosophila homolog of human AF10/AF17 leukemia fusion genes (Dalf) encodes a zinc finger/leucine zipper nuclear protein required in the nervous system for maintaining EVE expression and normal growth', *Mech Dev* 100(2): 291-301.

Bateman, J. M. and McNeill, H. (2006) 'Insulin/IGF signalling in neurogenesis', *Cell Mol Life Sci* 63(15): 1701-5.

Baumeister, R., Liu, Y. and Ruvkun, G. (1996) 'Lineage-specific regulators couple cell lineage asymmetry to the transcription of the Caenorhabditis elegans POU gene unc-86 during neurogenesis', *Genes Dev* 10(11): 1395-410.

Beck, Powell-Braxton, Widmer, Valverde and Hefti (1995) 'Igf1 gene disruption results in reduced brain size, CNS hypomyelination, and loss of hippocampal granule and striatal parvalbumin-containing neurons', *Neuron* 14(4): 717-30.

Blanchard, D., Parameswaran, P., Lopez-Molina, J., Gent, J., Saynuk, J. F. and Fire, A. (2011) 'On the nature of in vivo requirements for rde-4 in RNAi and developmental pathways in C. elegans', *RNA Biol* 8(3): 458-67.

Bokoch, G. M. (2003) 'Biology of the p21-activated kinases', *Annu Rev Biochem* 72: 743-81.

Bossinger, O., Klebes, A., Segbert, C., Theres, C. and Knust, E. (2001) 'Zonula adherens formation in Caenorhabditis elegans requires dlg-1, the homologue of the Drosophila gene discs large', *Dev Biol* 230(1): 29-42.

Bradford, D., Cole, S. J. and Cooper, H. M. (2009) 'Netrin-1: diversity in development', *Int J Biochem Cell Biol* 41(3): 487-93.

Brenner, S. (1974) 'The genetics of Caenorhabditis elegans', *Genetics* 77(1): 71-94.

Brose, K., Bland, K. S., Wang, K. H., Arnott, D., Henzel, W., Goodman, C. S., Tessier-Lavigne, M. and Kidd, T. (1999) 'Slit proteins bind Robo receptors and have an evolutionarily conserved role in repulsive axon guidance', *Cell* 96(6): 795-806.

Brunet, Bonni, Zigmond, Lin, Juo, Hu, Anderson, Arden, Blenis and Greenberg (1999) 'Akt promotes cell survival by phosphorylating and inhibiting a Forkhead transcription factor', *Cell* 96(6): 857-68.

Bruning, J. C., Gautam, D., Burks, D. J., Gillette, J., Schubert, M., Orban, P. C., Klein, R., Krone, W., Muller-Wieland, D. and Kahn, C. R. (2000) 'Role of brain insulin receptor in control of body weight and reproduction', *Science* 289(5487): 2122-5.

Buechling, T. and Boutros, M. (2011) 'Wnt signaling signaling at and above the receptor level', *Curr Top Dev Biol* 97: 21-53.

Bulow, H. E., Berry, K. L., Topper, L. H., Peles, E. and Hobert, O. (2002) 'Heparan sulfate proteoglycan-dependent induction of axon branching and axon misrouting by the Kallmann syndrome gene kal-1', *Proc Natl Acad Sci U S A* 99(9): 6346-51.

Burton, N. O., Burkhart, K. B. and Kennedy, S. (2011) 'Nuclear RNAi maintains heritable gene silencing in Caenorhabditis elegans', *Proc Natl Acad Sci U S A* 108(49): 19683-8.

Calixto, A., Jara, J. S. and Court, F. A. (2012) 'Diapause formation and downregulation of insulin-like signaling via DAF-16/FOXO delays axonal degeneration and neuronal loss', *PLoS Genet* 8(12): e1003141.

Candeias, E., Duarte, A. I., Carvalho, C., Correia, S. C., Cardoso, S., Santos, R. X., Placido, A. I., Perry, G. and Moreira, P. I. (2012) 'The impairment of insulin signaling in Alzheimer's disease', *IUBMB Life* 64(12): 951-7.

Cariboni, A., Andrews, W. D., Memi, F., Ypsilanti, A. R., Zelina, P., Chedotal, A. and Parnavelas, J. G. (2012) 'Slit2 and Robo3 modulate the migration of GnRH-secreting neurons', *Development* 139(18): 3326-31.

Carson, Behringer, Brinster and McMorris (1993) 'Insulin-like growth factor I increases brain growth and central nervous system myelination in transgenic mice', *Neuron* 10(4): 729-40.

Castelo-Branco, G., Sousa, K. M., Bryja, V., Pinto, L., Wagner, J. and Arenas, E. (2006) 'Ventral midbrain glia express region-specific transcription factors and regulate dopaminergic neurogenesis through Wnt-5a secretion', *Mol Cell Neurosci* 31(2): 251-62.

Cecere, G., Hoersch, S., Jensen, M. B., Dixit, S. and Grishok, A. (2013) 'The ZFP-1(AF10)/DOT-1 Complex Opposes H2B Ubiquitination to Reduce Pol II Transcription', *Mol Cell* 50(6): 894-907.

Ceol, C. J. and Horvitz, H. R. (2004) 'A new class of C. elegans synMuv genes implicates a Tip60/NuA4-like HAT complex as a negative regulator of Ras signaling', *Dev Cell* 6(4): 563-76.

Chai, X., Forster, E., Zhao, S., Bock, H. H. and Frotscher, M. (2009) 'Reelin stabilizes the actin cytoskeleton of neuronal processes by inducing n-cofilin phosphorylation at serine3', *J Neurosci* 29(1): 288-99.

Chan, S. S., Zheng, H., Su, M. W., Wilk, R., Killeen, M. T., Hedgecock, E. M. and Culotti, J. G. (1996) 'UNC-40, a C. elegans homolog of DCC (Deleted in Colorectal Cancer), is required in motile cells responding to UNC-6 netrin cues', *Cell* 87(2): 187-95.

Chang, Adler, Krause, Clark, Gertler, Tessier-Lavigne and Bargmann (2006) 'MIG-10/Lamellipodin and AGE-1/PI3K Promote Axon Guidance and Outgrowth in Response to Slit and Netrin', *Current Biology* 16(9): 854-862.

Chaplin, T., Ayton, P., Bernard, O. A., Saha, V., Della Valle, V., Hillion, J., Gregorini, A., Lillington, D., Berger, R. and Young, B. D. (1995) 'A novel class of zinc finger/leucine zipper genes identified from the molecular cloning of the t(10;11) translocation in acute leukemia', *Blood* 85(6): 1435-41.

Chen, W., Chen, S., Yap, S. F. and Lim, L. (1996) 'The Caenorhabditis elegans p21-activated kinase (CePAK) colocalizes with CeRac1 and CDC42Ce at hypodermal cell boundaries during embryo elongation', *J Biol Chem* 271(42): 26362-8.

Christensen, R., de la Torre-Ubieta, L., Bonni, A. and Colon-Ramos, D. A. (2011) 'A conserved PTEN/FOXO pathway regulates neuronal morphology during C. elegans development', *Development* 138(23): 5257-67.

Clark, S. G. and Chiu, C. (2003) 'C. elegans ZAG-1, a Zn-finger-homeodomain protein, regulates axonal development and neuronal differentiation', *Development* 130(16): 3781-94.

Claycomb, J. M., Batista, P. J., Pang, K. M., Gu, W., Vasale, J. J., van Wolfswinkel, J. C., Chaves, D. A., Shirayama, M., Mitani, S., Ketting, R. F. et al. (2009) 'The Argonaute CSR-1 and its 22G-RNA cofactors are required for holocentric chromosome segregation', *Cell* 139(1): 123-34.

Conine, C. C., Batista, P. J., Gu, W., Claycomb, J. M., Chaves, D. A., Shirayama, M. and Mello, C. C. (2010) 'Argonautes ALG-3 and ALG-4 are required for spermatogenesis-specific 26G-RNAs and thermotolerant sperm in Caenorhabditis elegans', *Proc Natl Acad Sci USA* 107(8): 3588-93.

Costa, M., Draper, B. W. and Priess, J. R. (1997) 'The role of actin filaments in patterning the Caenorhabditis elegans cuticle', *Dev Biol* 184(2): 373-84.

Costa, M., Raich, W., Agbunag, C., Leung, B., Hardin, J. and Priess, J. R. (1998) 'A putative catenin-cadherin system mediates morphogenesis of the Caenorhabditis elegans embryo', *J Cell Biol* 141(1): 297-308.

Coudreuse, D. Y., Roël, G., Betist, M. C., Destrée, O. and Korswagen, H. C. (2006) 'Wnt gradient formation requires retromer function in Wnt-producing cells', *Science* 312(5775): 921-4.

Cui, M., Chen, J., Myers, T. R., Hwang, B. J., Sternberg, P. W., Greenwald, I. and Han, M. (2006a) 'SynMuv genes redundantly inhibit lin-3/EGF expression to prevent inappropriate vulval induction in C. elegans', *Dev Cell* 10(5): 667-72.

Cui, M., Kim, E. and Han, M. (2006b) 'Diverse Chromatin Remodeling Genes Antagonize the Rb-Involved SynMuv Pathways in C. elegans', *PLoS Genet* 2(5): e74.

da Graca, L. S., Zimmerman, K. K., Mitchell, M. C., Kozhan-Gorodetska, M., Sekiewicz, K., Morales, Y. and Patterson, G. I. (2004) 'DAF-5 is a Ski oncoprotein homolog that functions in a neuronal TGF beta pathway to regulate C. elegans dauer development', *Development* 131(2): 435-46.

de la Torre-Ubieta, L., Gaudillière, B., Yang, Y., Ikeuchi, Y., Yamada, T., DiBacco, S., Stegmüller, J., Schüller, U., Salih, D. A., Rowitch, D. et al. (2010) 'A FOXO-Pak1 transcriptional pathway controls neuronal polarity', *Genes & Development* 24(8): 799-813.

Desai, C., Garriga, G., McIntire, S. L. and Horvitz, H. R. (1988) 'A genetic pathway for the development of the Caenorhabditis elegans HSN motor neurons', *Nature* 336(6200): 638-46.

Dhavan, R. and Tsai, L. H. (2001) 'A decade of CDK5', *Nat Rev Mol Cell Biol* 2(10): 749-59.

DiMartino, J. F., Ayton, P. M., Chen, E. H., Naftzger, C. C., Young, B. D. and Cleary, M. L. (2002) 'The AF10 leucine zipper is required for leukemic transformation of myeloid progenitors by MLL-AF10', *Blood* 99(10): 3780-5.

Driver, R. J., Lamb, A. L., Wyner, A. J. and Raizen, D. M. (2013) 'DAF-16/FOXO regulates homeostasis of essential sleep-like behavior during larval transitions in C. elegans', *Curr Biol* 23(6): 501-6.

Duchaine, T. F., Wohlschlegel, J. A., Kennedy, S., Bei, Y., Conte, D., Jr., Pang, K., Brownell, D. R., Harding, S., Mitani, S., Ruvkun, G. et al. (2006) 'Functional proteomics reveals the biochemical niche of C. elegans DCR-1 in multiple small-RNA-mediated pathways', *Cell* 124(2): 343-54.

Dudley, N. R., Labbe, J. C. and Goldstein, B. (2002) 'Using RNA interference to identify genes required for RNA interference', *Proc Natl Acad Sci U S A* 99(7): 4191-6.

Edgley, M. L., Baillie, D. L., Riddle, D. L. and Rose, A. M. (2006) 'Genetic balancers', *WormBook*: 1-32.

Edmondson, J. C. and Hatten, M. E. (1987) 'Glial-guided granule neuron migration in vitro: a high-resolution time-lapse video microscopic study', *J Neurosci* 7(6): 1928-34.

Edwards, Sanders, Bokoch and Gill (1999) 'Activation of LIM-kinase by Pak1 couples Rac/Cdc42 GTPase signalling to actin cytoskeletal dynamics', *Nat Cell Biol* 1(5): 253-9.

Esteve, P. and Bovolenta, P. (2010) 'The advantages and disadvantages of sfrp1 and sfrp2 expression in pathological events', *Tohoku J Exp Med* 221(1): 11-7.

Falkai, Schneider-Axmann and Honer (2000) 'Entorhinal cortex pre-alpha cell clusters in schizophrenia: quantitative evidence of a developmental abnormality', *Biol Psychiatry* 47(11): 937-43.

Ferguson, E. L. and Horvitz, H. R. (1989) 'The multivulva phenotype of certain Caenorhabditis elegans mutants results from defects in two functionally redundant pathways', *Genetics* 123(1): 109-21.

Fielenbach, N. and Antebi, A. (2008) 'C. elegans dauer formation and the molecular basis of plasticity', *Genes Dev* 22(16): 2149-65.

Fire, A., Xu, S., Montgomery, M. K., Kostas, S. A., Driver, S. E. and Mello, C. C. (1998) 'Potent and specific genetic interference by double-stranded RNA in Caenorhabditis elegans', *Nature* 391(6669): 806-11.

Fischer, S. E., Montgomery, T. A., Zhang, C., Fahlgren, N., Breen, P. C., Hwang, A., Sullivan, C. M., Carrington, J. C. and Ruvkun, G. (2011) 'The ERI-6/7 helicase acts at the first stage of an siRNA amplification pathway that targets recent gene duplications', *PLoS Genet* 7(11): e1002369.

Flamand, M. and Duchaine, T. F. (2012) 'Snapshot: endogenous RNAi [corrected] pathways', *Cell* 150(2): 442-442 e1.

Flames, N. and Hobert, O. (2009) 'Gene regulatory logic of dopamine neuron differentiation', *Nature* 458(7240): 885-9.

Fleming, T. C., Wolf, F. W. and Garriga, G. (2005) 'Sensitized genetic backgrounds reveal a role for C. elegans FGF EGL-17 as a repellent for migrating CAN neurons', *Development* 132(21): 4857-67.

Forrester and Garriga, G. (1997) 'Genes necessary for C. elegans cell and growth cone migrations', *Development* 124(9): 1831-43.

Forrester, W. C., Dell, M., Perens, E. and Garriga, G. (1999) 'A C. elegans Ror receptor tyrosine kinase regulates cell motility and asymmetric cell division', *Nature* 400(6747): 881-5.

Forrester, W. C., Kim, C. and Garriga, G. (2004) 'The Caenorhabditis elegans Ror RTK CAM-1 inhibits EGL-20/Wnt signaling in cell migration', *Genetics* 168(4): 1951-62.

Forrester, W. C., Perens, E., Zallen, J. A. and Garriga, G. (1998) 'Identification of Caenorhabditis elegans genes required for neuronal differentiation and migration', *Genetics* 148(1): 151-65.

Fox, J. W., Lamperti, E. D., Ekşioğlu, Y. Z., Hong, S. E., Feng, Y., Graham, D. A., Scheffer, I. E., Dobyns, W. B., Hirsch, B. A., Radtke, R. A. et al. (1998) 'Mutations in filamin 1 prevent migration of cerebral cortical neurons in human periventricular heterotopia', *Neuron* 21(6): 1315-25.

Franco, S. J., Martinez-Garay, I., Gil-Sanz, C., Harkins-Perry, S. R. and Muller, U. (2011) 'Reelin regulates cadherin function via Dab1/Rap1 to control neuronal migration and lamination in the neocortex', *Neuron* 69(3): 482-97.

Friedman and Johnson (1988) 'A mutation in the age-1 gene in Caenorhabditis elegans lengthens life and reduces hermaphrodite fertility', *Genetics* 118(1): 75-86.

Fujisawa, K., Wrana, J. L. and Culotti, J. G. (2007) 'The slit receptor EVA-1 coactivates a SAX-3/Robo mediated guidance signal in C. elegans', *Science* 317(5846): 1934-8.

Furuyama, Nakazawa, Nakano and Mori (2000) 'Identification of the differential distribution patterns of mRNAs and consensus binding sequences for mouse DAF-16 homologues', *Biochem J* 349(Pt 2): 629-34.

Gaglia, M. M. and Kenyon, C. (2009) 'Stimulation of movement in a quiescent, hibernation-like form of Caenorhabditis elegans by dopamine signaling', *J Neurosci* 29(22): 7302-14.

Garriga, G., Desai, C. and Horvitz, H. R. (1993) 'Cell interactions control the direction of outgrowth, branching and fasciculation of the HSN axons of Caenorhabditis elegans', *Development* 117(3): 1071-87.

Gelot, A., Billette de Villemeur, T., Bordarier, C., Ruchoux, M. M., Moraine, C. and Ponsot, G. (1995) 'Developmental aspects of type II lissencephaly. Comparative study of dysplastic lesions in fetal and post-natal brains', *Acta Neuropathol* 89(1): 72-84.

Gent, J., Schvarzstein, M., Villeneuve, A. M., Gu, S. G., Jantsch, V., Fire, A. and Baudrimont, A. (2009) 'A Caenorhabditis elegans RNA-directed RNA polymerase in sperm development and endogenous RNA interference', *Genetics* 183(4): 1297-314.

Gilleard, Barry and Johnstone (1997) 'cis regulatory requirements for hypodermal cell-specific expression of the Caenorhabditis elegans cuticle collagen gene dpy-7', *Mol Cell Biol* 17(4): 2301-11.

Gleason, Szyleyko and Eisenmann (2006) 'Multiple redundant Wnt signaling components function in two processes during C. elegans vulval development', *Developmental Biology* 298(2): 442-57.

Green, J. L., Inoue, T. and Sternberg, P. W. (2007) 'The C. elegans ROR receptor tyrosine kinase, CAM-1, non-autonomously inhibits the Wnt pathway', *Development* 134(22): 4053-62.

Green, J. L., Kuntz, S. G. and Sternberg, P. W. (2008) 'Ror receptor tyrosine kinases: orphans no more', *Trends Cell Biol* 18(11): 536-44.

Grishok, A., Hoersch, S. and Sharp, P. A. (2008) 'RNA interference and retinoblastoma-related genes are required for repression of endogenous siRNA targets in Caenorhabditis elegans', *Proc Natl Acad Sci U S A* 105(51): 20386-91.

Grishok, A., Sinskey, J. L. and Sharp, P. A. (2005) 'Transcriptional silencing of a transgene by RNAi in the soma of C. elegans', *Genes Dev* 19(6): 683-96.

Gu, S. G., Pak, J., Guang, S., Maniar, J. M., Kennedy, S. and Fire, A. (2012) 'Amplification of siRNA in Caenorhabditis elegans generates a transgenerational sequence-targeted histone H3 lysine 9 methylation footprint', *Nat Genet* 44(2): 157-64.

Gu, W., Shirayama, M., Conte, D., Vasale, J., Batista, P. J., Claycomb, J. M., Moresco, J. J., Youngman, E. M., Keys, J., Stoltz, M. J. et al. (2009) 'Distinct Argonaute-Mediated 22G-RNA Pathways Direct Genome Surveillance in the C. elegans Germline', *Molecular Cell*.

Guang, Bochner, Burkhart, Burton, Pavelec and Kennedy (2010) 'Small regulatory RNAs inhibit RNA polymerase II during the elongation phase of transcription', *Nature* 465(7301): 1097-101.

Gumbiner, B. M. (2005) 'Regulation of cadherin-mediated adhesion in morphogenesis', *Nat Rev Mol Cell Biol* 6(8): 622-34.

Halaschek-Wiener, J., Khattra, J. S., McKay, S., Pouzyrev, A., Stott, J. M., Yang, G. S., Holt, R. A., Jones, S. J., Marra, M. A., Brooks-Wilson, A. R. et al. (2005) 'Analysis of long-lived C. elegans daf-2 mutants using serial analysis of gene expression', *Genome Res* 15(5): 603-15.

Han, T., Manoharan, A. P., Harkins, T. T., Bouffard, P., Fitzpatrick, C., Chu, D. S., Thierry-Mieg, D., Thierry-Mieg, J. and Kim, J. K. (2009) '26G endo-siRNAs regulate spermatogenic and zygotic gene expression in Caenorhabditis elegans', *Proc Natl Acad Sci USA* 106(44): 18674-9.

Hao, Yu, Fujisawa, Culotti, J. G., Gengyo-Ando, Mitani, S., Moulder, Barstead, Tessier-Lavigne and Bargmann (2001) 'C. elegans slit acts in midline, dorsal-ventral, and anterior-posterior guidance via the SAX-3/Robo receptor', *Neuron* 32(1): 25-38.

Hardin, King, Thomas-Virnig and Raich (2008) 'Zygotic loss of ZEN-4/MKLP1 results in disruption of epidermal morphogenesis in the C. elegans embryo', *Dev Dyn* 237(3): 830-6.

Harris, J., Honigberg, L., Robinson, N. and Kenyon, C. (1996) 'Neuronal cell migration in C. elegans: regulation of Hox gene expression and cell position', *Development* 122(10): 3117-31.

Harterink, Kim, Middelkoop, Doan, Oudenaarden, v. and Korswagen (2011) 'Neuroblast migration along the anteroposterior axis of C. elegans is controlled by opposing gradients of Wnts and a secreted Frizzled-related protein', *Development* 138(14): 2915-24.

Hatten, M. E. (2002) 'New directions in neuronal migration', *Science* 297(5587): 1660-3.

Hedgecock, E. M., Culotti, J. G. and Hall, D. H. (1990) 'The unc-5, unc-6, and unc-40 genes guide circumferential migrations of pioneer axons and mesodermal cells on the epidermis in C. elegans', *Neuron* 4(1): 61-85.

Hedgecock, E. M., Culotti, J. G., Hall, D. H. and Stern (1987) 'Genetics of cell and axon migrations in Caenorhabditis elegans', *Development* 100(3): 365-82.

Henderson and Johnson (2001) 'daf-16 integrates developmental and environmental inputs to mediate aging in the nematode Caenorhabditis elegans', *Curr Biol* 11(24): 1975-80.

Herman, M. A., Vassilieva, L. L., Horvitz, H. R., Shaw, J. E. and Herman, R. K. (1995) 'The C. elegans gene lin-44, which controls the polarity of certain asymmetric cell divisions, encodes a Wnt protein and acts cell nonautonomously', *Cell* 83(1): 101-10.

Herman, R. K. and Hedgecock, E. M. (1990) 'Limitation of the size of the vulval primordium of Caenorhabditis elegans by lin-15 expression in surrounding hypodermis', *Nature* 348(6297): 169-71.

Hertweck, M., Göbel, C. and Baumeister, R. (2004) 'C. elegans SGK-1 is the critical component in the Akt/PKB kinase complex to control stress response and life span', *Dev Cell* 6(4): 577-88.

Hoekman, Jacobs, Smidt and Burbach (2006) 'Spatial and temporal expression of FoxO transcription factors in the developing and adult murine brain', *Gene Expr Patterns* 6(2): 134-40.

Hofmann, C., Shepelev, M. and Chernoff, J. (2004) 'The genetics of Pak', *J Cell Sci* 117(Pt 19): 4343-54.

Hong, S. E., Shugart, Y. Y., Huang, D. T., Shahwan, S. A., Grant, P. E., Hourihane, J. O., Martin, N. D. and Walsh, C. A. (2000) 'Autosomal recessive lissencephaly with cerebellar hypoplasia is associated with human RELN mutations', *Nat Genet* 26(1): 93-6.

Hsu, A. L., Murphy, C. T. and Kenyon, C. (2003) 'Regulation of aging and age-related disease by DAF-16 and heat-shock factor', *Science* 300(5622): 1142-5.

Hu, Sun, Owens, Gu, Wu, Chen, O'Flaherty and Edwards (2010) 'Syndecan-1-dependent suppression of PDK1/Akt/bad signaling by docosahexaenoic acid induces apoptosis in prostate cancer', *Neoplasia* 12(10): 826-36.

Hurtado-Chong, A., Yusta-Boyo, M., Vergaño-Vera, E., Bulfone, A., De Pablo, F. and Vicario-Abejón, C. (2009) 'IGF-I promotes neuronal migration and positioning in the olfactory bulb and the exit of neuroblasts from the subventricular zone', *Eur J Neurosci* 30(5): 742-55.

Hutvagner, G. and Simard, M. J. (2008) 'Argonaute proteins: key players in RNA silencing', *Nat Rev Mol Cell Biol* 9(1): 22-32.

Iino and Yamamoto (1998) 'Expression pattern of the C. elegans P21-activated protein kinase, CePAK', *Biochem Biophys Res Commun* 245(1): 177-84.

Ishii, Wadsworth, Stern, Culotti, J. G. and Hedgecock, E. M. (1992) 'UNC-6, a laminin-related protein, guides cell and pioneer axon migrations in C. elegans', *Neuron* 9(5): 873-81.

Jose, A. M., Garcia, G. A. and Hunter, C. P. (2011) 'Two classes of silencing RNAs move between Caenorhabditis elegans tissues', *Nat Struct Mol Biol* 18(11): 1184-8.

Kamath, R. S., Fraser, A. G., Dong, Y., Poulin, G., Durbin, R., Gotta, M., Kanapin, A., Le Bot, N., Moreno, S., Sohrmann, M. et al. (2003) 'Systematic functional analysis of the Caenorhabditis elegans genome using RNAi', *Nature* 421(6920): 231-7.

Kawano, Ito, Ishiguro, Takuwa, Nakajima and Kimura (2000) 'Molecular cloning and characterization of a new insulin/IGF-like peptide of the nematode Caenorhabditis elegans', *Biochem Biophys Res Commun* 273(2): 431-6.

Kee, Y., Hwang, B. J., Sternberg, P. W. and Bronner-Fraser, M. (2007) 'Evolutionary conservation of cell migration genes: from nematode neurons to vertebrate neural crest', *Genes Dev* 21(4): 391-6.

Kennerdell, J. R., Fetter, R. D. and Bargmann, C. I. (2009) 'Wnt-Ror signaling to SIA and SIB neurons directs anterior axon guidance and nerve ring placement in C. elegans', *Development* 136(22): 3801-10.

Kenyon, C. (2005) 'The plasticity of aging: insights from long-lived mutants', *Cell* 120(4): 449-60.

Kenyon, C. and Murphy, C. T. (2006) 'Enrichment of regulatory motifs upstream of predicted DAF-16 targets', *Nat Genet* 38(4): 397-8; author reply 398.

Ketting (2011) 'The many faces of RNAi', *Dev Cell* 20(2): 148-61.

Killeen, M. T. and Sybingco, S. S. (2008) 'Netrin, Slit and Wnt receptors allow axons to choose the axis of migration', *Developmental Biology* 323(2): 143-51.

Kim, C. and Forrester, W. C. (2003) 'Functional analysis of the domains of the C elegans Ror receptor tyrosine kinase CAM-1', *Dev Biol* 264(2): 376-90.

Kim, J. K., Gabel, H. W., Kamath, R. S., Tewari, M., Pasquinelli, A., Rual, J. F., Kennedy, S., Dybbs, M., Bertin, N., Kaplan, J. M. et al. (2005) 'Functional genomic analysis of RNA interference in C. elegans', *Science* 308(5725): 1164-7.

Kimura, Tissenbaum, H. A., Liu, Y. and Ruvkun, G. (1997) 'daf-2, an insulin receptor-like gene that regulates longevity and diapause in Caenorhabditis elegans', *Science* 277(5328): 942-6.

Kimura, K. D., Riddle, D. L. and Ruvkun, G. (2011) 'The C. elegans DAF-2 insulin-like receptor is abundantly expressed in the nervous system and regulated by nutritional status', *Cold Spring Harb Symp Quant Biol* 76: 113-20.

Koppen, M., Simske, J. S., Sims, P. A., Firestein, B. L., Hall, D. H., Radice, A. D., Rongo, C. and Hardin, J. D. (2001) 'Cooperative regulation of AJM-1 controls junctional integrity in Caenorhabditis elegans epithelia', *Nat Cell Biol* 3(11): 983-91.

Kops and Burgering (2000) 'Forkhead transcription factors are targets of signalling by the proto-oncogene PKB (C-AKT)', *J Anat* 197 Pt 4: 571-4.

Krause, M., Dent, E. W., Bear, J. E., Loureiro, J. J. and Gertler, F. B. (2003) 'Ena/VASP proteins: regulators of the actin cytoskeleton and cell migration', *Annu Rev Cell Dev Biol* 19: 541-64.

Kreis, P. and Barnier, J. V. (2009) 'PAK signalling in neuronal physiology', *Cell Signal* 21(3): 384-93.

Kwon, Narasimhan, Yen and Tissenbaum (2010) 'A new DAF-16 isoform regulates longevity', *Nature* 466(7305): 498-502.

Kwon, Zhu, Zhang, Knoop, Tharp, Smeyne, Eberhart, Burger and Baker (2001) 'Pten regulates neuronal soma size: a mouse model of Lhermitte-Duclos disease', *Nat Genet* 29(4): 404-11.

Lapierre, L. R. and Hansen, M. (2012) 'Lessons from C. elegans: signaling pathways for longevity', *Trends Endocrinol Metab* 23(12): 637-44.

Lee, R. C., Hammell, C. M. and Ambros, V. (2006) 'Interacting endogenous and exogenous RNAi pathways in Caenorhabditis elegans', *RNA* 12(4): 589-97.

Lee, R. Y., Hench, J. and Ruvkun, G. (2001) 'Regulation of C. elegans DAF-16 and its human ortholog FKHRL1 by the daf-2 insulin-like signaling pathway', *Curr Biol* 11(24): 1950-7.

Leinninger, Backus, Uhler, Lentz and Feldman (2004) 'Phosphatidylinositol 3-kinase and Akt effectors mediate insulin-like growth factor-I neuroprotection in dorsal root ganglia neurons', *FASEB J* 18(13): 1544-6.

Leonardo, Hinck, Masu, Keino-Masu, Ackerman and Tessier-Lavigne (1997) 'Vertebrate homologues of C. elegans UNC-5 are candidate netrin receptors', *Nature* 386(6627): 833-8.

Leung-Hagesteijn, C., Spence, A. M., Stern, B. D., Zhou, Y., Su, M. W., Hedgecock, E. M. and Culotti, J. G. (1992) 'UNC-5, a transmembrane protein with immunoglobulin and thrombospondin type 1 domains, guides cell and pioneer axon migrations in C. elegans', *Cell* 71(2): 289-99.

Levy-Strumpf, N. and Culotti, J. G. (2007) 'VAB-8, UNC-73 and MIG-2 regulate axon polarity and cell migration functions of UNC-40 in C. elegans', *Nat Neurosci* 10(2): 161-8.

Li, Kennedy and Ruvkun (2003) 'daf-28 encodes a C. elegans insulin superfamily member that is regulated by environmental cues and acts in the DAF-2 signaling pathway', *Genes & Development* 17(7): 844-58.

Li, H. S., Chen, J. H., Wu, W., Fagaly, T., Zhou, L., Yuan, W., Dupuis, S., Jiang, Z. H., Nash, W., Gick, C. et al. (1999) 'Vertebrate slit, a secreted ligand for the transmembrane protein roundabout, is a repellent for olfactory bulb axons', *Cell* 96(6): 807-18.

Li, J., Ebata, A., Dong, Y., Rizki, G., Iwata, T. and Lee, S. S. (2008) 'Caenorhabditis elegans HCF-1 functions in longevity maintenance as a DAF-16 regulator', *PLoS Biol* 6(9): e233.

Li, L. and Liu, Y. (2011) 'Diverse small non-coding RNAs in RNA interference pathways', *Methods Mol Biol* 764: 169-82.

Li, W., Gao, B., Lee, S. M., Bennett, K. and Fang, D. (2007) 'RLE-1, an E3 ubiquitin ligase, regulates C. elegans aging by catalyzing DAF-16 polyubiquitination', *Dev Cell* 12(2): 235-46.

Libina, N., Berman, J. R. and Kenyon, C. (2003) 'Tissue-specific activities of C. elegans DAF-16 in the regulation of lifespan', *Cell* 115(4): 489-502.

Lin, K., Dorman, J. B., Rodan, A. and Kenyon, C. (1997) 'daf-16: An HNF-3/forkhead family member that can function to double the life-span of Caenorhabditis elegans', *Science* 278(5341): 1319-22.

Lin, K., Hsin, Libina and Kenyon, C. (2001) 'Regulation of the Caenorhabditis elegans longevity protein DAF-16 by insulin/IGF-1 and germline signaling', *Nat Genet* 28(2): 139-45.

Liu, F., Jia, L., Thompson-Baine, A. M., Puglise, J. M., Ter Beest, M. B. and Zegers, M. M. (2010) 'Cadherins and Pak1 control contact inhibition of proliferation by Pak1-betaPIX-GIT complex-dependent regulation of cell-matrix signaling', *Mol Cell Biol* 30(8): 1971-83.

Liu, J. P., Baker, J., Perkins, A. S., Robertson, E. J. and Efstratiadis, A. (1993) 'Mice carrying null mutations of the genes encoding insulin-like growth factor I (Igf-1) and type 1 IGF receptor (Igf1r)', *Cell* 75(1): 59-72.

Lozano, E., Frasa, M. A., Smolarczyk, K., Knaus, U. G. and Braga, V. M. (2008) 'PAK is required for the disruption of E-cadherin adhesion by the small GTPase Rac', *J Cell Sci* 121(Pt 7): 933-8.

Lucanic, M., Kiley, M., Ashcroft, N., L'etoile, N. and Cheng, H. J. (2006) 'The Caenorhabditis elegans P21-activated kinases are differentially required for UNC-6/netrin-mediated commissural motor axon guidance', *Development* 133(22): 4549-59.

Ma, X., Kawamoto, S., Hara, Y. and Adelstein, R. S. (2004) 'A point mutation in the motor domain of nonmuscle myosin II-B impairs migration of distinct groups of neurons', *Mol Biol Cell* 15(6): 2568-79.

Maduro, M. F., Gordon, M., Jacobs, R. and Pilgrim, D. B. (2000) 'The UNC-119 family of neural proteins is functionally conserved between humans, Drosophila and C. elegans', *J Neurogenet* 13(4): 191-212.

Mahmoudi, T., Boj, S. F., Hatzis, P., Li, V. S., Taouatas, N., Vries, R. G., Teunissen, H., Begthel, H., Korving, J., Mohammed, S. et al. (2010) 'The leukemia-associated Mllt10/Af10-Dot1l are Tcf4/beta-catenin coactivators essential for intestinal homeostasis', *PLoS Biol* 8(11): e1000539.

Maloof, J. N., Whangbo, J., Harris, J. M., Jongeward, G. D. and Kenyon, C. (1999) 'A Wnt signaling pathway controls hox gene expression and neuroblast migration in C. elegans', *Development* 126(1): 37-49.

Maniar, J. M. and Fire, A. Z. (2011) 'EGO-1, a C. elegans RdRP, modulates gene expression via production of mRNA-templated short antisense RNAs', *Curr Biol* 21(6): 449-59.

Manser, J. and Wood, W. B. (1990) 'Mutations affecting embryonic cell migrations in Caenorhabditis elegans', *Dev Genet* 11(1): 49-64.

Mansisidor, A. R., Cecere, G., Hoersch, S., Jensen, M. B., Kawli, T., Kennedy, L. M., Chavez, V., Tan, M. W., Lieb, J. D. and Grishok, A. (2011) 'A conserved PHD finger protein and endogenous RNAi modulate insulin signaling in Caenorhabditis elegans', *PLoS Genet* 7(9): e1002299.

Marín and Rubenstein (2003) 'Cell migration in the forebrain', *Annu Rev Neurosci* 26: 441-83.

Marín, Valiente, Ge and Tsai (2010) 'Guiding neuronal cell migrations', *Cold Spring Harb Perspect Biol* 2(2): a001834.

Marin, O. and Rubenstein, J. L. (2001) 'A long, remarkable journey: tangential migration in the telencephalon', *Nat Rev Neurosci* 2(11): 780-90.

Marino, Krimpenfort, Leung, Korput, v. d., Trapman, Camenisch, Berns and Brandner (2002) 'PTEN is essential for cell migration but not for fate determination and tumourigenesis in the cerebellum', *Development* 129(14): 3513-22.

Marzluff, W. F., Wagner, E. J. and Duronio, R. J. (2008) 'Metabolism and regulation of canonical histone mRNAs: life without a poly(A) tail', *Nat Rev Genet* 9(11): 843-54.

Masse, Molin, Billaud and Solari (2005) 'Lifespan and dauer regulation by tissue-specific activities of Caenorhabditis elegans DAF-18', *Developmental Biology* 286(1): 91-101.

Matsunaga, Gengyo-Ando, Mitani, Iwasaki and Kawano (2012) 'Physiological function, expression pattern, and transcriptional regulation of a Caenorhabditis elegans insulin-like peptide, INS-18', *Biochem Biophys Res Commun* 423(3): 478-83.

McElwee, Schuster, Blanc, Thomas and Gems (2004) 'Shared transcriptional signature in Caenorhabditis elegans Dauer larvae and long-lived daf-2 mutants implicates detoxification system in longevity assurance', *J Biol Chem* 279(43): 44533-43.

McElwee, J., Bubb, K. and Thomas, J. H. (2003) 'Transcriptional outputs of the Caenorhabditis elegans forkhead protein DAF-16', *Aging Cell* 2(2): 111-21.

Meister, G. and Tuschl, T. (2004) 'Mechanisms of gene silencing by double-stranded RNA', *Nature* 431(7006): 343-9.

Mello, C. C., Kramer, J. M., Stinchcomb, D. and Ambros, V. (1991) 'Efficient gene transfer in C.elegans: extrachromosomal maintenance and integration of transforming sequences', *EMBO J* 10(12): 3959-70.

Mohan, M., Herz, H. M., Takahashi, Y. H., Lin, C., Lai, K. C., Zhang, Y., Washburn, M. P., Florens, L. and Shilatifard, A. (2010) 'Linking H3K79 trimethylation to Wnt signaling through a novel Dot1-containing complex (DotCom)', *Genes Dev* 24(6): 574-89.

Montell, D. J. (1999) 'The genetics of cell migration in Drosophila melanogaster and Caenorhabditis elegans development', *Development* 126(14): 3035-46.

Montgomery, M. K., Xu, S. and Fire, A. (1998) 'RNA as a target of double-stranded RNA-mediated genetic interference in Caenorhabditis elegans', *Proc Natl Acad Sci U S A* 95(26): 15502-7.

Morris, Tissenbaum, H. A. and Ruvkun, G. (1996) 'A phosphatidylinositol-3-OH kinase family member regulating longevity and diapause in Caenorhabditis elegans', *Nature* 382(6591): 536-9.

Murphy (2006) 'The search for DAF-16/FOXO transcriptional targets: approaches and discoveries', *Exp Gerontol* 41(10): 910-21.

Murphy, Lee and Kenyon (2007) 'Tissue entrainment by feedback regulation of insulin gene expression in the endoderm of Caenorhabditis elegans', *Proc Natl Acad Sci USA* 104(48): 19046-50.

Murphy, C. T., McCarroll, S. A., Bargmann, C. I. and Fraser, A. (2003) 'Genes that act downstream of DAF-16 to influence the lifespan of Caenorhabditis elegans', *Nature*.

Myers, T. R. and Greenwald, I. (2005) 'lin-35 Rb acts in the major hypodermis to oppose ras-mediated vulval induction in C. elegans', *Dev Cell* 8(1): 117-23.

Nadarajah, B., Brunstrom, J. E., Grutzendler, J., Wong, R. O. and Pearlman, A. L. (2001) 'Two modes of radial migration in early development of the cerebral cortex', *Nat Neurosci* 4(2): 143-50.

Nakamura, M., Ando, R., Nakazawa, T., Yudazono, T., Tsutsumi, N., Hatanaka, N., Ohgake, T., Hanaoka, F. and Eki, T. (2007) 'Dicer-related drh-3 gene functions in germ-line development by maintenance of chromosomal integrity in Caenorhabditis elegans', *Genes Cells* 12(9): 997-1010.

Nola, S., Daigaku, R., Smolarczyk, K., Carstens, M., Martin-Martin, B., Longmore, G., Bailly, M. and Braga, V. M. (2011) 'Ajuba is required for Rac activation and maintenance of E-cadherin adhesion', *J Cell Biol* 195(5): 855-71.

Nopoulos, Flaum, Andreasen and Swayze (1995) 'Gray matter heterotopias in schizophrenia', *Psychiatry Res* 61(1): 11-4.

Ogg, S., Paradis, S., Gottlieb, S., Patterson, G. I., Lee, L., Tissenbaum, H. A. and Ruvkun, G. (1997) 'The Fork head transcription factor DAF-16 transduces insulin-like metabolic and longevity signals in C. elegans', *Nature* 389(6654): 994-9.

Ogg, S. and Ruvkun, G. (1998) 'The C. elegans PTEN homolog, DAF-18, acts in the insulin receptor-like metabolic signaling pathway', *Mol Cell* 2(6): 887-93.

Oh, Mukhopadhyay, Svrzikapa, Jiang, Davis and Tissenbaum (2005) 'JNK regulates lifespan in Caenorhabditis elegans by modulating nuclear translocation of forkhead transcription factor/DAF-16', *Proc Natl Acad Sci USA* 102(12): 4494-9.

Oh, S. W., Mukhopadhyay, A., Dixit, B. L., Raha, T., Green, M. R. and Tissenbaum, H. A. (2006) 'Identification of direct DAF-16 targets controlling longevity, metabolism and diapause by chromatin immunoprecipitation', *Nat Genet* 38(2): 251-7.

Okada, Y., Feng, Q., Lin, Y., Jiang, Q., Li, Y., Coffield, V. M., Su, L., Xu, G. and Zhang, Y. (2005) 'hDOT1L links histone methylation to leukemogenesis', *Cell* 121(2): 167-78.

Otaegi, G., Yusta-Boyo, M. J., Vergano-Vera, E., Mendez-Gomez, H. R., Carrera, A. C., Abad, J. L., Gonzalez, M., de la Rosa, E. J., Vicario-Abejon, C. and de Pablo, F. (2006) 'Modulation of the PI 3-kinase-Akt signalling pathway by IGF-I and PTEN regulates the differentiation of neural stem/precursor cells', *J Cell Sci* 119(Pt 13): 2739-48.

Ozmen, M., Yilmaz, Y., Caliskan, M., Minareci, O. and Aydinli, N. (2000) 'Clinical features of 21 patients with lissencephaly type I (agyria-pachygyria)', *Turk J Pediatr* 42(3): 210-4.

Paik, Ding, Narurkar, Ramkissoon, Muller, Kamoun, Chae, Zheng, Ying, Mahoney et al. (2009) 'FoxOs cooperatively regulate diverse pathways governing neural stem cell homeostasis', *Cell Stem Cell* 5(5): 540-53.

Pak, J. and Fire, A. (2007) 'Distinct populations of primary and secondary effectors during RNAi in C. elegans', *Science* 315(5809): 241-4.

Pan, Howell, Clark, Hilliard, Cordes, Bargmann and Garriga (2006) 'Multiple Wnts and Frizzled Receptors Regulate Anteriorly Directed Cell and Growth Cone Migrations in Caenorhabditis elegans', *Dev Cell* 10(3): 367-377.

Pan, Peng, Chen and McIntire (2011) 'Genetic analysis of age-dependent defects of the Caenorhabditis elegans touch receptor neurons', *Proc Natl Acad Sci USA* 108(22): 9274-9.

Paradis, S., Ailion, M., Toker, A., Thomas, J. H. and Ruvkun, G. (1999) 'A PDK1 homolog is necessary and sufficient to transduce AGE-1 PI3 kinase signals that regulate diapause in Caenorhabditis elegans', *Genes Dev* 13(11): 1438-52.

Paradis, S. and Ruvkun, G. (1998) 'Caenorhabditis elegans Akt/PKB transduces insulin receptor-like signals from AGE-1 PI3 kinase to the DAF-16 transcription factor', *Genes Dev* 12(16): 2488-98.

Parker, G. S., Eckert, D. M. and Bass, B. L. (2006) 'RDE-4 preferentially binds long dsRNA and its dimerization is necessary for cleavage of dsRNA to siRNA', *RNA* 12(5): 807-18.

Parrini, M. C. (2012) 'Untangling the complexity of PAK1 dynamics: The future challenge', *Cell Logist* 2(2): 78-83.

Partovian, Ju, Zhuang, Martin and Simons (2008) 'Syndecan-4 regulates subcellular localization of mTOR Complex2 and Akt activation in a PKCalpha-dependent manner in endothelial cells', *Molecular Cell* 32(1): 140-9.

Patel, D. S., Garza-Garcia, A., Nanji, M., McElwee, J. J., Ackerman, D., Driscoll, P. C. and Gems, D. (2008) 'Clustering of genetically defined allele classes in the Caenorhabditis elegans DAF-2 insulin/IGF-1 receptor', *Genetics* 178(2): 931-46.

Peng, Li, Long, Li, Jia, Wang, Shen, Tang, Wen, Kung et al. (2010) 'Knockdown of FoxO3a induces increased neuronal apoptosis during embryonic development in zebrafish', *Neurosci Lett* 484(2): 98-103.

Peters, Gossett, Goldstein, Der and Reiner (2013) 'Redundant Canonical and Noncanonical Caenorhabditis elegans p21-Activated Kinase Signaling Governs Distal Tip Cell Migrations', *G3 (Bethesda)* 3(2): 181-95.

Pierce, S. B., Costa, M., Wisotzkey, R., Devadhar, S., Homburger, S. A., Buchman, A. R., Ferguson, K. C., Heller, J., Platt, D. M., Pasquinelli, A. A. et al. (2001) 'Regulation of DAF-2 receptor signaling by human insulin and ins-1, a member of the unusually large and diverse C. elegans insulin gene family', *Genes & Development* 15(6): 672-86.

Placzek, M. and Briscoe, J. (2005) 'The floor plate: multiple cells, multiple signals', *Nat Rev Neurosci* 6(3): 230-40.

Priess, J. R. and Hirsh, D. I. (1986) 'Caenorhabditis elegans morphogenesis: the role of the cytoskeleton in elongation of the embryo', *Dev Biol* 117(1): 156-73.

Qi, W., Huang, X., Neumann-Haefelin, E., Schulze, E. and Baumeister, R. (2012) 'Cell-nonautonomous signaling of FOXO/DAF-16 to the stem cells of Caenorhabditis elegans', *PLoS Genet* 8(8): e1002836.

Quinn, C. C., Pfeil, D. S., Chen, E., Stovall, E. L., Harden, M. V., Gavin, M. K., Forrester, W. C., Ryder, E. F., Soto, M. C. and Wadsworth, W. G. (2006) 'UNC-6/netrin and SLT-1/slit guidance cues orient axon outgrowth mediated by MIG-10/RIAM/lamellipodin', *Curr Biol* 16(9): 845-53.

Raj, Bogaard, Rifkin, Oudenaarden and Tyagi (2008) 'Imaging individual mRNA molecules using multiple singly labeled probes', *Nat Methods* 5(10): 877.

Rakic, P. (2007) 'The radial edifice of cortical architecture: from neuronal silhouettes to genetic engineering', *Brain Res Rev* 55(2): 204-19.

Rand, J. B. and Nonet, M. L. (1997) Synaptic Transmission. in D. L. Riddle T. Blumenthal B. J. Meyer and J. R. Priess (eds.) *C. elegans II*. Cold Spring Harbor (NY).

Renault, Rafalski, Morgan, Salih, Brett, Webb, Villeda, Thekkat, Guillerey, Denko et al. (2009) 'FoxO3 regulates neural stem cell homeostasis', *Cell Stem Cell* 5(5): 527-39.

Rhiner, C., Gysi, S., Fröhli, E., Hengartner, M. O. and Hajnal, A. (2005) 'Syndecan regulates cell migration and axon guidance in C. elegans', *Development* 132(20): 4621-33.

Rice, D. S. and Curran, T. (2001) 'Role of the reelin signaling pathway in central nervous system development', *Annu Rev Neurosci* 24: 1005-39.

Rocheleau, C., Cullison, K., Huang, K., Bernstein, Y., Spilker, A. and Sundaram, M. (2008) 'The Caenorhabditis elegans ekl (Enhancer of ksr-1 Lethality) Genes Include Putative Components of a Germline Small RNA Pathway', *Genetics* 178(3): 1431-1443.

Ross and Walsh (2001) 'Human brain malformations and their lessons for neuronal migration', *Annu Rev Neurosci* 24: 1041-70.

Rothberg, J. M., Jacobs, J. R., Goodman, C. S. and Artavanis-Tsakonas, S. (1990) 'slit: an extracellular protein necessary for development of midline glia and commissural axon pathways contains both EGF and LRR domains', *Genes Dev* 4(12A): 2169-87.

Ruby, J. G., Jan, C., Player, C., Axtell, M. J., Lee, W., Nusbaum, C., Ge, H. and Bartel, D. P. (2006) 'Large-scale sequencing reveals 21U-RNAs and additional microRNAs and endogenous siRNAs in C. elegans', *Cell* 127(6): 1193-207.

Rugarli, Schiavi, D., Hilliard, Arbucci, Ghezzi, Facciolli, Coppola, Ballabio and Bazzicalupo (2002) 'The Kallmann syndrome gene homolog in C. elegans is involved in epidermal morphogenesis and neurite branching', *Development* 129(5): 1283-94.

Salser, S. J. and Kenyon, C. (1992) 'Activation of a C. elegans Antennapedia homologue in migrating cells controls their direction of migration', *Nature* 355(6357): 255-8.

Schmidt-Strassburger, Schips, Maier, Kloiber, Mannella, Braunstein, Holzmann, Ushmorov, Liebau, Boeckers et al. (2012) 'Expression of constitutively active FoxO3 in murine forebrain leads to a loss of neural progenitors', *FASEB J* 26(12): 4990-5001.

Schneider, C. A., Rasband, W. S. and Eliceiri, K. W. (2012) 'NIH Image to ImageJ: 25 years of image analysis', *Nat Methods* 9(7): 671-5.

Schuster, E., McElwee, J. J., Tullet, J. M., Doonan, R., Matthijssens, F., Reece-Hoyes, J. S., Hope, I. A., Vanfleteren, J. R., Thornton, J. M. and Gems, D. (2010) 'DamID in C. elegans reveals longevity-associated targets of DAF-16/FoxO', *Mol Syst Biol* 6: 399.

She, X., Xu, X., Fedotov, A., Kelly, W. G. and Maine, E. M. (2009) 'Regulation of heterochromatin assembly on unpaired chromosomes during Caenorhabditis elegans meiosis by components of a small RNA-mediated pathway', *PLoS Genet* 5(8): e1000624.

Sijen, T., Fleenor, J., Simmer, F., Thijssen, K. L., Parrish, S., Timmons, L., Plasterk, R. H. and Fire, A. (2001) 'On the role of RNA amplification in dsRNA-triggered gene silencing', *Cell* 107(4): 465-76.

Sijen, T., Steiner, F. A., Thijssen, K. L. and Plasterk, R. H. (2007) 'Secondary siRNAs result from unprimed RNA synthesis and form a distinct class', *Science* 315(5809): 244-7.

Silhankova, M. and Korswagen, H. (2007) 'Migration of neuronal cells along the anterior–posterior body axis of C. elegans: Wnts are in control', *Current Opinion in Genetics & Development* 17(4): 320-325.

Smardon, A., Spoerke, J. M., Stacey, S. C., Klein, M. E., Mackin, N. and Maine, E. M. (2000) 'EGO-1 is related to RNA-directed RNA polymerase and functions in germ-line development and RNA interference in C. elegans', *Curr Biol* 10(4): 169-78.

Solari, Bourbon-Piffaut, Masse, Payrastre, Chan and Billaud (2005) 'The human tumour suppressor PTEN regulates longevity and dauer formation in Caenorhabditis elegans', *Oncogene* 24(1): 20-7.

Solecki, D. J. (2012) 'Sticky situations: recent advances in control of cell adhesion during neuronal migration', *Curr Opin Neurobiol* 22(5): 791-8.

Solecki, D. J., Model, L., Gaetz, J., Kapoor, T. M. and Hatten, M. E. (2004) 'Par6alpha signaling controls glial-guided neuronal migration', *Nat Neurosci* 7(11): 1195-203.

Song, S., Zhang, B., Sun, H., Li, X., Xiang, Y., Liu, Z., Huang, X. and Ding, M. (2010) 'A Wnt-Frz/Ror-Dsh pathway regulates neurite outgrowth in Caenorhabditis elegans', *PLoS Genet* 6(8).

Spalice, A., Parisi, P., Nicita, F., Pizzardi, G., Del Balzo, F. and Iannetti, P. (2009) 'Neuronal migration disorders: clinical, neuroradiologic and genetics aspects', *Acta Paediatr* 98(3): 421-33.

Steiner, F. A., Okihara, K. L., Hoogstrate, S. W., Sijen, T. and Ketting, R. F. (2009) 'RDE-1 slicer activity is required only for passenger-strand cleavage during RNAi in Caenorhabditis elegans', *Nat Struct Mol Biol* 16(2): 207-11.

Sternberg, P. W. (2005) 'Vulval development', *WormBook*: 1-28.

Stiles, J. and Jernigan, T. L. (2010) 'The basics of brain development', *Neuropsychol Rev* 20(4): 327-48.

Stranahan, A. M., Erion, J. R. and Wosiski-Kuhn, M. (2013) 'Reelin signaling in development, maintenance, and plasticity of neural networks', *Ageing Res Rev*.

Sulston, J. E. and Horvitz, H. R. (1977) 'Post-embryonic cell lineages of the nematode, Caenorhabditis elegans', *Developmental Biology* 56(1): 110-56.

Sulston, J. E., Schierenberg, White and Thomson, J. N. (1983) 'The embryonic cell lineage of the nematode Caenorhabditis elegans', *Developmental Biology* 100(1): 64-119.

Tabara, H., Yigit, E., Siomi, H. and Mello, C. C. (2002) 'The dsRNA binding protein RDE-4 interacts with RDE-1, DCR-1, and a DExH-box helicase to direct RNAi in C. elegans', *Cell* 109(7): 861-71.

Takahashi, Y., Daitoku, H., Hirota, K., Tamiya, H., Yokoyama, A., Kako, K., Nagashima, Y., Nakamura, A., Shimada, T., Watanabe, S. et al. (2011) 'Asymmetric arginine dimethylation determines life span in C. elegans by regulating forkhead transcription factor DAF-16', *Cell Metab* 13(5): 505-16.

Tank, Rodgers and Kenyon (2011) 'Spontaneous age-related neurite branching in Caenorhabditis elegans', *J Neurosci* 31(25): 9279-88.

Tessier-Lavigne, M. and Goodman, C. S. (1996) 'The molecular biology of axon guidance', *Science* 274(5290): 1123-33.

Thiery, J. P. (2003) 'Cell adhesion in development: a complex signaling network', *Curr Opin Genet Dev* 13(4): 365-71.

Thivierge, C., Makil, N., Flamand, M., Vasale, J. J., Mello, C. C., Wohlschlegel, J., Conte, D., Jr. and Duchaine, T. F. (2012) 'Tudor domain ERI-5 tethers an RNA-dependent RNA polymerase to DCR-1 to potentiate endo-RNAi', *Nat Struct Mol Biol* 19(1): 90-7.

Timmons, L. and Fire, A. (1998) 'Specific interference by ingested dsRNA', *Nature* 395(6705): 854.

Tissenbaum, H. A. and Ruvkun, G. (1998) 'An insulin-like signaling pathway affects both longevity and reproduction in Caenorhabditis elegans', *Genetics* 148(2): 703-17.

Toms, N., Cooper, J., Patchen, B. and Aamodt, E. (2001) 'High copy arrays containing a sequence upstream of mec-3 alter cell migration and axonal morphology in C. elegans', *BMC Dev Biol* 1: 2.

Trent, C., Tsuing, N. and Horvitz, H. R. (1983) 'Egg-laying defective mutants of the nematode Caenorhabditis elegans', *Genetics* 104(4): 619-47.

Tsai, L. H. and Gleeson, J. G. (2005) 'Nucleokinesis in neuronal migration', *Neuron* 46(3): 383-8.

Tullet, J. M., Hertweck, M., An, J. H., Baker, J., Hwang, J. Y., Liu, S., Oliveira, R. P., Baumeister, R. and Blackwell, T. K. (2008) 'Direct inhibition of the longevity-promoting factor SKN-1 by insulin-like signaling in C. elegans', *Cell* 132(6): 1025-38.

van Diepen, M. T. and Eickholt, B. J. (2008) 'Function of PTEN during the formation and maintenance of neuronal circuits in the brain', *Dev Neurosci* 30(1-3): 59-64.

Van Lieshout, R. J. and Voruganti, L. P. (2008) 'Diabetes mellitus during pregnancy and increased risk of schizophrenia in offspring: a review of the evidence and putative mechanisms', *J Psychiatry Neurosci* 33(5): 395-404.

Varela-Nieto, I., de la Rosa, E. J., Valenciano, A. I. and Leon, Y. (2003) 'Cell death in the nervous system: lessons from insulin and insulin-like growth factors', *Mol Neurobiol* 28(1): 23-50.

Vasale, J. J., Gu, W., Thivierge, C., Batista, P. J., Claycomb, J. M., Youngman, E. M., Duchaine, T. F., Mello, C. C. and Conte, D. (2010) 'Sequential rounds of RNA-dependent RNA transcription drive endogenous small-RNA biogenesis in the ERGO-1/Argonaute pathway', *Proc Natl Acad Sci USA* 107(8): 3582-7.

Vowels, J. J. and Thomas, J. H. (1992) 'Genetic analysis of chemosensory control of dauer formation in Caenorhabditis elegans', *Genetics* 130(1): 105-23.

Wadsworth, W. G., Bhatt, H. and Hedgecock, E. M. (1996) 'Neuroglia and pioneer neurons express UNC-6 to provide global and local netrin cues for guiding migrations in C. elegans', *Neuron* 16(1): 35-46.

Waite and Eickholt (2010) 'The neurodevelopmental implications of PI3K signaling', *Curr Top Microbiol Immunol* 346: 245-65.

Warner, A., Qadota, H., Benian, G. M., Vogl, A. W. and Moerman, D. G. (2011) 'The Caenorhabditis elegans paxillin orthologue, PXL-1, is required for pharyngeal muscle contraction and for viability', *Mol Biol Cell* 22(14): 2551-63.

Watari-Goshima, Ogura, Wolf, Goshima and Garriga (2007) 'C. elegans VAB-8 and UNC-73 regulate the SAX-3 receptor to direct cell and growth-cone migrations', *Nat Neurosci* 10(2): 169-76.

Welker, N. C., Habig, J. W. and Bass, B. L. (2007) 'Genes misregulated in C. elegans deficient in Dicer, RDE-4, or RDE-1 are enriched for innate immunity genes', *RNA* 13(7): 1090-102.

Wen, Wang, Little, Quirion and Zheng (2012) 'Forkhead family transcription factor FoxO and neural differentiation', *Neurogenetics* 13(2): 105-13.

Wen, Z. and Zheng, J. Q. (2006) 'Directional guidance of nerve growth cones', *Curr Opin Neurobiol* 16(1): 52-8.

Whangbo, J. and Kenyon, C. (1999) 'A Wnt signaling system that specifies two patterns of cell migration in C. elegans', *Molecular Cell* 4(5): 851-8.

White, J. G., Southgate, E., Thomson, J. N. and Brenner, S. (1986) 'The structure of the nervous system of the nematode Caenorhabditis elegans', *Philos Trans R Soc Lond B Biol Sci* 314(1165): 1-340.

Wightman, Clark, Taskar, Forrester, Maricq, Bargmann and Garriga, G. (1996) 'The C. elegans gene vab-8 guides posteriorly directed axon outgrowth and cell migration', *Development* 122(2): 671-82.

Wolf, Hung, Wightman, Way and Garriga, G. (1998) 'vab-8 is a key regulator of posteriorly directed migrations in C. elegans and encodes a novel protein with kinesin motor similarity', *Neuron* 20(4): 655-66.

Wolff, S. and Dillin, A. (2006) 'The trifecta of aging in Caenorhabditis elegans', *Exp Gerontol* 41(10): 894-903.

Yamamoto, T., Kato, Y., Kawaguchi, M., Shibata, N. and Kobayashi, M. (2004) 'Expression and localization of fukutin, POMGnT1, and POMT1 in the central nervous system: consideration for functions of fukutin', *Med Electron Microsc* 37(4): 200-7.

Ye and Field (2012) 'PAK signaling in cancer', *Cell Logist* 2(2): 105-116.

Yee, K. T., Simon, H. H., Tessier-Lavigne, M. and O'Leary, D. M. (1999) 'Extension of long leading processes and neuronal migration in the mammalian brain directed by the chemoattractant netrin-1', *Neuron* 24(3): 607-22.

Yigit, E., Batista, P., Bei, Y., Pang, K., Chen, C., Tolia, N., Joshuator, L., Mitani, S., Simard, M. and Mello, C. (2006) 'Analysis of the C. elegans Argonaute Family Reveals that Distinct Argonautes Act Sequentially during RNAi', *Cell* 127(4): 747-757.

Yue, Groszer, Gil, Berk, Messing, Wu and Liu (2005) 'PTEN deletion in Bergmann glia leads to premature differentiation and affects laminar organization', *Development* 132(14): 3281-91.

Zallen, J. A., Kirch, S. A. and Bargmann, C. I. (1999) 'Genes required for axon pathfinding and extension in the C. elegans nerve ring', *Development* 126(16): 3679-92.

Zecca, M., Basler, K. and Struhl, G. (1996) 'Direct and long-range action of a wingless morphogen gradient', *Cell* 87(5): 833-44.

Zegers, M. M., Forget, M. A., Chernoff, J., Mostov, K. E., ter Beest, M. B. and Hansen, S. H. (2003) 'Pak1 and PIX regulate contact inhibition during epithelial wound healing', *EMBO J* 22(16): 4155-65.

Zheng, W., Geng, A. Q., Li, P. F., Wang, Y. and Yuan, X. B. (2012) 'Robo4 regulates the radial migration of newborn neurons in developing neocortex', *Cereb Cortex* 22(11): 2587-601.

Zhu, G., Wang, Y., Huang, B., Liang, J., Ding, Y., Xu, A. and Wu, W. (2012) 'A Rac1/PAK1 cascade controls beta-catenin activation in colon cancer cells', *Oncogene* 31(8): 1001-12.

Zinovyeva, Yamamoto, Sawa and Forrester (2008) 'Complex network of Wnt signaling regulates neuronal migrations during Caenorhabditis elegans development', *Genetics* 179(3): 1357-71.

Zinovyeva, A. Y. and Forrester, W. C. (2005) 'The C. elegans Frizzled CFZ-2 is required for cell migration and interacts with multiple Wnt signaling pathways', *Dev Biol* 285(2): 447-61.

Appendix i: Analysis of *pak-1* transcriptional reporters containing mutated and non-mutated consensus DAF-16 binding sites

In Chapter 2 we show that the *pak-1* promoter in *C. elegans* contains consensus DAF-16 binding site sequences, which are conserved among the nematodes (Figure 2-12B) and highlight a ChIP-seq data set available from the modENCODE project, which shows that a DAF-16::GFP fusion protein occupies the endogenous *pak-1* promoter (Figure 2-12C). Before performing single-molecule fluorescent in situ hybridization (smFISH) to demonstrate that endogenous *pak-1* mRNA expression levels are reduced in *daf-16(mu86)* null embryos (Figure 2-13A-C), we had previously tried to test whether DAF-16 directly regulates *pak-1* expression by three additional methods. First, we created an extra chromosomal *ppak-1::tagrfp* transcriptional reporter to test whether expression was reduced in the *daf-16(null)* background. We analyzed embryos at the comma/1.5-fold stage when HSN migration is occurring but observed too much variation in TagRFP expression among embryos to conclude whether there was an overall reduction in expression in the *daf-16(null)* background compared to wild type (Figure appendix i-1).

ppak-1::tagrfp array in the wild type background

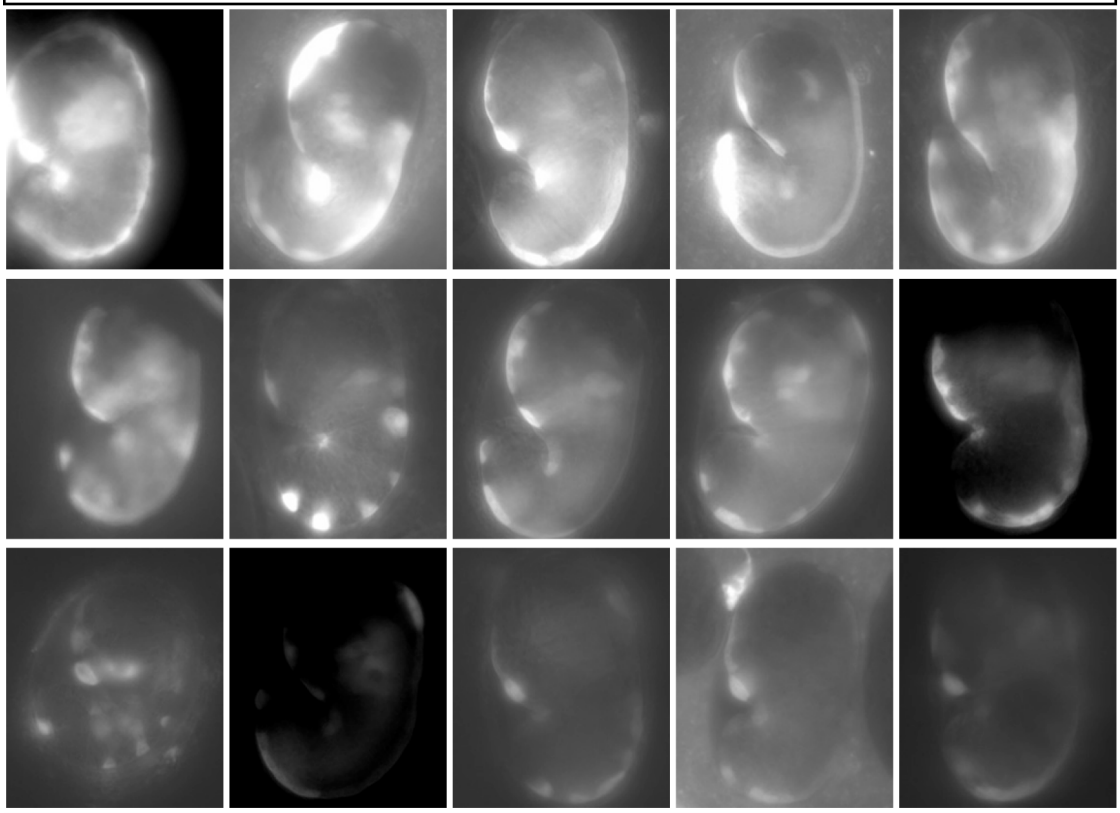

ppak-1::tagrfp array in the *daf-16(null)* background

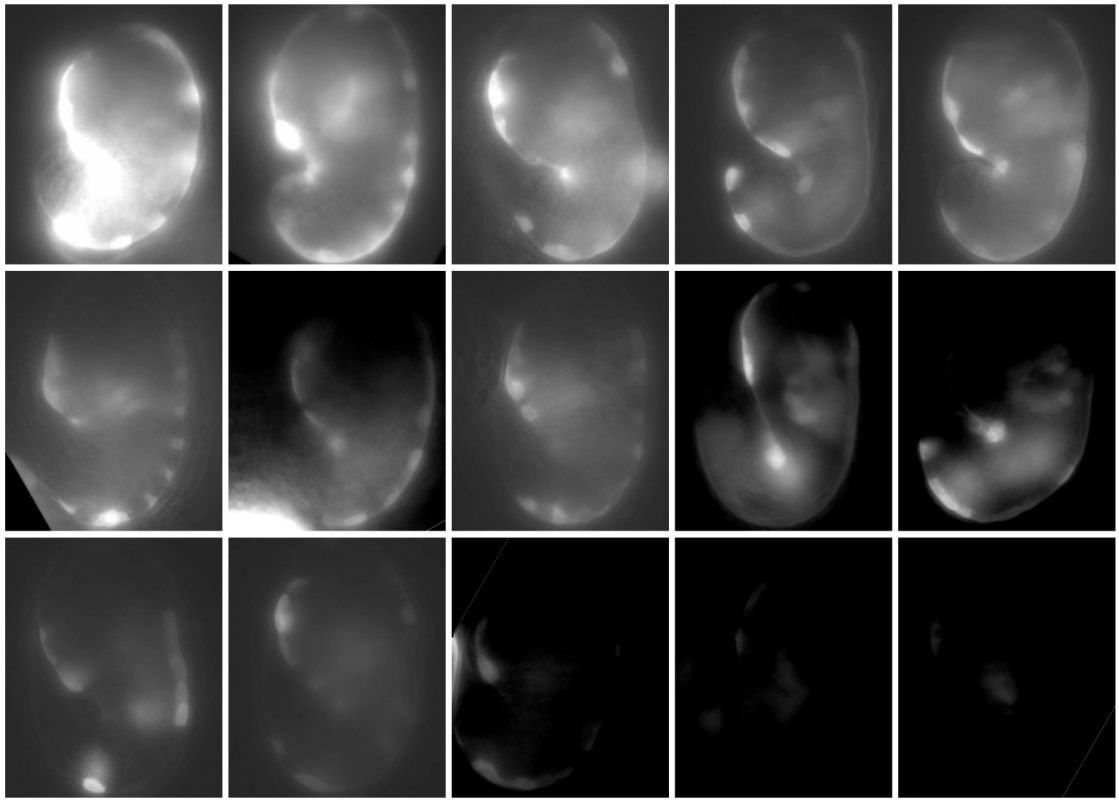

Figure appendix i-1. Expression of a *ppak-1::tagrfp* transcriptional reporter is variable in wild type and *daf-16* mutant backgrounds. Epifluorescent images of 15 individual comma/1.5-fold embryos expressing the *ppak-1::tagrfp* transcriptional reporter in the wild type background (top panel) and *daf-16(mu86)* background (bottom panel). Magnification, X630.

Second, we created another extra chromosomal *pak-1* promoter construct, but this time with an NLS tag (*ppak-1::NLS-tagrfp*), so that we could better identify the individual cells within the embryo and any possible differences in expression among cells in the *daf-16(null)* background. Furthermore, we injected this construct as a complex array to help stabilize transmission during development. However, similar to the *ppak-1::tagrfp* (created as a simple array) construct described above, we were unable to detect a difference in TagRFP expression between the wild type and *daf-16(null)* backgrounds (Figure appendix i-2).

ppak-1::NLS- tagrfp array in the wild type background

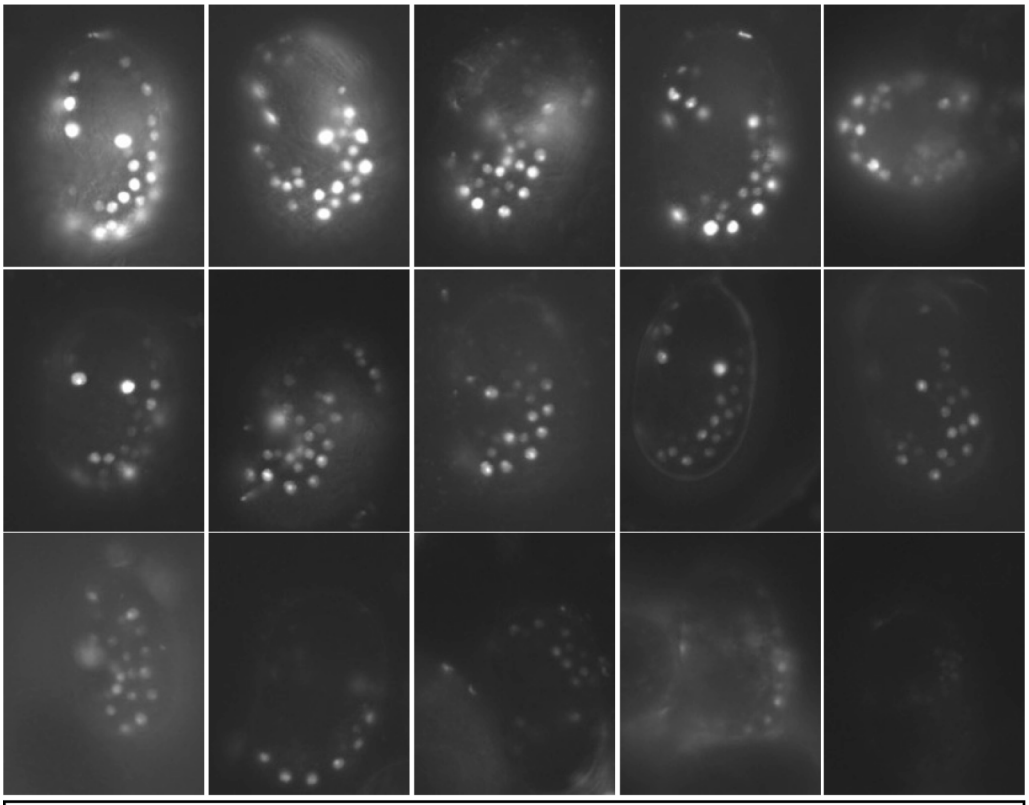

ppak-1::NLS-tagrfp array in the *daf-16(null)* background

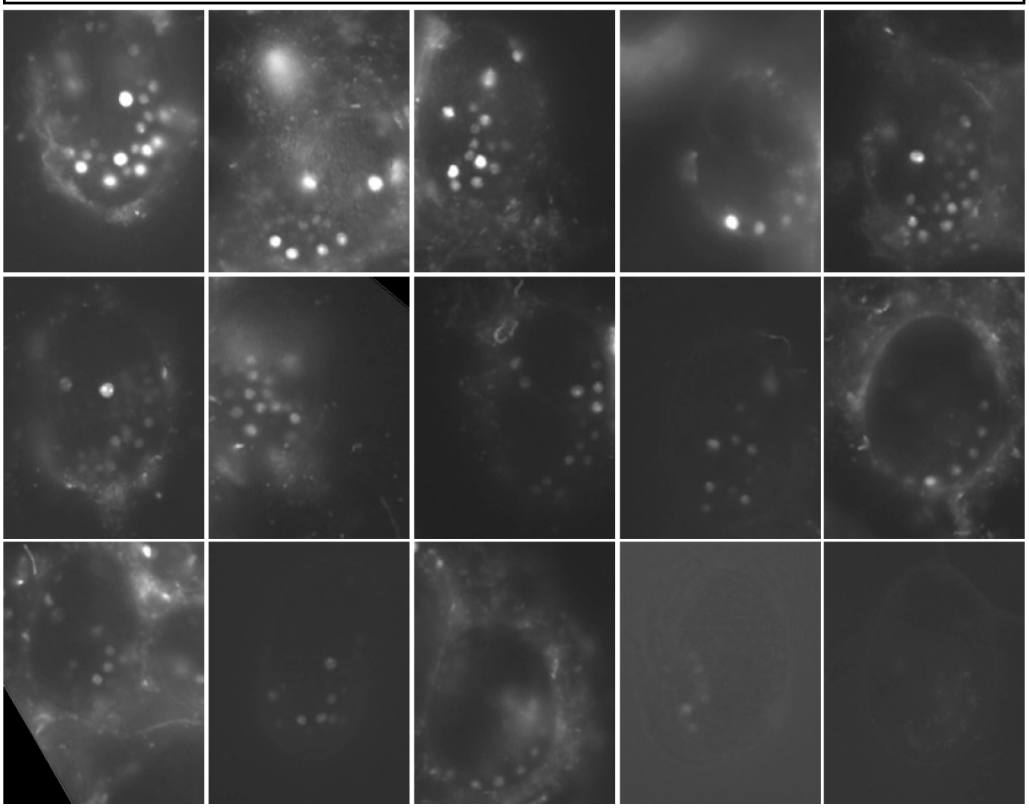

Figure appendix i-2. Expression of a *ppak-1::NLS-tagrfp* transcriptional reporter is variable in wild type and *daf-16* mutant backgrounds. Epifluorescent images of 15 individual comma/1.5-fold embryos expressing the *ppak-1::NLS-tagrfp* transcriptional reporter in the wild type background (top panel) and *daf-16(mu86)* background (bottom panel). Magnification, X400.

Third, we mutated all four consensus DAF-16 binding sites in the *pak-1* promoter to create the construct *ppak-1(1-4mut)::NLS-tagrfp*. We compared three independent lines containing this mutated construct with three independent lines containing the non-mutated *ppak-1::NLS-tagrfp* construct. Again, we were unable to conclude whether there was a reduction in TagRFP expression in the mutated lines compared to non-mutated lines since there was high variation in TagRFP expression among embryos within both the same line and among lines (Figure appendix i-3).

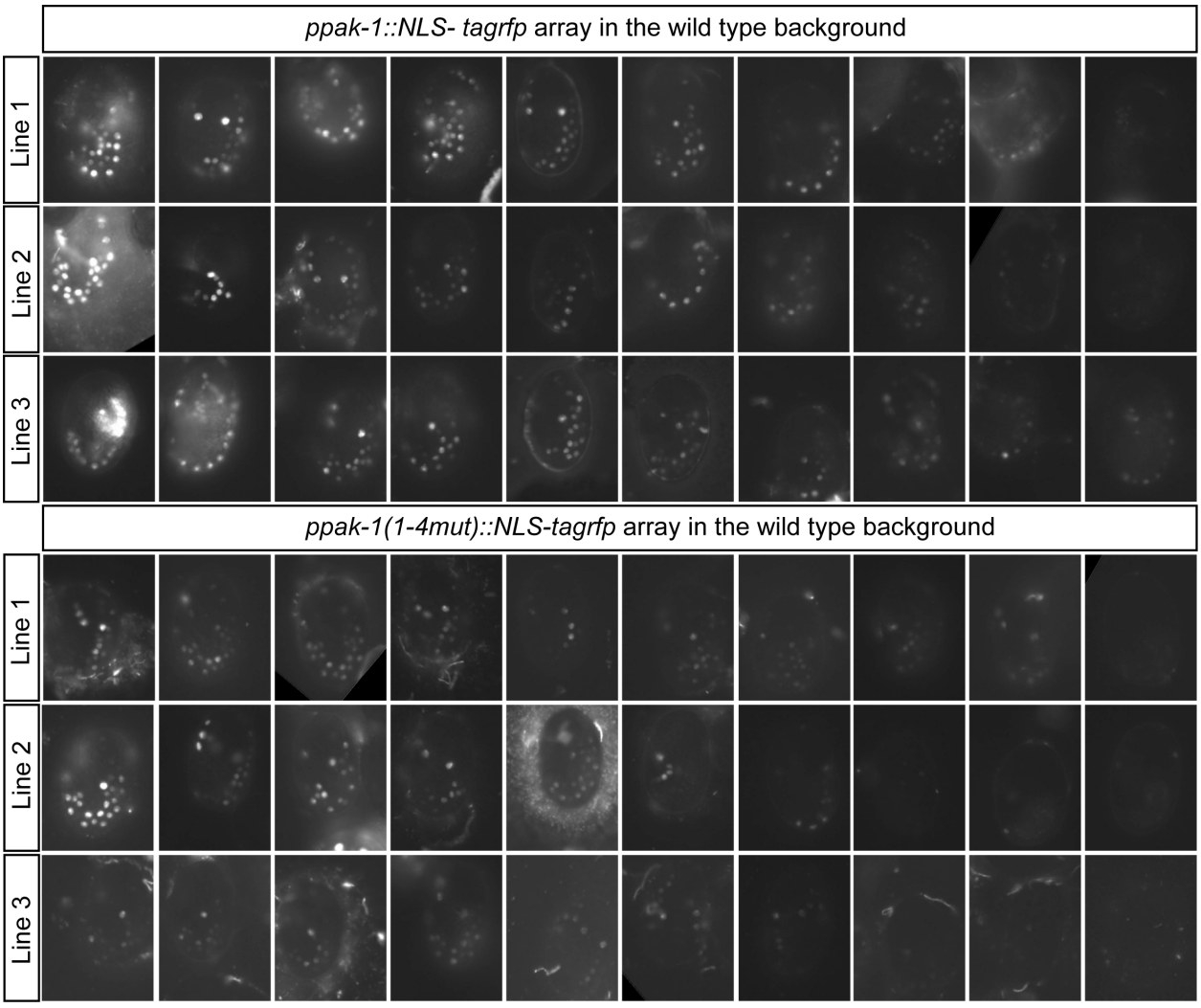

Figure appendix i-3. Mutating consensus DAF-16 binding sites in the *pak-1* promoter does not eliminate expression of a *ppak-1::NLS-tagrfp* transcriptional reporter. Epifluorescent images of 10 individual comma/1.5-fold embryos expressing the *ppak-1::NLS-tagrfp* (top panel) and the *ppak-1(1-4mut)::NLS-tagrfp* transcriptional reporter (bottom panel) in the wild type background. Three independent lines for each reporter were evaluated. Magnification, X400.

Materials and Methods

C. elegans Strains

Strains were maintained at 20°C unless otherwise noted, using standard methods (Brenner, 1974). Bristol N2 was the wild-type strain used. The following strain was obtained through the *Caenorhabditis* Genetics Center: LGI: CF1038 *daf-16(mu86).*

Molecular Biology and Transgenic Lines

Standard molecular biology techniques were used to construct transgenes. Germline transformation was performed by direct injection of various plasmid DNAs into the gonads of adult wild type animals as described (Mello et al., 1991). A 4kb fragment upstream of the *pak-1* ATG was isolated from genomic DNA by PCR and cloned into our modified fire vector with the forward primer containing a HindIII site 5'-CCGGCCAAGCTTCAATTCGATGCAATCCATTTAAAAG-3' and the reverse primer containing a BamHI site 5'-ATACGAGGATCCTTTGGCAAGCCTGGAAAATTGAAAC-3' to create the *ppak-1::tagrfp* reporter. The same primers were used to insert the 4kb *pak-1* promoter into a modified Fire Kit Vector pPD95.75 containing 2x NLS sequences and a gene encoding TagRFP (generously provided by the Greenwald Lab). The QuikChange II XL Site-Directed Mutagenesis kit (Agilent Technologies) was used to introduce mutations into the four consensus DAF-16 binding sites in the *pak-1* promoter. The consensus sites were changed from AT rich to GC rich sequences. The TATTTAC binding site sequences present at -1350 and -2918 relative to the *pak-1* ATG were changed to GCCCGAC. Primers used for the -1350 site are as follows: Primer_F: GGGTTTTTGCAGGTCTAGATTGTCGGGCTTCCCAAATTAACAGATTATG

and Primer_R:

CATAATCTGTTAATTTGGGAAGCCCGACAATCTAGACCTGCAAAAACCC.

Primers used for the -2918 site are as follows: Primer_F:

CTAATTCTGCATGTTTTGGTCGGGCTTTTTCAGTTCAGTTGATAG and Primer_R:

CTATCAACTGAACTGAAAAAGCCCGACCAAAACATGCAGAATTAG. The CTTATCA binding site sequence at -1867 was changed to GCCCGCA. Primers used are as follows: Primer_F: GGAAGCTCCAAATGCGGGCTGTCGAGAGGTCGAG and Primer_R: CTCGACCTCTCGACAGCCCGCATTTGGAGCTTCC. The TGTTTAC binding site sequence at -3238 was changed to GCCCGAC. Primers used are as follows: Primer_F: CCGTCGATCGTCGAAGCCCGACATAACCTATTCATAG and Primer_R:CTATGAATAGGTTATGTCGGGCTTCGACGATCGACGG. To create the *pak-1* transcriptional reporter lines, the corresponding transgenes were injected at 10 ng/µl together with pRF4 *(rol-6)* at 100 ng/µ1.

Microscopy

Live embryos were mounted on 2% agarose pads and examined using a Zeiss AxioImager Z1. Images that were compared were taken at the same exposure times.

Appendix ii: Pan-neuronal promoters are expressed in the *daf-18* mutant background

In chapter 2 we describe rescue experiments utilizing the pan-neuronal promoters *unc-119* and *rab-3* driving expression of a *daf-18* cDNA (Figure 2-5, 2-7). These constructs were simultaneously co-injected with a TagRFP transcriptional reporter to ensure proper promoter expression in the *daf-18(ok480)* null background (Figure appendix ii-1).

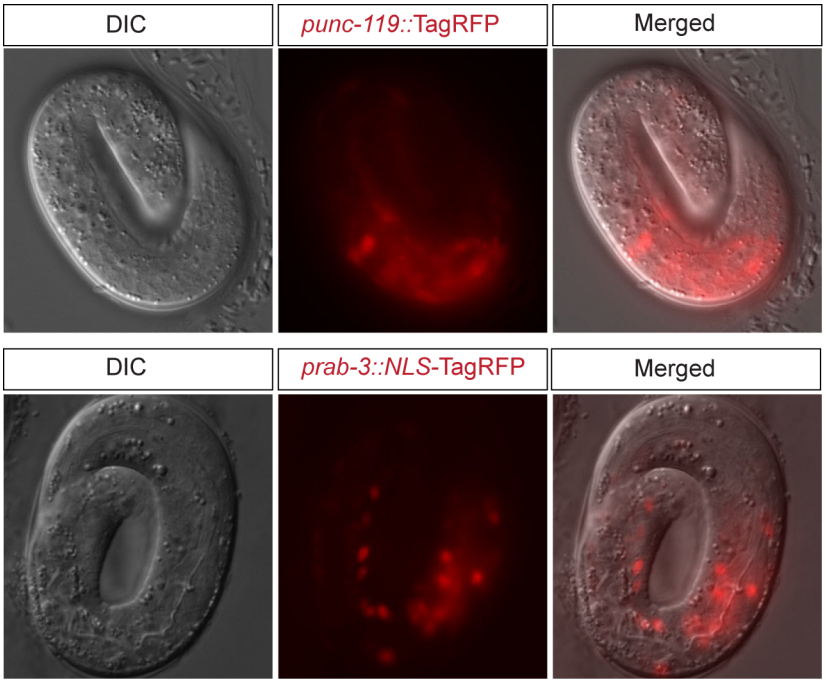

Figure appendix ii-1. Pan-neuronal transcriptional reporters are expressed in *daf-18(ok480)*. The *unc-119* (top panel) and *rab-3* (bottom panel) promoter-driven TagRFP

constructs are expressed in *daf-18* null mutants. Images of 3-fold embryos are shown. Magnification, X400.

Materials and Methods

See Chapter 2 for *C. elegans* strains, molecular biology, transgenic construction, and microscopy methods.

Appendix iii: DAF-16, ZFP-1 and RNAi mutants exhibit axon guidance defects

In addition to the HSN migration defects described in Chapters 2 and 3, the *daf-16, zfp-1* and RNAi mutants also display HSN axon guidance defects. In wild type animals HSN axon outgrowth begins during the L2 and L3 larval stages. The HSN axon extends ventrally to enter the ventral nerve cord in the midbody and then extends anteriorly in the nerve cord until it reaches the nerve ring by the late L4 stage. We have observed a variety of axon guidance defects in *daf-16*, *zfp-1* and RNAi mutants including: (1) axons that extend posteriorly along the body wall instead of anteriorly; (2) axons that wander along the body wall by either failing to remain in the ventral nerve cord or looping along the body wall and terminating before reaching the nerve ring; (3) axons that terminate prematurely in the ventral nerve cord before reaching the nerve ring (Figure appendix iii-1)

We find that loss-of-function mutations in *daf-16*, *zfp-1* or RNAi components cause 5-10% defects in axon guidance (Figure appendix iii-2). Moreover, a double mutant between the *daf-16(mu86)* null allele and the *zfp-1(ok554)* loss-of-function allele leads to enhanced axon guidance defects, suggesting that they act in parallel genetic pathways (Figure appendix iii-1). A double mutant between *daf-16(mu86)* and the *rde-4(ne299)* null allele leads to an enhancement of the *daf-16* single mutant phenotype but not the *rde-4* single mutant phenotype (Figure appendix iii-1). These data suggest that *rde-4* and *daf-16* work in parallel genetic pathways or that *rde-4* works upstream of *daf-16* to regulate axon guidance.

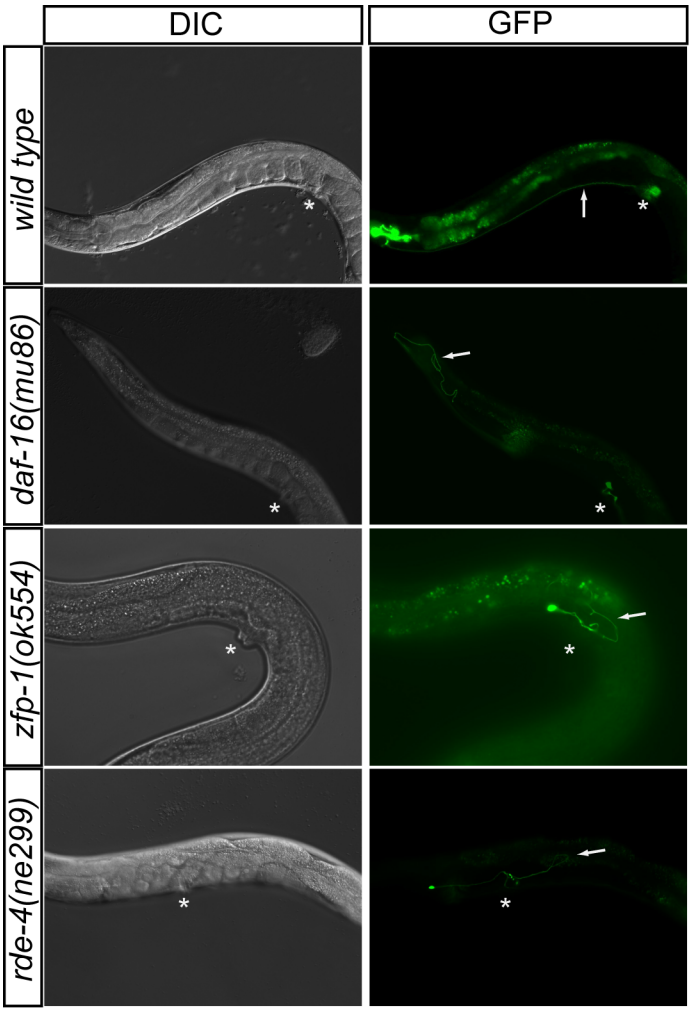

Figure appendix iii-1. Axon guidance defects in *daf-16, zfp-1* and *rde-4* mutants. In wild type animals the HSN axon extends ventrally to the ventral nerve cord and travels anteriorly to the nerve ring. Axons that fail to reach the ventral nerve cord and/or nerve ring are observed in *daf-16, zfp-1* and *rde-4* mutant animals. The HSN axons are visualized with a *tph-1::gfp* reporter in adult animals. Asterisks mark the vulva and arrows indicate the HSN axon. Magnification, X200.

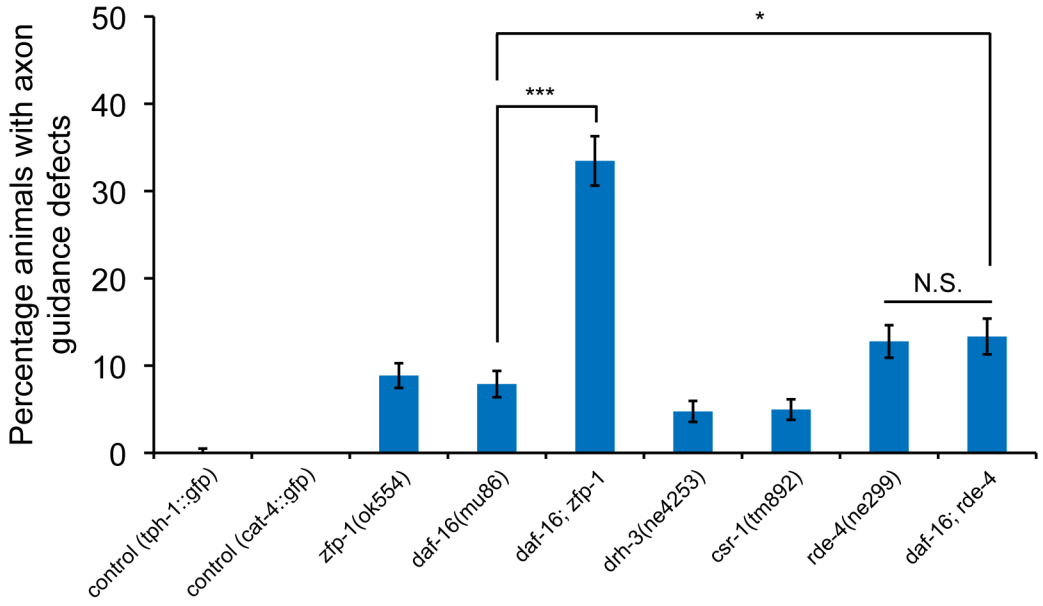

Figure appendix iii-2. Quantification of axon guidance defects in *daf-16, zfp-1* and RNAi mutants. Quantification of the percentage animals with axon guidance defects from a minimum of three pooled independent experiments per strain in controls *tph-1::gfp* (n=402), *cat-4::gfp* (n=263) versus *zfp-1(ok554)* (n=406), *daf-16(mu86)* (n=317), *daf-16; zfp-1* (n=275), *drh-3(ne4253)* (n=316), *csr-1(tm892)* (n=342), *rde-4(ne299)* (n=321), *daf-16; rde-4* (n=270). Note that the *cat-4::gfp* reporter was used to visualize the HSNs in the *csr-1(tm892)* mutant background. *p<0.05, ***p<0.001 (*z*-test). Error bars represent SEP.

Materials and Methods

C. elegans Strains

Strains were maintained at 20°C unless otherwise noted, using standard methods (Brenner, 1974). Bristol N2 was the wild-type strain used. The following strains were provided by the Hobert lab: SK4013 *zdIs13*(*tph-1::gfp)*IV (Clark and Chiu, 2003) and OH8482 *otIs225(cat-*

4::gfp)II; him-8IV. Compound mutant strains and transgenes used are as follows: AGK82: *zfp-1(ok554)*III; *tph-1::gfp*IV, AGK208: {*csr-1(tm892)*IV; *tph-1::*gfpIV; *neIs20* [pie-1::3xFLAG::csr-1 + unc-119(+)]}, AGK654: *drh-3(ne4253)*I; *tph-1::gfp*IV, AGK98: *rde-4(ne299)*III; *tph-1::gfp*IV, AGK580: *daf-16(mu86)*I; *tph-1::gfp*IV, AGK276: *daf-16(mu86)*I; *rde-4(ne299)*III; *tph-1::gfp* IV, AGK85: *daf-16(mu86)*I; *zfp-1(ok554)*III; *tph-1::gfp*IV.

Visualization of the HSN axons

The HSN axons were detected by by using the *zdIS13[tph-1::gfp]* or *otIs225[cat-4::gfp]* transcriptional reporters.

Microscopy and quantification

Live animals were mounted on 2% agarose pads and immobilized with 25 mM sodium azide (Sigma). Worms were examined using a Zeiss AxioImager Z1. Statistical significance was calculated using the *z*-test.

Appendix iv: Additional discussion on the *zfp-1(ok554)* allele

The *zfp-1(ok554)* allele has been characterized as a loss-of-function allele based on a variety of molecular and genetic experiments, which will be discussed below. The *zfp-1(ok554)* mutation leads to a truncated version of the protein that retains the N-terminal PHD fingers but lacks the C-terminal OM-LZ motifs, which are essential for DOT-1.1 interaction (Cui et al., 2006; Avgousti et al., 2013; Cecere et al., 2013). The recruitment of DOT-1.1 by ZFP-1 is required at the promoters of highly expressed genes throughout development as well as at the promoters of genes involved in the stress response and functions to negatively modulate transcription (Cecere et al., 2013). Moreover, in the *zfp-1(ok554)* mutant, the recruitment of DOT-1.1 by ZFP-1 to target promoters is reduced and an increase in transcription is observed (Cecere et al., 2013), which supports the classification of the *ok554* allele as a reduction-of-function mutation.

A genome-wide feeding RNAi screen to identify suppressors of the multivulva (Muv) phenotype of *lin-15AB(n765)* identified *zfp-1* and consistent with *zfp-1(RNAi)*, the *zfp-1(ok554)* mutant also significantly reduced the Muv phenotype (Cui et al., 2006). Moreover, the phenotype of the *zfp-1(ok554)* mutant was reported to display slow-growth, protruded vulva and a reduced brood size and was recapitulated using *zfp-1(RNAi)* (Cui et al., 2006). The *zfp-1(ok554)* allele has also been placed over a deficiency allele on chromosome III, nDF17, which leads to a more severe phenotype and causes lethality (Avgousti et al., 2013). Moreover, *zfp-1(RNAi)* also phenocopies the HSN migration defect observed in the *zfp-1(ok554)* mutant (Figure appendix iv-1), supporting that the HSN migration defect observed in the *ok554* mutant is due to reduced ZFP-1 activity. Also, in Chapter 3 we show that overexpressing the N-terminal fragment of the

ZFP-1 long isoform (PHD1-PHD2::FLAG), which represents the truncated fragment retained in the *zfp-1(ok554)* mutant (Avgousti et al., 2013), in the *zfp-1(ok554)* mutant background does not affect the HSN undermigration phenotype (Figure 3-3). This result supports that the residual fragment expressed in *zfp-1(ok554)* does not have neomorphic properties responsible for the HSN migration phenotype observed in the *zfp-1(ok554)* mutant. Combined, these genetic data are consistent with *zfp-1(ok554)* being a hypomorphic allele.

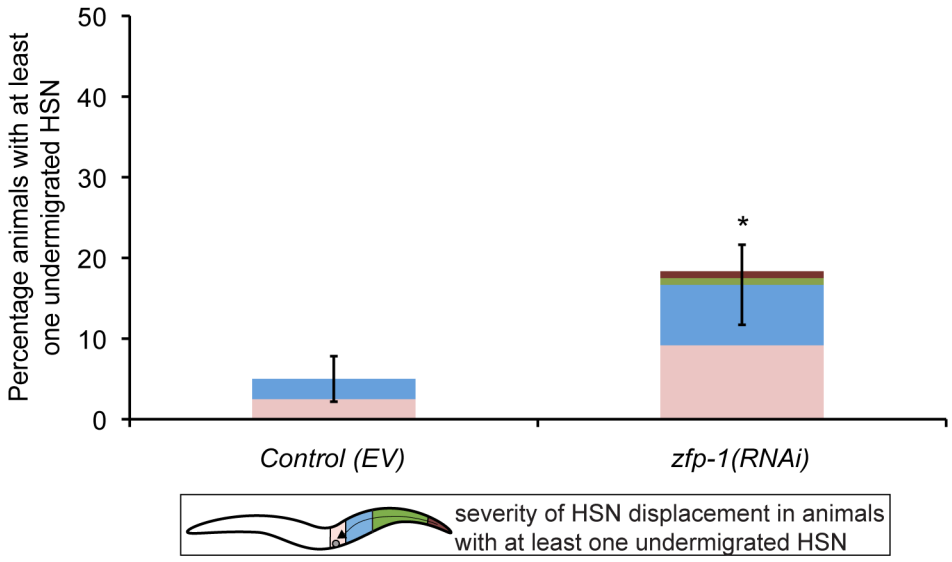

Figure appendix iv-1. Knockdown of *zfp-1* by RNAi leads to HSN undermigration. RNAi knockdown of *zfp-1* (long and short isoforms) results in HSN migration defects. Quantification of the percentage of animals with an undermigrated HSN from a minimum of three pooled independent experiments in control (EV) (n=60) and *zfp-1(RNAi)* (n=60) animals. EV = empty vector. HSNs were visualized with the *tph-1::gfp* reporter. Worm schematic legend: Stacked bars represent the proportion of HSNs at different positions along the A-P body axis within only those animals containing at least one undermigrated HSN. Thus, since there are two HSNs within each

animal and not every HSN is affected, one colored region (light pink) represents the wild type HSN that remains unaffected in animals containing a second undermigrated HSN, which is represented by either the red, green or blue region. *p<0.05 (*z*-test). Error bars represent standard error of the proportion.

Material and Methods

C. elegans Strains

Strains were maintained at 20°C using standard methods (Brenner, 1974). Bristol N2 was the wild-type strain used. The following strain was provided by the Hobert lab: SK4013 *zdIs13*(*tph-1::gfp)*IV (Clark and Chiu, 2003).

RNAi

RNA interference (RNAi) experiments were carried out by feeding at 20°C in the wild type background. L4 worms were fed dsRNA-producing bacteria, and their progeny scored for HSN migration defects. The following clone from the *C. elegans* feeding library (Kamath et al., 2003) were used: *zfp-1* (JA:F54F2.2). Bacteria containing each RNAi clone were grown via standard methods.

Microscopy and quantification

Live animals or embryos were mounted on 2% agarose pads and immobilized with 25 mM sodium azide (Sigma). Worms were examined using a Zeiss AxioImager Z1. All phenotypes were scored as percent animals with at least one undermigrated HSN and results are presented as stacked bar graphs to represent the proportion of HSNs in positions along the A-P body axis in

these animals. When one or both HSN cell bodies were located posterior to the vulva in adult animals, the animal was scored as mutant. Statistical significance was calculated using the *z*-test.

Appendix v: Genetic interaction between *rde-4* and *zfp-1* mutants

During our study on the involvement of RNAi and ZFP-1 in the process of HSN migration (Chapter 3) we created a double mutant between the *rde-4(ne299)* null mutant and the *zfp-1(ok554)* loss-of-function mutant to determine their genetic interaction. Surprisingly, we found that the *zfp-1(ok554)* mutant suppressed the *rde-4* mutant (Figure appendix v-1). ZFP-1 has been described as a negative regulator of gene expression (Cecere et al., 2013) and RNAi, although generally viewed as a negative regulator, has been recently shown to have a positive role in regulating gene expression (Avgousti et al., 2012). Therefore, one possibility is that *rde-4* and *zfp-1* regulate common target genes required for HSN migration but in opposite directions. Future experiments will be required to dissect the genetic and molecular interaction between *rde-4* and *zfp-1*.

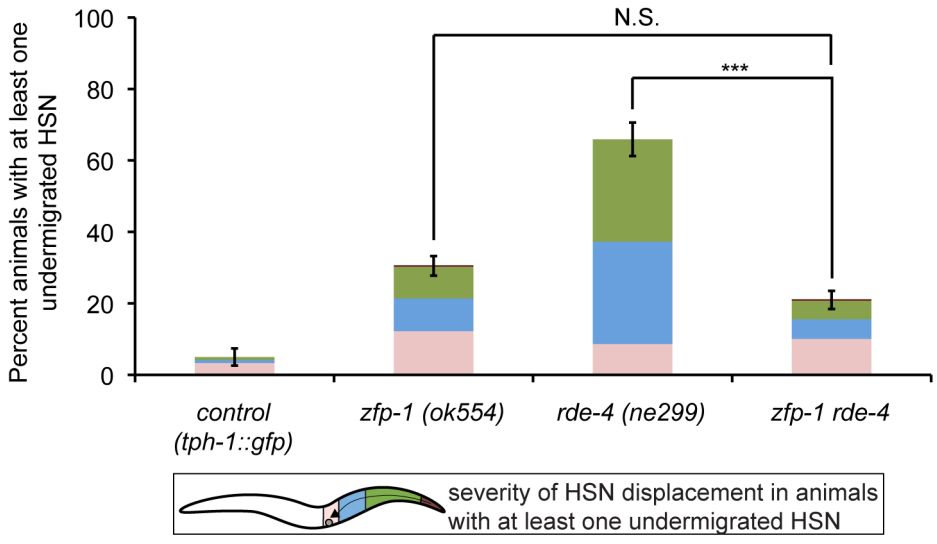

Figure appendix v-1. The *zfp-1* mutant suppresses the *rde-4* null mutant HSN undermigration phenotype. Quantification of the percentage of animals with an undermigrated HSN from a minimum of two pooled independent experiments per strain in control *tph-1::gfp* (n=120), *zfp-1(ok554)* (n=269), *rde-4(ne299)* (n=110), *zfp-1 rde-4* (n=267). HSNs were visualized with the *tph-1::gfp* reporter. Worm schematic legend: Stacked bars represent the proportion of HSNs at different positions along the A-P body axis within only those animals containing at least one undermigrated HSN. Thus, since there are two HSNs within each animal and not every HSN is affected, one colored region (light pink) represents the wild type HSN that remains unaffected in animals containing a second undermigrated HSN, which is represented by either the red, green or blue region. ***p<0.0001, N.S. (not significant) (*z*-test). Error bars represent standard error of the proportion.

Material and Methods

***C. elegans* Strains**

Strains were maintained at 20°C using standard methods (Brenner, 1974). Bristol N2 was the wild-type strain used. The following strain was provided by the Hobert lab: SK4013 *zdIs13*(*tph-1::gfp)*IV (Clark and Chiu, 2003). Compound mutant strains and transgenes used are as follows: AGK98: *rde-4(ne299)*III; *tph-1::gfp*IV, AGK82: *zfp-1(ok554)*III; *tph-1::gfp*IV, AGK397: *rde-4(ne299) zfp-1(ok554)*III*; tph-1::gfp*IV.

Microscopy and quantification

Live animals or embryos were mounted on 2% agarose pads and immobilized with 25 mM sodium azide (Sigma). Worms were examined using a Zeiss AxioImager Z1. All phenotypes

were scored as percent animals with at least one undermigrated HSN and results are presented as stacked bar graphs to represent the proportion of HSNs in positions along the A-P body axis in these animals. When one or both HSN cell bodies were located posterior to the vulva in adult animals, the animal was scored as mutant. Statistical significance was calculated using the *z*-test.